

NANOSCALE AND MICROSCALE HEAT TRANSFER IX



BERLIN 20 - 24 APRIL 2026



BOOK OF ABSTRACTS

Table of Contents

| | |
|--|-----------|
| Thermal Photonics in Non-Reciprocal Many-Body Systems | 1 |
| <u>Dr. Philippe Ben Abdallah</u> | |
| Simultaneous heat and electronic dynamics in photoexcited semiconductors investigated by time-resolved diffraction anomalous fine structure (TR-DAFS) | 2 |
| <u>Dr. Thomas C. Rossi</u> , Mr. Moritz Meißner, Dr. Matthias Rössle, Prof. John J. Rehr, Prof. Joshua Kas, Prof. Renske M. van der Veen | |
| Predictive Modeling of Non-Diffusive Heat Transport in 2D and 3D Materials under Transient Grating Excitations | 4 |
| <u>Ms. Almudena Diaz Serrano</u> , Mr. Jamie Harford, Dr. Albert Beardo, Mr. Jordi Tur Prats, Prof. Joshua Knobloch, Prof. Javier Bafaluy, Prof. F. Xavier Alvarez, Prof. Juan Camacho | |
| Thermal and electrical effects in polarized Ti/Si interface using cross-section scanning thermal and Kelvin probe force microscopies | 5 |
| <u>Dr. Juan Carlos Acosta Abanto</u> , Dr. Nicolas BERCU, Dr. Mélanie Brouillard, Prof. Jean-François Robillard, Prof. Nicolas Horny, Prof. Louis Giraudet, Prof. Pierre-Olivier Chapuis, Dr. Severine Gomes | |
| Revisiting Phonon Hydrodynamics in Graphene: Effects of High-Order Anharmonicity | 7 |
| <u>Mr. Jordi Tur Prats</u> , Dr. Zherui Han, Dr. Albert Beardo, Prof. Xiulin Ruan, Prof. F. Xavier Alvarez | |
| Higher-Order Perturbation Equation (HOPE) framework for thermal transport in semiconductors. | 9 |
| <u>Prof. F. Xavier Alvarez</u> , Dr. Albert Beardo, Mr. Jordi Tur Prats, Ms. Almudena Diaz Serrano | |
| Energy conversion at the nanoscale: exploiting non-thermal resources | 10 |
| <u>Ms. Elsa Danielsson</u> , <u>Dr. Henning Kirchberg</u> , Prof. Janine Splettstoesser | |
| Monte Carlo Modeling of Phonon Drag Effects on Thermoelectric Transport in Silicon Nanostructures | 11 |
| <u>Dr. Mohammad Ghanem</u> , Dr. Philippe Dollfus, Dr. Jelena Sjakste, Dr. Raja Sen, Prof. Jérôme Saint Martin | |
| A toolbox of pump-probe techniques to investigate phonons and thermal transport | 13 |
| <u>Dr. Begoña Abad Mayor</u> , Dr. Grazia Raciti, Mrs. Deeksha Sharma, Dr. Aswathi K. Sivan, Dr. Jose Manuel Sojo Gordillo, Dr. Ahmad Zenji, Prof. Ilaria Zardo | |
| Quantum and thermal light emission from time-modulated mid-infrared nanophotonic systems | 14 |
| <u>Mrs. Amaia Vertiz</u> , <u>Dr. Francisco Javier Alfaro Mozaz</u> , Dr. Iñigo Liberal | |
| Heat transport between nonreciprocal media | 15 |
| <u>Dr. Omar Jesus Franca Santiago</u> , Dr. Nico Strauß, Prof. Stefan Yoshi Buhmann | |
| Near-field thermal rectification and routing with Weyl Semi-Metals | 16 |
| <u>Dr. Alireza Naeimi</u> , Dr. S. Age Biehs | |
| Transition from far-field to enhanced near-field radiative heat transfer in a multi-body system involving two microspheres | 17 |
| <u>Dr. Ana Isabel Fernández-Tresguerres Mata</u> , Dr. Victor Guillemot, Dr. Yannick De Wilde | |

| | |
|---|-----------|
| Exceptional thermal stability and heat-induced structural transitions in individual Tobacco Mosaic Virus (TMV) | 19 |
| Dr. Diego Alonso Aldave, Mr. Alejandro Díez-Martínez, Dr. JaeHwan Jeong, Dr. Pedro J. de Pablo, Prof. Julio Gómez-Herrero, Dr. Pablo Ares | |
| Thermal characterization of nanolayers: silica, diamond and phase-change materials | 20 |
| Prof. Nicolas Horny, Ms. Ghadir OLLAIC , Dr. Sébastien Cueff, Dr. Georges Hamaoui, Dr. Lionel Rousseau, Dr. Mihaï Lazar, Ms. Evelyne Martin | |
| Giant Thermal Switching via Phase Transition in MoTe₂ | 21 |
| Mrs. Zhuyao Chang, Dr. Nemo McIntosh, Prof. Zhao Liu, Dr. Riccardo Rurali | |
| Phonon transport at the nanoscale: a wave-particle duality matter | 22 |
| Dr. Valentina Giordano | |
| Microscale Heat Transfer and Flexural Phonon Dynamics in Expanded Graphite–MWCNT Composites | 23 |
| Dr. Daria Szewczyk , Prof. Andrzej Jezowski, Dr. Maksym Barabashko, Prof. Galina Dovbeshko, Prof. Alexander Krivchikov | |
| Phonon transport in asymmetric nanostructures in the ballistic regime | 24 |
| Dr. Boris Brisuda , Dr. Olivier Bourgeois, Prof. Jean-François Robillard, Mr. Jon Canosa Diaz | |
| First principles calculations of thermal transport at metal/silicon interfaces: Evidence of interfacial electron-phonon coupling | 26 |
| Dr. Michael De SanFeliciano, Dr. Christophe Adessi , Dr. Julien El Hajj, Prof. Nicolas Horny, Dr. François Detcheverry, Dr. Manuel Cobian, Dr. Samy Merabia | |
| Phonon mean free path spectroscopy by Raman thermometry | 27 |
| Ms. Katharina Dudde , Mr. Mahmoud Elhajhasan, Mr. Guillaume Würsch, Mr. Julian Themann, Ms. Jana Lierath, Mrs. Elena Trukhan, Dr. Nakib Protik, Dr. Giuseppe Romano, Prof. Gordon Callsen | |
| Thermoelastic heat flux contribution opposing the thermal gradient in ultrathin MoS₂ and MoSe₂ | 28 |
| Dr. Albert Beardo , Mr. Jordi Tur Prats, Prof. F. Xavier Alvarez, Prof. Juan Camacho, Dr. Sebin Varghese, Prof. Klaas-Jan Tielrooij | |
| Machine Learning Guided Discovery of Extreme Lattice Thermal Conductivity in Si/Ge Superlattices | 29 |
| Dr. Shubham Tyagi , Dr. Julian Garcia Fernandez, Dr. Natalia Seoane, Prof. Antonio Garcia Loureiro, Prof. Marc Bescond | |
| Influence of electrical properties on thermal boundary conductance at metal/semiconductor interface | 31 |
| Prof. Nicolas Horny , Dr. Quentin Pompidou, Dr. Juan Carlos ACOSTA ABANTO, Dr. Mélanie Brouillard, Dr. Nicolas BERCU, Prof. Louis Giraudet, Dr. Raza Sheikh, Dr. Christophe Adessi, Dr. Samy Merabia, Dr. Severine Gomes, Dr. P-Olivier Chapuis, Prof. Jean-François Robillard, Prof. Mihaï Chirtoc | |
| Predictive modeling of nanoscale thermal transport in silicon using machine-learning molecular dynamics | 33 |
| Dr. Housseem Rezgui , Prof. Clivia Sotomayor-Torres | |
| Tutorial: Dilution Refrigerators | 35 |
| Dr. Leif Roschier | |

| | |
|--|-----------|
| Next-generation cryogenic refrigeration enabled by superconducting tunnel junctions | 36 |
| <u>Dr. Renan Loreto</u> , Dr. Arvind Kumar, Dr. Juho Luomahaara, Dr. Joel Hätingen, Dr. Jani Taskinen, Dr. Tuure Rantanen, Dr. Matilde Tubal, Dr. Emma Mykkänen, Dr. C. Wisa Förbom, Dr. Alberto Ronzani, Dr. Klaara Viisanen, Dr. Antti Kemppinen, Prof. Mika Prunnila | |
| Active and passive control of low-temperature thermal conduction with pillar-based phononic crystals | 37 |
| Mr. Tatu Korkiamäki, Dr. Tuomas Puurtinen, Prof. Bartłomiej Graczykowski, <u>Prof. Ilari Maasilta</u> | |
| From Single to Periodic Pulses: Fourier Expansion Analysis to Thermo-Reflectance Signal for Thermal Diffusivity Measurements | 38 |
| <u>Dr. Dmitry Sergeev</u> , Dr. Takahiro Baba, Prof. Tetsuya Baba, Mr. Yoshio Shinoda, Dr. Osamu Tsukamoto, Ms. Kazuko Ishikawa, Prof. Takao Mori | |
| Simulations of heat transfer with COMSOL Multiphysics | 40 |
| <u>Dr. Sébastien Denis</u> | |
| Microgels as Local Temperature Probes for Laser-Induced Heating of Plasmonic Metal Structures | 41 |
| <u>Dr. Yulia Gordievskaya</u> , Dr. Nino Lomadze, Ms. Shivani Kesarwani, Prof. Andrij Pich, Prof. Holger Lange, Prof. Svetlana Santer | |
| Tunable thermal conductivity in Silicon thin films via block copolymer nanostructuring | 42 |
| Mr. Alex Rodriguez-Iglesias, Dr. Jose Manuel Sojo Gordillo, Dr. Arianna Nigro, Mr. Marc Aceituno Pimentel, Dr. Iñigo Martín-Fernández, Dr. Francesc Perez-Murano, Dr. Luis Fonseca, Dr. Llibertat Abad, Prof. Ilaria Zardo, <u>Dr. Marc Salleras</u> , Dr. Marta Fernandez-Regulez | |
| Multi-scale temperature distribution for metal nano-particle solutions under CW illumination | 44 |
| <u>Mr. Mathis Noell</u> , Prof. Carsten Henkel | |
| Transient nonlinear transmission of thin gold nano-layers due to infrared pumping | 45 |
| Ms. Helena Poulouse, Mr. Mathis Noell, Ms. Athena Majlesi, Dr. Wouter Koopman, <u>Prof. Carsten Henkel</u> , Prof. Rike Müller-Werkmeister | |
| Broadband ultrafast probing of nonequilibrium interfacial thermal conductance in Au/substrate heterostructures | 46 |
| <u>Dr. Zhicheng Chen</u> , Prof. Qiye Zheng | |
| Polyvinyl Alcohol Silicon Dioxide Composite Material for Daytime Radiative Cooling | 47 |
| <u>Dr. Armande HERVE</u> , Mr. Yufei Yan, Ms. Rameeja Abdul Rasheed, Ms. Dhanya Jacob, Prof. Tarik Bourouina, Prof. Aldrin Antony, Dr. Elyes Nefzaoui | |
| Local probing of ion-doped regions of silicon carbide crystal via MIR photo-thermo-mechanical excitation of scanning probes | 48 |
| <u>Mr. Michael O'Shaughnessy-Gutierrez</u> , Dr. Rajasekhar Medapalli, Mr. Samuel Eserin, Ms. Xinyun Liu, Ms. Ella Schneider, Dr. Jessica Boland, Prof. Ben Murdin, Dr. Alexandros Elsachat, Prof. Oleg Kolosov | |
| Analogy between the thermal emission of nano objects and Hawking's radiation | 50 |
| <u>Prof. Karl Joulain</u> | |
| Near-field radiative heat transfer in plasmonic nanobubbles | 51 |
| Dr. Sreyash Sarkar, Mr. Jerome Sarr, Prof. Olivier Merchiers, <u>Dr. P-Olivier Chapuis</u> | |

| | |
|--|-----------|
| Near-field thermophotovoltaic conversion at room temperature with low-energy bandgap cells made of interband-cascade structure | 52 |
| Mr. Mathieu Thomas, Dr. Basile Roux, Dr. Lu Li, Dr. Jeremy A. Massengale, Prof. Rui Q. Yang, Prof. Michael B. Santos, Dr. Rodolphe Vaillon, <u>Dr. P-Olivier Chapuis</u> | |
| High order anharmonicity in the thermal conductivity of Transition Metal Dichalcogenides | 54 |
| <u>Ms. Marta Loletti</u> , Dr. Qi Ren, Dr. Riccardo Rurali | |
| Calibration of Scanning Joule Expansion Microscopy for nanoscale heat transport studies | 55 |
| <u>Dr. JaeHwan Jeong</u> , Dr. Diego Alonso Aldave, Prof. Julio Gómez-Herrero, Dr. Pablo Ares | |
| Cross-plane thermal conductivity in MXenes | 56 |
| Mr. Oscar Mateos-Lopez, Mr. Isaac Armstrong, Ms. Elvira Tornero, Dr. Miguel Muñoz, Prof. Hendrik Heinz, Dr. Guilherme Vilhena, Prof. Juan Carlos Cuevas | |
| Fabrication of large-area, suspended twisted WS2 bilayers | 57 |
| Mr. Daniel Capolat Palomar, Mr. JiaQi Yang, Mr. Pu Tan, Dr. Timm Swoboda, Dr. Maria Jose Esplandiu, Prof. Javier Rodriguez-Viejo, Dr. Marianna Sledzinska | |
| Enhancing phonon transmission across solid-superfluid helium interfaces by tuning phase coherence in nanometer-scale interlayer films | 59 |
| <u>Dr. Jay Amrit</u> , Prof. Kostiantyn Niemchenko, Dr. Varvara Luzik, Dr. Yehor Niemchenko, Dr. Akim Tonkonozhenko, Dr. Tetiana Vikhtynska | |
| Long-range radiative heat transfer along a Su-Schrieffer-Heeger chain coupled to a substrate | 60 |
| <u>Dr. Alireza Naeimi</u> , Dr. Florian Herz, Dr. Svend-Age Biehs | |
| Phonon-defect scattering in reciprocal space | 62 |
| <u>Mr. Alessandro Ciavatta</u> , Prof. Lorenzo Paulatto | |
| Thermal metrology for phase change materials | 63 |
| Mr. Tushar Chakrabarty, Dr. Akash Patil, Dr. Etienne Blandre, Dr. Pierre-Yves Cresson, Mrs. Yannick Le-Friec, Dr. Sarah Rubeck, Dr. Simon Jeannot, Prof. Emmanuel Dubois, Prof. Jean-François Robillard | |
| Investigating Thermal Transport in Freestanding SrTiO3 Membranes by Electro-Thermal Measurements | 65 |
| <u>Mr. Dominik M. Koch</u> , Dr. Jose Manuel Sojo Gordillo, Dr. Greta Segantini, Mr. Johannes Trautvetter, Dr. Aswathi K. Sivan, Dr. Riccardo Rurali, Prof. Andrea Caviglia, Prof. Ilaria Zardo | |
| Temperature-dependent anisotropic thermal conductivity of rutile GeO2 single crystals | 66 |
| <u>Mr. Pouria Emtenani</u> , Ms. Marta Loletti, Dr. Felix Nippert, Prof. Eduardo Bedê Barros, Dr. Zbigniew Galazka, Prof. Christian Thomsen, Dr. Sebastian Reparaz, Dr. Riccardo Rurali, Prof. Markus R. Wagner | |
| Heat Transfer at Interfaces: Mechanistic Insights from Molecular Dynamics Simulations | 68 |
| <u>Prof. Florian Müller-Plathe</u> | |
| From Amorphous to Amorphous-Crystalline Mixture Boron Nitride: Evolution of the Thermal Properties | 69 |
| <u>Dr. Marianna Sledzinska</u> , Mr. JiaQi Yang, Mr. Onurcan Kaya, Dr. Thomas Souvignet, Dr. Peng Xiao, Dr. Emigdio Chavez, Dr. Catherine Marichy, Prof. Catherine Journet-Gautier, Prof. Stephan Roche, Prof. Clivia Sotomayor-Torres | |
| Exact heat flux formula and its spectral decomposition in molecular dynamics for arbitrary many-body potentials | 71 |
| <u>Prof. Konstantinos Termentzidis</u> , Mr. Markos Poulos, Prof. Donatas Surblys | |

| | |
|---|----|
| Heat management via polymers and colloids | 72 |
| <u>Prof. Markus Retsch</u> | |
| Tailoring thermal transport in (Sc,Yb)AlN thin films to the glassy limit | 73 |
| <u>Prof. Qiye Zheng</u> | |
| Photothermal heterodyne imaging for 3D thermal microscopy | 74 |
| <u>Dr. Jeremie Maire, Prof. Stephane Chevalier, Dr. Jordan Letessier</u> | |
| Automated thermal characterization of multilayer nanostructures: from theory to applications in electrodeposited thermoelectric materials | 76 |
| <u>Mr. Miguel Ángel Tenaguillo, Ms. Elena Pérez Picazo, Dr. Olga Caballero Calero, Dr. Cristina Vicente Manzano, Prof. Marisol Martin-Gonzalez</u> | |
| Nanoscale thermal transport in van der Waals transition metal diselenide based nanolayers and nano-heterostructures | 77 |
| <u>Mr. Stuart Finch, Dr. Polychronis Tsipas, Ms. Stefania Skorda, Dr. Andrey Kretinin, Prof. Athanasios Dimoulas, Prof. Oleg Kolosov, Dr. Alexandros Elsachat</u> | |
| Moiré-Tuned Thermal Boundary Conductance in WS₂/MoS₂ Twisted Heterostructures | 79 |
| <u>Mr. Jiaqi Yang, Mr. Daniel Capolat Palomar, Mr. Onurcan Kaya, Dr. Timm Swoboda, Mr. Pu Tan, Dr. Aron Cummings, Prof. Javier Rodriguez-Viejo, Dr. Aitor Lopeandia, Prof. Stephan Roche, Dr. Maria Jose Esplandiu, Dr. Marianna Sledzinska</u> | |
| Nanoscale material design for heat transfer phenomena | 82 |
| <u>Prof. Saskia Fischer</u> | |
| Thermal emission of disks with radii close to the wavelength | 83 |
| <u>Ms. Kyriaki Kontou, Prof. Olivier Merchiers, Prof. Jean-Louis Leclercq, Prof. Taha Benyattou, Dr. Azeddine Tellal, Prof. Pierre-Olivier Chapuis</u> | |
| Direct observation of electroluminescence of hyperbolic phonon-polaritons and heat transfer in hBN-encapsulated graphene devices | 85 |
| <u>Dr. Yannick De Wilde, Dr. Loubnan Abou-Hamdan, Dr. Aurélien Schmitt, Dr. Patrick Bouchon, Prof. Jean-Jacques Greffet, Dr. Emmanuel Baudin</u> | |
| Development of Nanocomposites with Boron Nitride Nanomaterials for Thermal Transport and Related Applications | 87 |
| <u>Prof. Ya-Ping Sun</u> | |
| Investigating thermal conductivity anisotropy in Wurtzite semiconductors: AlN, GaN, ZnO, ZnS | 88 |
| <u>Mr. Sebastian Feulner, Dr. Kai Xu, Prof. Markus R. Wagner, Prof. Bartłomiej Graczykowski, Dr. Riccardo Rurali, Prof. Xavier Cartoixa, Dr. Vincent Linseis, Dr. Sebastian Reparaz</u> | |
| Scanning-probe based high-spatial-resolution thermoreflectance microscopy | 89 |
| <u>Dr. Mun Goung Jeong, Dr. Dong Uk Kim, Dr. Dongmok Kim, Mr. Chan Bae Jeong, Dr. Ki Soo Chang</u> | |
| Probing non-diffusive heat transport phenomena using spatiotemporally resolved pump-probe experiments in suspended graphite | 91 |
| <u>Mr. Bas van Dijck, Mr. Max van Hemert, Dr. Sebin Varghese, Prof. Samuel Huberman, Prof. Klaas-Jan Tielrooij</u> | |

| | |
|--|------------|
| Influencing parameters on SThM thermal conductivity measurements on nanostructured sample | 92 |
| <u>Dr. Sarah Douri</u> , Ms. Nolwenn Fleurence, Dr. Alexandra Délvallée, Dr. José Morán-Meza, Mr. Jacques Hameury, Dr. Nicolas Feltin, Mr. Bruno Hay | |
| Thermal diffusivity measurements using dual probe SThM | 94 |
| <u>Dr. Petr Klapetek</u> , Dr. Jan Martinek, Mr. Václav Hortvík, Dr. Miroslav Valtr | |
| Imaging heat transport in suspended diamond nanostructures with integrated spin defect thermometers | 95 |
| <u>Dr. Valentin Goblot</u> , Mr. Kexin Wu, Dr. Enrico Di Lucente, Ms. Yuchun Zhu, Mr. Claudio Jaramillo Concha, Prof. Nicola Marzari, Prof. Michele Simoncelli, Dr. Christophe Galland | |
| Thermodynamics of elementary mechanisms of quantum optics | 96 |
| <u>Dr. Alexia AUFFEVES</u> | |
| Noises in a two-channel charge Kondo model | 97 |
| <u>Dr. Jerome Rech</u> , Dr. Thanh Nguyen, Prof. Thierry Martin, Dr. Mikhail Kiselev | |
| Phase-Locked Exponential Growth: High-SNR Quantum Energy Storage at Dissipative Exceptional Points | 99 |
| <u>Dr. Borhan Ahmadi</u> | |
| Probing Coherent Phonon Contributions to Heat Conduction in Short-Period GaAs/AlAs 1D Phononic Crystals | 100 |
| <u>Prof. Markus R. Wagner</u> , Mr. Pouria Emtenani, Mr. Shazan Bhat, Dr. Jit Sarkar, Dr. Klaus Biermann, Dr. Felix Nippert, Ms. Marta Loletti, Dr. Kai Xu, Dr. Riccardo Rurali, Dr. Sebastian Reparaz | |
| Beyond Monte Carlo: Spectral and Mesoscopic Approaches to Real-Time and Space-Resolved BTE | 101 |
| <u>Dr. Aleksei Sokolov</u> , Prof. Samuel Huberman, Prof. Michele Simoncelli | |
| Precise Measurements from the Near Field to the Extreme Near Field under Ultra High Vacuum Conditions | 102 |
| Mr. Fridolin Geesmann, Mr. Philipp Thureau, Ms. Sophie Rodehutsors, Mr. Till Ziehm, Dr. Ludwig Worbes, Dr. S. Age Biehs, <u>Prof. Achim Kittel</u> | |
| Microscopic view of extreme near field heat transfer | 103 |
| <u>Dr. Samy Merabia</u> , Dr. Nadia Salami, Dr. Ali Rajabpour, Prof. Thomas Niehaus, Dr. Manuel Cobian, Dr. Fatemeh Tabatabaei | |
| Heat transfer across nanometre-sized water meniscus | 105 |
| <u>Mr. Oscar Mateos-Lopez</u> , Dr. Ruben Lopez-Nebreda, Mr. Pablo Martinez, Prof. Nicolas Agrait, Dr. Guilherme Vilhena, Prof. Juan Carlos Cuevas | |
| Polariton-activated Thermal Radiation of Guided Modes | 106 |
| <u>Dr. Sebastian VOLZ</u> | |
| Manipulation of phonon heat flow by nanostructuring of semiconductors: from room temperature to very low temperatures | 107 |
| <u>Dr. Olivier Bourgeois</u> | |
| Layer- and Field-Dependent Magnetic Order in 2D CrSBr Revealed by Pulsed Nanocalorimetry | 108 |
| <u>Dr. Aitor Lopeandia</u> , Mr. Hugo Gómez Torres, Dr. Roop K. Mech, Dr. Alessandra Canetta, Dr. Llibertad Abad, Dr. Pascal Gehring, Prof. Javier Rodriguez-Viejo | |

| | |
|---|------------|
| High electrical conductivity in PdCoO₂ epitaxial films: A pathway to next generation interconnects beyond copper | 109 |
| <i>Ms. Shivashree Shivamade Gowda, Mr. Bilal Azhar, Ms. Ramya Mohan, Dr. Saman Zare, Mr. Nazmun Sadat, Mr. Chung Ma, Prof. Ethan Scott, Prof. Ashutosh Giri, Prof. Joseph Poon, Prof. Hari Nair, Prof. Patrick Hopkins</i> | |
| Resolved thermal contact resistances in 1D and 2D nanomaterials using the 3-probe method | 110 |
| <i>Dr. Jose Manuel Sojo Gordillo, Mr. Alex Rodriguez-Iglesias, Mr. Dominik M. Koch, Dr. Marta Fernandez-Regulez, Dr. Marc Salleras, Prof. Ilaria Zardo</i> | |
| Optical characterization of anisotropic thermal conductivity in sub 50 nm thin single-wall carbon nanotube films | 112 |
| <i>Dr. Timm Swoboda, Dr. Martin Magg, Mr. Cristian Borja Peña, Mr. JiaQi Yang, Mr. Daniel Capolat Palomar, Mr. Pu Tan, Prof. Wim Wenseleers, Prof. Sofie Cambré, Dr. Benjamin Flavel, Prof. Javier Rodriguez Viejo, Dr. Marianna Sledzinska</i> | |
| Microfabricated Si-based planar μTEG platform for the integration and evaluation of novel thin-film thermoelectric materials | 114 |
| <i>Mr. Marc Aceituno Pimentel, Mr. Alex Rodriguez-Iglesias, Dr. Joaquin Santander, Mr. Shahadev Rodriguez-Miguel, Dr. Iñigo Martín-Fernández, Dr. Luis Fonseca, Dr. Llibertat Abad, Dr. Marc Salleras</i> | |
| Ultrafast phonon dynamics in free-standing and substrate-supported nanocrystalline silicon | 116 |
| <i>Dr. Tiago Magalhães, Dr. Housseem Rezgui, Dr. Gloria Conte, Dr. Tânia Ribeiro, Dr. Oili Ylivaara, Prof. Jouni Ahopelto, Prof. Clivia Sotomayor-Torres</i> | |
| Micro-Thermometry via Plasmon-Enhanced Metal Luminescence | 117 |
| <i>Ms. Athena Majlesi, Mr. Jan Kutschera, Dr. Marc Herzog, Prof. Matias Bargheer, Dr. Wouter Koopman</i> | |
| Inverted temperature gradients in Au-Pd and Au-Rh core-satellite systems | 118 |
| <i>Ms. Lisa Mehner, Ms. Maja Ruprecht, Mr. Ankit Dhankhar, Prof. Pramod Pillai, Ms. Shivani Kesarwani, Dr. Florian Schulz, Dr. Felix Stete, Prof. Matias Bargheer</i> | |
| Thickness- and temperature-dependent thermal conductivity of ScN using Time-Domain Thermoreflectance | 120 |
| <i>Mr. Moritz Metschl, Mr. Pouria Emtenani, Mr. Jamal Abou Haibeh, Dr. Felix Nippert, Dr. Duc Vinh Dinh, Mr. Abhilash Sanjay Ulhe, Prof. Gregor Koblmüller, Prof. Samuel Huberman, Prof. Christian Thomsen, Prof. Markus Raphael Wagner</i> | |
| Effect of π-conjugation in nanoscale heat transport | 122 |
| <i>Mr. Nelson Elías Rivas Chacón, Mr. Pablo Martinez, Prof. Juan Carlos Cuevas, Dr. Guilherme Vilhena</i> | |
| Ultrafast heat transport in metallic heterostructures tracked via strain responses measured by femtosecond X-ray diffraction | 123 |
| <i>Dr. Jan-Etienne Pudell, Dr. Maximilian Mattern, Dr. Marc Herzog, Dr. Alexander von Reppert, Dr. Jasmin Jarecki, Dr. Jörg Hallmann, Prof. Matias Bargheer, Prof. Anders Madsen</i> | |
| Why hybrid perovskites possess an ultralow thermal conductivity? | 124 |
| <i>Ms. Qinqin He, Prof. Yanguang Zhou</i> | |
| Optimizing Energy Conversion in Feedback-Controlled Nano Processes: Harnessing Time-Dependent Information | 125 |
| <i>Mr. Rasmus Hagman, Dr. Jonas Berx, Prof. Janine Splettstoesser, <u>Dr. Henning Kirchberg</u></i> | |

| | |
|--|------------|
| Phonon-mediated heat conduction in GaN/AlN superlattices grown on silicon | 126 |
| <u>Mr. Guillaume Würsch</u> , Mr. Pouria Emtenani, Dr. Sebastian Tamariz, Dr. Tim Grieb, Mr. Mahmoud Elhajhasan, Ms. Katharina Dudde, Ms. Jana Lierath, Prof. Nicolas Grandjean, Prof. Markus R. Wagner, Prof. Gordon Callsen | |
| Accurate Thermal Conductivity Measurement for Nano/Microscale Thermal Management: Advanced Models and Regression Methods for the Transient Plane Source Technique | 127 |
| <u>Mr. Jiaqi GU</u> , Prof. Qiye Zheng | |
| Thermophotonic coupling as a function of distance between the LED and the photovoltaic cell | 129 |
| Ms. Wissal Sghaier, Mr. Luc M. van der Krabben, Dr. Natasha Gruginskie, Dr. John J. Schermer, Dr. Somendu Maurya, Dr. Jonna Tiira, Dr. Tuomas Vaimala, Dr. Kirsi Tappura, Prof. Mika Prunnila, Dr. Benoit Behaghel, Dr. Ivan Radevici, Dr. Ahmad Shahahmahdi, Dr. Jani Oksanen, <u>Dr. P-Olivier Chapuis</u> | |
| Direct Measurement of the Heat Capacity of Monolayer MoSe₂ by Ultrafast Nanocalorimetry | 131 |
| <u>Mr. Hugo Gómez Torres</u> , Dr. Sebin Varghese, Prof. Klaas-Jan Tielrooij, Dr. Aitor Lopeandia, Prof. Javier Rodriguez-Viejo | |
| Controlling phonon transport in low-dimensional structures using phonon tunneling | 132 |
| <u>Prof. Ilari Maasilta</u> , Dr. Zhuoran Geng | |
| Thermal Transport Evolution in WS₂ Polymorphs: From 2H to the Low-Symmetry 2M Phase | 133 |
| <u>Dr. Qi Ren</u> , Ms. Marta Loletti, Dr. Riccardo Rurali | |
| Studying Phonon vs. Electron Contributions to Heat Transport of Single-Flake Metallic Ti₃C₂T_x MXene using Spatiotemporal Microscopy | 135 |
| <u>Mr. Max van Hemert</u> , Dr. Hugh Ramsden, Dr. Sebin Varghese, Dr. Bohai Lui, Ms. Elvira Tornero, Dr. Stefano Ippolito, Dr. Miguel Muñoz, Prof. Yury Gogotsi, Dr. Hai Wang, Prof. Klaas-Jan Tielrooij | |
| Investigating the effect of temperature and relative humidity on thermal transport in Covalent organic frameworks (COFs) | 136 |
| <u>Ms. Sudeshna Sahoo</u> , Mr. Yannick Eich, Prof. Seema Agarwal, Prof. Juergen Senker, Prof. Markus Retsch | |
| Thermal anisotropy in layered oxide Bragg stacks | 137 |
| <u>Mr. Simon Freund</u> , Mr. Ingmar Pietsch, Prof. Josef Brey, Prof. Markus Retsch | |
| Localizing heat at the nanoscale via dissipation – Testing 3-temperature models by ultrafast x-ray diffraction and transient absorption | 138 |
| <u>Prof. Matias Bargheer</u> | |
| Couplings between heat carriers (electrons, phonons and magnons) in complex systems | 139 |
| <u>Prof. Yanguang Zhou</u> | |
| Engineering Transport and Thermoelectric Properties of Cs₂NaYbCl₆ Perovskite via Doping and Nano-engineering | 141 |
| <u>Dr. Antonio Cappai</u> , Prof. Claudio Melis, Prof. Luciano Colombo | |
| Fast Ionic Transport Governed by Collective Vibrational Dynamics | 142 |
| <u>Dr. Yixin Xu</u> , Prof. Yanguang Zhou | |
| Anomalous thermal transport in 2D layered metal organic frameworks | 144 |
| <u>Dr. Riccardo Dettori</u> , Prof. David Beljonne, Prof. Luciano Colombo, Prof. Claudio Melis | |

| | |
|--|------------|
| Using heterodyned, deep-ultraviolet transient gratings to measure non-diffusive heat transport in crystalline silicon membranes | 145 |
| <u>Ms. Emma Nelson</u> , Mr. Yunhao Li, Mr. Theodore Culman, Ms. Jiayi Liu, Dr. Albert Beardo, Dr. Brendan McBen- | |
| nett, Prof. Joshua Knobloch, Prof. Henry Kapteyn, Prof. Margaret Murnane | |
| Thermoelectric characterization of 2D materials on a micro-chip platform | 146 |
| <u>Dr. Nathan Aubergier</u> , Dr. Peng Xiao, Dr. Eva Desgue, Dr. Pierre Legagneux, Mr. Nicolas Claus, Dr. Daniel | |
| Bourgault, Dr. Paolo Bondavalli, Dr. Aymen Mahjoub, Dr. Olivier Bourgeois | |
| Non-local heating in semiconductor membranes | 147 |
| Mr. Mahmoud Elhajhasan, Ms. Katharina Dudde, Ms. Elena Trukhan, Mr. Guillaume Würsch, Mr. Julian | |
| Themann, Ms. Jana Lierath, Dr. Nakib Protik, Dr. Giuseppe Romano, <u>Prof. Gordon Callsen</u> | |
| Out-of-plane thermal conductivity of Ti3C2Tx MXene flakes depending on temperature and thickness | 149 |
| <u>Ms. Elvira Tornero</u> , Dr. Bohai Lui, Dr. Stefano Ippolito, Mr. Max van Hemert, Dr. Hugh Ramsden, Dr. David | |
| Saleta, Dr. Aaron Schmidt, Dr. Katja Klinar, Prof. Yury Gogotsi, Prof. Klaas-Jan Tielrooij, Dr. Miguel Muñoz | |
| Experimental Study of Atomic and Single-Molecule Scale Heat Transport: From molecular phononics to near-field hot-carrier thermal radiation | 150 |
| <u>Dr. Longji Cui</u> | |
| Room-temperature phonon interference in single-molecule junctions | 151 |
| Mr. Sai C. Yelishala, Dr. Yunxuan Zhu, <u>Mr. Pablo Martinez</u> , Dr. Hongxuan Chen, Mr. Mohammad Habibi, Dr. | |
| Giacomo Prampolini, Prof. Juan Carlos Cuevas, Prof. Wei Zhang, Dr. Guilherme Vilhena, Dr. Longji Cui | |
| Cryogenic STM Break Junction Measurements of Heat Transport in Atomic Contacts | 153 |
| <u>Ms. Valentina Grieci</u> , Dr. Bernd Gotsmann | |
| Reverse design of SmxNd1-xNiO3 thin films for radiative transfer applications | 155 |
| <u>Mr. Pierre-Antoine Tostivint</u> , Dr. Jérémie Drévillon, Dr. Simon Hurand, Dr. Arthur Tausch, Dr. Fabien Capon | |
| Ballistic phonon dissipation in 2D, thermal conductivity suppression function and the ‘collective diffusion’ regime | 156 |
| Dr. Juan Carlos ACOSTA ABANTO, Dr. Raja Sen, Dr. Jelena Sjakste, Dr. Nathalie Vast, Dr. Ali Alkurdi, Dr. Carolina | |
| Abs Da Cruz, Dr. Elyes Nefzaoui, Dr. Severine Gomes, <u>Dr. P-Olivier Chapuis</u> | |
| A Novel High-Throughput Approach to Studying the Quasi-Ballistic Thermal Transport Regime | 158 |
| <u>Dr. Sebastian Reparaz</u> , Dr. Kai Xu, Dr. Clemens Petersen, Dr. Filippo Bencivenga, Dr. Laura Foglia, Dr. Riccardo | |
| Mincigrucci, Prof. Markus R. Wagner, Dr. Holger von Wenckstern, Dr. Riccardo Rurali | |

Thermal Photonics in Non-Reciprocal Many-Body Systems

Monday, 20th April - 09:00: Invited - Invited talk

Dr. Philippe Ben Abdallah¹

1. Laboratoire Charles Fabry, CNRS, Institut d'Optique

In this lecture, I investigate the radiative properties of many-body systems [1] composed of magneto-optical materials. In the first part, I highlight a variety of out-of-equilibrium phenomena that emerge under the action of temperature gradients and spatially varying external magnetic fields. I show how these systems provide a powerful platform for exploring thermal analogs of condensed-matter phenomena, including the thermal Hall effect [2,3] and the inverse spin Hall effect [4]. These effects open exciting perspectives for spin caloritronics, driven by the interplay between the spin angular momentum of light and radiative heat transport.

In the second part of the presentation, I demonstrate that the orientation of an external magnetic field acts as a genuine control parameter capable of driving geometric phase transitions of electromagnetic modes in magneto-optical systems. In particular, I show that tiny changes in the magnetic-field orientation can induce giant modulations of the local density of electromagnetic states and lead to non-analytic behavior of the electromagnetic free energy [5]. These phenomena are formally analogous to Landau-type phase transitions [6] and reveal a new route for controlling thermal radiation through geometric and topological effects.

References

- [1] S.-A. Biehs, R. Messina, P. S. Venkataram, A. W. Rodriguez, J. C. Cuevas, and P. Ben-Abdallah, *Rev. Mod. Phys.*, **93**, 025009 (2021).
- [2] P. Ben-Abdallah, *Phys. Rev. Lett.*, **116**, 084301 (2016).
- [3] A. Ott, P. Ben-Abdallah, and S.-A. Biehs, *Phys. Rev. B*, **97**, 205414 (2018).
- [4] P. Ben-Abdallah, *Phys. Rev. Lett.*, **134**, 113804 (2025).
- [5] P. Ben-Abdallah, *Phys. Rev. B*, **109**, 245409 (2024).
- [6] I. Latella and P. Ben-Abdallah, In progress

Simultaneous heat and electronic dynamics in photoexcited semiconductors investigated by time-resolved diffraction anomalous fine structure (TR-DAFS)

Monday, 20th April - 09:50: Ultrafast Transport - Oral

***Dr. Thomas C. Rossi*¹, *Mr. Moritz Meißner*², *Dr. Matthias Rössle*¹, *Prof. John J. Rehr*³, *Prof. Joshua Kas*³, *Prof. Renske M. van der Veen*¹**

1. HZB, 2. Paul-Drude-Institut für Festkörperelektronik, 3. University of Washington

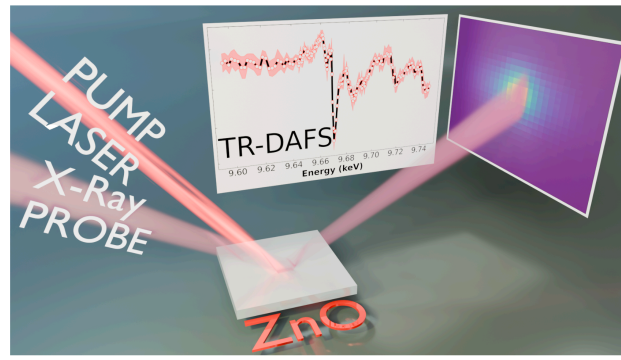
Photoexcitation of materials inevitably leads to lattice heating, while transient electronic states coexist and interact with the evolving lattice. Disentangling these coupled structural and electronic responses calls for experimental techniques that are simultaneously sensitive to atomic-scale lattice dynamics and electronic effects. Here, we present the first demonstration of time-resolved diffraction anomalous fine structure (TR-DAFS) measurements implemented using a stroboscopic pump-probe scheme. The experiment is performed at the Zn K-edge of photoexcited epitaxial ZnO thin films. We show that the non-resonant and resonant parts of the excited-state DAFS spectra provide complementary insights: from lattice heating at different length scales, to photoinduced electronic effects.

In the non-resonant part of the DAFS spectrum, the observed changes are dominated by an increase of the crystallographic Debye-Waller factor and an expansion of the lattice parameter. Notably, the lattice expansion exceeds the value expected from purely thermal effects, indicating an additional contribution arising from the screening of the piezoelectric potential by photoexcited carriers. In the resonant part of the DAFS spectrum, changes are attributed to the Coulomb screening of the core-hole potential, providing sensitivity to the density and distribution of photoexcited carriers (1, 2).

Both the structural and electronic responses are reproduced by *ab initio* calculations within the full multiple scattering theory framework. By combining crystallographic and spectroscopic sensitivity within a single experiment, TR-DAFS enables a unified view of the coupled lattice and electronic dynamics following optical excitation of semiconductors. These results establish TR-DAFS as a powerful new tool for time-resolved studies of photoexcited materials and lay the foundations for its application at next-generation synchrotrons and X-ray free-electron lasers.

References

1. T. C. Rossi, C. P. Dykstra, T. N. Haddock, R. Wallick, J. H. Burke, C. M. Gentle, G. Doumy, A. M. March, R. M. van der Veen, Charge Carrier Screening in Photoexcited Epitaxial Semiconductor Nanorods Revealed by Transient X-ray Absorption Linear Dichroism *Nano Letters* **21**, 9534–9542 (2021).
2. T. C. Rossi, L. Qiao, C. P. Dykstra, R. Rodrigues Pela, R. Gnewkow, R. F. Wallick, J. H. Burke, E. Nicholas, A. M. March, G. Doumy, D. B. Buchholz, C. Deparis, J. Zúñiga-Pérez, M. Weise, K. Ellmer, M. Fondell, C. Draxl, R. M. van der Veen, Dynamic control of X-ray core-exciton resonances by Coulomb screening in photoexcited semiconductors *Communications Materials* **6**, 191 (2025).



Pump-probe DAFS measurement on photoexcited ZnO epitaxial layers.

Figure pump probe dafs.png

Predictive Modeling of Non-Diffusive Heat Transport in 2D and 3D Materials under Transient Grating Excitations

Monday, 20th April - 10:10: Ultrafast Transport - Oral

***Ms. Almudena Diaz Serrano*¹, *Mr. Jamie Harford*², *Dr. Albert Beardo*¹, *Mr. Jordi Tur Prats*¹, *Prof. Joshua Knobloch*², *Prof. Javier Bafaluy*¹, *Prof. F. Xavier Alvarez*¹, *Prof. Juan Camacho*¹**

1. Universitat Autònoma de Barcelona, Campus UAB, ES-08193 Bellaterra, Spain, 2. Utah State University

Transient grating (TG) experiments have emerged as a powerful, non-destructive, and contactless technique for investigating ultrafast heat and charge carrier dynamics at ultrasmall length scales in semiconductors [1]. The TG configuration has been employed to quantify a size-dependent decrease in thermal conductivity at elevated temperatures and to identify second-sound propagation in graphite at lower temperatures [2]. While these effects can be predicted using microscopic solvers of the phonon dynamics based on the full Boltzmann transport equation (BTE), theoretical modelling of the TG experiment, providing physical intuition beyond the Fourier diffusion framework and the fundamental mechanisms for their emergence, remains an open area of study. In particular, the interplay of these effects at different temperatures and length and time scales is still not understood.

In this work, we address this fundamental question within the framework of the Guyer-Krumhansl equation, as derived from the BTE [3]. We model and compare the non-diffusive transient relaxation in both cases, layered 2D structures, such as graphite, and bulk 3D materials, such as silicon. This approach allows us to characterize the transition from diffusive to hydrodynamic regimes as a function of temperature and length scales, including the emergence of weak hydrodynamic signatures in intermediate regimes. To correctly capture ultrafast phenomena present in TG experiments and discriminate non-equilibrium phonon effects from other nanoscale phenomena, we incorporate an electron-phonon coupling model, accounting for hot-electron physics immediately after excitation. At later times, we analyse the competition between in-plane and cross-plane dissipation mechanisms.

Overall, our work provides a unified theoretical description of TG experiments across low-dimensional and bulk materials, explaining the different forms of non-diffusive transport observed at varying temperatures and grating periods. The model captures key experimental signatures such as the reduction of effective thermal conductivity with decreasing TG period and second sound propagation, offering a complete framework for interpreting TG ultrafast heat transport beyond the diffusive limit.

[1] Emma E. Nelson et. al. Tabletop deep-ultraviolet transient grating for ultrafast nanoscale carrier-transport measurements in ultrawide-band-gap materials. *Phys. Rev. Appl.* 22, 54007 (2024).

[2] S. Huberman, et. al. Observation of second sound in graphite at temperatures above 100 K. *Science* 364, 375–79 (2019).

[3] Lluc Sendra et. al Derivation of a hydrodynamic heat equation from the phonon Boltzmann equation for general semiconductors. *Phys. Rev. B* 103, L140301 (2021).

Thermal and electrical effects in polarized Ti/Si interface using cross-section scanning thermal and Kelvin probe force microscopies

Monday, 20th April - 10:30: Ultrafast Transport - Oral

***Dr. Juan Carlos Acosta Abanto*¹, *Dr. Nicolas BERCU*², *Dr. Mélanie Brouillard*³, *Prof. Jean-François Robillard*³, *Prof. Nicolas Horny*⁴, *Prof. Louis Giraudet*², *Prof. Pierre-Olivier Chapuis*¹, *Dr. Severine Gomes*¹**

1. CETHIL, CNRS-INSA Lyon, France, 2. L2N, Univ. Reims Champagne-Ardenne, Reims, France, 3. IEMN (Institut d'électronique de microélectronique et de nanotechnologie), 4. ITHEMM, Université de Reims Champagne-Ardenne

Management of heat dissipation and generation or cooling through coupled charge/heat transport phenomena is critical in modern micro- and nano-electronic devices. In this work, we present an experimental investigation of thermal and electrical transports as well as thermoelectric effect in an electrically-biased Ti/Si structure, using Scanning Thermal Microscopy (SThM) and Kelvin Probe Force Microscopy (KPFM) (see Fig. 1 for the experimental setups). The sample consists of a 200 nm Ti layer deposited on a 400 μm thick N-doped Si substrate (few 10^{14} cm^{-3} doping concentration), representative of metal/semiconductor (M/S) systems widely used in microelectronic technologies. Measurements were performed on the cross section of the structure, enabling correlated mapping of local temperature and surface potential with nanometric spatial resolution [1-2]. This original cross-sectional approach provides direct access to out-of-plane transport phenomena and interface effects under operating conditions, allowing the investigation of non-equilibrium heat and charge transfer at the M/S interface. Electrical characteristics, such as the depletion region width, and features consistent with thermoelectric phenomena, such as an increase of temperature due to the Seebeck effect, are determined (see Fig. 2 for the temperature profile across the junction) and discussed in relation to material properties and interface. These results demonstrate the potential of combined SThM-KPFM measurements for investigating and optimizing thermal and energy-related phenomena in micro- and nano-electronic devices. They also provide new insights into nanoscale thermal and thermoelectric phenomena in M/S heterostructures.

[1] S. Gomès, A. Assy, and P.-O. Chapuis, Scanning thermal microscopy: A review, *Physica status solidi (a)* 212, 477-494 (2015)

[2] Y. Rosenwaks, et al., Kelvin probe force microscopy of semiconductor surface defects, *Physical Review B* 70, 085320 (2004)

Authors acknowledge funding from ANR project EFICACE.

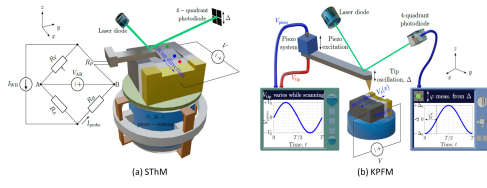


Fig. 1. Schematic of the experiments.

Fig1.jpg

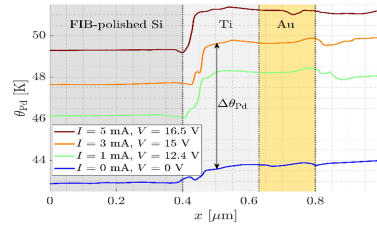


Fig. 2. SThM probe temperature rise profiles measured while scanning the Ti/N-doped Si cross-section under applied bias voltage V . In this configuration, sample polarization induces electrons to flow from silicon to Ti. The increased thermal contrast between Ti and Si under forward bias suggests heating of the Ti layer by incoming charge carriers.

Fig2.jpg

Revisiting Phonon Hydrodynamics in Graphene: Effects of High-Order Anharmonicity

Monday, 20th April - 10:50: Ultrafast Transport - Oral

Mr. Jordi Tur Prats¹, **Dr. Zherui Han**², **Dr. Albert Beardo**¹, **Prof. Xiulin Ruan**³, **Prof. F. Xavier Alvarez**¹

1. *Universitat Autònoma de Barcelona, Campus UAB, ES-08193 Bellaterra, Spain*, **2.** *chool of Mechanical Engineering and the Birck Nanotechnology Center, Purdue University, West Lafayette, Indiana 47907-2088*, **3.** *School of Mechanical Engineering and the Birck Nanotechnology Center, Purdue University, West Lafayette, Indiana 47907-2088*

Recent *ab initio* calculations of graphene that explicitly include four-phonon scattering processes [1] compel a fundamental revision of the conventional picture of phonon hydrodynamics. In contrast to the traditional view—where dominant momentum-conserving (normal) three-phonon collisions lead to a fully collective phonon fluid—we show that the inclusion of four-phonon processes qualitatively alters the nature of hydrodynamic transport. Rather than reinforcing collective behavior, higher-order anharmonicity introduces efficient momentum-dissipating channels that drive the system away from the pure collective limit and fundamentally reshape the non-equilibrium phonon distribution.

Using the Kinetic Collective Model (KCM), we analyze the converged solution of the phonon Boltzmann transport equation in graphene including four-phonon scattering. We demonstrate that the *ab initio* phonon distribution cannot be described by a purely collective form: in particular, the slope of the distribution near the Brillouin-zone center deviates from that expected in a momentum-dominated hydrodynamic regime. This reveals an unexpected result: hydrodynamic signatures in graphene can only be properly understood by accounting for the simultaneous action of kinetic and collective processes. By interpolating between kinetic and collective limits, the KCM accurately reconstructs both the phonon distribution function and thermal transport properties, offering significantly higher predictive capability than models based on purely collective assumptions. This enhanced predictability arises from the ability of the KCM to capture the non-intuitive role of resistive four-phonon scattering in shaping hydrodynamic transport.

As a consequence, the distinction between graphene and conventional semiconductors such as silicon or germanium becomes significantly less sharp once higher-order anharmonicity is properly accounted for.

Finally, we explore the implications of this revised hydrodynamic picture for nanoscale thermal evolution. Using *ab initio* inputs, we compute key hydrodynamic parameters, including the non-local length scale and the heat-flux relaxation time, and demonstrate that non-diffusive phenomena such as second-sound propagation can persist even in regimes far from the pure collective limit. These results lead to an unexpected conclusion: phonon hydrodynamics in graphene does not require the full dominance of normal processes, prompting a critical reassessment of the criteria traditionally used to identify hydrodynamic heat transport [2].

[1] Z. Han, X. Ruan. *Thermal conductivity of monolayer graphene: Convergent and lower than diamond*, Phys. Rev. B 2023, 108, L121412.

[2] J. Tur-Prats et al. *High-Order Anharmonicities Shape Phonon Hydrodynamic Effects in Graphene*. Nano Lett. 2025, 25, 11203-11209.

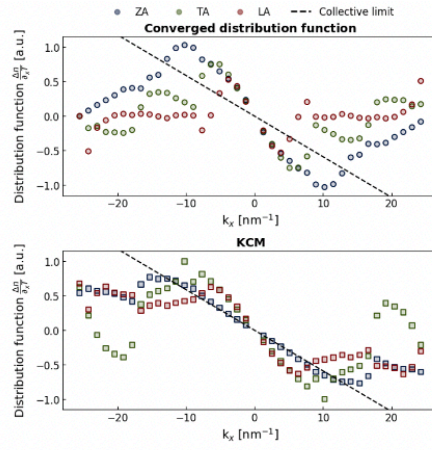


Figure 1: (top) Converged distribution function achieved by the iterative method when including four-phonon scattering processes at 300K [1]. **(bottom)** Distribution function reconstructed with RTA inputs according to the Kinetic Collective Model (KCM) at 300K.

Convergeddistribution vs kcmdistribution.png

Higher-Order Perturbation Equation (HOPE) framework for thermal transport in semiconductors.

Monday, 20th April - 11:30: Beyond Local Equilibrium - Featured talk

***Prof. F. Xavier Alvarez*¹, *Dr. Albert Beardo*¹, *Mr. Jordi Tur Prats*¹, *Ms. Almudena Diaz Serrano*²**

1. Universitat Autònoma de Barcelona, Campus UAB, ES-08193 Bellaterra, Spain, 2. Departament de Física, Universitat Autònoma de Barcelona, 08193 Bellaterra

We introduce the Higher-Order Perturbation Equation (HOPE) framework, a predictive multiscale theory for phonon heat transport in semiconductors. HOPE provides quantitative predictions of thermal conductivity in silicon across all length scales and temperatures, from the bulk limit to deeply nanoscale structures, with accuracy that rivals or surpasses state-of-the-art models.

Starting from the Boltzmann transport equation, we expand the phonon distribution in a flux-based moment hierarchy within the relaxation-time approximation. This produces a coupled two-level description: a differential equation for the macroscopic heat flux, solved with finite-element methods, and a Monte Carlo transport equation for higher-order moments that is solved using a variance-reduced particle scheme.

In the second part, we will present a new form of the boundary conditions that treats the relaxation of heat flux and higher-order fluxes separately. Rather than switching between different phenomenological models for different materials, this physically grounded formulation provides a single unified boundary description that naturally bridges hydrodynamic, quasiballistic, and diffusive regimes.

Together, HOPE and the new boundary conditions establish a unified framework for non-Fourier heat transport, explaining phenomena ranging from thermal conductivity reduction in nanostructured silicon to Poiseuille flow and second sound in graphite or germanium. Effects that were previously viewed as unrelated are revealed to be different manifestations of the same underlying phonon physics, bringing new coherence to nanoscale thermal transport.

Energy conversion at the nanoscale: exploiting non-thermal resources

Monday, 20th April - 12:00: Beyond Local Equilibrium - Oral

Ms. Elsa Danielsson¹, Dr. Henning Kirchberg¹, Prof. Janine Splettstoesser¹

1. Chalmers University of Technology

Nanoscale engines – such as on-chip thermoelectric devices – are increasingly used to transduce energy and particles between reservoirs for *useful* tasks like cooling. Unlike macroscopic engines, these systems often operate under conditions where environmental reservoirs are constantly out-of-equilibrium and cannot be described by well-defined thermal distributions. Consequently, temperature and chemical potential lose their meaning, and fluctuations in energy and particle flows become significant.

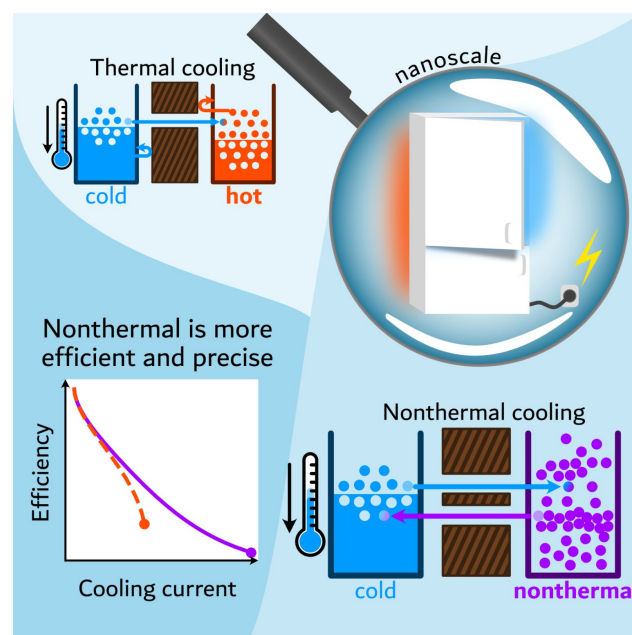
Rather than treating this non-thermal nature as a limitation, we exploit it as a *resource* to design devices that can even outperform traditional engines in performance. We investigate a prototype quantum thermoelectric device operating between a non-thermal and thermal reservoir, analyzing energy and particle flows in the coherent transport regime via scattering theory [1].

Our approach seeks to optimize the device's performance based on the efficiency, precision, or a trade-off between the two at a given output cooling current while the usual heat-work distinction breaks down. We introduce entropy currents as resources and exploit a Lagrange multiplier method to optimize the particle transmission characteristics to achieve the optimal performance. We find that the resulting optimal transmission filters are directly shaped by the non-thermal distribution.

Our work provides a framework for characterizing and leveraging non-thermal resources, opening pathways for unconventional energy conversion strategies in quantum thermodynamics and nanoscale physics.

Reference:

[1] E. Danielsson, H. Kirchberg, J. Splettstoesser, *Phys. Rev. B* **112**, 195434 (2025)



Nonthermal.jpeg

Monte Carlo Modeling of Phonon Drag Effects on Thermoelectric Transport in Silicon Nanostructures

Monday, 20th April - 12:20: Beyond Local Equilibrium - Oral

***Dr. Mohammad Ghanem*¹, *Dr. Philippe Dollfus*¹, *Dr. Jelena Sjakste*², *Dr. Raja Sen*², *Prof. Jérôme Saint Martin*³**

1. C2N, Paris Saclay University, 2. LSI, CNRS, Ecole Polytechnique, Palaiseau, France, 3. SATIE, ENS Paris Saclay

Thermoelectric transport have been investigated in silicon nanostructures using a self-consistent electro-thermal Monte Carlo (MC) framework that explicitly couples electron dynamics to a non-equilibrium phonon bath with a spatially nonuniform temperature profile. In this study is the direct inclusion of phonon-drag effects at the level of individual electron–phonon scattering events, is achieved by modifying the momentum exchange according to the local deviation of the phonon distribution from equilibrium. Unlike prior approaches based on linearized Boltzmann transport equations and semi-analytical formulations, our method computes thermoelectric properties from current–voltage characteristics without analytical approximations. In addition to steady-state operation, our model is also able to examine the transient response of the thermoelectric device. The model is validated against experimental data for bulk silicon and nanofilms.thermoelectric regime.

I. MODEL

The particle Monte Carlo code, coupled with Poisson’s equation, is based on analytical conduction band [1,2]. The model is coupled with a non-uniform temperature phonon bath, allowing us to include phonon drag effect at the particle scattering level to simulate realistic nanofilms.

II. SIMULATED DEVICE and RESULTS.

Figure 1 shows a silicon nanofilm of length L and with doping concentration N in a cross-plane configuration. The nanofilm is sandwiched between two 10 nm Ohmic contacts with n-doping of 10^{19}cm^{-3} , and a thermal gradient and a voltage difference are applied between contacts.

Figure 2 shows the diffusive Seebeck coefficient as a function of doping concentration for different temperatures.

Figure 2(b) presents the coefficient for different device lengths, revealing that thermopower grows with device length, particularly at low doping where electron–impurity scattering is weak and longer devices enhance energy asymmetry in carrier transport.

Figure 3 shows the total and phonon-drag Seebeck coefficients versus doping concentration at 300 K. The phonon-drag contribution decreases with doping due to enhanced scattering, which shortens the phonon mean free path and limits momentum exchange with electrons. The Seebeck coefficient shows good agreement with experimental and theoretical data [3], [4], thereby validating our model.

[1] T. T. T. Nghiem, et. al, JAP, Vol 116, 2014.

[2] P. Dollfus, JAP, Vol 82, 1997.

[3] J. Zhou et al. APS, Vol 112, 2015.

[4] T. H. Geballe et al. , PR, Vol 98, 1955.

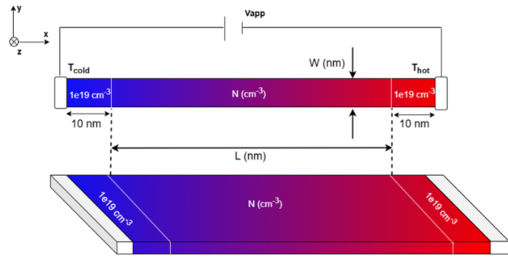


Image1.png

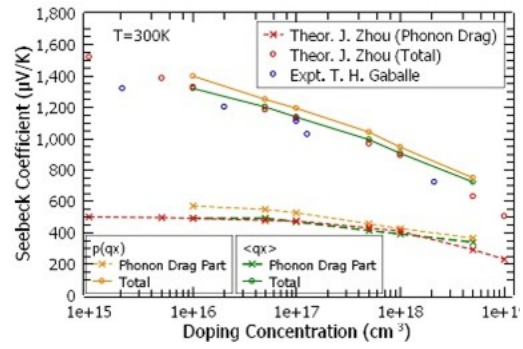


Image3.jpg

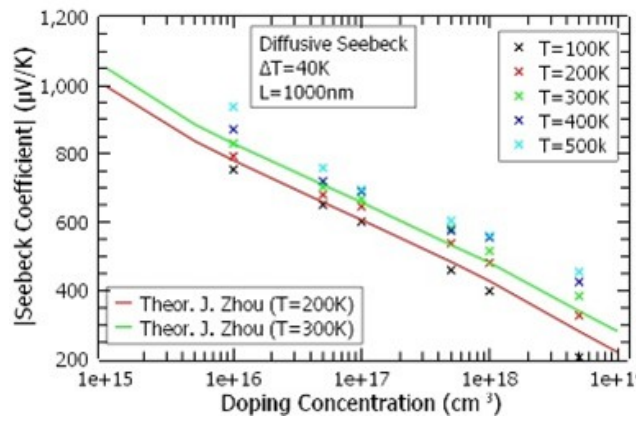


Image2.jpg

A toolbox of pump-probe techniques to investigate phonons and thermal transport

Monday, 20th April - 14:00: Invited - Invited talk

*Dr. Begoña Abad Mayor*¹, *Dr. Grazia Raciti*¹, *Mrs. Deeksha Sharma*¹, *Dr. Aswathi K. Sivan*¹, *Dr. Jose Manuel Sojo Gordillo*¹, *Dr. Ahmad Zenji*¹, *Prof. Ilaria Zardo*¹

1. University of Basel

Controlling nanoscale heat transfer is crucial to design next-generation electronic devices as heat management becomes a bottleneck to increase their efficiency. However, the governing mechanisms for heat transfer at these length scales are completely different from bulk-counterparts and are not well understood [1]. Therefore, as electronic devices continue to shrink in size, the demand for precise and efficient characterization tools becomes increasingly crucial to overcome or complement the limitations of conventional measurement approaches.

We have built a powerful toolbox of noncontact pump-probe techniques, that combines frequency-domain thermoreflectance, transient thermal grating, time-resolved Raman spectroscopy and transient reflectivity [2]. They are based on a pump laser that heats up the material's surface, while a subsequent probe beam monitors its change in reflectivity, diffraction efficiency or Raman spectrum, depending on the technique, as a function of time or frequency. We will, therefore, introduce the principles and applications of these techniques, which offer unique insights into the thermal property and dynamic behavior of phonon processes, such as direct observations of phonon lifetime given by anharmonic effects.

We applied these techniques to various material systems, from classic semiconductors, to graphene and perovskites, showing diverse mechanisms responsible for the energy flow after laser excitation, critical to understand heat dissipation in miniaturized devices [3]. These results shed light on the intricate interplay between lattice dynamics and thermal transport phenomena, and prove that the combination of these techniques is an effective approach to investigate materials for efficient next-generation electronic devices.

[1] G. Chen, *Nature Reviews Physics*, 3, 555-569 (2021)

[2] B. Abad et al., *Renewable and Sustainable Energy Reviews*, 76, 1348-1370 (2017)

[3] G. Raciti, B. Abad, et al. *Advanced Science*, in press (2025). DOI: 10.1002/advs.202515470

Quantum and thermal light emission from time-modulated mid-infrared nanophotonic systems

Monday, 20th April - 14:50: Near-Field Heat Radiation - Oral

Mrs. Amaia Vertiz¹, Dr. Francisco Javier Alfaro Mozaz¹, Dr. Iñigo Liberal¹

1. Universidad Pública de Navarra

Recent efforts of the nanophotonic community have been focused on the ultra-fast modulation of macroscopic material parameters. Harnessing time as an additional degree of freedom empowers new forms of wave control and manipulation, including simultaneous beamforming, frequency shift, amplification and pulse-shaping. Beyond classical fields, nonadiabatic time-modulations facilitate new forms of quantum light emission. Our team has pioneered angle dependent squeezing and squeezing combs from anisotropic temporal boundaries [1], as well as broadband and ultrafast quantum state frequency shifting, and thermal noise management based on quantum antireflection temporal coatings [2].

Temporal modulation also fundamentally changes the physics of thermal emission, granting access to super-Planckian, nonreciprocal and nonequilibrium thermal emission. Our team has pioneered the first-principle approach to model thermal emission from time-modulated systems [3], and has highlighted the important role of dispersion [4], and the need to use a quantum theory of light [5].

Finally, the ultra-fast modulation of material parameters can be engineered to produce synthetic motion, i.e., spatiotemporal modulations that mimic mechanical motion. Because no mass is being moved, synthetic motion facilitates high-speed motion, and grant access to luminal and superluminal regimes that cannot be realized with mechanical motion. Recently, we have proposed the concept of synthetically rotating crystals, showing that simple pump-probe configurations can mimic the rotation of an anisotropic crystal [6]. At high rotational frequency, the interaction with light results in spin-modulated ultra-fast pulses, and frequency-polarization locked sidebands.

[1] J.E. Vázquez-Lozano and I. Liberal, “Shaping the quantum vacuum with anisotropic temporal boundaries”, *Nanophotonics*, **12**(3), 539-548 (2023).

[2] I. Liberal, J.E. Vázquez-Lozano and V. Pacheco-Peña, “Quantum antireflection temporal coatings: quantum state frequency shifting and inhibited thermal noise amplification”, *Laser & Photonics Reviews*, **17**(9), 2200720 (2023).

[3] J.E. Vázquez-Lozano and I. Liberal, “Incandescent temporal metamaterials”, *Nature Communications*, **14**(1), 4606, (2023).

[4] A. Vertiz-Conde, I. Liberal and J.E. Enrique Vázquez-Lozano, “Dispersion effects in thermal emission from temporal metamaterials: high-frequency cutoffs”, *Optics Letters*, **50**(4), 1097-1100 (2025).

[5] I. Liberal, J.E. Vázquez-Lozano and A. Ganfornina-Andrades, “Can thermal emission from time-varying media be described semiclassically?”, *Optical Materials Express*, **15**(7), 1483-1495 (2025).

[6] I. Liberal and A. Manjavacas. “Synthetic crystal rotation with spacetime metamaterials”, *preprint arXiv:2506.02495* (2025).

Heat transport between nonreciprocal media

Monday, 20th April - 15:10: Near-Field Heat Radiation - Oral

***Dr. Omar Jesus Franca Santiago*¹, *Dr. Nico Strauß*¹, *Prof. Stefan Yoshi Buhmann*¹**

1. Institute of Physics, University of Kassel

The second law of thermodynamics dictates that heat flows from warm to cold objects, thereby providing a direction of time [1]. In the optics of nonreciprocal media [2], an arrow of time is alternatively provided by the observation that optical paths cannot be reversed. How are these two notions compatible at the level of quantum electro-dynamics? In order to answer this question, we analyse the near-field heat transfer in a three-layer system constituted by nonreciprocal media with special focus on three-dimensional topological insulators, which break time-reversal symmetry. We investigate the impact of these materials on the heat transfer.

References

[1] Volokitin, A. I.; Persson, B. N. *J. Rev. Mod. Phys.* 4, 79 (2007).

[2] S. Y. Buhmann et al., *New J. Phys.* 14, 083034 (2012).

[3] Nico Strauß, Heat transfer in macroscopic electrodynamics. Doctoral Dissertation, University Kassel, 2025.

Near-field thermal rectification and routing with Weyl Semi-Metals

Monday, 20th April - 15:30: Near-Field Heat Radiation - Oral

Dr. Alireza Naeimi¹, Dr. S. Age Biehs¹

1. Oldenburg University

Near-field radiative heat transfer proposes a robust framework to control heat flows at the nanoscale, where surface and evanescent modes play a dominant role [1]. Using fluctuational electrodynamics, it has been clearly realized that heat transfer between objects with a separation smaller than the corresponding thermal wavelength can break the ideal blackbody radiation limit by several orders of magnitude. This significant increase in heat transfer has numerous applications in the field of thermal management, such as thermophotovoltaics or devices like thermal diodes and routers [2].

In this oral talk (poster presentation), I will focus on our two recent publications [3, 4] on thermal rectifiers and routers based on Weyl semi-metals. Weyl semi-metals are a family of materials, such as $\text{Co}_3\text{Se}_2\text{S}_2$ or $\text{Co}_3\text{Sn}_2\text{S}_2$, that can show intrinsic non-reciprocal properties like magneto-optical materials. The direction of the Weyl node separation vector determines the direction of the intrinsic magnetic field, and the modulus determines its strength. The non-reciprocity allows us to control the directionality of the heat transport of two spherical nanoparticles coupled to a nearby substrate, leading to a substantial thermal rectification and routing between the nanoparticles. I will further discuss the underlying spin-spin interactions and surface-mode coupling giving rise to strong thermal diode and routing effects, offering new opportunities to experimental realization and near-field thermal engineering.

- [1] S.-A. Biehs et al., Rev. Mod. Phys. 93, 025009 (2021).
- [2] Z. Zhang and L. Zhu, Phys. Rev. Appl. 18, 027001 (2022).
- [3] A. Naeimi and S.-A. Biehs, Phys. Rev. Mater. 9, 045201 (2025).
- [4] A. Naeimi and S.-A. Biehs, Appl. Phys. Lett. 127, 101601 (2025).

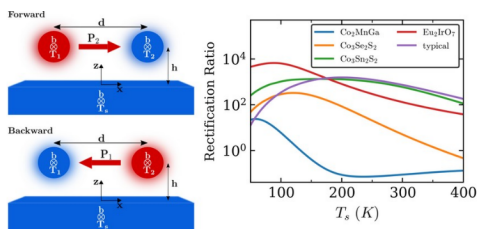


Fig1. Thermal rectification setup consisting of two Weyl nanoparticles in the vicinity of a substrate where the cold particle and substrate have temperatures T_s while the hot particle has the temperature $T_s + 20$ K for both forward and backward scenarios. We show that the rectification ratio can be up to 6700 at temperatures close to $T_s = 100$ K for Eu_2IrO_7 .

Fig1.png

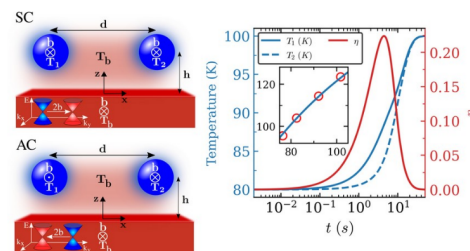


Fig2. Thermal routing effect between two cold Weyl nanoparticles with initial temperatures $T_1 = T_2 = 80$ K in the vicinity of a hot substrate with fixed temperature $T_s = 100$ K. The dynamical routing effect can be up to 22.5 % for $\text{Co}_3\text{Sn}_2\text{S}_2$.

Fig2.png

Transition from far-field to enhanced near-field radiative heat transfer in a multi-body system involving two microspheres

Monday, 20th April - 15:50: Near-Field Heat Radiation - Oral

***Dr. Ana Isabel Fernández-Tresguerres Mata*¹, *Dr. Victor Guillemot*¹, *Dr. Yannick De Wilde*¹**

1. Institut Langevin, ESPCI Paris, Université PSL, CNRS

Ana I. F. Tresguerres-Mata^{1,*}, Victor Guillemot¹, Riccardo Messina², Valentina Krachmalnicoff¹, Rémi Carminati^{1,3}, Philippe Ben-Abdallah², Wilfrid Poirier⁴, and Yannick De Wilde^{1,*}

¹Institut Langevin, ESPCI Paris, Université PSL, CNRS, 75005 Paris, France. ²Laboratoire Charles Fabry, UMR 8501, Institut d'Optique, CNRS, Université Paris-Saclay, 2 Avenue Augustin Fresnel, 91127 Palaiseau Cedex, France. ³Institut d'Optique Graduate School, Université Paris-Saclay, 91127 Palaiseau, France. ⁴Laboratoire National de Métrologie et d'Essais (LNE), 29 avenue Roger Hennequin, 78197 Trappes, France.

*email : anaif.tresguerres-mata@espci.fr ; yannick.dewilde@espci.fr

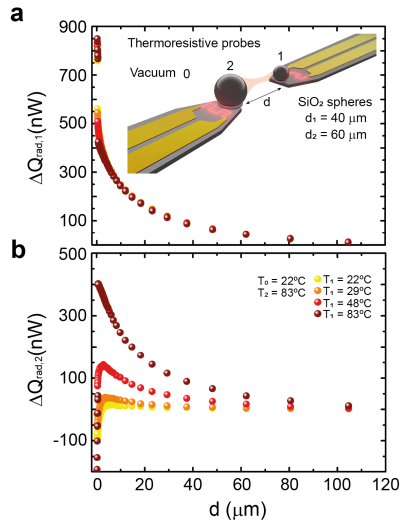
Thermal radiation is responsible for heat transfer between bodies in vacuum. In the far-field regime, when object dimensions and separations are large compared to the thermal wavelength, a well-defined limit exists, known as the blackbody limit and described by Planck's radiation law. However, at micrometric or nanometric length scales below the thermal wavelength, this description breaks down and new physical mechanisms become dominant. In this near-field regime, radiative heat transfer can be mediated by evanescent fields, enabling it to surpass the blackbody limit [1].

While radiative heat transfer in the sphere-plane geometry has recently been revisited in our group [2], this work presents a novel experimental study investigating radiative heat transfer between multiple bodies within a two-sphere geometry. We use two silicon dioxide microspheres of various diameters supporting localized surface phonon polaritons. These excitations play a central role in near-field heat transfer. A highly sensitive platform based on thermoresistive probes combined with Wheatstone bridges enables the detection of very small resistance changes associated with minute temperature variations, as well as precise control of the sphere separation from micrometers down to nanometers, allowing investigation of the transition from far- to near-field regimes.

In this way, we directly probe radiative exchange in a multi-body system where the surrounding environment plays a significant role. Results with microspheres of various diameters reveal a strong modification of near-field radiative heat transfer, dominated by localized surface polaritonic modes that significantly enhance energy exchange. Two independent thermal probes in our setup enable one to find where exactly radiative heat flows between the bodies involved in the system. Our findings highlight fundamental differences between far- and near-field radiative heat transfer and demonstrate the importance of near-field effects for achieving control over thermal radiation at the nanoscale.

[1] Rousseau, E., Siria, A. *et al. Nature Photonics* **3**, 514-517 (2009).

[2] Guillemot, V. *et al. Phys. Rev. Lett.* **134**, 193801 (2025).



Experimental measurements of the transition from the far- to the near-field regime in a multi-body system. a. Gap-size dependence of the flux variation in sphere 1 (40 μm diameter), considering sphere 1 temperatures ranging from 22 to 83 °C and a constant temperature of 83 °C for sphere 2. Inset: schematic of the two-sphere multi-body system. **b.** Same as (a), but for sphere 2 (60 μm diameter). When the temperature of sphere 1 is lower than that of sphere 2, the measured flux becomes non-monotonic as a function of distance. This non-monotonic behaviour is the result of a competition between two radiative mechanisms: propagating-wave exchange with the environment and near-field interaction between the spheres.

Figure1 anaiftresguerres-mata.png

Exceptional thermal stability and heat-induced structural transitions in individual Tobacco Mosaic Virus (TMV)

Monday, 20th April - 16:30: Phase Change Materials - Featured talk

*Dr. Diego Alonso Aldave*¹, *Mr. Alejandro Díez-Martínez*¹, *Dr. JaeHwan Jeong*¹, *Dr. Pedro J. de Pablo*¹,
*Prof. Julio Gómez-Herrero*¹, *Dr. Pablo Ares*¹

¹. Departamento de Física de la Materia Condensada, IFIMAC and INC, Universidad Autónoma de Madrid, 28049, Madrid, Spain

Thermal processes in biological nanostructures play a critical role in their functionality, stability, and integration into nanoengineered systems. However, experimental access to heat-induced transformations at the level of individual biomolecular objects remains limited. In this work, we investigate the thermal response of single Tobacco Mosaic Virus (TMV) particles subjected to high temperatures in air, using Atomic Force Microscopy (AFM) as a nano/microscale thermal metrology platform [1].

TMV particles adsorbed on solid substrates were heated from room temperature up to 250 °C, both ex situ and in situ using integrated microheaters, enabling direct correlation between thermal loading and nanoscale structural evolution. By statistically analyzing height and lateral dimensions at the single-particle level, we identify three distinct thermal regimes: i) a stable regime up to ~175 °C with minimal structural change, ii) a transition regime between ~195 °C and 235 °C characterized by progressive flattening and lateral expansion, and iii) complete structural collapse above ~240-250 °C (Figure 1). A melting temperature of approximately 215 °C is extracted, consistent with ensemble diffraction measurements while revealing substantial heterogeneity in degradation pathways that is inaccessible to bulk techniques.

Remarkably, partially degraded TMV nanorods remain morphologically stable for at least one week after thermal treatment, indicating irreversible but long-lived thermally driven reconfigurations. In situ AFM experiments further demonstrate rapid thermal equilibration and stability over extended heating times, underscoring the low thermal mass and robust energy dissipation characteristics of individual virions.

These results provide quantitative insight into thermal processes in biological systems at the nanoscale, highlighting the role of interfacial constraints, hydration loss, and protein reorganization under extreme thermal stress. Beyond biological relevance, this work establishes AFM-based approaches as powerful tools for nano/microscale thermal metrology of soft and hybrid materials and supports the use of virus-based nanostructures as model systems and functional components in thermally demanding nano/micro devices.

References

[1] D. A. Aldave, A. Díez-Martínez, J. H. Jeong, P. J. de Pablo, J. Gómez-Herrero, P. Ares, Probing the structural resilience of tobacco mosaic virus under thermal stress, *Materials & Design* 257, 114482 (2025).

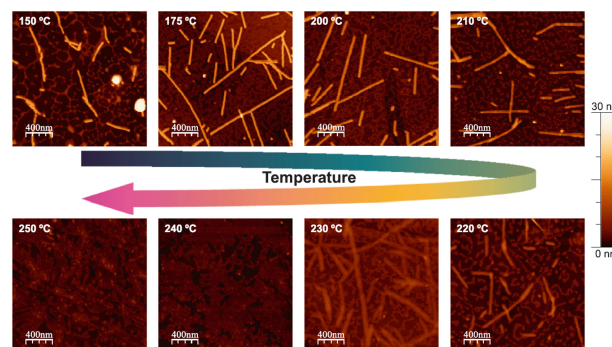


Figure 1. Evolution of the structure of TMVs deposited on HOPG heated in air from room temperature up to 250 °C.

Fig pabloares.jpg

Thermal characterization of nanolayers: silica, diamond and phase-change materials

Monday, 20th April - 17:00: Phase Change Materials - Oral

Prof. Nicolas Horny¹, **Ms. Ghadir OLLAIC**¹, **Dr. Sébastien Cueff**², **Dr. Georges Hamaoui**³, **Dr. Lionel Rousseau**³, **Dr. Mihai Lazar**⁴, **Ms. Evelyne Martin**⁵

1. ITHEMM, Université de Reims Champagne-Ardenne, 2. INL, Ecole centrale Lyon, 3. ESYCOM, Gustave Eiffel University, 4. L2n, Université de Technologie de Troyes, 5. ICube, Unistra

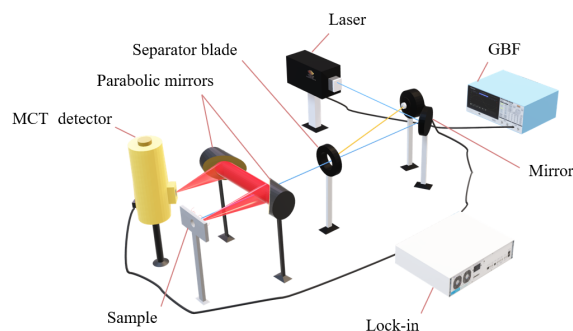
Understanding heat transport at the nanoscale is becoming increasingly important for many micro- and nanoelectronic technologies, especially as devices get smaller and the heat flow becomes more confined. In this work, we looked at several thin-film systems with different thicknesses, including 300 nm SiO₂ and 300 nm to 1 μm diamond layers on 370 μm SiC, as well as 10 to 200 nm GST and Sb₂S₃, and VO₂ films grown on silicon. The measurements were performed with frequency-domain photothermal radiometry (FD-PTR), and we analysed the data using a standard 1D multilayer heat diffusion model.

For the SiC substrate, we were able to retrieve the thermal effusivity and diffusivity quite reliably, which then allowed us to calculate the conductivity. In contrast, for the SiO₂ films, the model mainly gave us access to the conductivity and the volumetric heat capacity. We are currently comparing these two strategies: either extract k and C first and then compute the diffusivity and effusivity, or do the opposite.

Some samples turned out to be more challenging. The VO₂ films show strong correlations between the thermal parameters in the 1D model, which makes it difficult to obtain thermal property values. For the diamond layers, the 1D model seems to be not sufficient to fit experimental data because lateral heat spreading becomes significant due to the very high conductivity of diamond. This points toward the need for a 2D model for such configurations.

Overall, the results help clarify how heat flows in these different nanolayers and underline the importance of choosing the right modelling approach depending on the material and geometry.

This work was supported by ANR PRC (ANR-24-CE09-5163-03) and the NANOPHOT graduate school (ANR-18-EURE-0013).



Ptr setup.png

Giant Thermal Switching via Phase Transition in MoTe₂

Monday, 20th April - 17:20: Phase Change Materials - Oral

*Mrs. Zhuyao Chang*¹, *Dr. Nemo McIntosh*², *Prof. Zhao Liu*¹, *Dr. Riccardo Rurali*²

1. Hebei Normal University, 2. Institut de Ciència de Materials de Barcelona, ICMAB-CSIC, ES-08193 Bellaterra, Spain

Designing materials with tailor made thermal properties is an important challenge in current condensed matter and nanoscience, particularly for the implications on efficient thermal management in electronics and for applications related to energy harvesting, such as thermoelectricity. Even more interesting is the possibility to dynamically access different heat conduction states, as it potentially leads to real-time control of heat flow. Here, we leverage on phase-engineering in MoTe₂, a 2D van der Waals transition metal dichalcogenide (TMD), showing that the thermal conductivity, κ , undergoes a giant threefold increase ($\sim 270\%$ at room temperature) upon the phase transition between the common 2H and 1T' polymorphs. Exploiting polymorphism to dynamically modulate the properties of TMDs is particularly promising in the case of MoTe₂, as it possesses one of the lowest energy barriers for the transition between the 2H and 1T' phases. Our first-principles calculations trace back this very large change of κ to the different effect that four-phonon processes have on the two crystal phases. Importantly, the 2H \rightarrow 1T' phase transition is ultrafast and reversible and can be triggered by external electric fields, light absorption, and THz pulses.

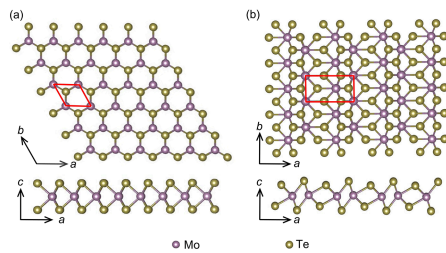


Figure 1: Top and side views of (a) 2H-MoTe₂ and (b) 1T'-MoTe₂. The red wireframes indicate the unit cell.

Figure1.png

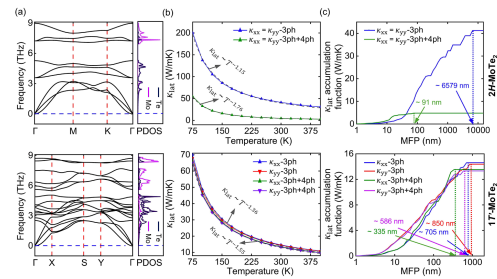


Figure 2: (a) Phonon dispersions and projected density of states (PDOS). (b) κ_{tot} versus temperature. The grey dashed line represents the fitting based on $\kappa_{\text{tot}} \sim T^{-\alpha}$. (c) The accumulation function of κ_{tot} versus phonon mean free path (MFP) at 300 K. The top and bottom panels represent the results of 2H-MoTe₂ and 1T'-MoTe₂, respectively.

Figure2.png

Phonon transport at the nanoscale: a wave-particle duality matter

Tuesday, 21st April - 09:00: Invited - Invited talk

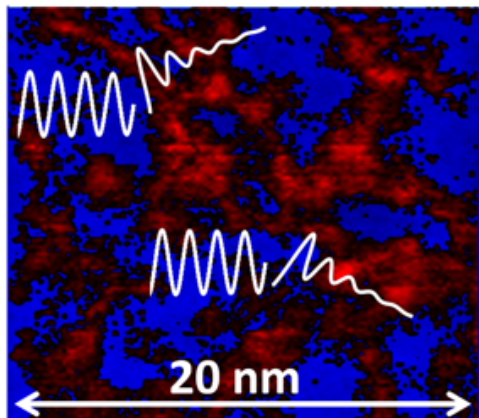
Dr. Valentina Giordano¹

1. ILM, Université Claude Bernard Lyon1

Phonons, the quanta of lattice vibrations, are ubiquitous in our daily life, since they control elastic properties, sound propagation, and heat transport. As such, phonon manipulation has come to the forefront of current research, e.g., for engineering efficient thermoelectric devices or for the thermal management in micro/nanoelectronics. Like electrons, phonons exhibit a dual particle-wave nature, a duality which plays a key role in determining, among others, thermal transport properties.

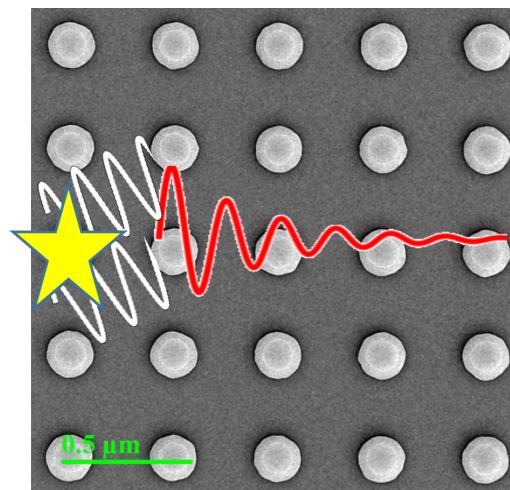
Historically, thermal transport by phonons in crystals has been described using the particle approach: a phonon is seen as a quasi-particle carrying its quantum of energy and travelling across the sample, until it collides against an obstacle. In this view, nanostructuring has proved to be very efficient in reducing thermal conductivity through phonon scattering at interfaces (Figure 2). This strategy is based on phonon incoherent scattering, or particle behavior. Another strategy has recently been proposed, based on exploiting phonon wave behavior through the realization of periodic nanostructures, able to generate constructive and destructive phonon interferences that profoundly change phonon dynamics, with direct consequences on thermal transport (Figure 1).

In this talk, I will survey the problem of thermal transport in nanostructured materials, from random to periodic, and the current open questions and technical challenges that remain to face.



In nanocomposites, interfaces scatter phonons, reducing their contribution to thermal transport. A particles description may capture the physics at play.

Figure1.png



In periodic nanostructures, when reflected by the interfaces, phonons preserve their phase and wave behavior. They can interfere with each other, leading for example to the modification of phonon dispersions.

Figure2.png

Microscale Heat Transfer and Flexural Phonon Dynamics in Expanded Graphite–MWCNT Composites

Tuesday, 21st April - 09:50: Phonon Transport - Oral

Dr. Daria Szewczyk¹, Prof. Andrzej Jezowski¹, Dr. Maksym Barabashko², Prof. Galina Dovbeshko³, Prof. Alexander Krivchikov²

1. Institute of Low Temperature and Structure Research PAS, 2. Verkin Institute for Low Temperature Physics and Engineering NASU, 3. Institute of Physics NASU

This study provides an in-depth analysis of low-temperature heat capacity and phonon dynamics in expanded graphite (EG) and EG–multiwalled carbon nanotube (MWCNT) composites (1.0 and 3.0 wt.% MWCNT) over a temperature range of 2–300 K. The research reveals that thermal behavior in these carbon-based systems is primarily governed by low-frequency out-of-plane phonons with quadratic dispersion, characteristic of two-dimensional layered structures. These flexural phonon modes dominate vibrational properties at cryogenic temperatures, as confirmed by consistently negative C_5 coefficients in the heat capacity model.

Calorimetric measurements combined with structural characterization techniques—including Raman spectroscopy, X-ray diffraction (XRD), and energy-dispersive X-ray spectroscopy (EDS)—demonstrate that structural disorder and material density critically influence thermal transport. Compared to crystalline graphite, EG exhibits significantly higher heat capacity at low temperatures, driven by increased defect density, reduced interlayer coherence, and chemical oxidation effects. The linear term (C_1T) in the three-term polynomial model ($C_1T + C_3T^3 + C_5T^5$) was markedly elevated in low-density EG samples, correlating strongly with the Raman I_{2D}/I_G ratio and confirming the link between vibrational heat capacity and structural disorder.

Interestingly, the incorporation of MWCNTs up to 3 wt.% produced only minor changes in overall heat capacity, indicating that the intrinsic disorder within the EG matrix plays a more dominant role than nanotube concentration. Mechanical compaction of low-density samples significantly reduced the C_1 term, suggesting suppression of defect-related vibrational modes, whereas high-density samples exhibited minimal changes, reflecting structural stabilization through prior processing.

A notable observation is the absence of the low-temperature hump (boson peak) typically associated with disordered solids, further supporting the dominance of flexural phonons and the suppression of localized vibrational states. The effective application of the three-term model across all samples underscores its ability to capture contributions from defects, Debye-like phonons, and non-linear dispersion effects.

These findings provide new insights into nanoscale and microscale heat transfer in anisotropic carbon systems, highlighting the interplay between structural disorder, phonon dispersion, and mechanical processing. The results have implications for thermal management in advanced carbon-based materials, where tuning defect density and layer coherence can modulate vibrational heat capacity and thermal transport properties.

Phonon transport in asymmetric nanostructures in the ballistic regime

Tuesday, 21st April - 10:10: Phonon Transport - Oral

Dr. Boris Brisuda¹, ***Dr. Olivier Bourgeois***¹, ***Prof. Jean-François Robillard***², ***Mr. Jon Canosa Diaz***²

1. Institut Néel, CNRS, 25 avenue des Martyrs, F-38000 Grenoble, France, 2. IEMN (Institut d'électronique de microélectronique et de nanotechnologie)

The manipulation of heat fluxes is possible by acting on the transport of phonons at the nanoscale using advanced nanostructuring in what is currently called thermal metamaterials. This is one of the major challenges of the current small-scale energy management.

In our experiment we propose a suspended double-membrane based sensor, (see Figure 1 left), functioning at very low temperatures (<100mK) using the state-of-the-art niobium nitride thermometry with attowatt sensitivity [1]. This will enable us to demonstrate innovative thermal effects involving large phonon mean-free-paths and long phonon-wavelength (>100nm) in the non-Fourier regime.

The sample (nanostructured layer of SiN), see Figure 1 right, is installed in between two suspended membranes, allowing the measurement of heat flux in both directions and the evaluation of thermal rectification. They are nanostructured using microelectronic technology at the length scale of the phonon wavelength, which is on the order of 100 nm at 1K in the case of silicon nitride. The length of the sample is inferior to the phonon mean-free path, ensuring ballistic regime of phonon transport. The nanostructuring of the sample is an asymmetric lattice meant for the study of thermal rectification.

This presentation will focus on the asymmetric sample shown in Figure 1 and the impact of the structure on the heat flow in the system [2]. In Figure 2, an example of a heat flux measurement is represented as a function of the temperature gradient applied between the two membranes (T1-T2) at 900 mK, showing a difference depending on the heat flux direction. This work sheds some light on the often-debated area of non-trivial heat management at ultra low temperatures.

[1] A. Tavakoli, K. Lulla, T. Crozes, E. Collin, and O. Bourgeois, "Heat conduction in a ballistic 1D phonon waveguide indicate breakdown of the thermal conductance quantization", *Nature Commun.* 9, 4287 (2018).

[2] B. Brisuda, J. Canosa Diaz, C. Polanco, V. Doebele, T. Crozes, J.-F. Robillard, N. Mingo, L. Saminadayar, O. Bourgeois, article in preparation

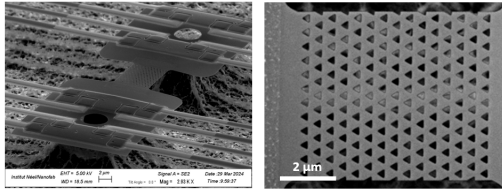


Figure 1. SEM images of the suspended SiN double-membranes (left) and the nanostructured SiN strip (right).

Figure 1- sem of sample.png

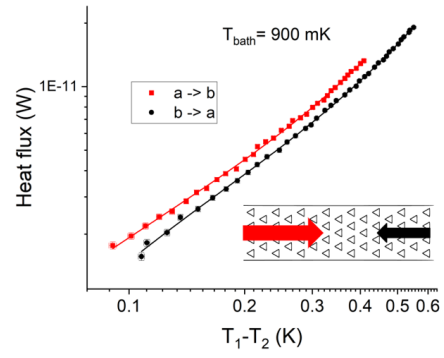


Figure 2. Plot of heat flux as a function of temperature gradient across the nanostructured SiN sample at 900 mK, showing a difference between the heat flux in the forward (red arrow) and reverse (black arrow) directions.

Figure 2- heat flux.png

First principles calculations of thermal transport at metal/silicon interfaces: Evidence of interfacial electron-phonon coupling

Tuesday, 21st April - 10:30: Phonon Transport - Oral

Dr. Michael De SanFeliciano¹, **Dr. Christophe Adessi**¹, **Dr. Julien El Hajj**¹, **Prof. Nicolas Horny**², **Dr. François Detcheverry**¹, **Dr. Manuel Cobian**³, **Dr. Samy Merabia**¹

1. ILM, Université Claude Bernard Lyon1, 2. ITHEMM, Université de Reims Champagne-Ardenne, 3. PMCS2I, École Centrale de Lyon

With the increasing miniaturization of electronic components and the need to optimize thermal management, it has become essential to understand heat transport at metal-semiconductor interfaces. While it has been recognized decades ago that an electron phonon channel may exist at metal-semiconductor interfaces, its existence is still controversial. Here, we investigate thermal transport at metal-silicon interfaces using the combination of first principles calculations and nonequilibrium Green's function (NEGF).

We explain how to correct NEGF formalism to account for the out-of-equilibrium nature of the energy carriers in the vicinity of the interface. The relative corrections to the equilibrium distribution are shown to arise from the spectral mean free paths of silicon and may reach 15%. Applying these corrections, we compare the predictions of NEGF to available experimental data for Au-Si, Pt-Si and Al-Si interfaces. Based on this comparison, we infer the value of the electron-phonon interfacial thermal conductance by employing the two temperature model. We find that interfacial thermal transport at Au-Si interfaces is mainly driven by phonon-phonon processes, and that electron-phonon processes play a negligible role at this interface.

By contrast, for Al-Si interfaces, we show that phonon-phonon scattering alone can not explain the experimental values reported so far, and we estimate that the electron phonon interfacial conductance accounts for one third of the total conductance. This work demonstrates the importance of the electron-phonon conductance at metal-silicon interfaces and calls for systematic experimental investigation of thermal transport at these interfaces at low temperatures. It opens also the door for the building of an accurate model to predict the conductance associated to the interfacial electron-phonon channel.

Phonon mean free path spectroscopy by Raman thermometry

Tuesday, 21st April - 10:50: Phonon Transport - Oral

Ms. Katharina Dudde¹, Mr. Mahmoud Elhajhasan¹, Mr. Guillaume Würsch¹, Mr. Julian Themann¹, Ms. Jana Lierath¹, Mrs. Elena Trukhan², Dr. Nakib Protik², Dr. Giuseppe Romano³, Prof. Gordon Callsen¹

1. Universität Bremen, 2. Humboldt-Universität zu Berlin, 3. MIT-IBM Watson AI Lab

In this work, we exemplify on a bulk silicon sample that Raman thermometry is capable of phonon mean free path (PMFP) spectroscopy [1]. Our experimental approach is similar to the variation of different characteristic length scales l_c during thermal reflectance measurements in the time or frequency domain (TDTR and FDTR) and transient thermal grating (TTG) spectroscopy. In place of l_c , we vary the laser focus spot size (w_e) and the light penetration depth (h_α) during one-laser Raman thermometry (1LRT) measurements, enabling control over the size of the temperature probe volume V . For our largest w_e values, the derived effective thermal conductivities κ_{eff} converge towards the bulk thermal conductivity κ_{bulk} for silicon, which we confirm by two-laser Raman thermometry and *ab initio* theory. However, towards smaller w_e values, we observe a pronounced increase of κ_{eff} , which amounts up to a factor of 5.3 at 293 K and even 8.3 at 200 K. We mainly assign this phenomenon to quasi-ballistic phonon transport and the generation of an initial non-thermal phonon distribution due to our optically induced heating. As a result, we can compare our measured $\kappa_{\text{eff}}(w_e)$ trends with the thermal accumulation function κ_{cum} and its dependence on the phonon mean free path l_{ph} , which we derive from *ab initio* solutions of the linearized phonon Boltzmann transport equation (BTE). For small w_e or h_α values, 1LRT mimics the situation of a local and/or surfacic heat source in a large matrix, which allows us to probe κ_{eff} values that exceed κ_{bulk} . From a theoretical point of view, this was first predicted by Chiloyan *et al.* [2], who calculated $\kappa_{\text{eff}}(w_e)$ for different initial phonon distributions in qualitative agreement with our data, cf. Fig. 1. Our results shall seed future PMFP spectroscopy based on 1LRT, which can directly be benchmarked against state-of-the-art theory to probe the effect of, e.g., any nano-structuring by comparison of κ_{cum} trends and not only κ values, aiming to test our understanding of intricate phonon transport physics.

[1] K. Dudde, M. Elhajhasan, G. Würsch, J. Themann, J. Lierath, D. Paul, N.H. Protik, G. Romano, G. Callsen, *Material Today Physics* 57, 101784 (2025).

[2] V. Chiloyan, S. Huberman, A.A. Maznev, K.A. Nelson, G. Chen, *Appl. Phys. Lett.* **116**, 163102 (2020).

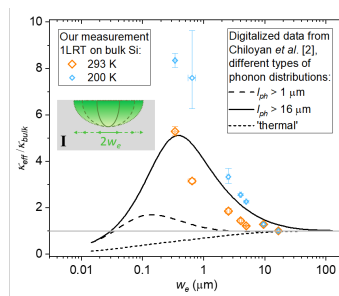


Fig. 1: κ_{eff} normalized to the bulk value calculated for single-crystalline bulk silicon at room temperature based on the steady-state phonon BTE for a 3D Gaussian heat source for various radii w_e and for three different generated phonon distributions. This theoretical results originate from Ref. [2] and treat a thermal phonon distribution (short-dashed line) and two phonon distributions with either $l_{\text{ph}} > 1 \mu\text{m}$ (long-dashed line) or $l_{\text{ph}} > 16 \mu\text{m}$ (solid line). In comparison we plot our 1LRT data normalized to $\kappa_{\text{eff}}(\kappa_{\text{cum,max}})$ for bulk silicon at $T_{\text{amb}} = 293\text{K}$ (orange symbols) and $T_{\text{amb}} = 200\text{K}$ (blue symbols).

Phonon mean free path spectroscopy by raman thermometry fig 1.png

Thermoelastic heat flux contribution opposing the thermal gradient in ultrathin MoS₂ and MoSe₂

Tuesday, 21st April - 11:30: Thin Films, Machine Learning - Featured talk

***Dr. Albert Beardo*¹, *Mr. Jordi Tur Prats*¹, *Prof. F. Xavier Alvarez*¹, *Prof. Juan Camacho*¹, *Dr. Sebin Varghese*², *Prof. Klaas-Jan Tielrooij*²**

1. Universitat Autònoma de Barcelona, Campus UAB, ES-08193 Bellaterra, Spain, 2. Eindhoven University of Technology

The ability to actively control the thermal energy dissipation rates in semiconductor nanostructures via external perturbations is key to enhance efficiency and increase the life-time of nanoelectronic devices. Here, we experimentally reveal a hidden contribution to heat transport directly opposing the established thermal gradient in ultrathin suspended layers of MoS₂ and MoSe₂. By exposing the sample to pulsed ultrafast optical excitations, we identify a thermoelastic heat flux contribution that flows from cold and compressed regions toward hot and expanded regions.

This novel regime of non-diffusive heat transport results from the interplay between hydrodynamic and thermoelastic effects under strongly inhomogeneous strain profiles at the nanoscale. Beyond standard thermal expansion and thermo-mechanical energy exchange, we measure the emergence of this thermoelastic heat flux contribution, which was theoretically predicted more than 70 years ago [1] but never observed until now. This non-diffusive phenomenon, in combination with hydrodynamic effects [2], induces an apparent reduction in the apparent thermal diffusivity by more than one order of magnitude in monolayers. We develop the required theoretical framework to model the transient evolution of the sample using intrinsic material properties calculated from first principles and provide a physical interpretation in terms of the strain-induced local modification of the phonon dispersion relations.

We furthermore demonstrate control over these effects via the thickness and the type of heating: By controlling the thickness from multilayer to monolayer, a transition occurs from the usual diffusive regime to a regime where hydrodynamic effects play a role, and by applying pulsed heating instead of continuous heating, the unconventional thermoelastic effects occur, leading to a transition to a hydro-thermoelastic regime. This work thus establishes unprecedented active control over heat flow in solids, all at room temperature, with potential applications ranging from thermal management in electronic devices to thermoelectrics and other forms of energy conversion.

[1] Kronig, R. On the hydrodynamics of non-viscous fluids and the theory of helium II. Part III. *Physica* 19, 535-544 (1953).

[2] Guyer, R. A. & Krumhansl, J. A. Thermal conductivity, second sound, and phonon hydro-dynamic phenomena in nonmetallic crystals. *Phys. Rev.* 148, 778-788 (1966).

Machine Learning Guided Discovery of Extreme Lattice Thermal Conductivity in Si/Ge Superlattices

Tuesday, 21st April - 12:00: Thin Films, Machine Learning - Oral

Dr. Shubham Tyagi¹, **Dr. Julian Garcia Fernandez**², **Dr. Natalia Seoane**³, **Prof. Antonio Garcia Loureiro**³, **Prof. Marc Bescond**⁴

1. IM2NP UMR-CNRS, Aix Marseille Université, France, **2.** Departamento de Electrónica e Computación, USC, Santiago de Compostela, Spain, **3.** Centro Singular de Investigación en Tecnoloxías Intelixentes, USC, 15782, Santiago de Compostela, Spain,

4. IM2NP UMR-CNRS, Aix Marseille Université, France; Institute of Industrial Science, University of Tokyo, Japan

The increasing thermal loads in nanoscale electronic systems demand materials and engineered nanostructures that can either dissipate heat efficiently or strongly suppress it, a challenge that ultimately depends on controlling phonon-mediated thermal transport. Si/Ge superlattices (SLs) remain a powerful platform for exploring this dual objective because their lattice thermal conductivity (κ_l) can be tuned from strongly localized to highly coherent transport regimes via interface engineering. However, systematic exploration of the large design space, even for fixed-length SLs, requires computational tools that can efficiently identify structures yielding extreme κ_l values.

In this work, we develop a workflow that couples non-equilibrium Green's function (NEGF) simulations with a convolutional neural network (CNN) in an iterative loop to accelerate the discovery of Si/Ge superlattices exhibiting ultra-low and ultra-high κ_l . Starting from harmonic force constants obtained from first-principles calculations and a fixed total superlattice length, we generate phonon transport data across diverse interface arrangements. The resulting NEGF-based thermal conductances (G) form the training dataset, and κ_l is obtained by multiplying G with the superlattice length. Structural sequences are encoded as 1D arrays and mapped into a higher-dimensional embedded representation before entering the CNN, enabling the network to resolve spatial patterns relevant to coherent and localized phonon transport. In contrast to recent machine learning frameworks applied to 2D van der Waals heterostructures [npj Comput. Mater., 11, 158 (2025)], our study targets Si/Ge multilayers and employs a purely data-driven NEGF–CNN pipeline without manual feature engineering. To efficiently learn structure–property relationships, we design a CNN architecture (Fig. 1) to detect spatial patterns associated with interference design. The workflow proceeds through data preprocessing, sequence embedding, CNN training, and the rapid prediction of κ_l . The resulting plot (Fig. 2) shows excellent agreement between predicted and simulated values, with R^2 values exceeding 0.98.

Once trained, the model enables a rapid exploration of the fixed-length design space and identifies superlattice configurations that span the two extremes of κ_l . Structures with dense interface clustering exhibit strong elastic backscattering and localization, resulting in lower κ_l values. In contrast, arrangements containing short locally periodic fragments support enhanced coherent transmission, producing high κ_l values. Direct NEGF simulations validate both extremes.

Overall, our NEGF-ML framework offers a scalable approach for discovering superlattice designs with application-specific thermal transport properties. Beyond Si/Ge SLs, this model can be extended to other heterostructures where identifying rare, high-impact thermal transport behaviors is crucial for nanoscale cooling and heat-spreading technologies.

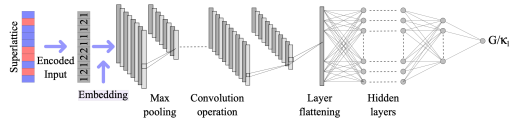


Fig 1.png

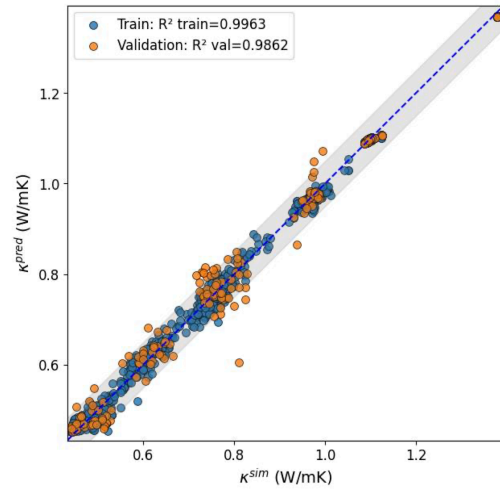


Fig 2.png

Influence of electrical properties on thermal boundary conductance at metal/semiconductor interface

Tuesday, 21st April - 12:20: Thin Films, Machine Learning - Oral

Prof. Nicolas Horny¹, **Dr. Quentin Pompidou**¹, **Dr. Juan Carlos ACOSTA ABANTO**², **Dr. Mélanie Brouillard**³, **Dr. Nicolas BERCU**⁴, **Prof. Louis Giraudet**⁴, **Dr. Raza Sheikh**⁵, **Dr. Christophe Adessi**⁶, **Dr. Samy Merabia**⁶, **Dr. Severine Gomes**², **Dr. P-Olivier Chapuis**², **Prof. Jean-François Robillard**³, **Prof. Mihai Chirtoc**¹

1. ITHEMM, Université de Reims Champagne-Ardenne, 2. CETHIL, CNRS-INSA Lyon, France, 3. IEMN (Institut d'électronique de microélectronique et de nanotechnologie), 4. L2N, Univ. Reims Champagne-Ardenne, Reims, France, 5. Department of Mechanical Engineering and Materials Science, University of Pittsburgh, 6. ILM, Université Claude Bernard Lyon1

Recent experiments reveal that thermal boundary conductance (TBC) at metal/semiconductor interfaces can significantly increase with doped semiconductor. This study explores how electrical properties affect heat transfer across metal/doped semiconductor junctions. Using frequency domain photothermal radiometry, TBC is measured under varying conditions, analyzing the impact of doping levels, barrier height, and the space charge region. A key finding is an increase in TBC when an electric current is applied to n-doped silicon/titanium interfaces, attributed to the reduction of the surface charge area, suggesting that interfacial heat transfer can be modulated through electrical tuning.

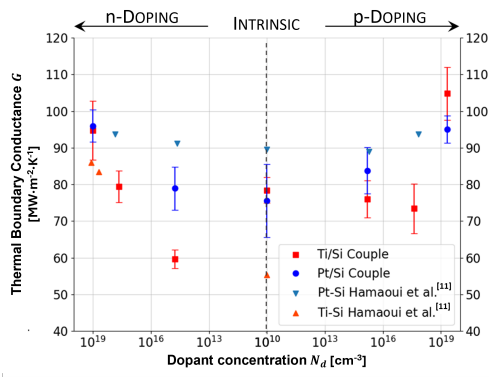
TBC depends on the transmission of heat carriers across the interface. While phonons dominate thermal conduction in both materials, the presence of a metal introduces a significant electronic contribution, complicating energy transfer. Majumdar and Reddy [1] demonstrated that electron-phonon coupling in the metal, followed by phonon transmission, is insufficient to explain the observed TBC. They proposed that electronic transport must also be considered. Lombard et al. [2] later confirmed this, highlighting the importance of direct coupling between metal electrons and semiconductor phonons. A recent first-principles study further clarified that while TBC is primarily governed by phonon-phonon scattering, electrons contribute when the metal's Debye frequency approaches that of silicon, involving localized electron-phonon coupling near the interface.

In doped semiconductors, a third conduction pathway emerges due to electrical charges. The overall TBC results from three main mechanisms: (i) energy transfer from metal electrons to metal phonons, followed by phonon coupling between the metal and semiconductor; (ii) direct coupling between metal electrons and semiconductor phonons; and (iii) energy transfer from metal electrons to charges in the semiconductor, which then dissipate within the crystal.

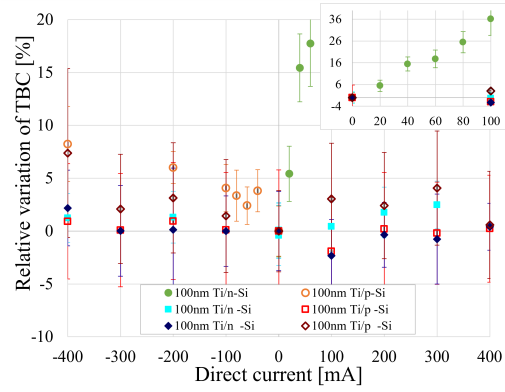
This study introduces a comprehensive experimental methodology to characterize heat transfer at metal/semiconductor interfaces and analyze the influence of electrical properties on TBC. Key parameters include the Schottky barrier height, semiconductor doping level, and applied electrical potential. Titanium and platinum contacts with doped silicon are examined to understand the electronic contribution to thermal transport under polarization. The samples, designed specifically for this study, undergo electrical characterization before TBC measurements using frequency domain photothermal radiometry.

This research advances the understanding of thermal transport mechanisms and offers new possibilities for modulating heat dissipation in electronic devices, paving the way for more efficient thermal management in technology.

This work was supported by ANR PRC (ANR-24-CE09-5163-03) and the NANOPHOT graduate school (ANR-18-EURE-0013).



Tbc vs dop newer.png



Final tbc vs current.png

Predictive modeling of nanoscale thermal transport in silicon using machine-learning molecular dynamics

Tuesday, 21st April - 12:40: Thin Films, Machine Learning - Oral

Dr. Housseem Rezgui¹, Prof. Clivia Sotomayor-Torres¹

1. International Iberian Nanotechnology Laboratory (INL), Braga 4715-330, Portugal

Understanding and controlling phonon-mediated heat transport in silicon is essential for the design of next-generation nanoelectronic and nanomechanical devices, where thermal dissipation is strongly influenced by atomic-scale structure and interfacial effects. In this work, we investigate the capability of modern machine-learning interatomic potentials (MLIPs), specifically the Multi-Atomic Cluster Expansion (MACE) and the Gaussian Approximation Potential (GAP), to model thermal transport properties in nanocrystalline silicon with high accuracy and computational efficiency. Their performance is systematically compared with classical Stillinger-Weber and Tersoff potentials.

By combining machine-learning-based molecular dynamics with lattice-dynamical calculations, we extend the standard Phonopy/Phono3py workflow by using MLIP-derived forces to compute second- and third-order interatomic force constants. This unified framework enables the evaluation of key phonon properties, including dispersion relations, vibrational densities of states, phonon lifetimes, and lattice thermal conductivity. The results demonstrate that MLIPs provide a more accurate and physically consistent description of both harmonic and anharmonic phonon behavior.

To extend this analysis to interfacial thermal transport, we investigate phonon transmission across silicon grain boundaries using a combined atomistic Green's function (AGF) and non-equilibrium molecular dynamics (NEMD) approach within the machine-learning framework. The AGF method provides a frequency-resolved description of phonon transmission and interfacial thermal conductance, revealing that heat transfer is dominated by low-frequency acoustic phonons, while higher-frequency modes are increasingly suppressed by interfacial mismatch. Anharmonic effects are incorporated through frequency-dependent phonon lifetimes derived from third-order force constants, leading to a significant reduction in transmission and interfacial conductance. Complementary NEMD simulations capture full anharmonic and non-equilibrium effects, enabling direct evaluation of the thermal boundary resistance and its dependence on the interatomic potential and interface structure.

This work highlights the potential of machine-learning approaches to bridge the gap between atomistic simulations and experimentally measurable thermal transport properties. This work contributes to the development of predictive, multiscale modeling frameworks for thermal transport in complex materials. Future work will extend this methodology to nanostructured and two-dimensional twisted systems, enabling direct comparison with experimental techniques such as time-domain thermoreflectance and Raman thermometry.

Figure 1. Graphical overview of the computational workflow. Machine-learning interatomic potentials trained on DFT enable efficient MD simulations.

Figure 2. Summary of phonon properties for bulk silicon computed using MLP: (a) vibrational DOS, (b) band structure, (c) phonon lifetimes obtained using the GAP potential, and (d) temperature-dependent thermal conductivity.

Figure 3. (a) AGF schematic of the grain-boundary system. (b) Cumulative interfacial thermal conductance at T=300 K using the GAP potential.

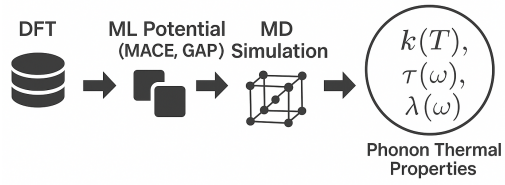


Figure 1.png

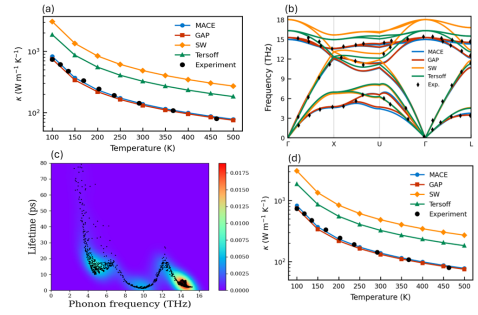


Figure 2.png

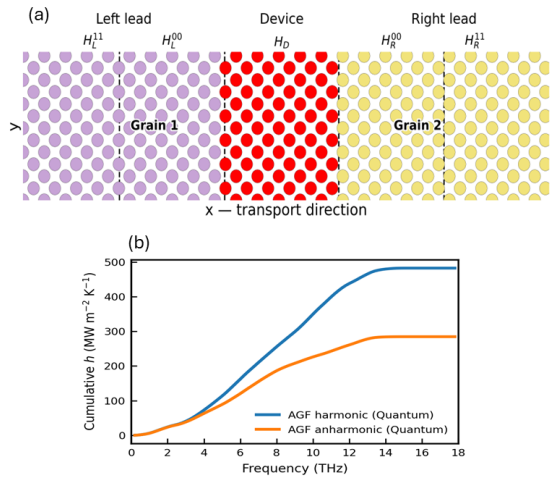


Figure 3.png

Tutorial: Dilution Refrigerators

Tuesday, 21st April - 14:00: Tutorial - Invited talk

Dr. Leif Roschier¹

1. Bluefors

This tutorial talk covers dilution refrigerators from the base principles to real world machines.

Next-generation cryogenic refrigeration enabled by superconducting tunnel junctions

Tuesday, 21st April - 14:50: Low Temperature and Industry Talks - Oral

Dr. Renan Loreto¹, Dr. Arvind Kumar¹, Dr. Juho Luomahaara¹, Dr. Joel Häätinen¹, Dr. Jani Taskinen¹, Dr. Tuure Rantanen¹, Dr. Matilde Tubal¹, Dr. Emma Mykkänen¹, Dr. C. Wisa Förbom¹, Dr. Alberto Ronzani¹, Dr. Klaara Viisanen¹, Dr. Antti Kemppinen¹, Prof. Mika Prunnila¹

1. VTT, Espoo, Finland

Achieving temperatures in the deep cryogenic regime down to sub 1 K-range is critical for a wide range of technologies, from superconducting quantum information processing and ultra-sensitive radiation detection to space applications. Today, such temperatures are typically achieved with complex and large dilution refrigerators based on pumping mixtures of 3He-4He isotopes. Solid-state electrical refrigeration offers a compelling alternative to replace or supplement these solutions by providing a fully electrical cooling systems that are significantly simpler, smaller, more efficient and affordable.

Superconducting tunnel junction based electrical on-chip cooling has been studied for several decades [1], yielding different proof-of-concept demonstrators at various temperatures below 1 K [2]. Our recent work has concentrated on utilizing phonon engineering and 3D integration techniques to create fully scalable and efficient solid-state cooling platforms [3,4,5]. Furthermore, we have demonstrated electron temperature reduction from a temperature of 2.4 K compatible with conventional 4He-coolers to below 1.6 K (34% relative cooling) against the phonon bath [6], using Al-AlO_x-Nb tunnel junctions. These discoveries represent a major milestone toward building a fully solid-state cooling platform capable of bridging the gap between 4He pulse-tube temperatures and the mK range without the need of rare and expensive 3He.

In this communication, we discuss the latest developments of fabrication, characterization and capabilities of these junction-based cooling devices, including thermometry methods. We also report on the thermal modeling of the devices and outline the roadmap for cascading multiple cooling stages to reach dilution refrigerator-equivalent temperatures of 100 mK temperature range and below.

[1] J. T. Muhonen, M. Meschke, and J. P. Pekola, Rep. Prog. Phys. **75**, 046501 (2012).

[2] O. Quaranta et al., Appl. Phys. Lett. **98**, 032501 (2011).

[3] E. Mykkänen et al., Science Adv. **6**, 15 (2020).

[4] A. Kemppinen et al., Appl. Phys. Lett. **119**, 052603 (2021).

[5] J. Häätinen et al., Appl. Phys. Lett. **123**, 152202 (2023).

[6] J. Häätinen et al., Phys. Rev. Applied **22**, 064048 (2024).

Active and passive control of low-temperature thermal conduction with pillar-based phononic crystals

Tuesday, 21st April - 15:10: Low Temperature and Industry Talks - Oral

Mr. Tatu Korkiamäki¹, Dr. Tuomas Puurtinen¹, Prof. Bartłomiej Graczykowski², Prof. Ilari Maasilta¹

1. Nanoscience Center, Department of Physics, University of Jyväskylä, 2. Faculty of Physics, Adam Mickiewicz University, PL-61-614 Poznań, Poland

Phononic crystals (PnCs) can be used to control phonon thermal conduction, with particularly strong effects observed at low temperatures where coherent effects through modification of the phonon dispersions have been demonstrated [1,2]. Most earlier studies have concentrated on geometries with periodic array of holes, but recently, more interest has been given to pillar-based PnCs including localized resonances [3].

Here, we report sub-Kelvin thermal transport experiments of several nano- to microscale pillar-based PnCs, demonstrating up to an order of magnitude reduction in thermal conductance. The samples consist of superconducting aluminum pillars on a suspended SiN membrane. Finite element method simulations were used to compute the phonon dispersion relations and calculate the thermal conductance of all the PnCs, and Brillouin light spectroscopy was used to validate the dispersion calculations. For the two smaller lattice constant (300 nm and 1 μm) structures, the coherent calculations qualitatively match the experimental data. The thermal conductance reduction for those devices thus appears to originate from the coherent mechanism of group velocity reduction induced by the hybridization of the pillar phonon modes with the plate modes.

However, with the larger structures, the thermal conductance begins to disagree with the coherent theory simulations, a trend seen for the larger hole-based PnCs before [2]. Incoherent Monte Carlo simulations in the diffusive surface scattering limit provide an explanation for this trend. Thus, a breakdown in the coherent modification of the dispersion relations takes place around a crossover of $a \approx 1 \mu\text{m}$, most likely caused by the surface and sidewall roughness of the Al pillars.

We have also demonstrated the active control of thermal conductance on such PnCs using a magnetic field. By switching the superconductivity of the Al pillars on and off with the applied field, we observe a change in the conductance. This effect is only visible in the coherent scattering regime. The origin of this effect is likely phonon-electron scattering, which is insignificant in the superconducting state. It is not visible in the larger lattice constants because diffusive boundary scattering overshadows the ph-e scattering. As ph-e scattering is the only diffusive process in the coherent case, turning it on and off can be observed there.

References

- [1] N. Zen et al., *Nat. Commun.* **5**, 3435 (2014).
- [2] Y. Tian et al, *Phys. Rev. Applied* **12**, 014008 (2019).
- [3] Y. Jin et al., *Rep. Prog. Phys.* **84** 086502 (2021).

From Single to Periodic Pulses: Fourier Expansion Analysis to Thermo-Reflectance Signal for Thermal Diffusivity Measurements

Tuesday, 21st April - 15:30: Low Temperature and Industry Talks - Oral

***Dr. Dmitry Sergeev*¹, *Dr. Takahiro Baba*², *Prof. Tetsuya Baba*³, *Mr. Yoshio Shinoda*², *Dr. Osamu Tsukamoto*², *Ms. Kazuko Ishikawa*², *Prof. Takao Mori*⁴**

1. NETZSCH-Gerätebau GmbH, Selb, 2. NETZSCH Japan, Yokohama, 3. National Institute of Advanced Industrial Science and Technology, Tsukuba, 4. National Institute for Materials Science, Tsukuba

Laser Flash Analysis (LFA) and Time Domain Thermo-Reflectance (TDTR) represent two distinct approaches for thermophysical property measurement, each optimized for different sample thickness regimes. LFA uses a transient heat pulse and infrared detection, making it well-suited for bulk and thick films but limited in accuracy for samples with thickness below $\sim 50\ \mu\text{m}$ due to pulse duration and detector delay effects. In contrast, TDTR employs a pump-probe electronic timing with high temporal resolution up to 1 ps and observation time of 50 ns for PicoTR device and up to 20 μs for NanoTR (1 ns resolution), enabling precise characterization of nanoscale films and interfaces (Fig. 1). Through the development of both the conventional laser flash method and ultrafast laser flash methods (including picosecond and nanosecond thermo-reflectance techniques), it has become possible to consistently measure thermal diffusivity across a wide range of materials — from ultrathin films (tens of nanometers) to bulk samples (several millimeters thick) - by observing one-dimensional heat diffusion following impulse heating, under a unified principle.

Instead of laser flash method, which observe the temperature response for single shot, pulsed light thermo-reflectance method applies periodic light pulses to the sample, and the resulting signal contains the total temperature response for multiple shots, and the mathematical treatment has been an difficult problem to solve.

In the present work, the Fourier expansion analysis was applied to the temperature response curve (signal amplitude) of NanoTR and PicoTR devices, and the model fitting was applied in the frequency space for the determination of thermophysical properties. The results were inversely converted to real space and confirmed that completely fits to the measured curve over the entire observation time [1], [2]. Good agreement was obtained between the analytical expression and the reference materials, such as TiN, Pt and ITO samples, in both the time and frequency domains, enabling thermal diffusivity to be determined.

References

- [1] T. Baba, T. Baba, K. Ishikawa, T. Mori, Determination of thermal diffusivity of thin films by applying Fourier expansion analysis to thermo-reflectance signal after periodic pulse heating, *Journal of Applied Physics* 130, 225107 (2021)
- [2] T. Baba, T. Baba, and T. Mori, Fourier Transform Thermoreflectance Method Under Front-Heat Front-Detect Configuration, *Int. J. Thermophys.* 45, 61 (2024)

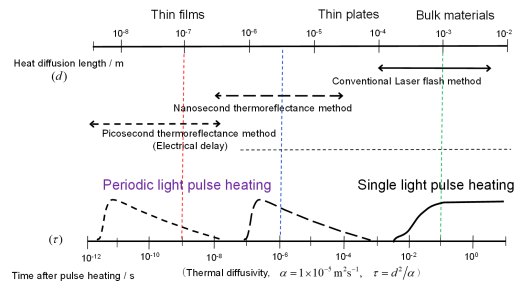


Fig. 1 Block diagram of the pico and nano second light pulse heating thermo-reflectance apparatus

Screenshot 2025-12-14 222405.png

Simulations of heat transfer with COMSOL Multiphysics

Tuesday, 21st April - 15:50: Low Temperature and Industry Talks - Oral

Dr. Sébastien Denis¹

1. COMSOL, 26 rue Gustave Eiffel, 38100 Grenoble, France

The talk will provide an overview of COMSOL Multiphysics® software dedicated to numerical solutions for heat transfer in the stationary and transient regimes. Particular emphasis is paid to the handling of material properties and boundary/interface conditions. The current performance is highlighted with a brief demonstration ranging from geometry definition to postprocessing and visualization of results.

Microgels as Local Temperature Probes for Laser-Induced Heating of Plasmonic Metal Structures

Tuesday, 21st April - 16:50: Poster I - Poster

Dr. Yulia Gordievskaya¹, **Dr. Nino Lomadze**¹, **Ms. Shivani Kesarwani**², **Prof. Andrij Pich**³, **Prof. Holger Lange**¹, **Prof. Svetlana Santer**¹

1. Institute of Physics and Astronomy, University of Potsdam, 14476 Potsdam, Germany, 2. University of Potsdam, Institute of Physics and Astronomy, 3. RWTH Aachen University, Aachen, Germany

Microgels are well known for their remarkable responsiveness to changes in environmental conditions [1]. In this work, we demonstrate a novel method for local temperature determination in aqueous solutions by observing the spatially inhomogeneous collapse of microgels near a substrate. We investigated two scenarios in which localized laser irradiation of plasmonic metal structures generates heat through light absorption. In the first scenario, gold (Fig.1) and silver thin layers were irradiated. In the second scenario, involving laser irradiation of gold nanoparticle solutions, we showed that microgels can adsorb a sufficient number of nanoparticles to enable measurable heating. The effects of laser wavelength and power on the size and shape of thermosensitive PNIPAM microgels were systematically analyzed. The experimental data showed good agreement with numerical simulations performed in COMSOL. These measurements allowed us to construct a comprehensive temperature distribution profile relative to the irradiation point.

Figure 1: COMSOL simulations of the temperature distribution under 1.72 mW blue laser irradiation of a 30 nm gold layer (left) and the corresponding temperature profile of the aqueous solution measured using microgels (right).

Acknowledgments

We thank SFB 1636: Elementary processes of light driven reactions at the nanoscale.

[1] J. Jelken, S.-H. Jung, N. Lomadze, Yu.D. Gordievskaya, E.Yu. Kramarenko, A. Pich, S. Santer. *Adv. Funct. Mater.* **32(2)**, 2107946 (2022)

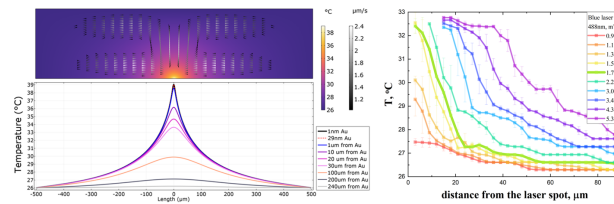


Fig1.png

Tunable thermal conductivity in Silicon thin films via block copolymer nanostructuring

Tuesday, 21st April - 16:50: Poster I - Poster

Mr. Alex Rodriguez-Iglesias¹, Dr. Jose Manuel Sojo Gordillo², Dr. Arianna Nigro², Mr. Marc Aceituno Pimentel¹, Dr. Iñigo Martín-Fernández¹, Dr. Francesc Perez-Murano¹, Dr. Luis Fonseca¹, Dr. Llibertat Abad¹, Prof. Ilaria Zardo², Dr. Marc Salleras¹, Dr. Marta Fernandez-Regulez¹

1. Institute of Microelectronics of Barcelona, 2. University of Basel

Controlling the thermal conductivity of thin films is of great interest for a wide range of applications, including thermoelectric energy harvesting, thermal management in microelectronics, and sensors [1, 2]. In this work, we demonstrate a precise approach to tune the thermal conductivity of silicon thin films by introducing nanoscale cylindrical patterns using block copolymers (PS-b-PMMA in this work) as a lithographic template [3]. The fabrication of the nanostructured layers is achieved through a direct pattern transfer of the block copolymer film pattern onto silicon, combining both wet and dry etching techniques to define the depth and morphology of the nano-features (Figure 1 - Nanostructuring). The thermal properties of the resulting nanostructured silicon layers are characterized using a 3-probe method [4,5]. In this setup, a focused laser heats the suspended membrane, and the thermal resistance of the layer is extracted through a heat balance analysis, allowing precise determination of the thermal conductivity without the contribution of the thermal contacts.

The results reveal a clear correlation between the depth of the nano-structuring and the thermal conductivity: as the etch depth increases, the thermal conductivity of the silicon layer decreases significantly (Figure 2 - ThermalConductivity). This trend demonstrates that the thermal transport in these films can be systematically controlled by adjusting the etching depth, providing a versatile tool to engineer thermal properties at the nanoscale. These findings highlight the potential of block copolymer-directed nanostructuring as a scalable and reproducible approach to tune thermal conductivity in silicon thin films, which is particularly relevant for thermoelectric applications, where optimizing the balance between electrical and thermal transport is essential [2]. Beyond thermoelectrics, the ability to precisely adjust thermal conductivity opens opportunities for on-chip thermal management, phononic devices, and thermal insulation at the micro- and nano-scale.

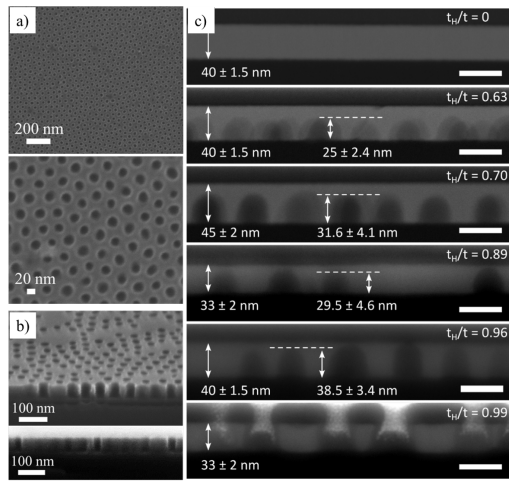
[1] D. G. Cahill et al. *Journal of Applied Physics*, 93(2), 793–818 (2003)

[2] P. Pichanusakorn et al. *Materials Science and Engineering: R: Reports*, 67(2–4), 19-63 (2010)

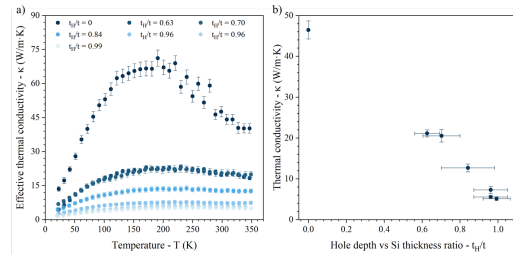
[3] C. Pinto-Gómez et al. *polymers*, 12(10), 2432 (2020)

[4] D. Liu et al. *Nanoletters*, 14, 806-812 (2014)

[5] P. Y. Huang et al. *Applied Physics Letters*, 124, 182201 (2024)



Nanostructuring.png



Thermalconductivity.png

Multi-scale temperature distribution for metal nano-particle solutions under CW illumination

Tuesday, 21st April - 16:50: Poster I - Poster

Mr. Mathis Noell¹, ***Prof. Carsten Henkel***¹

1. University of Potsdam, Institute of Physics and Astronomy

We present a multiple-scale framework for describing steady-state temperature distributions in solutions of metal nano-particles under continuous-wave illumination. The particles are modeled as point-like heat sources embedded in a homogeneous medium, leading to a heat equation with singular source terms. To account for the intrinsic disorder of a nano-particle solution, the temperature field is decomposed into a macroscopic background contribution and a microscopic temperature peaked around the nearest nano-particle. The microscopic problem is formulated within an effective volume per particle and solved under boundary conditions that suppress heat flux across neighboring volumes. This construction ensures exact recovery of the underlying point-source heat equation while providing a physically transparent separation of length scales. The resulting framework allows to understand heating and steady-state temperatures in light-absorbing suspensions.

Transient nonlinear transmission of thin gold nano-layers due to infrared pumping

Tuesday, 21st April - 16:50: Poster I - Poster

**Ms. Helena Poulouse¹, Mr. Mathis Noell², Ms. Athena Majlesi², Dr. Wouter Koopman²,
Prof. Carsten Henkel³, Prof. Rike Müller-Werkmeister¹**

1. University of Potsdam, Institute of Chemistry, Germany, 2. University of Potsdam, Institute of Physics and Astronomy, 3. Uni Potsdam

Infrared spectroscopy is a versatile analytic tool in physics and chemistry because organic and other substances can be identified from their spectral fingerprints. In this context, thin layers of noble metals are used quite frequently, for example in electrochemistry, as functionalised surfaces in attenuated total reflection (shift of surface plasmon resonance), in surface-enhanced IR absorption (SEIRA), to name a few. In Potsdam, we are interested in the impact of strong coupling between molecular vibrations and microcavity modes on energy transport and chemical reactions [1].

Our ultrafast techniques like transient IR transmission and two-dimensional spectroscopy [2] typically require high fluences (100 $\mu\text{J}/\text{cm}^2$) to achieve decent signal levels. We have observed a nonlinear response of gold layers with thicknesses in the 10-50nm range. This complicates the interpretation of transient IR signals. Although the pulses are far from the visible range and the surface plasmon resonance, the explanation is likely that a pump pulse deposits enough heat in the free electrons of the metal to transiently change its dielectric function. Due to the small electronic specific heat, transient electron temperatures up to 1000K may appear. This can be modelled with a shift of the carrier density and of the Drude scattering rate on time scales of up to 10ps, where electrons are not yet in equilibrium with the gold ion lattice (two-temperature model [3]). We apply transfer matrix theory to simulate the transmission of the IR cavity with hot layers and propose to disentangle metallic and molecular nonlinearities by comparing with experimental observations.

[1] *Strong Light-Matter Coupling*, edited by A. Auffèves et al., World Scientific 2014; J. A. Hutchison, T. Schwartz, C. Genet, E. Devaux, and T. W. Ebbesen, *Angew. Chem. Int. Ed.* **51** (2012) 1592–96; N. Azarova, A. J. Ferguson, J. van de Lagemaat, E. Rengnath, W. Park, and J. C. Johnson, *J. Phys. Chem. Lett.* **4** (2013) 2658–63.

[2] P. Hamm and M. Zanni, *Concepts and Methods of 2D Infrared Spectroscopy*, Cambridge University Press 2011; H. M. Müller-Werkmeister, Y.-L. Li, E.-B. W. Lerch, D. Bigourd, and J. Bredenbeck, *Angew. Chem. Int. Ed.* **52** (2013) 6214–17.

[3] V. E. Gusev and O. B. Wright, *Phys. Rev. B* **57** (1998) 2878–88; N. Singh, “Two-Temperature Model of Nonequilibrium Electron Relaxation: A Review”, *Int. J. Mod. Phys. B* **24** (2010) 1141–58.

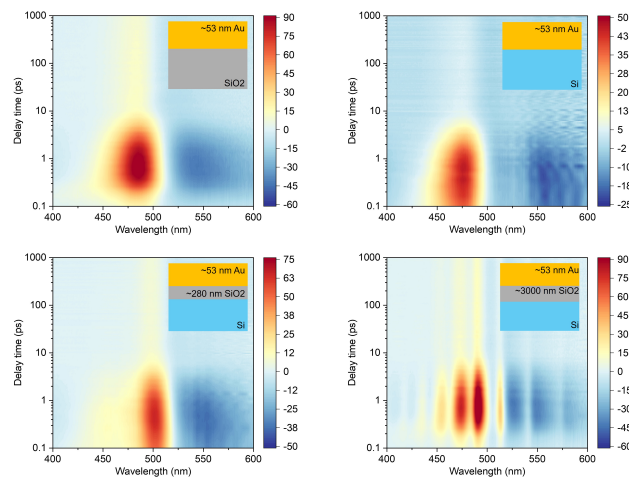
Broadband ultrafast probing of nonequilibrium interfacial thermal conductance in Au/substrate heterostructures

Tuesday, 21st April - 16:50: Poster I - Poster

*Dr. Zhicheng Chen*¹, *Prof. Qiye Zheng*¹

1. The Hong Kong University of Science and Technology

As microelectronic devices continue to scale down to the nanoscale, interfacial heat transfer between metals and non-metals becomes a critical bottleneck for thermal management. In metals, heat is carried by both electrons and phonons, leading to complex nonequilibrium energy transport at nanometer length scales and ultrafast time scales. Conventional interfacial thermal conductance (ITC) measurements, typically performed at a single probe wavelength, provide an incomplete description of these dynamics. Here, we investigate the visible-wavelength (400–600 nm) ultrafast thermal dynamics of 50 nm gold films deposited on Si, SiO₂, and SiO₂/Si substrates using time-domain thermoreflectance (TDTR). Broadband pump-probe measurements combined with global fitting using the Drude-Lorentz optical model, the two-temperature model, and electromagnetic field calculations enable extraction of ITC. The results show that optical transmission through the 50 nm gold film is non-negligible, and that non-transparent substrates strongly modify the transient reflectivity response. Notably, surface plasmon polariton-mediated thermal radiation is found to significantly enhance interfacial heat transfer in the Au/SiO₂/Si system. This work demonstrates the importance of broadband probing and nonequilibrium modeling for accurately characterizing interfacial heat transport in nanoscale metal-based structures.



1.jpg

Polyvinyl Alcohol Silicon Dioxide Composite Material for Daytime Radiative Cooling

Tuesday, 21st April - 16:50: Poster I - Poster

Dr. Armande HERVE¹, Mr. Yufei Yan¹, Ms. Rameeja Abdul Rasheed², Ms. Dhanya Jacob², Prof. Tarik Bourouina¹, Prof. Aldrin Antony², Dr. Elyes Nefzaoui¹

1. *ESYCOM, Univ. Gustave-Eiffel, France*, 2. *Department of Physics, Cochin University of Science and Technology, Cochin, Kerala 682022, India*

Global warming increases the need for effective thermal management, especially in urban areas affected by heat-island effects. Radiative cooling provides electricity-free daytime cooling by combining high reflectance in the solar spectrum with strong thermal emission in the 8-13 μm atmospheric window. Materials designed with these properties can reach lower temperatures than conventional surfaces and, in some cases, below ambient air temperature.

In this work, we investigate polyvinyl alcohol (PVA) composites containing SiO_2 microspheres as potential radiative cooling coatings, with a view to cost-effective and scalable integration in building applications. The radiative properties of several PVA composite formulations were characterized, revealing promising cooling performance and significant room for further optimization, as illustrated in Figure 1.

From these properties, we calculated the contribution of each term to the overall radiative cooling and estimated the cooling power potential of each PVA film, as presented in Figure 2.

We also evaluated the most promising formulation in an outdoor radiative cooling experiment with continuous monitoring over a 24-hour cycle.

Based on spectral measurement and outdoor tests, the PVA-based composites achieved substantial cooling, with temperature reductions of around 5°C below ambient over the day-night period and peak cooling performance of up to 7 °C below ambient under maximum solar irradiance.

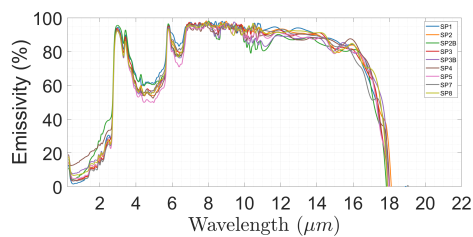


Figure1.png

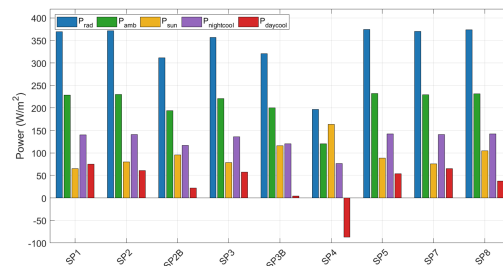


Figure2.png

Local probing of ion-doped regions of silicon carbide crystal via MIR photo-thermo-mechanical excitation of scanning probes

Tuesday, 21st April - 16:50: Poster I - Poster

Mr. Michael O'Shaughnessy-Gutierrez¹, Dr. Rajasekhar Medapalli¹, Mr. Samuel Eserin², Ms. Xinyun Liu³, Ms. Ella Schneider⁴, Dr. Jessica Boland³, Prof. Ben Murdin², Dr. Alexandros Elsachat⁵, Prof. Oleg Kolosov¹

1. Physics department, Lancaster University, 2. Physics Department, University of Surrey, 3. Department of Materials, University of Manchester, UK, 4. Surrey Ion Beam Centre, University of Surrey, UK, 5. National Center for Scientific Research "Demokritos"

Combining nanoscale resolution of scanning probe microscopy (SPM) with chemical sensitivity of vibrational microscopy using either mid-infrared (MIR) light absorption, or inelastic (Raman) light scattering, allows to reveal key chemical features of nanoscale materials, devices and biological objects. Any such technique relies on transduction of local spectroscopic information to the response of the scanning probe. One of highly efficient methods is a detection of the local temperature rise of the absorbed MIR light via local photo-thermomechanical (PTM) expansion of the sample surface probed by the atomic force microscope (AFM) cantilever with nanoscale tip in contact with sample, the AFM-IR [1].

For typical MIR non-transparent samples, the AFM-IR requires efficient top illumination of the area of AFM tip while minimising the effects of spurious PTM response due to direct heating of the AFM cantilever, using either quantum cascade lasers (QCL) that can be modulated at MHz frequencies, or a free electron laser (FEL) producing only short powerful pulses of microsecond duration at a very low (a few Hz) repetition rate.

Here we report mapping of the spatial PTM response of the AFM cantilever in contact with the measured sample using the QCL excitation at 10 μm wavelength modulated at the contact resonance frequency, in one of the operational modes of novel HiWiN system at Radboud University. By comparison of reflected MIR light map (Fig.1a) with the PTM response (Fig1,b), we found that PTM response is relatively constant for the beam positioned along the central line of the AFM cantilever, with a slight amplitude increase at the cantilever base. At the same time, the light focused at some distance off the apex of the tip (about two MIR wavelength) produces much larger localised PTM response with the lateral dimensions of about 20x20 μm (Fig 1 b).

We then located the implanted areas using AFM topography mapping that picks-up areas of the high implantation dose (Fig 1c), and nanomechanical mapping via ultrasonic force microscopy (UFM), sensitive to the lower doses, possibly via strain generated by the implantation (Fig.1d). Finally, we measure the local PTM response of ion-implanted SiC sample using QCL in 8-11 μm wavelength range and absorption of SiC substrate using FEL in the broader wavelength range from 10 to 20 μm (Fig.1e).

This work is funded by the European Union (ERC, TheMA, 101117958)

[1] Dazzi A, et al, *Appl Spectroscopy* **66**, 1365-1384 (2012).

[2] <https://hiwin-felix.org/>

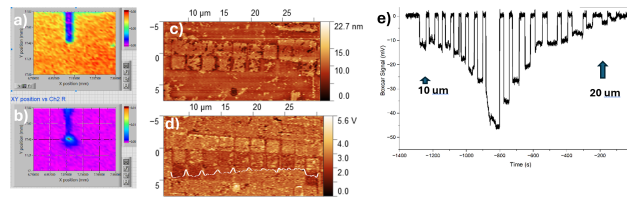


Figure 1. Maps of a) light reflection and b) photo-thermo-mechanical (PTM) response of the AFM cantilever to MIR excitation; c) AFM topography and d) UFM nano-mechanical maps, the line profile in d) shows detection of the implanted areas, e) wavelength sweep of FEL PTM response on SiC (10 to 20 μm , 1 μm increments).

Afm-ir fig 1.png

Analogy between the thermal emission of nano objects and Hawking's radiation

Tuesday, 21st April - 16:50: Poster I - Poster

Prof. Karl Joulain¹

1. University of Poitiers

We analyze in this work some analogies between thermal emission of nano objects and Hawking's radiation. We first focus on the famous expression of the black hole radiating temperature derived by Hawking in 1974 [1] and consider the case of thermal emission of a small aperture made into a cavity (Ideal Blackbody). We show that an expression very similar to Hawking's temperature determines a temperature below which an aperture in a cavity cannot be considered as a standard blackbody radiating like T^4 . Hawking's radiation therefore appears as radiation at a typical wavelength which is of the size of the horizon radius. In a second part, we make the analogy between the emission of particle-anti particle pairs near the black hole horizon and the scattering and coupling of thermally populated evanescent waves by a nano objects. We consider two different systems. The first one is a disk constituted of a material supporting surface waves. The analog of the particle-anti particle pairs separated by a black hole horizon are here the thermally populated surface waves scattered by the disk [2]. We show that this scattering occurs for a typical temperature taking the form of an analog of an Hawking temperature where the Schwarzschild radius is replaced by the disk radius. In a second situation, we consider a spherical object and show that for suitable permittivities, thermal emission scales as T^2 below a typical temperature here again very similar to the Hawking temperature.

[1] S.W. Hawking. Black Hole Explosions? *Nature*, 248:30–31, 1974.

[2] Karl Joulain, Younes Ezzahri, and Remi Carminati. Thermal emission by a subwavelength aperture. *Journal of Quantitative Spectroscopy and Radiative Transfer*, 173:1–6, April 2016.

Near-field radiative heat transfer in plasmonic nanobubbles

Tuesday, 21st April - 16:50: Poster I - Poster

Dr. Sreyash Sarkar¹, Mr. Jerome Sarr¹, Prof. Olivier Merchiers¹, Dr. P-Olivier Chapuis¹

1. CETHIL, CNRS-INSA Lyon, France

Illuminating metallic nanoparticles spread into liquid environment enables localized heating, generating nanobubbles around the particles with applications in optical hyperthermia, microbiology, and solar thermal systems [1]. This process involves complex dynamics associated with vaporization, molecular heat transfer, and multiple scattering of light. However, the radiative thermal interactions in such systems, especially for nanoparticles smaller than Wien's wavelength (few micrometers), have been overlooked, while effects such as apparent nanoparticle emissivity exceeding unity and near-field photon tunnelling between the nanoparticle and liquid being present certainly requiring accurate description. In order to address this issue, we use fluctuational electrodynamics, incorporate electric and magnetic dipole contributions within a spherical cavity, and compare results to those of Mie theory, therefore accounting for multireflections and wave-related effects in a nanoparticle-bubble-liquid system. Interestingly, we include the small-thickness regime of the bubble, which requires accounting for nonlocal effects in the metal and the liquid (here gold and water [2]). In the local regime, original results are observed, such as temperature-dependent scaling deviating from classical Stefan-Boltzmann predictions, with radiative power scaling as T^2 for small bubbles and $T^{5.5}$ particle for larger ones at elevated temperatures. Volumetric near-field absorption exhibits a sixth-power dependence on distance from the origin and a third-power dependence on bubble size, with resonant water spectral features dominating radiative exchange. These findings enhance the understanding of radiative heat transfer in confined nanoparticle-liquid systems.

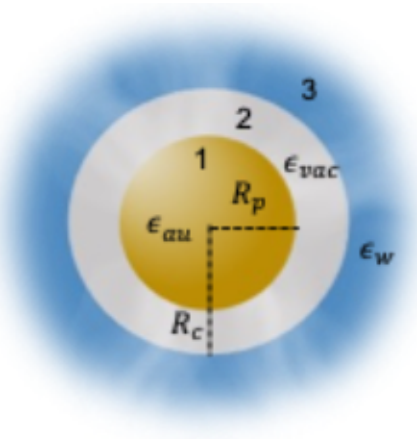
Fig. 1. Gold nanoparticle surrounded by a bubble and water.

Fig. 2. Thermal radiative exchange between the gold nanoparticle and water as a function of the bubble thickness. Blue: macroscopic thermal radiation (erroneous) prediction.

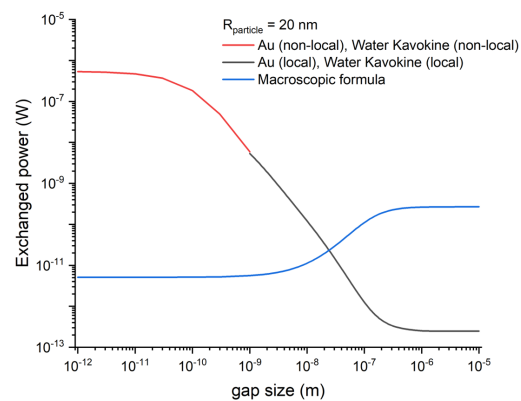
[1] M. Lukianova-Hleb et al., Plasmonic nanobubbles for biomedical applications, *Nano Today* 30, 100785 (2020).

[2] N. Kavokine et al., *Nature* 602, 84 (2022)

We acknowledge funding from ANR project CASTEX, and discussions with S. Merabia.



Sreyashsarkar-fig1.png



Sreyashsarkar-fig2.png

Near-field thermophotovoltaic conversion at room temperature with low-energy bandgap cells made of interband-cascade structure

Tuesday, 21st April - 16:50: Poster I - Poster

Mr. Mathieu Thomas¹, **Dr. Basile Roux**², **Dr. Lu Li**³, **Dr. Jeremy A. Massengale**³, **Prof. Rui Q. Yang**³,
Prof. Michael B. Santos³, **Dr. Rodolphe Vaillon**⁴, **Dr. P-Olivier Chapuis**¹

1. CETHIL, CNRS-INSA Lyon, France, 2. IES, Université de Montpellier, CNRS, Montpellier, France, 3. University of Oklahoma, Norman, USA, 4. LAAS-CNRS, Université de Toulouse, CNRS, Toulouse, France

Radiative heat exchange is strongly enhanced when the distance between a hot emitter and a room-temperature receiver decreases to a size below the spectrum characteristic wavelength. It is typically given by Wien's wavelength, i.e. 10 μm for an emitter close to room temperature and 3 μm for an emitter around 1000 K. Such increase of thermal radiation can be beneficial for thermal-energy harvesting, for instance by converting the radiated flux into electrical power by thermophotovoltaics (TPV). In TPV, another size enters into play: the cell's bandgap wavelength. Indeed, if the radiation emitted below the bandgap wavelength is only a fraction of the total flux, TPV is inefficient. While TPV cells with bandgap wavelength in near infrared are well established (i.e. at bandgap energies above 0.7 eV, like Ge, Si or GaAs for instance), cells with bandgaps tailored for mid-infrared (i.e. below 0.5 eV) are still in their infancy [1]. Experiments with single-junction cells in InAsSb at room temperature (0.3 eV) [2] or InSb cooled at 77 K (0.25 eV) [3] have been demonstrated, but room-temperature operation of an efficient low bandgap-energy cell is still required. Here, we report on near-field thermophotovoltaic conversion at room temperature by means of an advanced interband cascade architecture [4], which aims at converting infrared thermal radiation. The cells are made of multiple junctions in order to avoid large current that lead to self-heating. Our emitter is a graphite microsphere glued to an atomic-force microscope tip [3], which is brought toward contact of the sample and allows determining power-distance curves as a function of emitter temperature in the sub-1 μm distance regime. Analyzing the data, we are able to estimate the power and efficiency of a size-optimized parallel-plate device, which would allow reaching power density of 200 $\text{W}\cdot\text{m}^{-2}$ for emitter temperatures below 1000 K, well below those typically required for TPV.

Fig. 1. Schematic of experiment

Fig. 2. Power-voltage curves at tip-cell distance of $\sim 2 \mu\text{m}$

Fig. 3. Generated photocurrent as a function of emitter-cell distance. The green area is due to near-field TPV conversion.

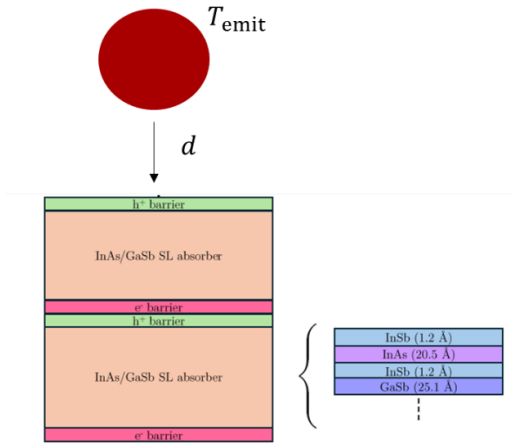
[1] B. Roux et al., *Journal of Photonics for Energy* 14, 042403 (2024)

[2] A. Fiorino et al., *Nature Nanotechnology* 13, 806 (2018)

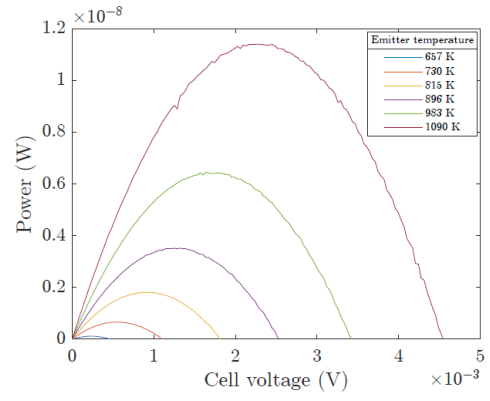
[3] C. Lucchesi et al., *Nano Letters* 21, 4524 (2021)

[4] R. Yang et al., *Solar Energy Materials and Solar Cells* 238, 111636 (2022)

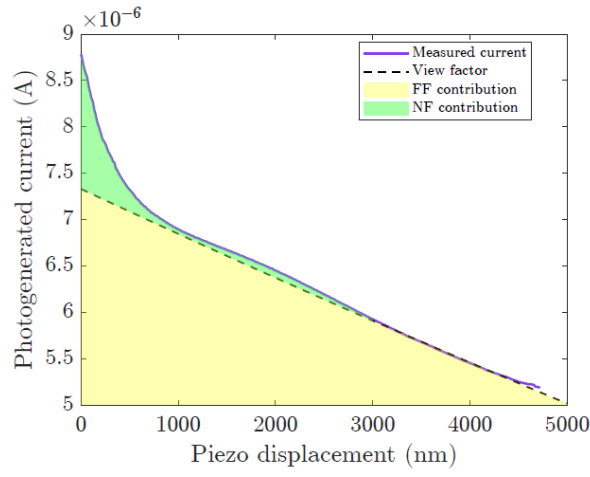
We acknowledge funding from EU project TPX-Power and ANR projects STORE and Low-Gap-TPV.



Mathieuthomas-fig1.png



Mathieuthomas-fig2.png



Mathieuthomas-fig3.png

High order anharmonicity in the thermal conductivity of Transition Metal Dichalcogenides

Tuesday, 21st April - 16:50: Poster I - Poster

Ms. Marta Loletti¹, Dr. Qi Ren¹, Dr. Riccardo Rurali¹

1. Institut de Ciència de Materials de Barcelona, ICMAB-CSIC, ES-08193 Bellaterra, Spain

In 2D semiconductors' field, transitional metal dichalcogenides (TMDs) have a strong and prominent position due to their favourable properties. A direct bandgap and the possibility of constructing van der Waals layered systems that enable the tuning of electronic, optical and mechanical properties make them great materials for flexible electronic and thermoelectric sensors [1]. An accurate understanding of phonon transport in two-dimensional materials is a fundamental challenge for the design of next-generation devices. In layered materials of the TMDs family, the contribution of four-phonon scattering has recently been found to be crucial for correctly describing thermal properties [2].

Preliminary results from our group are already available for MoTe₂ material in its two polymorphic phases 2H and 1T' by resolving the Boltzmann transport equation (BTE) with the inclusion of four-phonon scattering. For the 2H polymorph, adding this contribution results in a substantial reduction in thermal conductivity compared to the three-phonon limit. However, for the 1T' one, this effect is negligible, indicating a saturation of scattering processes already at the third order. This discrepancy in behavior indicates that the significance of the fourth order is not consistent across all systems but rather dependent on the specific crystal structure and the nature of the phonon modes involved. However, despite its accuracy, the canonical DFT-BTE approach is extremely computationally intensive in most cases. This makes it difficult to conduct a systematic study on a wide range of materials and phases. To overcome this limitation, in this work we propose the use of the machine-learning potential based MACE [3], a pre-trained framework capable of reproducing with high fidelity the potential energies obtained from DFT, drastically reducing the computational cost. We then present a benchmark study to evaluate the impact of the four-phonon contribution in TMDs. Our aim is to verify whether this contribution is relevant only for specific materials or polymorphs, and to determine which structural or electronic factors depend on it. The results pave the way for a more efficient and generalizable approach to phononic transport engineering, with implications for the design of thermoelectric materials and heat management in 2D devices.

[1] Nat Rev Mater 2, 17033 (2017)

[2] Materials Today Physics 40, 101314 (2024)

[3] arXiv:2401.00096 [physics.chem-ph]

Calibration of Scanning Joule Expansion Microscopy for nanoscale heat transport studies

Tuesday, 21st April - 16:50: Poster I - Poster

Dr. JaeHwan Jeong¹, Dr. Diego Alonso Aldave¹, Prof. Julio Gómez-Herrero¹, Dr. Pablo Ares²

1. Departamento de Física de la Materia Condensada, IFIMAC and INC, Universidad Autónoma de Madrid, 28049, Madrid, Spain, 2. Departamento de Física de la Materia Condensada, Universidad Autónoma de Madrid, Madrid, Spain

Nanoscale thermal measurement is an important aspect of current technological developments. Atomic Force Microscopy (AFM) is a widely used technique to analyze nanoscale properties of surfaces, including thermal properties. Among the AFM thermal analysis techniques, Scanning Thermal Microscopy (SThM) is predominantly used for thermal property measurements. However, SThM has several limitations, including the need for expensive specially fabricated probes, customized electronic instrumentation for the SThM probe, and lateral resolution lower than standard AFM measurements.^[1]

Several alternative AFM-based thermal measurement techniques have been explored to address the limitations of SThM. Scanning Joule Expansion Microscopy (SJEM)^[2] stands out as an alternative candidate for studying thermal properties at the nanoscale. SJEM measures the thermal properties of surfaces through thermal expansion. It offers several advantages, such as high lateral resolution due to the use of standard probes, ease of use, fast measurement, and versatile probe and instrument choices. These attributes make SJEM an attractive tool for studying heat transport, especially in two-dimensional (2D) materials.^[3]

Despite its benefits, SJEM remains essentially a qualitative technique: it provides relative information about heat transfer speed and does not provide quantitative temperature values. To address the hurdles limiting the wider adoption of SJEM, we aim to develop a calibration process that converts SJEM into a quantitative tool for studying heat transport processes.

In this talk, I will present various techniques and their requirements to be employed to calibrate the SJEM measurements. Through the comparison of thermal decomposition of viral particles, Raman thermometry using silicon nanoparticles (Si NPs), and Finite Element Method (FEM) simulations onto specifically fabricated microheater circuits, SJEM can be calibrated and used to measure thermal profiles of surfaces for various materials and structures.

References

- [1] Zhang, Y., Zhu, W., Hui, F., Lanza, M., Borca-Tasciuc, T., & Muñoz Rojo, M. *Advanced functional materials*, 30(18), 1900892. (2020)
- [2] de Pablo, P. J., Colchero, J., Gómez-Herrero, J., Serena, P. A., & Baró, A. M. *Nanotechnology*, 12, 113. (2001)
- [3] Grosse, K. L., Dorgan, V. E., Estrada, D., Wood, J. D., Vlasiouk, I., Eres, G., ... & Pop, E. *Applied Physics Letters*, 105(14). (2014)

Cross-plane thermal conductivity in MXenes

Tuesday, 21st April - 16:50: Poster I - Poster

Mr. Oscar Mateos-Lopez¹, **Mr. Isaac Armstrong**², **Ms. Elvira Tornero**¹, **Dr. Miguel Muñoz**¹, **Prof. Hendrik Heinz**², **Dr. Guilherme Vilhena**¹, **Prof. Juan Carlos Cuevas**³

1. Instituto de Ciencia de Materiales de Madrid, Madrid, Spain, 2. University of Colorado Boulder, 3. Departamento de Física Teórica de la Materia Condensada, Universidad Autónoma de Madrid

Two-dimensional (2D) transition metal carbides and nitrides, known as MXenes, have emerged as a promising family of materials for thermal management applications due to their unique combination of high electrical conductivity and extreme thermal anisotropy. With the general formula $M_{n+1}X_nT_x$ (where M is a transition metal, X is carbon/nitrogen, and T represents surface terminations), MXenes offer tunable properties via surface chemistry. However, their development is hampered by significant discrepancies in reported cross-plane thermal conductivity values, which vary by nearly an order of magnitude across recent experimental studies [1].

In this work, we address this puzzle through a systematic theoretical investigation of the cross-plane thermal transport in $Ti_3C_2T_x$ using non-equilibrium molecular dynamics (NEMD) simulations. We demonstrate that the observed discrepancies result from differences in the stereo-chemical repulsion between layers, which is dictated by the diverse nature of surface terminations (e.g., -O, -OH, -F). Our results unveil that thermal boundary resistance is ultimately controlled by these termination groups in a rather unexpected manner, which is unnoticeable from x-ray or other structural or bulk-phase analysis. Our findings not only clarify the mechanism behind the intrinsic low cross-plane thermal conductivity of MXenes but also highlight the critical importance of controlling surface terminations, and hence emphasizing the importance of transitioning from a solution-based to a bottom-up growth that offers a high degree of control on such terminations.

1. T. Hasan, C. Park, S. M. Naqvi, J. Kim, H. Kim, Z. Khalid, S. Jung, Y. Gogotsi, C. M. Koo, ACS Nano, **19**, 48, 40703-40732 (2025)

Fabrication of large-area, suspended twisted WS₂ bilayers

Tuesday, 21st April - 16:50: Poster I - Poster

Mr. Daniel Capolat Palomar¹, Mr. JiaQi Yang¹, Mr. Pu Tan¹, Dr. Timm Swoboda¹, Dr. Maria Jose Esplandiu¹, Prof. Javier Rodriguez-Viejo², Dr. Marianna Sledzinska¹

1. Catalan Institute of Nanoscience and Nanotechnology, 2. Universitat Autònoma de Barcelona, Campus UAB, ES-08193 Bellaterra, Spain

Since the discovery of the magic angle in twisted bilayer graphene, twisted bilayer systems have attracted substantial research interest due to their potential for next-generation electronic devices. These structures exhibit a wide range of emergent phenomena, including strongly correlated electronic states and significant modifications of electronic and phononic band structures, with properties that can be efficiently tuned via the relative twist angle between layers [1,2]. Among the most intensively studied materials in this context are transition metal dichalcogenides (TMDs), a class of semiconducting van der Waals materials [3].

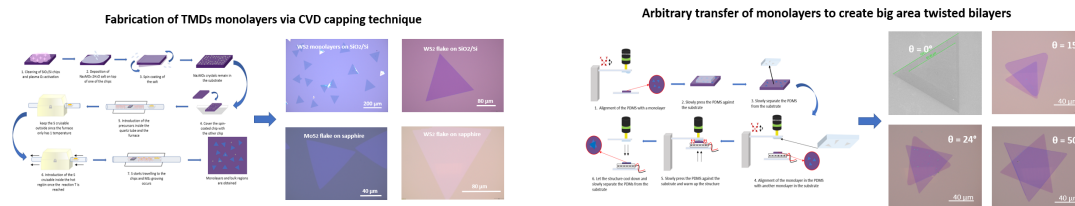
With respect to thermal transport, molecular dynamic simulations predict a pronounced anisotropy between in-plane and cross-plane thermal conductivities in twisted TMD bilayers, strongly dependent on the angle.

To experimentally confirm this theory, a combination of measurements on the supported and free-standing samples should be performed to obtain the cross- and in-plane components of the thermal conductivity, respectively. In particular, the in-plane thermal measurements require large-area, suspended samples [4], which are still challenging to achieve.

The present work focuses on the fabrication of twisted bilayer WS₂ samples featuring suspended regions of approximately 80 μm², suitable for in-plane thermal conductivity measurements via two-laser Raman thermometry. High-quality WS₂ monolayers with lateral dimensions up to 200 μm are grown by chemical vapor deposition and subsequently transferred with controlled rotational alignment to form twisted bilayers. These bilayers are then precisely transferred onto perforated substrates using a clean and alignment-controlled process to create large suspended areas. The resulting samples are characterized by photoluminescence spectroscopy, Raman spectroscopy, atomic force microscopy (AFM), and transmission electron microscopy (TEM) to assess structural quality and accurately determine the twist angle prior to in-plane thermal conductivity measurements. Experimental confirmation of the predicted thermal anisotropy would support the integration of twisted TMD bilayers into nanoscale electronic devices, where efficient thermal management remains a key challenge.

References

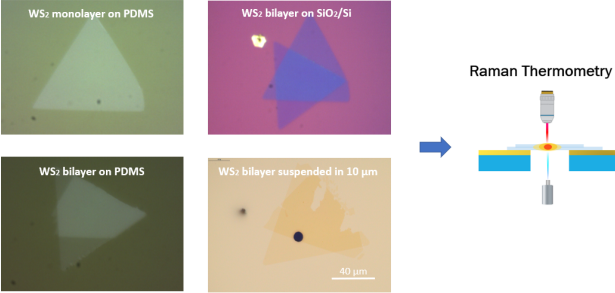
- [1] Cao, Y et. al. Nature 2018, 556 (7699), 43-50.
- [2] Tang, B et. al. Small Structures, 2(5).
- [3] Xiong, H et. al. ACS Applied Nano Materials 2023, 6 (17), 15685-15696.
- [4] Sledzinska, M. et. al. 2D Materials 2016, 3 (3), 035016



1.png

2.png

Samples for in-plane Raman thermometry



3.png

Enhancing phonon transmission across solid-superfluid helium interfaces by tuning phase coherence in nanometer-scale interlayer films

Tuesday, 21st April - 16:50: Poster I - Poster

***Dr. Jay Amrit*¹, *Prof. Kostiantyn Niemchenko*², *Dr. Varvara Luzik*², *Dr. Yehor Niemchenko*², *Dr. Akim Tonkonozhenko*², *Dr. Tetiana Vikhtynska*²**

1. LISN, Paris-Saclay University, CNRS, 2. V.N.Karazin Kharkiv National University

It has been demonstrated that the Kapitza resistance at a solid–superfluid helium interface is governed by phonon-scattering processes that occur on the scale of nanoscale boundary roughness [1–2]. Motivated by this, we investigate phonon transmission by introducing a nanoscale interlayer between superfluid ⁴He and the solid. The analysis is carried out within the acoustic-mismatch model, while explicitly accounting for phonon phase coherence in the interlayer. Because phonons in superfluid helium form an isotropic thermal gas, heat transfer involves a broad spectrum of wavelengths and incidence angles. This diversity gives rise to a rich set of wave phenomena at layered interfaces, including interference patterns, partial resonances, total internal reflection, and coupling to both bulk and surface modes. The presence of a thin film introduces additional channels for constructive interference, thereby increasing the number of conditions under which reflection—and thus thermal resistance—is suppressed.

Analytical expressions are derived describing phonon transmission through the three-layer system consisting of helium, film, and a solid substrate. A key result is that the maximum transmission is achieved when the film thickness L is comparable to the phonon wavelength in the interlayer material. Under this condition, multiple reflections within the film interfere constructively in the transmission direction, effectively canceling a significant part of the reflection at both interfaces. This mechanism is analogous to the operation of optical quarter-wave antireflection coatings but must account for the broad, temperature-dependent phonon spectrum characteristic of superfluid helium. The expressions obtained in this study provide a practical guide for selecting optimal impedance combinations and film thicknesses of different materials to enhance thermal coupling [3]. The proposed approach may serve as a foundation for developing advanced thermal management strategies in quantum technologies, cryogenic detectors, and ultra-low temperature experimental platforms where precise control of phonon transport is essential.

References

- [1]. A. Ramiere, S. Volz, and J. Amrit, *Nature Materials*, **15**, 512 (2016)
- [2]. I. N. Adamenko and I. M. Fuks, *Sov. Phys. JETP* **32**, 1123 (1971)
- [3]. J. Amrit, V. Luzik, K. Niemchenko, Ye. Niemchenko, A. Tonkonozhenko, T. Vikhtynska, submitted (2025)

Long-range radiative heat transfer along a Su-Schrieffer-Heeger chain coupled to a substrate

Tuesday, 21st April - 16:50: Poster I - Poster

***Dr. Alireza Naeimi*¹, *Dr. Florian Herz*¹, *Dr. Svend-Age Biehs*¹**

1. Carl von Ossietzky University Oldenburg

This work combines two efficient long-range heat flux mechanisms: surface waves and topologically protected edge modes. Substrate-excited surface waves are known to enhance long-range heat fluxes between objects [1, 2], and non-reciprocal materials can even enable uni-directional transfer similar to a thermal diode [3-5]. On the other hand, Su-Schrieffer-Heeger (SSH) chains in a topologically non-trivial phase support edge modes that facilitate dominant long-range radiative heat transfer [6]. The synergy of these two effects remains largely unexplored.

We demonstrate how an InSb substrate influences the SSH chain's band structure for the configuration in Fig.1. By adjusting the substrate's charge carrier density, we can control this interaction. We investigate the emergence of topological edge modes by calculating the Zak phase and evaluating the chain's eigenfrequencies in presence of the substrate. As shown in Fig.2, the emergence of these modes is evident in both in-plane and out-of-plane configurations.

Finally, we evaluate the heat transfer between the first and last particles of the SSH chain in Fig.3. The results indicate that the heat transfer length scale depends on the surface modes' propagation length. When this length exceeds the lattice constant, edge modes significantly enhance heat transfer in the non-trivial phase compared to the trivial phase. However, if the propagation length is restricted to the lattice constant, this enhancement occurs only in short chains of comparable length.

[1] J. Dong, J. Zhao, and L. Liu, *Long-distance near-field energy transport via propagating surface waves*, Phys. Rev. B **97**, 075422 (2018).

[2] R. Messina, S.-A. Biehs and P. Ben-Abdallah, *Surface-mode-assisted amplification of radiative heat transfer between nanoparticles*, Phys. Rev. B **97**, 165437 (2018).

[3] A. Ott, R. Messina, P. Ben-Abdallah, and S.-A. Biehs, *Radiative thermal diode driven by nonreciprocal surface waves*, Appl. Phys. Lett. **114**, 163105 (2019).

[4] Y. Zhang, C.-L. Zhou, H.-L. Yi, and H.-P. Tan, *Radiative Thermal Diode Mediated by Nonreciprocal Graphene Plasmon Waveguides*, Phys. Rev. Appl. **13**, 034021 (2020).

[5] A. Naeimi and S.-A. Biehs, *Efficiency and mechanism of heat flux rectification with non-reciprocal surface waves in Weyl-Semi-Metals*, Phys. Rev. Mat. **9**, 045201 (2025).

[6] A. Ott and S.-A. Biehs, *Radiative heat flux through a topological Su-Schrieffer-Heeger chain of plasmonic nanoparticles*, Phys. Rev. B **102**, 115417 (2020).

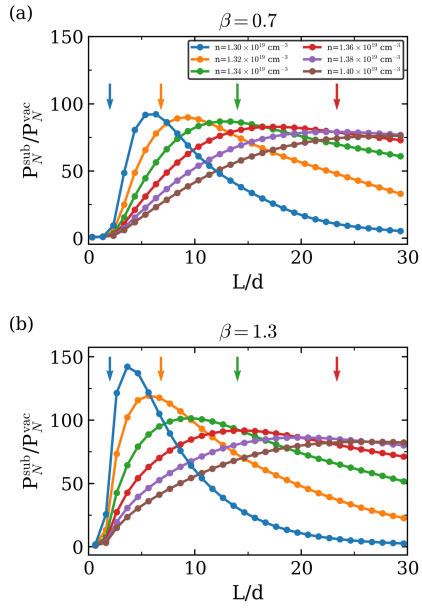


Figure 3: Total power P_N^{sub} received by particle N in nanoparticle chains with $N = 2, \dots, 60$ nanoparticles, i.e. with varying chain lengths L , normalized to the power P_N^{vac} of the same chain without substrate choosing different carrier concentrations n_{sub} in the substrate in topologically trivial (a) and non-trivial phase (b).

Fig3 cap.png

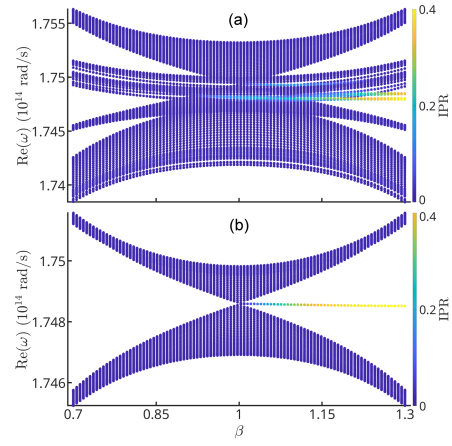


Figure 2: Real part of the in-plane (a) and out-of-plane (b) eigenfrequencies for a finite chain of 60 particles and charge carrier density of $n_{\text{sub}} = 1.36 \times 10^{19} \text{ cm}^{-3}$. The parameter $\beta = 2t/d$ characterizes the topological phase transition at $\beta = 1$. To highlight the edge modes, we introduce the inverse participation ratio (IPR) quantifying the mode's localization.

Fig2 cap.png

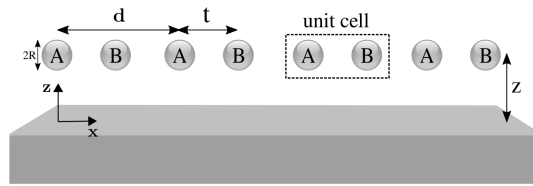


Figure 1: Sketch of the considered system. A bipartite SSH chain of nanoparticles of radius R with lattice constant d in each sublattice A and B and separation distance t within each unit cell is placed at a distance z in close vicinity of a semi-infinite planar substrate.

Fig1 cap.png

Phonon-defect scattering in reciprocal space

Tuesday, 21st April - 16:50: Poster I - Poster

***Mr. Alessandro Ciavatta*¹, *Prof. Lorenzo Paulatto*¹**

1. Sorbonne Universite

Since defect scattering theory was developed in the seventies, analytical models have been available to describe non-perturbative phenomena that govern the spectral and transport properties of phonons. The growth of computing power now makes it possible to solve the corresponding ab initio problem with high accuracy. Working in reciprocal space provides a clearer interpretation of the diagrammatic expansion and allows for an efficient interpolation of the phonon–phonon potential. This approach reaches the level of accuracy required to interpret disorder-activated spectroscopy and thermal transport in doped semiconductors.

Thermal metrology for phase change materials

Tuesday, 21st April - 16:50: Poster I - Poster

Mr. Tushar Chakrabarty¹, Dr. Akash Patil¹, Dr. Etienne Blandre², Dr. Pierre-Yves Cresson², Mrs. Yannick Le-Friec¹, Dr. Sarah Rubeck¹, Dr. Simon Jeannot¹, Prof. Emmanuel Dubois², Prof. Jean-François Robillard²

1. STMicroelectronics, 2. IEMN (Institut d'électronique de microélectronique et de nanotechnologie)

Our group at IEMN aims at developing a thermal metrology platform combining Raman Thermometry, 3ω , Scanning Thermal Microscopy and the Thermoreflectance method to fully characterize thermal transport in microelectronic devices. In this frame, we are currently working on quantifying the thermal properties of the materials used in phase change memory (PCM) devices: SiN (used as surrounding electrical insulator) and Ge-enriched GeSbTe (GGST) as phase change material. PCM has emerged as an alternative to its counterpart flash memories for non-volatile applications, and its performance is influenced by the thermal properties of these materials since it is thermally activated. The thermal conductivity and the thermal boundary resistance (TBR) between GGST and SiN influences the temperature field, thereby influencing the programming current [1]. In this study, we report on the thermal conductivity of SiN and GGST as well as the thermal boundary resistance (TBR) between them using 3ω method, and show that the GGST thermal conductivity value is consistent with earlier measurements using Raman thermometry. For this purpose, we have prepared two types of samples: SiN samples with varying SiN thickness (d_{SiN}) on Si wafers, and GGST samples consisting of a 55 nm SiN/GGST/55 nm SiN stacks with varying GGST thickness (d_{GGST}) on Si wafers.

The effective thermal resistance $R1$ obtained with the measurements of the third harmonic voltage $V_{3\omega}$ for the SiN samples can be expressed by:

$$R1 = (d_{\text{SiN}}/K_{\text{SiN}}) + \text{TBR}_{\text{Au-SiN-Si}} + R_{\text{Si}} \quad (1)$$

The corresponding graph is shown in Fig. 1, and $R1$ increases with the increase of SiN thickness. Fitting the results with equation 1 provides the SiN thermal conductivity, K_{SiN} as $0.91 \pm 0.01 \text{ Wm}^{-1}\text{K}^{-1}$ and $\text{TBR}_{\text{Au-SiN-Si}}$ as $1.8 \pm 1 \times 10^{-9} \text{ m}^2\text{KW}^{-1}$.

Next, 3ω measurements are done on GGST samples, and the thermal resistance of the SiN/GGST/SiN stack, $R2$ are plotted against d_{GGST} in Fig. 2.

$$R2 = (d_{\text{GGST}}/K_{\text{GGST}}) + (2 \times d_{\text{SiN}}/K_{\text{SiN}}) + 2 \times \text{TBR}_{\text{SiN-GGST}} + \text{TBR}_{\text{Au-SiN-Si}} \quad (2)$$

By fitting with equation 2, we obtained the GGST thermal conductivity of $0.39 \pm 0.01 \text{ Wm}^{-1}\text{K}^{-1}$ and the $\text{TBR}_{\text{SiN-GGST}}$ as $3.16 \pm 0.36 \times 10^{-8} \text{ m}^2\text{KW}^{-1}$. The K_{GGST} values obtained by 3ω method are in agreement with the value obtained by Raman Thermometry, as shown in Fig. 3.

These values are crucial as they can be incorporated in CAD simulations for optimizing PCM cell design and performance.

[1] S. Durai, et al., *IEEE Trans. Comput.-Aided Des. Integr. Circuits Syst.*, 39, 1834–1840 (2020).

[2] A. Patil et al., *J. Appl. Phys.* 136, 175102 (2024).

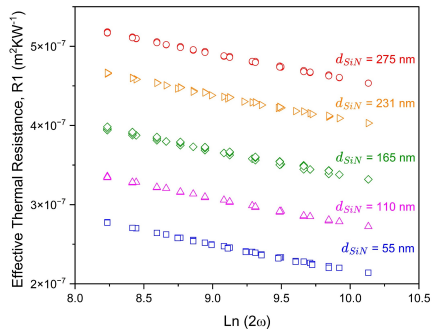


Fig. 1 Measured effective thermal resistance, R1 as a function of $\ln(2\omega)$ for several thickness (d_{SiN}) of SiN.

Sin effective thermal resistance.jpg

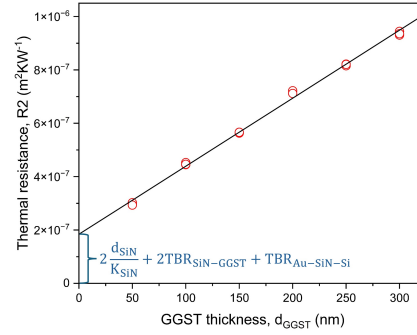


Fig. 2 Thermal resistance of SiN/GGST/SiN stack, R2 as a function of GGST thickness, d_{GGST} .

Sin-ggst-sin stack thermal resistance.jpg

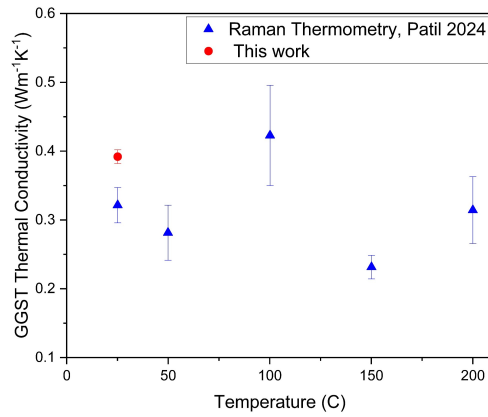


Fig. 3 As-deposited GGST thermal conductivity, K_{GGST} as a function of temperature.

Ggst thermal conductivity.jpg

Investigating Thermal Transport in Freestanding SrTiO₃ Membranes by Electro-Thermal Measurements

Tuesday, 21st April - 16:50: Poster I - Poster

***Mr. Dominik M. Koch*¹, *Dr. Jose Manuel Sojo Gordillo*¹, *Dr. Greta Segantini*², *Mr. Johannes Trautvetter*¹, *Dr. Aswathi K. Sivan*¹, *Dr. Riccardo Rurali*³, *Prof. Andrea Caviglia*², *Prof. Ilaria Zardo*¹**

1. University of Basel, 2. University of Geneva, 3. Institut de Ciència de Materials de Barcelona, ICMAB-CSIC, ES-08193 Bellaterra, Spain

Functional oxides attract significant attention due to their wide range of properties including superconductivity, ferroelectricity, ferromagnetism, and multiferroicity. This plethora of properties arises from the strong interactions between charge, orbital, spin, and structural properties, leading to a wide range of functionalities. Among functional oxides, perovskites stand out as one of the most versatile, thanks to their integrability as thin-films into silicon-based electronics. They are suitable for applications ranging from memory transistors to optical circuits, sensors, and transducers [1]. In addition to the intrinsic properties of the bulk crystals, the possibility of nanostructuring them in a thin-film fashion opens a further degree of freedom to control their properties [2]. However, the thermal behavior of this family of materials when shaped as thin-films radically changes and it has not been fully investigated yet.

In this work, the thermal properties of suspended SrTiO₃ films, with thickness between 30 and 200 nm are studied. The films were epitaxially grown onto a sacrificial layer of Sr₃Al₂O₆ using the pulsed laser deposition technique [3] and then transferred onto a substrate with patterned holes that allows to suspend them. Firstly, we study the temperature evolution of the phonon modes by Raman spectroscopy, as phonons are the fingerprint of the phase transition (from a cubic to a tetragonal). Secondly, a temperature dependent study of the in-plane thermal conductivity was conducted using a combination of the thermal bridge method [4] and the three probe technique [5], which uses a scanning laser as a heat source to correct for contact resistance. Finally, the experimental results were corroborated by second-principles density-functional theory calculations. This combination of Raman spectroscopy and electro-thermal measurements allows to relate the thermal properties with the phase-changes of the studied SrTiO₃ thin-films, highlighting the impact of structural phase transitions on their thermal behavior. Understanding these effects is key to optimize the integration of functional oxide thin films in novel advanced electronic devices.

[1] L. Han et al., *Advanced Functional Materials*, 2024, 34, 2309543.

[2] F. M. Chiabrera et al., *ANNALEN DER PHYSIK*, 2022, 534, 2200084.

[3] G. Segantini et al., *Nano Letters*, 2024, 24 (45), 14191-14197.

[4] L. Shi et al., *Journal of Heat Transfer*, 2003, 125, 881.

[5] D. Liu et al., *Nano Letters*, 2014, 14 (2), 806-812.

Temperature-dependent anisotropic thermal conductivity of rutile GeO₂ single crystals

Tuesday, 21st April - 16:50: Poster I - Poster

Mr. Pouria Emtenani¹, **Ms. Marta Loletti**², **Dr. Felix Nippert**¹, **Prof. Eduardo Bedê Barros**³, **Dr. Zbigniew Galazka**⁴, **Prof. Christian Thomsen**¹, **Dr. Sebastian Reparaz**², **Dr. Riccardo Rurali**², **Prof. Markus R. Wagner**⁵

1. Technische Universität Berlin, Institute of Physics and Astronomy, Hardenbergstr. 36, 10623 Berlin, Germany, **2.** Institut de Ciència de Materials de Barcelona, ICMA-B-CSIC, ES-08193 Bellaterra, Spain, **3.** Department of Physics, Universidade Federal do Ceará, Fortaleza, Ceará, 60455-760, Brazil, **4.** Leibniz-Institut für Kristallzüchtung, Max-Born-Str. 2, 12489 Berlin, Germany, **5.** Paul-Drude-Institut für Festkörperelektronik, Leibniz-Institut im Forschungsverbund Berlin e.V., Hausvogteiplatz 5–7, 10117 Berlin, Germany

Demand for power-electronics devices is growing rapidly, driven by higher efficiency and improved system reliability. Rutile germanium dioxide (r-GeO₂) is gaining attention as an Ultrawide Bandgap (UWBG) semiconductor candidate for power electronics with a 4.64 eV direct bandgap [1] and promising electronic properties, including high electron mobility and the ability to achieve high free-electron concentrations for n-type doping [2–4]. As in other UWBG candidates, heat removal limits device performance; to date, experimental κ values have been reported only for polycrystalline r-GeO₂ at room and elevated temperatures [5], while temperature-dependent directional measurements on single crystals have not been reported, to the best of our knowledge.

In this study, we used our home-built TDTR to measure the through-plane κ of single-crystal r-GeO₂ along the [001] and [110] directions. The crystals were grown by the Top-Seeded Solution Growth method at Leibniz-Institut für Kristallzüchtung [2]. Measurements were performed from 80 K to 350 K (Fig.1). At room temperature, we obtain $\kappa[001] = 47.5$ W/mK and $\kappa[110] = 32.5$ W/mK, corresponding to an anisotropy ratio of approximately 1.46. The anisotropy decreases with temperature and approaches near-isotropy at low temperature (Fig.2).

To interpret these trends, we compare our measurements with ab initio phonon-transport calculations based on density-functional theory and solution of the phonon Boltzmann transport equation. The calculations reproduce the temperature dependence and capture the evolution of anisotropy, indicating that phonon velocities are the predominant contributors: phonons with $v_z > v_x$ are concentrated in the mid-frequency range around ~10 THz, but at 80 K these modes are weakly populated and therefore contribute little to κ .

In addition, we extract the thermal boundary conductance, TBC(T), of the Al/r-GeO₂ interface for both orientations and observe that TBC decreases with decreasing temperature (Fig.3). Scaling TBC(T) by the r-GeO₂ lattice heat capacity integrated up to ~10 THz, $C_v(\leq 10$ THz), yields an almost temperature-independent behavior, indicating that elastic phonons are the primary heat carriers across the Al/r-GeO₂ interface and that transmission is limited by the ~10THz pass band of Al [6].

- [1] Mengle, K. A.; Chae, S.; Kioupakis, E. J. Appl. Phys. 126, 085703 (2019).
- [2] Galazka, Z. et al. Phys. Status Solidi B 2400326 (2024).
- [3] Bushick, K. et al. Appl. Phys. Lett. 117, 182104 (2020).
- [4] Takane, H. et al. Phys. Rev. Mater. 6, 084604 (2022).
- [5] Chae, S. et al. Appl. Phys. Lett. 117, 102106 (2020).
- [6] Koh, Y. R. et al. Phys. Rev. B 102, 205304 (2020).

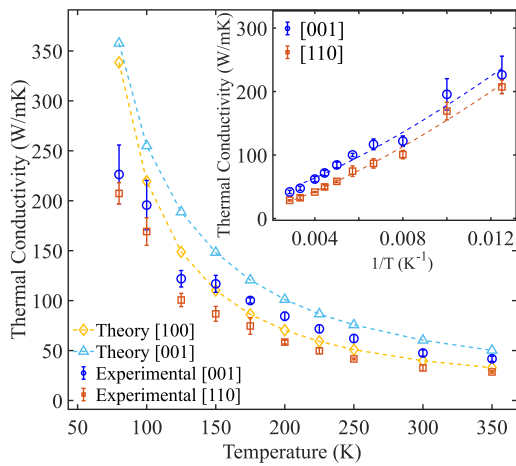


Fig.1.png

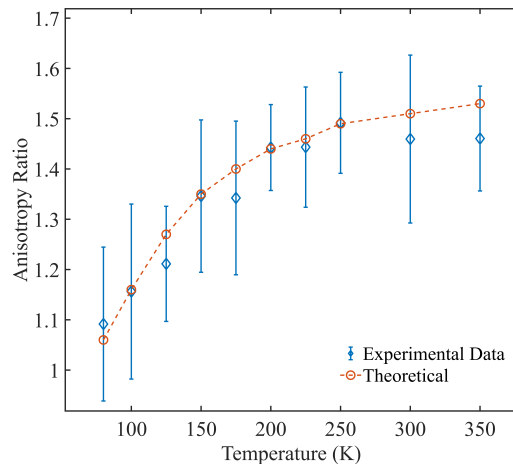


Fig.2.png

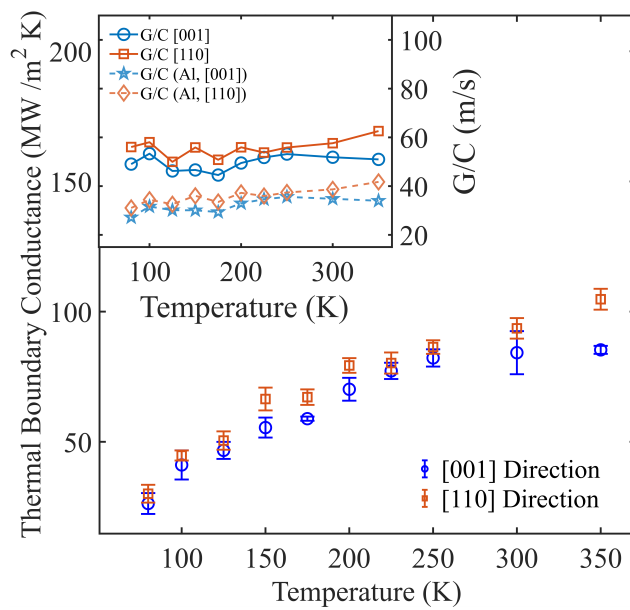


Fig.3.png

Heat Transfer at Interfaces: Mechanistic Insights from Molecular Dynamics Simulations

Wednesday, 22nd April - 09:00: Invited - Invited talk

Prof. Florian Müller-Plathe¹

1. Technical University of Darmstadt

This invited talk will give an overview over various applications of molecular-simulation methods of the thermal transport which were performed in our group. The focus will be on systems involving interfaces, which may be as varied as polymer nanocomposites, heat storage, droplet evaporation from surfaces, and even biological membranes. A central point is always the molecular mechanism of heat transfer and how it might be modified or exploited for different applications.

Selected references

- “Thermal Conductivity of a Carbon Nanotube – Polyamide-6,6 Composite: Reverse Nonequilibrium Molecular Dynamics Simulations”, M. Alaghemandi, M.C. Böhm, and F. Müller-Plathe, *J. Chem. Phys.* **135**, 184905 (2011). [DOI: 10.1063/1.3660348]
- “Evaporation of nanodroplets on heated substrates: a molecular dynamics simulation study”, J. Zhang, F. Leroy, and F. Müller-Plathe, *Langmuir* **29**, 9770–9782 (2013). [DOI: 10.1021/la401655h]
- “Molecular dynamics study on the thermal conductivity of the end-grafted carbon nanotubes filled polyamide-6.6 nanocomposites”, Y. Gao and F. Müller-Plathe, *J. Phys. Chem. C* **122**, 1412–1421 (2018). [DOI: 10.1021/acs.jpcc.7b11310]
- “Solid-liquid interface thermal resistance affects the evaporation rate of droplets from a surface: A study of perfluorohexane on chromium using molecular dynamics and continuum theory”, H. Han, C. Schlawitschek, N. Katyal, P. Stephan, T. Gambaryan-Roisman, F. Leroy, and F. Müller-Plathe, *Langmuir* **33**, 5336–5343 (2017). [DOI: 10.1021/acs.langmuir.7b01410]

From Amorphous to Amorphous-Crystalline Mixture Boron Nitride: Evolution of the Thermal Properties

Wednesday, 22nd April - 09:50: Amorphous and Heterogeneous Materials - Oral

Dr. Marianna Sledzinska¹, **Mr. JiaQi Yang**¹, **Mr. Onurcan Kaya**¹, **Dr. Thomas Souvignet**², **Dr. Peng Xiao**¹, **Dr. Emigdio Chavez**¹, **Dr. Catherine Marichy**², **Prof. Catherine Journet-Gautier**², **Prof. Stephan Roche**¹, **Prof. Clivia Sotomayor-Torres**³

1. Catalan Institute of Nanoscience and Nanotechnology, 2. Univ Lyon, ENS Lyon, UCBL, CNRS, Inria, LIP, F-69342, Lyon Cedex 07, France, 3. International Iberian Nanotechnology Laboratory (INL), Braga 4715-330, Portugal

2D boron nitride (BN) has gained significant attention as a nanoscale electrical insulator. Among its different polymorphs, hexagonal BN (h-BN), exhibits remarkable electrical, optical and thermal properties. It has been commonly used as a dielectric material for 2D material-based transistors, thanks to ultra-flat surface and dielectric constant ~ 3 in the out-of-plane direction^[1]. On the other hand amorphous BN (a-BN) is an emerging material with low dielectric constant (1.78-1.16), and high mechanical robustness, with applications in electronics^[2], batteries^[3] and coatings.

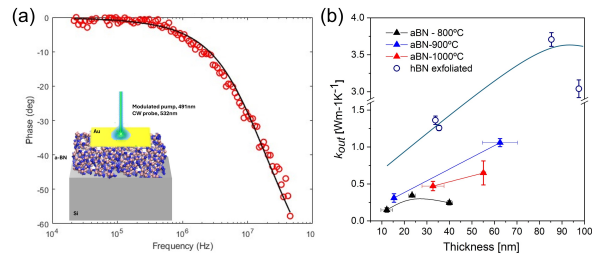
In this work, we show structural, thermal and elastic characterization of BN prepared by chemical vapor deposition using borazine precursor as a function of deposition temperature (800 – 1000 °C). Completely amorphous growth (a-BN) is achieved at 800°C, while partial crystallization becomes evident as the temperature increases to 900°C, resulting in a mixed amorphous-crystalline phase, where BN crystallites are embedded in an amorphous matrix. From 1000°C, the film starts to be mainly polycrystalline.

The cross-plane k of the aBN films was experimentally studied using frequency-domain thermoreflectance (FDTR) technique, closely resembling the gate dielectric-electrode interface. Effective aBN thermal conductivity k_{out} as a function of thickness and growth temperature is plotted in Fig3b. The k_{out} shows systematic increase as a function of increased film thickness, which is consistent with previous studies on the thermal properties of thin films. It can be attributed to the increased influence of the contribution from the thin film to the overall measured thermal conductance as the film thickness increases. A-BN synthesized at 800°C exhibits the lowest k_{out} , below 0.5 W/mK. With the increased synthesis temperature and improved crystalline structure, k_{out} increases to up to 1 W/mK. The experimental findings are compared to the theoretical predictions, modelled via classical equilibrium molecular dynamic (EMD) approach. Using EMD calculations, thermal conductivity, and spatial features of lattice vibrations (localized vs extended) were explored. The dependence of k as a function of degree of amorphization, sp²/sp³ ratio, film thickness and interface combinations were also addressed. Further, we also probe the change of thermal properties against the typical contaminants, such as carbon and oxygen.

[1] A. Pierret, et al. *Mater. Res. Express* **2022**, *9*, 065901.

[2] S. Hong, et al. *Nature* **2020**, *582*, 511.

[3] H. Kim, et al. *Nano Lett.* **2025**, *25*, 13850.



Picture2.jpg

Exact heat flux formula and its spectral decomposition in molecular dynamics for arbitrary many-body potentials

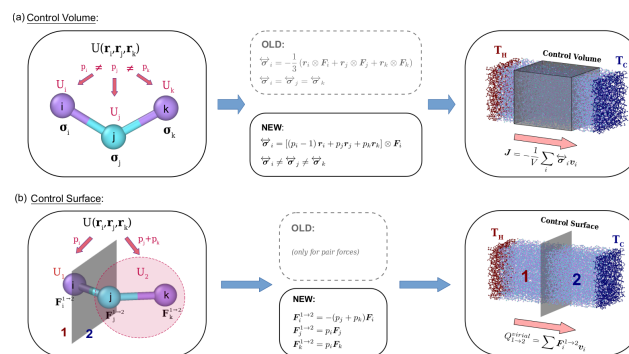
Wednesday, 22nd April - 10:10: Amorphous and Heterogeneous Materials - Oral

Prof. Konstantinos Termentzidis¹, Mr. Markos Poulos², Prof. Donatas Surblys³

1. cnrs, 2. CETHIL, CNRS-INSA Lyon, France, 3. Un. Tohoku

Molecular Dynamics (MD) is a powerful tool for studying the thermal properties of materials in the nanoscale. Within MD there are two principal and widely used methods for calculating thermal properties, namely the Green-Kubo (GK) method and the Non-Equilibrium MD (NEMD) method. The GK method is a statistical technique that uses the auto-correlation function of the instantaneous heat flux of a system in equilibrium to calculate the thermal conductivity κ from the fluctuation-dissipation theorem, while NEMD is based on the application of a temperature gradient to a system by means of connecting thermal reservoirs at a temperature difference ΔT . In both methods, the heat flux (HF) is a central quantity needed in order to calculate κ . For GK the time-dependent HF is calculated as an average over the system volume from the instantaneous atomic velocities and forces acting on the atoms. However, for GK, the calculation of the heat flux is based on the calculation of the atomic stress tensor, for which LAMMPS originally used a formula that is valid only for pair potentials

In this study the exact framework for the calculation of the HF and its spectral decomposition in MD for arbitrary many-body potentials have been derived. The current work addresses several lacks and limitations of previous approaches and allows for the accurate computational study of thermal properties in a wide variety of many-body systems with MD (see figure: Visualization of the HF calculation workflow for a 3-body interaction with arbitrary weights p_i . a. Average HF in a Control Volume, b. HF across a Control Surface). We have tested our modifications with GK and NEMD simulations for various 2D and 3D material systems using the Tersoff and Stillinger-Weber potentials as test examples. The spectral decomposition of the heat current was also calculated for 1ML graphene and MoS₂, for different system lengths. Our results show that the heat current calculated by our method is consistently in agreement with the thermostat current in NEMD, while previous implementations can estimate quite poorly the thermal conductivity both under GK and NEMD simulations, and both for 2D and 3D materials. The decomposition of the heat current also sheds light on the contribution of different phonon modes to thermal conductivity and its dependence on length. Our methodology is implemented in LAMMPS code specifically for the Tersoff and SW potentials, and it is applicable to the vast majority of many-body MD potentials.



Visual abstract.png

Heat management via polymers and colloids

Wednesday, 22nd April - 10:30: Amorphous and Heterogeneous Materials - Oral

Prof. Markus Retsch¹

1. University of Bayreuth

Controlling heat and cold across various scales is a key prerequisite to mitigating the severe effects of global warming. Mesoscale materials play a vital role in this context. The transport of temperature and heat is intricately governed by the material's composition, its interfaces, and its mesostructure.

In this presentation, I will comprehensively demonstrate how colloidal particles and polymers can contribute to heat management across various applications. Throughout the talk, I will emphasize the interplay among interfaces, order, disorder, percolation, and anisotropy in high and low thermal conductivity systems. Depending on the precise application, this will comprise particle-based systems, nanofiber structures, and bulk polymers. I will discuss how disorder in binary colloidal mixtures can lower the thermal conductivity by nearly 50%,¹ how silica nanospheres function as outstanding thermal insulators² (at least at ambient temperatures)³, and how anisotropic building blocks can influence temperature distributions.⁴ Engineering high thermal conductivity in polymer materials remains challenging. I will, therefore, discuss how polymer processing can contribute to this important capability.⁵ Heat spreading in nanofibrous nonwovens fundamentally depends on interfiber interactions and fiber alignment, which various external stimuli can further trigger. I will also elaborate on the anisotropic temperature spreading in such systems.

Overall, this presentation will focus on thermal conductance in polymers and colloids and provide, at times, unexpected insights into the interplay among composition, structure, and thermal transport.

(1) Nutz, F. A.; Philipp, A.; Kopera, B. A. F.; Dulle, M.; Retsch, M. Low Thermal Conductivity through Dense Particle Packings with Optimum Disorder. *Adv. Mater.* **2018**, *30* (14), e1704910. DOI: 10.1002/adma.201704910

(2) Ruckdeschel, P.; Philipp, A.; Retsch, M. Understanding Thermal Insulation in Porous, Particulate Materials. *Adv. Funct. Mater.* **2017**, *27* (38), 1702256. DOI: 10.1002/adfm.201702256.

(3) Neuhöfer, A. M.; Herrmann, K.; Lebeda, F.; Lauster, T.; Kathmann, C.; Biehs, S. A.; Retsch, M. High-Temperature Thermal Transport in Porous Silica Materials: Direct Observation of a Switch from Conduction to Radiation. *Adv. Funct. Mater.* **2021**, *32* (8), 2108370. DOI: 10.1002/adfm.202108370

(4) Lebeda, F.; Demleitner, M.; Pongratz, A.; Ruckdaschel, H.; Retsch, M. Shaping Thermal Transport and Temperature Distribution via Anisotropic Carbon Fiber Reinforced Composites. *ACS Omega* **2024**, *9* (37), 39232-39241. DOI: 10.1021/acsomega.4c06558

(5) Klein, I.; Tran, T.; Reiser, R.; Theis, M.; Rosenfeldt, S.; Schöttle, M.; Schirmeister, C.; Bösecke, P.; Rettinger, S.; Mülhaupt, R.; et al. High and tuneable anisotropic thermal conductivity controls the temperature distribution of 3D printed all-polyethylene objects. *Journal of Materials Chemistry A* **2023**, *11* (41), 22492-22502. DOI: 10.1039/d3ta04483a

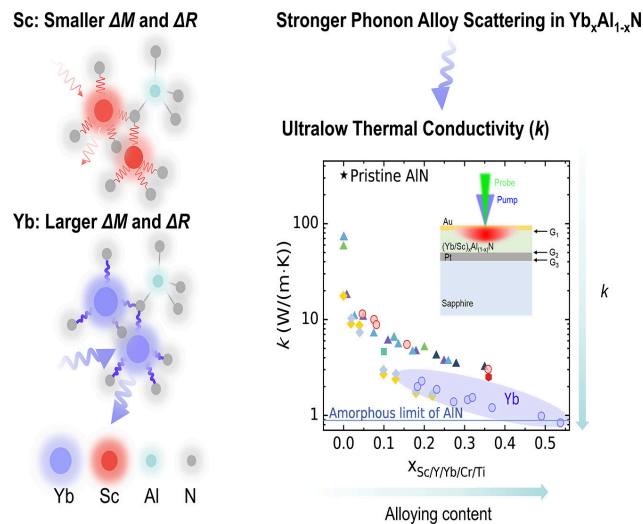
Tailoring thermal transport in (Sc,Yb)AlN thin films to the glassy limit

Wednesday, 22nd April - 10:50: Amorphous and Heterogeneous Materials - Oral

Prof. Qiye Zheng¹

1. The Hong Kong University of Science and Technology

AlN-based ternary nitride thin films are promising for radio-frequency (RF) devices, power electronics, and thermal barrier coatings due to their tunable properties, where thermal conductivity (k) critically impacts performance. Here, we establish rational design principles for achieving ultralow k by investigating epitaxial thin films of novel $\text{Yb}_x\text{Al}_{1-x}\text{N}$ alongside classic $\text{Sc}_x\text{Al}_{1-x}\text{N}$ alloys from RF sputtering, where dramatic Yb-Al ionic mismatch creates significant structural perturbation within the wurtzite lattice. Frequency-domain thermoreflectance measurements reveal unprecedented k reduction through Yb alloying ($0.184 \leq x \leq 0.538$): from 320 W/(m·K) in pristine AlN to 0.98 W/(m·K) at $x = 0.491$, merely 10% above the amorphous limit of AlN and 18% above measured glassy $\text{Yb}_{0.538}\text{Al}_{0.462}\text{N}$, while Sc-alloying reduces k to 3.03 W/(m·K) ($x = 0.359$), at room temperature. Both systems exhibit monotonic k increase with temperature (100-500 K), defying conventional Debye-Callaway predictions. To elucidate mechanisms, we combine machine-learning-based molecular dynamics with quasi-harmonic Green-Kubo analysis and achieve excellent agreement with experiments. We reveal that low-frequency thermal diffusivity remains anomalously constant with Yb concentration due to unusual invariance of generalized group velocities for heat-carrying vibrational modes below 5 THz, which opposes conventional alloying expectations. This work provides predictive insights for engineering crystalline materials with amorphous-like k , establishing $\text{Yb}_x\text{Al}_{1-x}\text{N}$ as a scalable platform for thermal-barrier applications while guiding thermal management in electronics.



1-s2.0-s1359645425010547-ga1 lrg.jpg

Photothermal heterodyne imaging for 3D thermal microscopy

Wednesday, 22nd April - 11:30: Imaging and Thin Films - Featured talk

***Dr. Jeremie Maire*¹, *Prof. Stephane Chevalier*¹, *Dr. Jordan Letessier*¹**

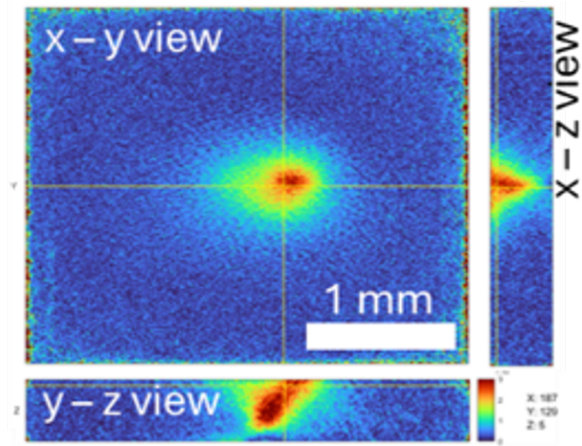
1. 1) Univ. Bordeaux, CNRS, Bordeaux INP, I2M, UMR 5295, F-33400, Talence, France. 2) Arts et Metiers Institute of Technology, CNRS, Bordeaux INP, I2M, UMR 5295, F-33400 Talence, France

3D field measurements are achievable with several techniques, and have been applied broadly, such as in medical imaging. Such 3D measurements are a powerful source of information, and likewise 3D temperature measurements are highly sought after. To get volumetric thermal information, however, the most common way consists in performing surface measurements and combine them to inverse methods. Infrared thermography is well suited to identify emerging defects and changes in material properties, but identifying underlying defects, although theoretically possible with thermography, is a mathematically ill-posed problem. Nonetheless, many works have tackled this issue, including with pure inverse methods or Bayesian approaches [1,2].

In this work, we introduce a technique that combines thermal measurements with 3D acquisition in semi-transparent materials: 3D infrared thermography. To overcome some of the limits of classical infrared thermography and expand it to semi-transparent materials without the need to uniformize the sample's emissivity, we use our recent development of the transmission photothermal heterodyne imaging technique. In semi-transparent materials, the partial transmission of light carries information about light-matter interactions along the optical beam path. As temperature varies, so does the optical index, and detecting these variations thus provides information about the temperature variations along the optical path.

Our technique is based on the use of a modulated broadband IR source going through the sample of interest before being detected by an IR camera. A laser is modulated and used to heat the sample and the recorded signal is demodulated at the heterodyne frequencies, highlighting the field of temperature variation caused by the modulated laser and sensed by the optical index of the transmitted broadband probe. It is possible to calibrate the coefficient linking the variations of temperature with the variation of transmitted light, called the thermotransmittance coefficient, which allows for quantitative temperature variation measurements.

We first show the application of this technique in 2D on three materials commonly used in microfluidic experiments, namely Borofloat glass, PDMS and a micro-layer of water. We show the variation of temperature induced by the laser beam at different frequencies, and by calibrating the thermotransmittance coefficients, we demonstrate a sensitivity as low as 30 mK in PDMS. We then combine this technique with a laminography setup and show direct reconstruction of the 3D temperature variation field at the microscale (Fig. 1) in a homogeneous material. These first results offer promising perspectives for 3D microscale temperature measurements.



Measured 3D temperature variations induced by laser heating in a glass wafer

Figure 1.png

Automated thermal characterization of multilayer nanostructures: from theory to applications in electrodeposited thermoelectric materials

Wednesday, 22nd April - 12:00: Imaging and Thin Films - Oral

Mr. Miguel Ángel Tenaguillo¹, Ms. Elena Pérez Picazo¹, Dr. Olga Caballero Calero¹, Dr. Cristina Vicente Manzano¹, Prof. Marisol Martin-Gonzalez¹

1. Instituto de Micro y Nanotecnología CSIC

Precise thermal conductivity determination in multilayer structures remains a critical challenge, particularly for electrodeposited materials where inherent surface roughness severely limits conventional optical pump-probe techniques such as Time-Domain Thermoreflectance (TDTR). We present a fully automated, MATLAB-based inverse analysis framework for photoacoustic (PA) thermal characterization that circumvents these limitations by exploiting the thermal piston effect rather than optical reflectivity, providing intrinsic robustness against topographic artifacts.

Our methodology operationalizes generalized thermal wave theory for N-layer systems (Figure 1), through an automated inverse solver employing a constrained non-linear optimization algorithm designed to minimize phase shift discrepancies between experimental and theoretical data. We have also implemented a dynamic iterative fitting strategy that navigates complex error surfaces to ensure convergence to a global minimum, overcoming local minimal traps inherent to conventional static solvers. Furthermore, a sensitivity analysis module quantifies the influence of each physical parameter, confirming that the signal is statistically dominated by the film's thermal conductivity, validating our measurement's physical significance.

Validation against standard Bi_2Te_3/AAO nanocomposites¹ reproduced literature values with deviations below 3% (Figure 2). Subsequently, we applied the tool to characterize a series of electrodeposited Cu_xSe films², a system which thermal conductivity was previously unmeasurable due to the roughness constraints mentioned earlier. The model achieved excellent fits across the frequency spectrum for all compositions. Results indicate a systematic drop in thermal conductivity as copper content rises, a trend which could be likely driven by enhanced lattice anharmonicity in the superionic phase. In summary, this work provides a validated, accessible tool for non-destructive thermal profiling of structurally non-ideal energy harvesting materials.

References

1 A. Ruiz-Clavijo, O. Caballero-Calero, C. V. Manzano, X. Maeder, A. Beardo, X. Cartoixà, F. X. Álvarez and M. Martín-González, *ACS Appl Energy Mater*, 2021, 4, 13556–13566.

2 D. Byeon, R. Sobota, K. Delime-Codrin, S. Choi, K. Hirata, M. Adachi, M. Kiyama, T. Matsuura, Y. Yamamoto, M. Matsunami and T. Takeuchi, *Nat Commun*, DOI:10.1038/s41467-018-07877-5.

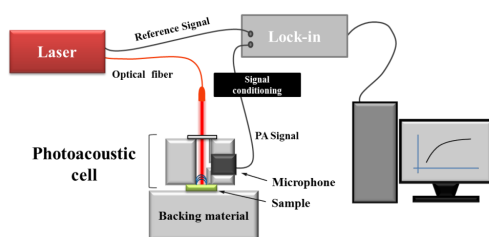


Fig. 1: Schematic of the photoacoustic setup used for thermal characterization (Adapted from B. Abad, PhD Thesis, UAM/CSIC, 2015).

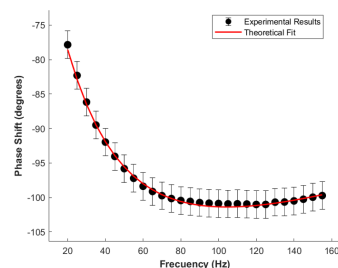


Fig. 2: Methodology validation showing high-fidelity fit for reference Bi_2Te_3/AAO composites.

Experimental setup.png

Method validation.png

Nanoscale thermal transport in van der Waals transition metal diselenide based nanolayers and nano-heterostructures

Wednesday, 22nd April - 12:20: Imaging and Thin Films - Oral

***Mr. Stuart Finch*¹, *Dr. Polychronis Tsipas*², *Ms. Stefania Skorda*², *Dr. Andrey Kretinin*³, *Prof. Athanasios Dimoulas*², *Prof. Oleg Kolosov*⁴, *Dr. Alexandros Elsachat*²**

1. Physics Department, Lancaster University, 2. National Center for Scientific Research "Demokritos", 3. Department of Materials, University of Manchester, UK, 4. Physics department, Lancaster University

ITRS roadmap puts two-dimensional materials (2DM's) as the key platform for microelectronics from 2030. In addition to exciting electronic properties, 2DMs that consist of tightly covalently bound atomic planes stacked together via weaker van der Waals (vdW) interactions, also possess high in-plane thermal conductivity, allowing to effectively dissipate the local heat of microelectronic devices. This, although, requires good knowledge of heat conduction across 2DM layers and interfaces, to understand the heat transport from the device through adjacent 2D layers.

To quantify this, we use scanning thermal microscopy (SThM) that measures the local heat conductance via the nanoscale sized tip [1] to quantify of the heat conductance in 2DM layers consisting of a few layer Se-based transition metal dichalcogenides (TMD) - HfSe₂, ZrSe₂, SnSe₂ and MoSe₂. The 2DMs were grown using molecular beam epitaxy (MBE) on sapphire substrates with homogeneous TMD of varied thickness of 2, 8 and 16 layers and a study of a 4 layer homogenous ZrSe₂ and HfSe₂ vs 2+2 layer heterostructure of the same materials.

The SThM measurements were performed in the high vacuum (10⁻⁵ torr) environment so the heat transport from the tip apex to the sample was measured exclusively, using KNT-2 resistive microfabricated thermal probe [1] and multiple measurements in the topographically and thermally uniform areas. The measurements (Fig 1) provide the ratio of temperature drop of the probe due to contact with the sample with respect to the temperature out of contact $\Delta T/T_{nc}$. By calibration the thermal resistances of the probe, R_p and the tip, R_t , the thermal resistance of the probe-TMD contact, can be determined as $R_{TMD} = R_p T_{nc} / \Delta T - R_t$. Each set of SThM TMD measurements included the measurements of reference SiO₂ layer with known thermal conductivity of 1.4 W m⁻¹K⁻¹ allowing to evaluate the tip-surface contact area and, hence, the relative thermal conductivity of the TMD layer. Our results indicates that heterostructuring of ZrSe₂ and HfSe₂ degrades the cross-sectional thermal conductivity, whereas increasing the TMD layer thickness reduces the thermal conductivity only for the relatively thick (16 layers) TMDs. Both observations suggest that the interfacial thermal resistance between the layers may play a dominant role in these materials. These data provide a solid base for theoretical modelling that would allow better understand of the heat transport in TMD layers and heterostructures.

The work was supported by the European Union grant (ERC, TheMA 101117958).

[1] Gonzalez-Munoz S, et al. *Adv Mater Interfaces* 10, 2300081 (2023).

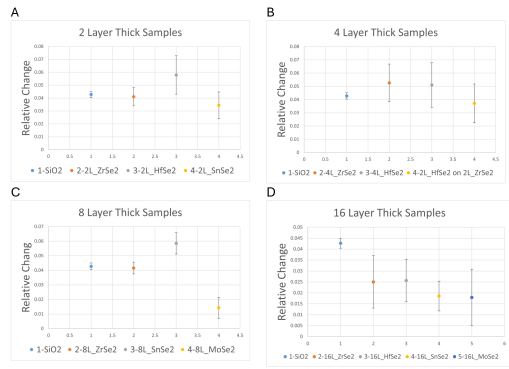


Figure 1. Relative change $\delta T = \Delta T / T_{\infty}$ STHM reading for the different number of TMD layers.

| Thickness | SiO ₂ | ZrSe ₂ | HfSe ₂ | MoSe ₂ | SnSe ₂ | HfSe ₂ /ZrSe ₂ |
|-----------|--------------------------|---------------------------|--------------------------|--------------------------|--------------------------|--------------------------------------|
| 2 Layers | 6.4±0.4x10 ⁻⁷ | 6.2±1.1 x10 ⁻⁷ | 9±2x10 ⁻⁷ | | 5.2±1.6x10 ⁻⁷ | |
| 4 Layers | | 8±2x10 ⁻⁷ | 8±3x10 ⁻⁷ | | | 6±2x10 ⁻⁷ |
| 8 Layers | | 6.3±0.6x10 ⁻⁷ | | 2.2±1.1x10 ⁻⁷ | 8.8±1.1x10 ⁻⁷ | |
| 16 Layer | | 3.8±1.8x10 ⁻⁷ | 3.9±1.5x10 ⁻⁷ | 3±2x10 ⁻⁷ | 2.8±1.0x10 ⁻⁷ | |

Table 1. Values of thermal conductance in WK⁻¹m⁻¹ for the different thicknesses of TMDs.

Tmd tab 1.png

Tmd fig 1.png

Moiré-Tuned Thermal Boundary Conductance in WS₂/MoS₂ Twisted Heterostructures

Wednesday, 22nd April - 12:40: Imaging and Thin Films - Oral

*Mr. Jiaqi Yang*¹, *Mr. Daniel Capolat Palomar*¹, *Mr. Onurcan Kaya*¹, *Dr. Timm Swoboda*¹, *Mr. Pu Tan*¹, *Dr. Aron Cummings*¹, *Prof. Javier Rodriguez-Viejo*², *Dr. Aitor Lopeandia*², *Prof. Stephan Roche*¹, *Dr. Maria Jose Esplandiu*¹, *Dr. Marianna Sledzinska*¹

1. Catalan Institute of Nanoscience and Nanotechnology, 2. Universitat Autònoma de Barcelona, Campus UAB, ES-08193 Bellaterra, Spain

Two-dimensional (2D) materials provide a tunable platform for interfacial heat transport, where a rotational degree of freedom (twist angle) generates moiré superlattices that can modulate phonon coupling across van der Waals interfaces.^[1-2] Previous theoretical and experimental studies further suggest that the thermal boundary conductance (TBC) of twisted 2D bilayers can exhibit a pronounced twist-angle dependence, with the strongest modulation expected at small angles ($\approx 0-5^\circ$).^[3-4] Notably, the magnitude of this twist-angle dependence varies significantly across different material systems. These discrepancies can be attributed to intrinsic structural differences between material systems, as well as differences in research methodologies.

In this study, we investigate MoS₂/WS₂ heterobilayers to determine how interfacial phonon spectral mismatch reshapes the small-angle twist dependence of TBC. We fabricate twisted bilayer stacks with a series of twist angles using a water-assisted transfer method (three examples shown in Fig. 1), and further confirm the twist angle by selected-area electron diffraction (SAED) (Fig. 2). We then quantify the twist-angle dependence of TBC using frequency-domain thermoreflectance (FDTR). In particular, we focus on the contrast between the near-0° (nearly aligned) state and the small-angle regime where TBC suppression is most pronounced and evaluate whether the resulting TBC ratio differs from that in homobilayers. Guided by our WS₂/WS₂ measurements ($\approx 2\times$ variation between near-aligned and small-angle states, Fig. 3), this work provides an experimental comparison of twist-tunable TBC in homo- versus heterobilayer TMD interfaces.

By extending from homobilayers to MoS₂/WS₂ heterobilayers, this study establishes a like-for-like metric—the 0°-to-small-angle-minimum TBC ratio—to compare how strongly twist modulates interfacial heat transport across material systems. We hypothesize that twist-driven changes in local registry and moiré relaxation reshape interlayer coupling and phonon transmission, while additional phonon spectral mismatch in heterobilayers further suppresses cross-plane transport and enhances this contrast. If validated, these insights provide a practical guideline for tuning interfacial heat flow in 2D moiré interfaces via twist angle.

Reference:

- [1] S, Carr et. al. Nat. Rev. Mater. 2020, 5 (10), 748–763.
- [2] K. S, Novoselov et. al. Science 2016, 353 (6298), 461.
- [3] L, Zhang et. al. Nano Lett. 2023, 23, 17, 7790–7796.
- [4] X, Bin et. al. Adv. Funct. Mater. 2025, 2422761.

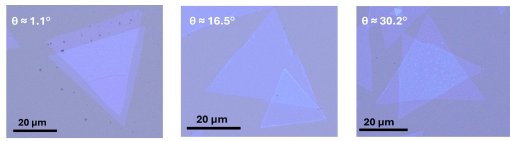


Fig 1. Optical micrographs of WS₂ twisted bilayers on sapphire ($\theta \approx 1.1^\circ, 16.5^\circ, 30.2^\circ$)

Fig.1.jpg

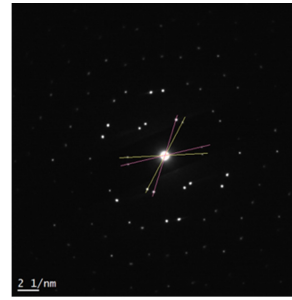


Fig 2. Electron diffraction pattern of a WS₂ bilayer ($\theta \approx 13^\circ$)

Fig.2.jpg

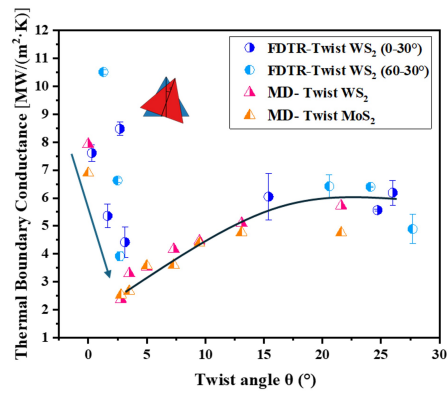


Fig 3. Effective thermal conductance G_{eff} as a function of twist angle (0-30°) measured by FDTR (with MD results shown for comparison), ratio $\approx 2\times$ contrast between near-0° and the small-angle minimum.

Fig.3.jpg

Nanoscale material design for heat transfer phenomena

Wednesday, 22nd April - 14:00: Invited - Invited talk

Prof. Saskia Fischer¹

1. Humboldt-Universität zu Berlin

Material design at the nanoscale may be used to tailor heat transfer processes. According to an *inverse Bauhaus principle* - “function follows form” - the material size and geometry influence transport properties. The understanding of charge and heat transfer in electronic materials is important for developing routes, both, for energy materials, low- and high-power electronics as well for future applications in quantum, nano and power electronics.

In this talk size effects on the charge carrier and phonon scattering and their interaction cross-sections are outlined. First, scattering mechanisms in nanoscale metals are regarded. As an example, in high-quality single crystalline silver nanowires [1] the electrical and thermal conductivity are reduced by surface scattering. Therefore, the residual resistance ratio (RRR) is no longer suitable as a quality measure for the material's purity. However, the ratio, the Lorenz number turns out to be independent of surface scattering and the temperature dependent characteristic is determined by the material's purity. Further, a method for high-precision nanometrology for determining the absolute Seebeck coefficient of individual metallic nanowires was demonstrated [2]. Knowledge of the thermodiffusion and phonon drag contributions to the absolute Seebeck coefficient are relevant for nanopatterned metallic interconnects as used in low-noise applications.

Second, scattering mechanisms in semiconductor films are considered. As an example $\beta\text{-Ga}_2\text{O}_3$ is discussed: A ultra-wide bandgap (4,7-4,9 eV) semiconductor of topical research interest for e.g. high power electronic applications. A challenge is heat dissipation due to the low room temperature thermal conductivity [3-6]. For high-quality epitaxial layers a *cross-over from resistive to ballistic* phonon transport [7] is reported, proving highly phonon-transparent interfaces. Generally, this opens a route to harness the phonon-drag to enhance the thermoelectric functionality by decoupling of the cross sections of electron-phonon and phonon-phonon interaction. Tailoring of the phonon drag becomes possible if the phonon-drag interaction length is larger than the phonon mean free path and the film thickness is smaller than both.

[1] D. Kojda, *et al.*, Phys. Rev. B **91**, 024302 (2015).

[2] M. Kockert, *et al.*, Scientific Reports **9**, 20265 (2019).

[3] A. J. Green, *et al.*, APL Mater. **10**, 029201 (2022).

[4] M. Handwerg, *et al.*, Semicond. Sci. Technol. **30**, 024006 (2015)

[5] M. Handwerg, *et al.*, Semiconductor Science and Technology **31**, 125006 (2016).

[6] J. Boy, *et al.*, APL Mater. **7**, 022526 (2019).

[7] R. Ahrling, *et al.*, Phys. Rev. B **110**, 085302 (2024).

Thermal emission of disks with radii close to the wavelength

Wednesday, 22nd April - 14:50: Conduction and Radiation - Oral

Ms. Kyriaki Kontou¹, **Prof. Olivier Merchiers**¹, **Prof. Jean-Louis Leclercq**², **Prof. Taha Benyattou**², **Dr. Azeddine Tellal**², **Prof. Pierre-Olivier Chapuis**¹

1. CETHIL, CNRS-INSA Lyon, France, 2. INL, CNRS-INSA Lyon-EC Lyon-UCBL

The study of thermal emission by sub- or wavelength sized objects is key for improved control of micro- and nanoscale heat transfer, and also for better characterization methods of surface contaminants. Different classes of such objects have been recently considered in literature such as single spherical nanoparticles [1], objects on substrates [2-3] and holes [4]. In this work we focus on the emission by dielectric bulks covered with a metal coating which has circular apertures (see Fig. 1). We aim to measure the emissivities of these objects and assess the validity of theoretical models. To characterize thermal emission, one needs to account for the diffraction of electromagnetic waves through the apertures. The ratio of the hole size (R_0) over the wavelength (λ_0) of the incident radiation, defines different regimes: the Kirchhoff regime ($R_0 / \lambda_0 > 1$), the small hole or Bethe regime ($R_0 / \lambda_0 \ll 1$) and the intermediate regime ($0.1 < R_0 / \lambda_0 < 1$). Our system consists of a silica substrate covered with a 100 nm thick gold layer. The silica substrate is a good emitter and acts as the radiation source when heated above room temperature. We performed FTIR microscopy measurements in reflection and compared the results with numerical calculations building further upon the work by Joulain et al. [4]. The measurements were performed on hole sizes ranging from 8 microns up to 55 microns in diameter and for temperatures between 50 °C and 250 °C. In Fig. 2, the emissivity over an area of $(100 \mu\text{m})^2$ is plotted as a function of wavelength at 200 °C. As expected, the emissivity decreases with decreasing hole size due to the dominating effect of the gold emissivity for small holes. For the considered sizes and temperatures, the ratio sits between the Kirchhoff and intermediate regimes. We compare those results with numerical simulations of the directional emissivity in the Kirchhoff approximation including the scattering of surface modes. We discuss the agreement between simulation and experiments of the spectrally integrated emitted flux as function of temperature.

[1] K.L. Nguyen, et al., Appl. Phys. Lett. 112, 111906 (2018)

[2] D. Langevin et al. Phys. Rev. Lett. 132, 043801 (2024)

[3] C. Li et al., Phys. Rev. Lett. 121, 233901 (2018).

[4] K. Joulain et al., J. Quant. Spectrosc. Radiat. Transf. 173, 1-6 (2016)

We acknowledge funding from ANR project STORE and discussion with X. Letartre.

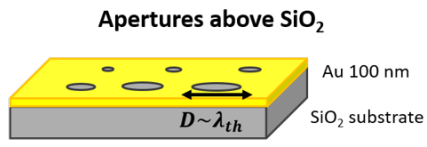


Fig. 1. Schematic of the samples

Fig1 schematic samples caption.png

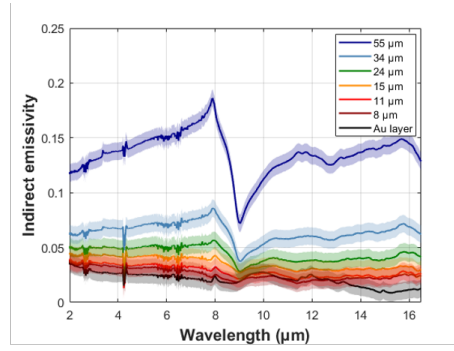


Fig. 2. Emissivity as a function of wavelength for different hole sizes and a sample temperature of 200 °C.

Fig2 emissivity vs wavelength 200 caption.png

Direct observation of electroluminescence of hyperbolic phonon-polaritons and heat transfer in hBN-encapsulated graphene devices

Wednesday, 22nd April - 15:10: Conduction and Radiation - Oral

Dr. Yannick De Wilde¹, **Dr. Loubnan Abou-Hamdan**¹, **Dr. Aurélien Schmitt**², **Dr. Patrick Bouchon**³,
Prof. Jean-Jacques Greffet⁴, **Dr. Emmanuel Baudin**²

1. Institut Langevin, ESPCI Paris, Université PSL, CNRS, 2. Laboratoire de Physique de l'Ecole Normale Supérieure, ENS, Université PSL, CNRS, Sorbonne Université, Université Paris Cité, Paris, France, 3. DOTA, ONERA, Université Paris-Saclay, Palaiseau, France, 4. Université Paris-Saclay, Institut d'Optique Graduate School, CNRS, Laboratoire Charles Fabry, Palaiseau, France

Electroluminescence corresponds to the emission of electromagnetic radiation beyond incandescence. It usually occurs at visible wavelengths in light emitting devices made of doped semiconductors. However, electroluminescence of hyperbolic phonon-polaritons (HPhPs) has been first proposed to occur within hexagonal boron nitride (hBN)-encapsulated graphene transistors based on electrical transport measurements using noise thermometry, giving indirect evidence [1]. We recently collaborated with the LPENS group of E. Baudin which performed this pioneer observation, to help them search for direct evidence of electroluminescence in hBN-encapsulated graphene transistors [2]. The structure of the devices is shown in figure 1a. Infrared microscopy combined with high sensitivity modulation spectroscopy has been used to investigate the radiation produced by high quality hBN-encapsulated graphene transistors with a mobility of tens of thousands of $\text{cm}^2 \text{V}^{-1}\text{s}^{-1}$. At large bias voltage between the source and the drain, electron-hole pair injection occurs as a result of interband Zener-Klein tunneling [1]. We observe then a substantial mid-infrared emission from the device channel, as shown in Figure 1b.

The IR emission appears above the threshold voltage of the Zener-Klein tunneling effect [2]. Indeed, as hBN is a hyperbolic material, interband electron-hole recombination in graphene gives rise to the emission of HPhPs in hBN. We show that electroluminescence is due to propagating small-wavevector HPhPs scattered elastically at discontinuities in the van der Waals heterostructure. This produces a spectral peak at ~ 190 meV beyond incandescence. Large wavevector HPhPs are also produced by electron-hole recombination above the Zener-Klein threshold voltage. Their dissipation occurs over nanometer length scales near the graphene layer, producing the heating of hBN and out-of-plane energy transfer through the silica layer at the gate of the device. Incandescent emission results from the hot SiO_2 layer, whose intensity makes it possible to quantify the heat transfer [2].

Collaboration:

LPENS (E. Baudin's group), LCF-IOGS (JJ Greffet's group), ONERA (P. Bouchon's group),

References

1. Yang, W. et al. "A graphene Zener-Klein transistor cooled by a hyperbolic substrate.", *Nature Nanotechnol.*, 13, 47 (2018).
2. Abou-Hamdan, L., Schmitt, A., Bretel, R., Rossetti, S., Tharrault, M., Mele, D., Pierret, A., Rosticher, M., Taniguchi, T., Watanabe, K., Maestre, C., Journet, C., Toury, B., Garnier, V., Steyer, P., Edgar, J. H., Janzen, E., Berroir, J-M., Fève, G., Ménard, G., Plaçais, B., Voisin, C., Hugonin, J-P., Bailly, E., Vest, B., Greffet, J-J., Bouchon, P., De Wilde, Y., and Baudin, E. " Electroluminescence and Energy Transfer Mediated by Hyperbolic Polaritons", *Nature*, 639, 909 (2025)

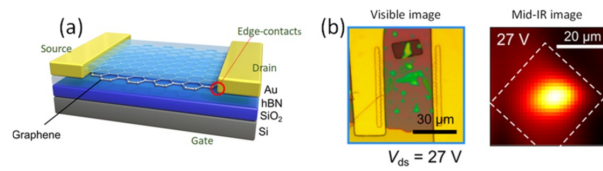


Figure 1: (a) Sketch of the hBN-encapsulated graphene transistors; (b) Visible microscopy image and spatial scan of the spectrally integrated mid-IR emission of the device biased above the Zener Klein threshold voltage.

Figure nmht dewilde.jpg

Development of Nanocomposites with Boron Nitride Nanomaterials for Thermal Transport and Related Applications

Wednesday, 22nd April - 15:30: Conduction and Radiation - Oral

Prof. Ya-Ping Sun¹

1. *Clemson University*

Hexagonal boron nitride (h-BN) and exfoliated nanosheets (BNNs) not only resemble their carbon counterparts graphite and graphene nanosheets in structural configurations and many excellent materials characteristics, especially the ultra-high thermal conductivity, but also offer other unique properties such as being electrically insulating, and the extreme chemical stability and oxidation resistance even at elevated temperatures. In fact, BNNs as a special class of 2-D nanomaterials have been widely pursued for technological applications that are beyond the reach of their carbon counterparts. Highlighted in this presentation are significant recent effects in our program, in reference to those in the relevant research field, on the development of more effective and efficient exfoliation techniques for high-quality BNNs, the understanding of their characteristic properties, and the use of BNNs in polymeric nanocomposites for thermally conductive yet electrically insulating materials and systems. Major challenges and opportunities for further advances are also discussed.

[1] Song, W.-L.; Wang, P.; Cao, L.; Anderson, A.; Mezziani, M. J.; Farr, A. J.; Sun, Y.-P. "Polymer/Boron Nitride Nanocomposite Materials for Superior Thermal Transport Performance" *Angew. Chem. Int. Ed.* **2012**, *51*, 6498.

[2] Mezziani, M. J.; Song, W.-L.; Wang, P.; Lu, F.; Hou, Z.; Anderson, A.; Maimaiti, H.; Sun, Y.-P. "Boron Nitride Nanomaterials for Thermal Management Applications" *ChemPhysChem* **2015**, *16*, 1339.

[3] Wang, Z.; Mezziani, M. J.; Patel, A. K.; Priego, P.; Wirth, K.; Wang, P.; Sun, Y.-P. "Boron Nitride Nanosheets from Different Preparations and Correlations with Their Materials Properties" *Ind. Eng. Chem. Res.* **2019**, *58*, 18644.

[4] Wang, Z.; Priego, P.; Mezziani, M. J.; Wirth, K.; Bhattacharya, S.; Rao, A.; Wang, P.; Sun, Y.-P. "Dispersion of High-Quality Boron Nitride Nanosheets in Polyethylene for Nanocomposites of Superior Thermal Transport Properties" *Nanoscale Adv.* **2020**, *2*, 2507.

[5] Mezziani, M. J.; Sheriff, K.; Parajuli, P.; Priego, P.; Bhattacharya, S.; Rao, A. M.; Quimby, J. L.; Qiao, R.; Wang, P.; Hwu, S.-J.; Wang, Z.; Sun, Y.-P. "Advances in Studies of Boron Nitride Nanosheets and Nanocomposites for Thermal Transport and Related Applications" *ChemPhysChem* **2022**, *23*, e202100645 (journal cover, January, 2022).

[6] Singh, B.; Han, J.; Mezziani, M. J.; Cao, L.; Yerra, S.; Collins, J.; Dumra, S.; Sun, Y.-P. "Polymeric Nanocomposites of Boron Nitride Nanosheets for Enhanced Directional or Isotropic Thermal Transport Performance" *Nanomaterials* **2024**, *14*, 1259.

Investigating thermal conductivity anisotropy in Wurtzite semiconductors: AlN, GaN, ZnO, ZnS

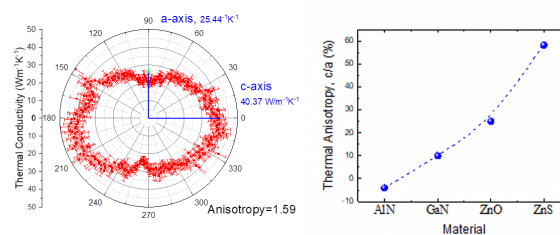
Wednesday, 22nd April - 15:50: Conduction and Radiation - Oral

Mr. Sebastian Feulner¹, Dr. Kai Xu², Prof. Markus R. Wagner³, Prof. Bartłomiej Graczykowski⁴, Dr. Riccardo Rurali², Prof. Xavier Cartoixa¹, Dr. Vincent Linseis⁵, Dr. Sebastian Reparaz²

1. Universitat Autònoma de Barcelona, Campus UAB, ES-08193 Bellaterra, Spain, 2. Institut de Ciència de Materials de Barcelona, ICMAB-CSIC, ES-08193 Bellaterra, Spain, 3. Technische Universität Berlin, Institut für Festkörperphysik, D-10623 Berlin, Germany, 4. Faculty of Physics, Adam Mickiewicz University, PL-61-614 Poznań, Poland, 5. Linseis Messgeräte GmbH, R&D Department, D-95100 Selb, Germany

Wurtzite-structured III-nitride (AlN, GaN) and II-oxide (ZnO) semiconductors are foundational materials for next-generation devices. They offer exceptional performance in high-power electronics, UV/blue lasers, and robust sensing applications due to their wide bandgaps, high breakdown fields, and outstanding thermal stability. Meanwhile, wurtzite ZnS holds significant promise for visible-light optoelectronics. While these applications critically rely on efficient thermal management, there remains a significant lack of consensus and consistent experimental data regarding their intrinsic thermal anisotropy. Specifically, previous studies often lack systematic investigation across different crystallographic planes, hindering the precise thermal design required for optimal device performance.

To address the limitations of conventional thermometry—which struggles to provide reliable, non-destructive, and orientation-specific thermal conductivity data on the same sample—this work employs two novel, recently developed, and patented experimental methodologies (licensed by **Linseis Messgeräte GmbH**). These are suitable for investigating thermal conductivity along in-plane directions, thereby providing direct access to thermal anisotropy. We systematically investigated the thermal properties along the primary m-, a-, and c-crystallographic planes of these wurtzite semiconductors using Anisotropic Thermoreflectance Thermometry¹ (ATT) and Beam-Offset Thermoreflectance.² A key development in this approach is the use of a 1-dimensional heat source, which offers several advantages for probing heat transport along selected crystallographic orientations. Employing these techniques, we determine the complete thermal conductivity tensor for each wurtzite material. To provide a fundamental understanding of the observed heat transfer, the experimental results are complemented by an analysis of their acoustic vibrational properties, achieved through Raman and Brillouin scattering measurements conducted on the same samples. Furthermore, we conducted *ab initio* calculations to model the phonon dispersion and scattering mechanisms that govern the thermal anisotropy. The resulting data resolve long-standing inconsistencies and provide the precise parameters necessary for thermal modeling. **Figure 1** displays an example of our findings regarding the thermal anisotropy ratio at room temperature, as well as an angular-dependent thermal conductivity polar map for ZnS. This work delivers a complete experimental and theoretical framework essential for maximizing the thermal performance of next-generation wurtzite-based power and optoelectronic devices.



Results thermal anisotropy wurtzite materials.png

Scanning-probe based high-spatial-resolution thermoreflectance microscopy

Wednesday, 22nd April - 16:30: Scanning Probes - Oral

Dr. Mun Goung Jeong¹, Dr. Dong Uk Kim¹, Dr. Dongmok Kim¹, Mr. Chan Bae Jeong¹, Dr. Ki Soo Chang¹

1. Korea Basic Science Institute

We demonstrate a non-contact, scanning-probe based thermoreflectance microscopy that achieves thermal imaging beyond the diffraction limit. A subwavelength-aperture fiber probe (<100 nm), attached to a quartz tuning fork, is positioned near a nanometer-scale resistive heater to collect reflected light through the aperture (see Fig. 1). The optical fiber probe is approached to the sample device closely enough to minimize the diffraction at the fiber tip by employing a quartz-tuning-fork based positioning system with piezoelectric stage. The resonant frequency of quartz tuning fork with optical fiber is 32 kHz. A phase-locked loop (PLL) mechanism is utilized to maintain stable and precise distance during the measurement process using XY piezoelectric scanner (i.e., two-dimensional sample scanning). The reflected light from the poly-Si heater is collected back through the optical fiber and transferred to the photomultiplier tube for maximizing the sensitivity to the reflection signal. Figure 2(a) shows the optical microscopy image of a poly-Si heater with a width of 500 nm and a resistance of 72.5 k Ω . Here, a patterned poly-Si layer is deposited to a thickness of 200 nm on the 500-nm-thick silicon dioxide layer. Figure 2(b) is a thermoreflectance image from wide-field thermoreflectance microscopy using a blue LED as the light source and a $\times 100$ objective lens (NA = 0.7) for near-diffraction-limit resolution (~ 300 nm). As shown in Fig. 2(b), the 500-nm-width poly-Si heater edges are barely distinguishable due to limited resolution. On the other hand, thermoreflectance image from the high-spatial-resolution thermoreflectance microscopy shows the border lines of the poly-Si heater are distinctly visible, as depicted in Fig. 2(c). The border line visibility obviously indicates the spatial resolution of the present thermoreflectance microscopy is beyond the diffraction limit (< 300 nm). Given that the wavelength of the present thermoreflectance microscopy ($\lambda = 657$ nm) exceeds that of the wide-field thermoreflectance microscopy ($\lambda = 462$ nm), the spatial resolution in the present thermoreflectance microscopy is independent of the wavelength. Consequently, it is expected that the inherent limitation of the thermoreflectance method, specifically wavelength dependency of thermoreflectance sensitivity, will be overcome, thereby ensuring no trade-offs between spatial resolution and sensitivity. This approach enables characterization of localized thermal behavior and will serve as a versatile tool for thermal analysis of advanced electronic devices.

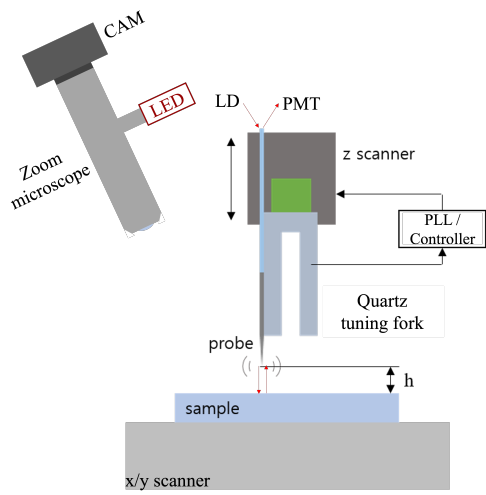


Fig1 schematic thermoreflectance microscope.png

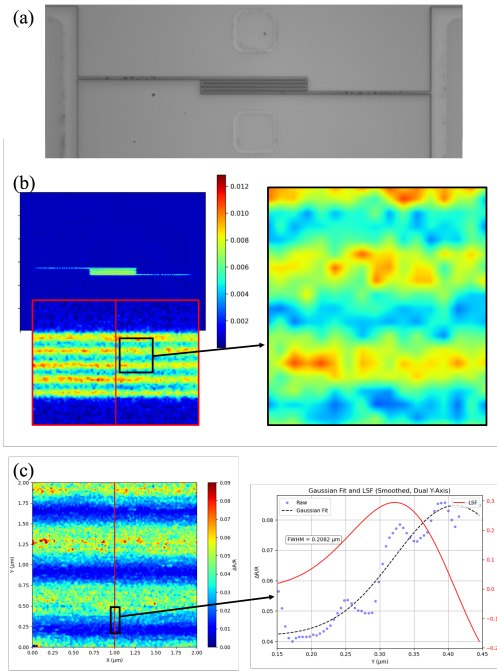


Fig2 thermoreflectance images polysil heater.png

Probing non-diffusive heat transport phenomena using spatiotemporally resolved pump-probe experiments in suspended graphite

Wednesday, 22nd April - 16:50: Scanning Probes - Oral

***Mr. Bas van Dijk*¹, *Mr. Max van Hemert*¹, *Dr. Sebin Varghese*¹, *Prof. Samuel Huberman*², *Prof. Klaas-Jan Tielrooij*¹**

1. Eindhoven University of Technology, 2. McGill University

As device dimensions continue to shrink, effective heat management has become essential for the future of technological applications such as transistors and interconnects. Two-dimensional (2D) materials are promising building blocks in these devices. This makes certain 2D materials, such as graphene with its high thermal conductivity, an interesting topic of research both theoretically and experimentally. Despite the large interest in research into heat management, existing experimental techniques to study heat transport remain limited. Many techniques often rely on the knowledge of certain material parameters, require invasive probing methods, need substantial temperature increases or require a need for complex modelling. This hinders the study into more exotic types of heat transport in 2D materials and their application into devices.

We have developed a technique [1] that addresses these challenges by following heat diffusion in thin films directly in space and time. Recently, we have expanded this technique by extending our range of wavelength operation towards the near-/mid infrared regime. Furthermore, we can make use of a supercontinuum laser that is equipped with a controllable repetition rate that is tunable to observe long-lived processes up to microseconds, enabling the study of both short and long-lived heat in the system. The broad wavelength tunability gives us access to a previously under-researched optical regime in these kinds of materials.

Making use of this broad wavelength tunability we conduct spatiotemporal pump-probe experiments in the near infrared on graphite. We suspect that we will be more sensitive to heat related phenomena in this optical regime, in contrast to the more conventionally studied visible- and terahertz optical regimes. These graphite flakes are suspended above circular drums with diameters exceeding 10 μm , allowing the measurement of pure in-plane diffusion. In these suspended geometries, we observe non-trivial interference-like effects in our temporal- and spatial profiles not observed for more trivial materials. We anticipate that these observations can be attributed to non-Fourier like heat flow, possibly hydrodynamic, which has been shown to exist in graphite at low temperatures [2], and has been predicted to occur at room temperature [3].

[1] S. Varghese *et al.* A pre-time-zero spatiotemporal microscopy technique for the ultrasensitive determination of the thermal diffusivity of thin films, *Rev. Sci. Inst* 94 034903, 2023

[2] S. Huberman *et al.* Observation of second sound in graphite at temperatures above 100 K, *Science* 364,375-379, (2019)

[3] Cepellotti *et al.* Phonon hydrodynamics in two-dimensional materials. *Nat Commun* 6, 6400 (2015).

Influencing parameters on SThM thermal conductivity measurements on nanostructured sample

Wednesday, 22nd April - 17:10: Scanning Probes - Oral

***Dr. Sarah Douri*¹, *Ms. Nolwenn Fleurence*¹, *Dr. Alexandra Délvallée*¹, *Dr. José Morán-Meza*¹, *Mr. Jacques Hameury*¹, *Dr. Nicolas Feltin*¹, *Mr. Bruno Hay*¹**

1. Laboratoire National de métrologie et d'essais (LNE)

Understanding heat transport at the nanoscale is essential for the development and reliability of recent electronic devices [1], where characteristic dimensions approach the energy carriers mean free path. At these scales, local variations in thermal properties and interfacial effects strongly influence heat transfers, challenging classical diffusive models.

Scanning Thermal Microscopy (SThM) enables the investigation of local thermal properties at micro/nanoscale [2]. Measurements can be performed in different environments, such as air and vacuum, allowing separation of heat transfers inside the material from environmental heat transfers. For the moment, the thermal conductivity measurement traceability, in air, using SThM has been established for materials with characteristic length higher than the energy carriers mean free paths [2,3].

We present an experimental thermal study of a nanostructured silicon-based sample using SThM. This sample consists of a silicon (Si) substrate overlaid with silicon dioxide (SiO₂) films of varying thicknesses, upon which pads of gold (Au) with different diameters lie [4]. The thermal responses of these nanostructures were investigated with a palladium thermo-resistive probe. The measurements were done both in ambient air and in vacuum conditions to study the influence of environmental heat transfer. As seen in Figure 1, SThM measurements were performed to map local thermal conductivity contrasts and to assess the experimental lateral thermo-spatial resolution.

We observed that increasing the SiO₂ thickness leads to thermal signals approaching the bulk SiO₂ thermal response, indicating a transition from substrate-dominated heat dissipation to a behavior characteristic of the oxide layer. Moreover, the thermo-spatial resolution of the SThM thermal maps depends on the size of the Au pads. Our comparative analysis in ambient air and in vacuum reveals that the environmental heat transfer contributes significantly to the probe-sample thermal interaction, thus affecting both quantitative contrast, lateral thermo-spatial resolution and, consequently, the interpretation of the results.

1. Bhandari, P., Singh, J., Kumar, K., & Ranakoti, L. (2022). Acta Innovations
2. N. Fleurence, S. Demeyer, A. Allard, S. Douri. and B. Hay, Nanomaterials, 13 (2023), 2424
3. A. Charvátová Campbell, P. Klapetek, R. Šlesinger, J. Martinek, V. Hortvík, V. Witkovský and G.
4. Piquemal, F.; Morán-Meza, J.; Delvallée, A.; Richert, D.; Kaja, K. Nanomaterials 2021, 11, 820.

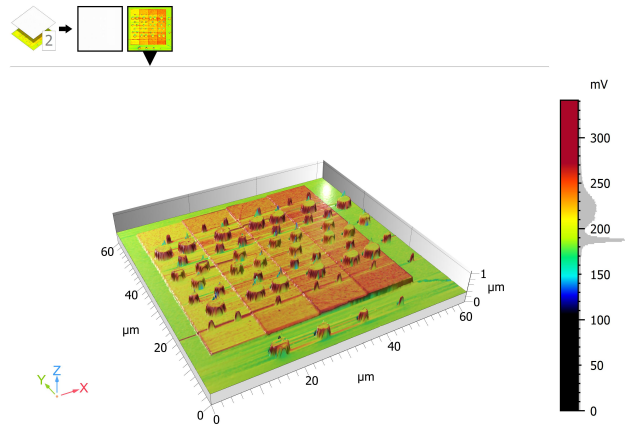


Figure 1 thermal contrast image.jpg

Thermal diffusivity measurements using dual probe SThM

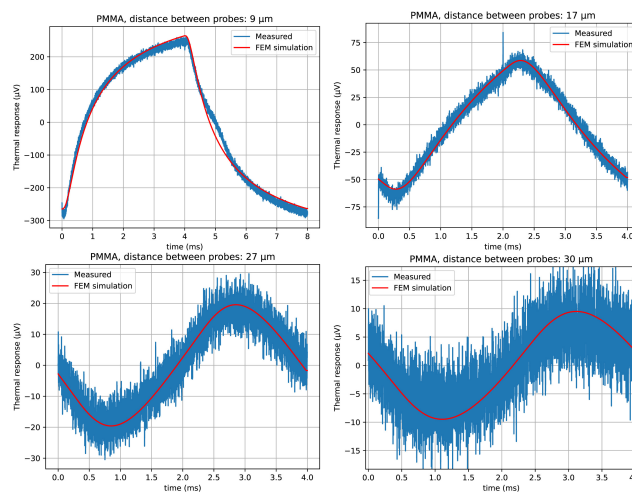
Wednesday, 22nd April - 17:30: Scanning Probes - Oral

Dr. Petr Klapetek¹, Dr. Jan Martinek¹, Mr. Václav Hortvík¹, Dr. Miroslav Valtr¹

1. Czech Metrology Institute

Dual probe Scanning Thermal Microscopy is a tool enabling better control over the heat flow between two SThM probes at micro- to nanoscale distances with accurate control of the probe-probe distance. Due to the high probe-sample contact thermal resistance, the heat flux between probe and sample is very low and the lower it is when two probe-sample contacts are in the circuit. The relevant signals in the dual probe setup are therefore very weak and experiments have to be designed very carefully to detect them. Here we present a measurement configuration and protocol enabling to detect thermal response when time dependence of the heat flow is measured, addressing thermal diffusivity measurements. Various steps had to be taken to remove different types of parasitic signals, including air thermal conductivity impact removal by reduction of air pressure, subtraction of radiative heat transfer contribution by measurements in different combinations of probe contacts to sample, detection of probe-probe zero distance and a massive averaging. When all these measures had been taken, signals sensitive to thermal diffusivity could be obtained and thermal diffusivity could be evaluated from them with a help of a numerical modeling, as illustrated in Fig. 1¹. Diffusivity measurements will be demonstrated on glasses and polymer samples. Potential uncertainty sources and suggested methodology improvements will be discussed as well.

1 Jan Martinek, Václav Hortvík, Miroslav Valtr, Petr Klapetek, Thermal diffusivity measurements using dual probe Scanning Thermal Microscopy, Int. J. of Thermal Sciences 220 (2026) 11293, DOI: <https://doi.org/10.1016/j.ijthermalsci.2025.110293>



Pmm diffusivity measurement.jpg

Imaging heat transport in suspended diamond nanostructures with integrated spin defect thermometers

Wednesday, 22nd April - 17:50: Scanning Probes - Poster

Dr. Valentin Goblot¹, **Mr. Kexin Wu**¹, **Dr. Enrico Di Lucente**¹, **Ms. Yuchun Zhu**¹, **Mr. Claudio Jaramillo Concha**¹, **Prof. Nicola Marzari**¹, **Prof. Michele Simoncelli**², **Dr. Christophe Galland**¹

1. Ecole polytechnique fédérale de Lausanne (EPFL), 2. Columbia University

Among all materials, mono-crystalline diamond has one of the highest measured thermal conductivities, with values above 2000 W/m/K at room temperature. This stems from momentum-conserving ‘normal’ phonon-phonon scattering processes dominating over momentum-dissipating ‘Umklapp’ processes, a feature that also suggests diamond as an ideal platform to experimentally investigate phonon heat transport phenomena that violate Fourier’s law.

However, a major challenge in the study of thermal transport at the nanoscale is to find appropriate temperature sensors. Here, we introduce dilute nitrogen-vacancy color centers as in-situ, highly precise spin defect thermometers in single-crystal diamond. I will show how we can image the heat flow in diamond nanostructures of arbitrary geometry, with a combined diffraction-limited spatial resolution, below 1 μm , and a temperature accuracy below 0.15 K (Fig. 1). This technique is contactless, non-perturbative and does not require additional sample engineering or transducer material.

Further, we analyze cantilevers with cross-sections in the range from about 0.2 to 2.6 μm^2 , observing a strong reduction of the cantilevers’ conductivity as width decreases (Fig. 2). We use first-principles simulations based on the linearized phonon Boltzmann transport equation and viscous heat equations to quantitatively predict the cantilevers’ thermal transport properties, rationalizing how the interplay between intrinsic and extrinsic phonon scattering mechanisms determines the observed non-diffusive behavior.

Our temperature-imaging method paves the way for the exploration of unconventional, non-diffusive heat transport phenomena in devices and nanostructures of arbitrary geometries.

[1] Goblot et al., arXiv:2411.04065 (2024)

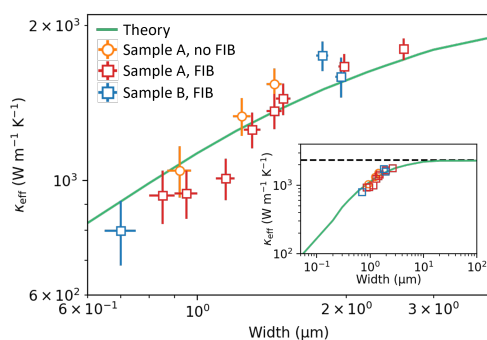


Figure 2 – Effective thermal conductivity of 1D diamond cantilevers of various width, measured on different diamond samples fabricated with two different methods. Solid line is the theoretical prediction from our model, based on the viscous heat equations.

Figure2.png

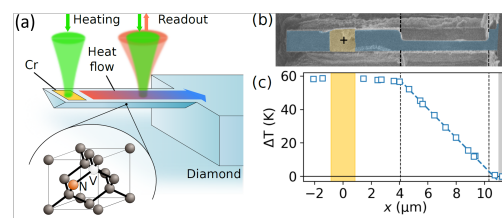


Figure 1 - (a) Schematic representation of the experiment. The temperature-dependent zero-field splitting of the NV centers spin can be readout optically, giving access to local temperature. A heat flow can be generated by laser light absorption in the Cr patch at the tip of the cantilever. (b) SEM image of a fabricated diamond cantilever, with sections of different width. (c) Corresponding temperature profile measured for an applied heating power $P_h = 1.5$ mW on the Cr patch.

Figure1.png

Thermodynamics of elementary mechanisms of quantum optics

Thursday, 23rd April - 09:00: Invited - Invited talk

Dr. Alexia AUFFEVES¹

1. MajuLab, CNRS-UCA-SU-NUS-NTU International Joint Research Laboratory, Centre for Quantum Technologies, National University of Singapore

An important motivation of quantum thermodynamics is to explore how quantum features impact energy and entropy exchanges in the quantum realm. Energetic footprint of quantum coherence and entanglement, irreversibility of quantum measurement and decoherence are typical research topics in the field. By staging simple interacting systems like atoms and photons, quantum optics provides a convenient scenery to study these effects. In this talk I will present a new framework to analyse energy and entropy exchanges in quantum optics, and apply it to elementary mechanisms: spontaneous and stimulated emission, coherent driving, driven-dissipative dynamics. I will showcase a few recent experimental results to illustrate the operability of this framework before concluding on the impact of this research on the energy cost of quantum technologies.

References:

I. Maillette de Buy Wenniger, S.E. Thomas, M Maffei, S.C. Wein, M. Pont, N. Belabas, S. Prasad, A. Harouri, A. Lemaître, I. Sagnes, N. Somaschi, A. Auffèves, P. Senellart, Experimental analysis of energy transfers between a quantum emitter and light fields, *Phys. Rev. Lett.* **131** (26), 260401 (2023), covered in phys.org.

S. Campbell, et al, Roadmap on quantum thermodynamics, arXiv:2504.20145

R. Dassonneville, et al, Amplifying microwave pulses with a single qubit engine fueled by quantum measurements, arXiv:2501.17069

S. Prasad, et al, Thermodynamics of autonomous optical Bloch equations, arXiv:2404.09648

Noises in a two-channel charge Kondo model

Thursday, 23rd April - 09:50: Quantum or Coherent - Oral

***Dr. Jerome Rech*¹, *Dr. Thanh Nguyen*², *Prof. Thierry Martin*¹, *Dr. Mikhail Kiselev*³**

1. CPT, Aix Marseille Université, CNRS, 2. Institute of Physics, Vietnam Academy of Science and Technology, 3. The Abdus Salam International Centre for Theoretical Physics

Recently, thermoelectric transport through quantum dot (QD) systems has garnered significant attention from both theorists and experimentalists.

Indeed, due to its ability to be precisely controlled by external fields, this platform provides valuable insights into the effects of strong electron interactions and resonant scattering. A fundamental phenomenon that encapsulates both of these quantum effects is the Kondo effect where a local spin is coupled to conduction electrons. Similar physical situations can be realized using an iso-spin implementation of the charge quantization, a scenario known as the charge Kondo effect [1]. This charge Kondo model has been implemented in pioneering experiments involving integer quantum Hall edge states [2].

Current noise measurement is known to offer crucial understanding of the fundamental mechanisms of quantum transport and electron interactions. In this context, it is natural to wonder whether noise can probe the non-Fermi-liquid characteristics in a multi-channel charge Kondo model.

In this work, we calculate the electric, heat and mixed noises (charge-heat current correlations) at the weak link connecting a reservoir to a two-channel charge Kondo (2CK) circuit, in the presence of a voltage or a temperature bias [3]. The setup consists of a large metallic quantum dot that is weakly coupled to the left lead via a tunnel barrier and strongly coupled to the right lead through an almost transparent single-mode quantum point contact (fig. 1).

We find that the voltage-driven electric and heat noises show oscillatory behavior with respect to the gate voltage, mirroring the pattern observed in the thermoelectric coefficient G_T (fig. 2). On the other hand, the temperature-driven electric and heat noises display a behavior similar to that of the thermal coefficient G_H or the electric conductance G (fig. 3). In contrast, the mixed noise in both situations exhibits a trend opposite to that of the aforementioned noises.

The logarithmic temperature dependence of these noises signals non-Fermi-liquid behavior, while their oscillations with gate voltage reflect the roles of particle-hole and time-reversal symmetries in thermoelectric transport. Our results demonstrate that the fundamental relations linking voltage- and temperature-induced noises to thermoelectric transport across a tunnel junction persist beyond the Fermi-liquid paradigm.

[1] K. A. Matveev, Phys. Rev. B 51, 1743 (1995).

[2] Z. Iftikhar et al., Nature 526, 233 (2015).

[3] T. K. T. Nguyen, J. Rech, T. Martin, M. N. Kiselev, arXiv:2511.02590 (2025).

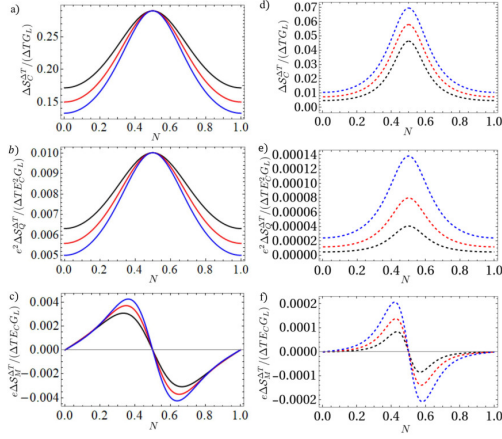


FIG. 3. Temperature-driven charge noise ($\Delta S_C^{\Delta T}/G_L$ [panels a) and d)], temperature-driven heat noise $e^2 \Delta S_Q^{\Delta T}/(E_C^2 G_L)$ [panels b) and e)], and temperature-driven mixed noise $e \Delta S_M^{\Delta T}/(E_C G_L)$ [panels c) and f)] over the temperature difference ΔT between two sides of the weak link $\Delta T/E_C$ as a function of the gate voltage N . For the plots on the left [a), b), and c)], $T/E_C = 0.01$, black, red, and blue lines correspond to $|r|^2 = 0.06$, $|r|^2 = 0.08$, and $|r|^2 = 0.1$. For the plots on the right [d), e), and f)], $|r|^2 = 0.1$, black, red, and blue lines correspond to $T/E_C = 0.008$, $T/E_C = 0.01$, and $T/E_C = 0.012$.

Fig3 results t.jpg

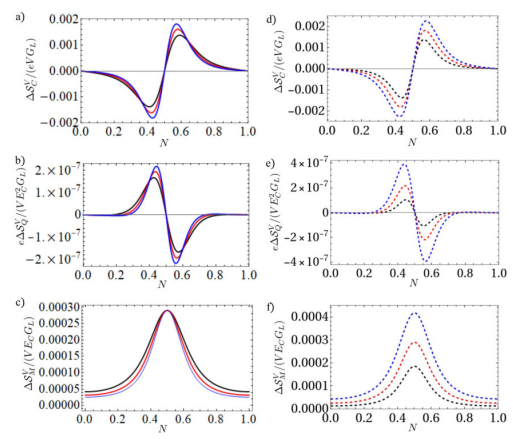


FIG. 2. Voltage-driven electric noise $\Delta S_C^V/(eG_L)$ [panels a) and d)], voltage-driven heat noise $e \Delta S_Q^V/(E_C^2 G_L)$ [panels b) and e)], and voltage-driven mixed shot noise $\Delta S_M^V/(E_C G_L)$ [panels c) and f)] over the voltage difference V between two sides of the weak link as a function of the gate voltage N . For the plots on the left [a), b), and c)], $T/E_C = 0.01$, black, red, and blue lines correspond to $|r|^2 = 0.06$, $|r|^2 = 0.08$, and $|r|^2 = 0.1$. For the plots on the right [d), e), and f)], $|r|^2 = 0.1$, black, red, and blue lines correspond to $T/E_C = 0.008$, $T/E_C = 0.01$, and $T/E_C = 0.012$.

Fig2 results v.jpg

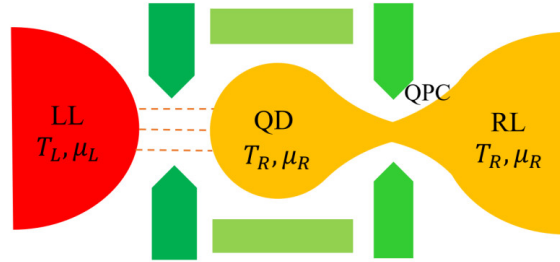


FIG. 1. Schematic of a single-electron transistor device in which a large metallic quantum dot (QD) is embedded into two-dimensional electron gas (2DEG) and connects weakly to the left lead (LL) through a tunnel barrier and strongly coupled to the right one (RL) through an almost transparent single-mode quantum point contact (QPC). The QD and the right lead (yellow color) are at potential μ_R temperature $T_R = T$ while the left lead (red color) is at higher voltage $\mu_L = \mu_R - eV$ and temperature $T_L = T + \Delta T$. The voltage or temperature drops at the weak link. The green patches demonstrate the gate voltage and the voltages controlling the tunnel barrier and the QPC.

Fig1 setup.jpg

Phase-Locked Exponential Growth: High-SNR Quantum Energy Storage at Dissipative Exceptional Points

Thursday, 23rd April - 10:10: Quantum or Coherent - Oral

Dr. Borhan Ahmadi¹

¹. University of Gdańsk

Exceptional points (EPs) are spectral singularities where both eigenvalues and eigenvectors coalesce, producing a sharp change in dynamics and an enhanced response to perturbations. Leveraging EP physics for quantum energy storage has remained challenging because most proposals rely on gain media, finely balanced loss, or explicitly non-Hermitian Hamiltonians—ingredients that can be difficult to implement and may obscure the physical origin of the stored energy.

We present an energy-storage mechanism that generates EP dynamics within a fully trace-preserving, completely positive open-system description. A charging mode and a storage mode are coupled indirectly through a dissipative mediator engineered by a common reservoir, yielding an effective complex interaction that produces an EP in the drift matrix of the Heisenberg–Langevin (first-moment) equations while maintaining a microscopic Lindblad model. In the passive setting, microscopic constraints restrict the dynamics to a stable regime with bounded response under coherent driving. Building on this near-passive EP engineering, we then show how adding a weak, experimentally standard incoherent pump on the charger mode provides a transparent work source and enables controlled access to the broken side, where the driven response is exponentially enhanced. Our framework clarifies when reduced Markovian descriptions are valid, resolves apparent runaway-from-vacuum paradoxes, and offers a practical route to EP-assisted, high-rate charging protocols in platforms such as optomechanical devices, superconducting circuits, and magnonic systems.

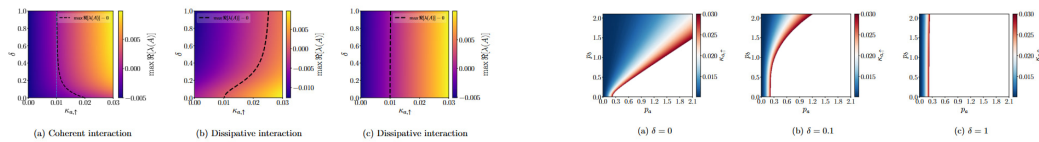


Photo 1 2026-03-10 14-25-43.jpg

Photo 2 2026-03-10 14-25-43.jpg

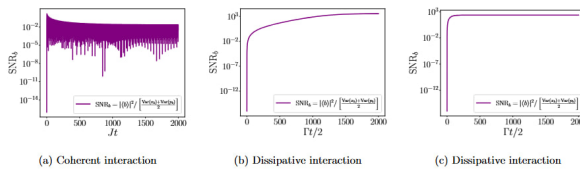


Photo 3 2026-03-10 14-25-43.jpg

Probing Coherent Phonon Contributions to Heat Conduction in Short-Period GaAs/AlAs 1D Phononic Crystals

Thursday, 23rd April - 10:30: Quantum or Coherent - Oral

Prof. Markus R. Wagner¹, **Mr. Pouria Emtenani**², **Mr. Shazan Bhat**¹, **Dr. Jit Sarkar**¹, **Dr. Klaus Biermann**¹, **Dr. Felix Nippert**³, **Ms. Marta Loletti**⁴, **Dr. Kai Xu**⁴, **Dr. Riccardo Rurali**⁴, **Dr. Sebastian Reparaz**⁵

1. Paul-Drude-Institut für Festkörperelektronik, Leibniz-Institut im Forschungsverbund Berlin e.V., Hausvogteiplatz 5–7, 10117 Berlin, Germany, **2.** Technische Universität Berlin, Institut für Festkörperphysik, **3.** Technische Universität Berlin, Institute of Physics and Astronomy, Hardenbergstr. 36, 10623 Berlin, Germany, **4.** Institut de Ciència de Materials de Barcelona, ICMAB-CSIC, ES-08193 Bellaterra, Spain, **5.** Universitat Autònoma de Barcelona, Campus UAB, ES-08193 Bellaterra, Spain

One-dimensional phononic crystals based on semiconductor superlattices are key model systems to probe the transition between incoherent and coherent phonon heat conduction. In GaAs/AlAs and related III–V multilayers, strong reductions of cross-plane thermal conductivity relative to bulk have been reported, but the extent to which these reductions arise from wave-like phonon interference, as opposed to purely incoherent interface and alloy scattering, remains under active debate. Coherent heat conduction has been inferred in selected systems, while other studies show that modest interface mixing or roughness is sufficient to suppress coherence and drive transport toward an alloy-like limit. A quantitative, experimentally grounded picture for ultra-short-period, lattice-matched III–V superlattices with monolayer-scale control is still missing.

Here, molecular-beam epitaxy is used to grow a comprehensive series of GaAs/AlAs superlattices on GaAs with fixed total thickness of 576 monolayers (≈ 163 nm) and systematically varied period from 2 to 64 monolayers per bilayer, corresponding to period thicknesses of 0.565–18.1 nm and interface densities from ≈ 1.8 down to ≈ 0.06 nm⁻¹. High-resolution x-ray diffraction and atomic-force microscopy confirm abrupt, atomically smooth interfaces with sub-0.15 nm rms roughness for the nominal series. To isolate the role of disorder, we additionally investigate selected superlattices with increased roughness, as well as reference layers of pure AlAs and random AlGaAs alloy with the same total thickness and average composition.

Temperature-dependent cross-plane thermal conductivities of all samples are measured by time-domain and frequency-domain thermorefectance (TDTR and FDTR) between 50 K and 450 K. This wide temperature range allows us to track the evolution from interface- and boundary-limited transport at low temperatures to predominantly Umklapp-limited transport at high temperatures, and to identify the temperature window where deviations from an incoherent transport baseline, and thus possible interference-related contributions, are most pronounced. In parallel, *ab-initio* lattice-dynamics and Boltzmann transport calculations (DFT + BTE) are employed for bulk, alloy and superlattice structures to obtain mode-resolved phonon dispersions, lifetimes and spectral thermal conductivities. Comparison between the calculated incoherent limit and the measured trends across ordered, roughened and alloyed samples provides quantitative insight into how interface density, roughness and alloy disorder reshape the phonon mean-free-path spectrum and delimit the magnitude and temperature range of any coherent contributions to heat conduction in short-period GaAs/AlAs phononic crystals.

Beyond Monte Carlo: Spectral and Mesoscopic Approaches to Real-Time and Space-Resolved BTE

Thursday, 23rd April - 10:50: Quantum or Coherent - Oral

*Dr. Aleksei Sokolov*¹, *Prof. Samuel Huberman*², *Prof. Michele Simoncelli*³

1. Technische Universität Berlin, 2. McGill University, 3. Columbia University

Recent advances in thermal measurement techniques have brought anomalous heat conduction to the forefront of research. A breakdown of Fourier's law was demonstrated in [1], while others have revealed exotic phenomena including thermal rectification and phonon focusing [2]. Traditionally, anomalous heat transport has been investigated through the size dependence of thermal conductivity. However, this approach suffers from important limitations: Fourier's law is no longer valid in these regimes, and such measurements provide limited insight into the microscopic phonon dynamics, offering no mode-resolved information.

More advanced experimental techniques, such as Transient Thermal Grating (TTG) spectroscopy [4], provide direct time-resolved measurement, however provide limited spatial resolution. Recently developed approaches, including two-laser time-resolved Raman thermometry [3], now enable simultaneous time- and space-resolved temperature mapping and phonon mean free path spectroscopy. Interpreting these experiments requires theoretical models of heat conduction that remain valid beyond the diffusive regime.

Heat transport in dielectric crystals is fundamentally governed by the Boltzmann Transport Equation (BTE), which is applicable across a wide range of length scales and temperatures. Despite its generality, practical solutions of the BTE are often restricted to Monte Carlo methods, which become computationally prohibitive for transient simulations or complex geometries.

In this work, we introduce two alternative modeling strategies that address these challenges. The first is a spectral decomposition of the BTE, in which the full phonon transport spectrum is precomputed once and subsequently enables efficient computation of thermal transients for arbitrary initial conditions in infinite domains. The second approach is based on the recently proposed viscous heat equations (VHE) [5], which generalize Fourier's law to account for nonlocal and hydrodynamic effects and allow direct finite-element discretization. We develop and implement a finite-element solver for the VHE within the FEniCS framework, capable of capturing non-Fourier heat transport with manageable computational cost.

We apply both approaches to the modeling of experimental configurations such as TTG [4], transient hydrodynamic lattice cooling [6], and two-laser Raman thermometry [3], demonstrating their ability to capture key features of anomalous thermal transport in both real time and space domains.

1. Chang, C.-W., et al. **Phys. Rev. Lett.** 101, 075903 (2008).
2. Anufriev, R., et al. **Nat. Commun.** 8, 15505 (2017).
3. Dudde, K., et al. **Materials Today Physics** (2025), 101784.
4. Huberman, S., et al. **Science** 364, 375–379 (2019).
5. Simoncelli, M., et al. **Phys. Rev. X** 10, 011019 (2020).
6. Jeong, J., et al. **Phys. Rev. Lett.** 127, 085901 (2021).

Precise Measurements from the Near Field to the Extreme Near Field under Ultra High Vacuum Conditions

Thursday, 23rd April - 11:30: Radiation and Conduction - Featured talk

Mr. Fridolin Geesmann¹, Mr. Philipp Thureau¹, Ms. Sophie Rodehutsors¹, Mr. Till Ziehm¹, Dr. Ludwig Worbes¹, Dr. S. Age Biehs¹, Prof. Achim Kittel¹

1. Oldenburg University

We report on precise measurements of the heat transfer on the nanometer scale by means of a ultra high vacuum (UHV) near-field scanning thermal microscope. This microscope is based on a scanning tunneling microscope which is equipped with a sub-micron sized, coaxial thermocouple. In principle, the microscope is able to measure lateral changes in heat transfer with a spatial resolution of about 5 nm. The conversion factor of the sensor is defined as the thermal flux through the sensor, from a thermal reservoir at its back to its tip, divided by the thermopower generated in the sensor's coaxial thermocouple. The achieved accuracy of the conversion factor is about 8% including the precision of each piece of equipment used in the calibration procedure.

The tip and the sample are cleaned *in-situ*, i. e. under UHV conditions, leading to clean sample surface which can be easily imaged by the STM capabilities of our setup. This can be verified by recording the result of each individual cleaning step. Furthermore, any contamination by various adsorbate substances can be ruled out by imaging the surface topography. To prove this, ultrapure water was applied as a submonolayer to the sample surface in UHV and then imaged (see Fig. (a)). The water contamination on the surface is clearly visible. After ensuring that the surfaces were clean, measurements were taken in the transition from near-field heat transfer to extreme near-field heat transfer.

With a calibrated sensor we perform quantitative measurements of the heat transfer between a sphere glued to the coaxial thermocouple sensor (see Fig. (a)) and a flat surface. The observed heat transfer between a gold plated sphere and a flat gold surface can be determined for separations of a few nanometers to some hundred nanometers (see Fig. (b) black and blue dots for uncleaned and cleaned surfaces, respectively). For large distances, the measurement results of the heat transfer can be described perfectly by the theory of fluctuational electrodynamics combined with the so-called Derjaguin approximation (red solid line in Fig. (c)). At smaller distances smaller than 18 nm (see Fig. (c)), a strong deviation from the theory can be seen (blue circles). This large deviation was already observed in previous measurements with a sharp NSThM tip. The origin of the peculiarity at shorter distances is still under heavy debate.

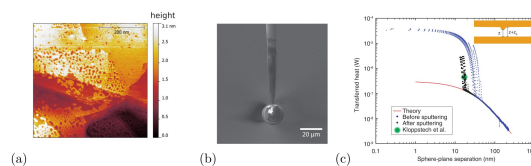


Figure 1: (a) STM image of a subatomic water film on gold. (b) SEM image of the spherical sensor tip. A 20 μm glass sphere was glued to the very end of a completely processed coaxial thermocouple tip. For some experiments, this sphere was gold plated by evaporation afterwards. (c) Distance dependence of the near field heat transfer for a gold plated sphere and a flat gold surface. For distances larger than about 18 nm, the experimental data follow the fluctuational electrodynamics together with Derjaguin approximation.

Figures with captions.jpg

Microscopic view of extreme near field heat transfer

Thursday, 23rd April - 12:00: Radiation and Conduction - Oral

***Dr. Samy Merabia*¹, *Dr. Nadia Salami*², *Dr. Ali Rajabpour*³, *Prof. Thomas Niehaus*⁴, *Dr. Manuel Cobian*⁵, *Dr. Fatemeh Tabatabaei*⁴**

1. ILM, Université Claude Bernard Lyon1, 2. Islamic Azad University, Tehran, 3. Imam Khomeiny University, Qazvin, 4. Institut Lumière Matière, 5. PMCS2I, École Centrale de Lyon

Heat transfer in the extreme near field has shown recently an increased interest driven by the development of scanning probe techniques allowing one to measure thermal transport across a nanoscale gap [1]. The thermal conductance of single molecule junctions has been also recently determined experimentally [2] opening the door to confirm the high thermoelectric efficiency displayed by these junctions.

In this contribution, we model heat transfer across nanometer gaps and across single-molecule junctions using a combination of molecular dynamics and ab-initio calculations. First, we demonstrate that phonons dominate heat transport at nanometer distances, even in the presence of molecules in the gap [3-5]. We use these results to interpret recent experiments [1,4,5]. We also discuss extreme near field heat transfer across gaps between polar materials, and unveil limitations of fluctuational electrodynamics theory [5]. The second issue to be covered concerns the thermoelectric properties of single molecule junctions. We focus on junctions made of OPE3 derivatives, a single molecule commonly synthesized by experimentalists and which electronic transport properties have been extensively investigated. We first demonstrate that first-principles calculations yield values of figure of merit in good agreement with experiments [6]. We also show that these molecule junctions may realize Peltier cooling by applying a bias voltage in a three-gate terminal device [7]. We discuss how to reach optimal conditions amounting to nanoWatt cooling powers [7]. We eventually show that cross-linking OPE3 is a promising strategy to enhance the figure of merit ZT of the molecule junction. The increase of ZT is shown to be controlled by the broadening and shift of the lowest unoccupied molecular orbital (LUMO) level of the molecule induced by cross-linking [8]. These results unveil an innovative strategy to improve the thermoelectric properties of molecule junctions.

[1] L. Cui et al., *Nature Communications*, 2017; K. Kloppstech et al., *Nature Communications*, 2017

[2] Nico Mosso et al., *Nano Letters*, 2019; Cui et al., *Nature*, 2019

[3] A. Alkurdi, C. Adessi, K. Termentzidis and S. Merabia, *Int. J. Heat Mass Transf.*, 2020

[4] Y. Guo, M. Cobian, C. Adessi and S. Merabia, *Phys. Rev. B* (2022);

[5] Y. Guo, M. Gómez Vioria, R. Messina, P. Ben-Abdallah, S. Merabia, *Phys. Rev. B*, (2023); A. Rajabpour et al. *Appl. Phys. Lett.* (2024)

[6] A. Gemma, F. Tabatabaei et al., *Nature Communications* (2023)

[7] F. Tabatabaei et al. *Nanoscale* (2022)

[8] N. Salami et al., in preparation

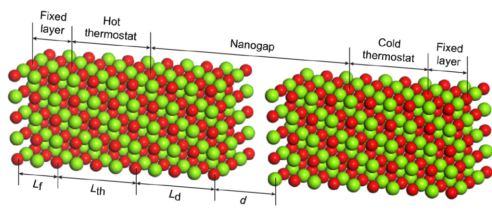
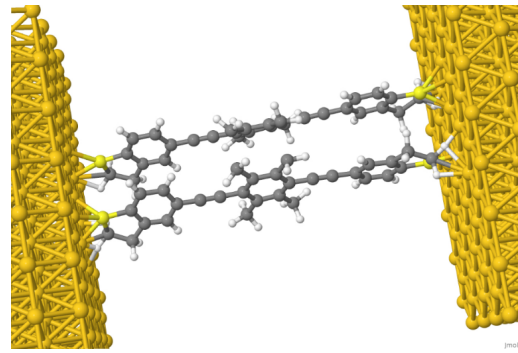
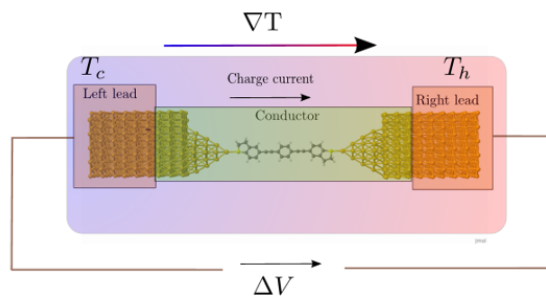


Illustration polar gap.png



Molecular-junction.png



Thermoelectricity-molecule.png

Heat transfer across nanometre-sized water meniscus

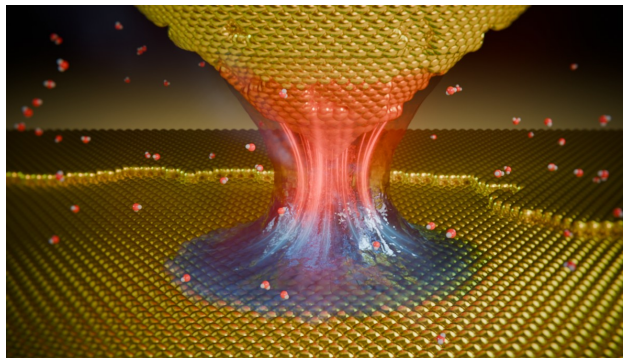
Thursday, 23rd April - 12:20: Radiation and Conduction - Oral

Mr. Oscar Mateos-Lopez¹, **Dr. Ruben Lopez-Nebreda**², **Mr. Pablo Martinez**³, **Prof. Nicolas Agrait**², **Dr. Guilherme Vilhena**¹, **Prof. Juan Carlos Cuevas**⁴

1. Instituto de Ciencia de Materiales de Madrid, Madrid, Spain, 2. Departamento de Fisica de la Materia Condensada, Universidad Autonoma de Madrid, Madrid, Spain, 3. Instituto de Ciencia de Materiales de Madrid, 4. Departamento de Fisica Teorica de la Materia Condensada, Universidad Autonoma de Madrid

Heat transfer in nanoscale gaps is of key relevance for a variety of technologies. Recent experiments have reported contradictory results shedding doubts about the fundamental mechanisms for heat exchange when bodies are separated by nanometre-sized gaps. Here, we aim at resolving this controversy by measuring the thermal conductance of gold atomic-sized contacts with a custom-designed scanning tunnelling microscope that incorporates a novel thermal probe. This technique enables the measurement of thermal and electrical conductance in different transport regimes. When the electrodes are separated by a nanometre-sized gap, we observe thermal signals whose magnitude and gap size dependence cannot be explained with standard heat transfer mechanisms. With the help of non-equilibrium molecular dynamic simulations, we elucidate that these anomalous signals are due to the thermal conduction through water menisci that form between tip and sample under customary operation conditions¹. Our work resolves this fundamental puzzle and suggests avenues for the investigation of heat conduction in atomic and molecular junctions.

1. R. Lopez-Nebreda, O. Mateos-Lopez, P. M. Martinez, J. J. Garcia-Esteban, A. Ibabe, N. Roca-Gimenez, P. Segovia, E. Garcia, E. J. H. Lee, J. G. Vilhena, J. C. Cuevas, N. Agrait, *Nature Communications*, **16**, 7345 (2025)



Water bridge.jpg

Polariton-activated Thermal Radiation of Guided Modes

Thursday, 23rd April - 12:40: Radiation and Conduction - Oral

Dr. Sebastian VOLZ¹

1. CNRS-Ecole Polytechnique-CEA

Thermal radiation is classically divided into near- and far-field regimes; however, recent advances highlight the existence of intermediate radiative mechanisms governed by geometry, diffraction, and modal hybridization. In this work, we investigate thermal emission shaped by the hybridization of guided electromagnetic modes with surface phonon polaritons (SPhPs) in polar microcavities, with a particular focus on the Fresnel-zone regime. Using fluctuational electrodynamics implemented through boundary-element simulations, we show that SPhPs supported by SiO₂ interfaces can couple to cavity geometries to form thermally excited guided modes (TEGMs). These modes are partially confined yet radiative, enabling a conversion from two-dimensional polaritonic transport into three-dimensional thermal emission. Spatial mappings of the cavity-induced Poynting vector reveal a waveguiding behavior that redirects thermal flux through the cavity aperture, in sharp contrast with purely geometric resonances observed in non-polar materials.

Spectrally resolved analyses demonstrate that TEGMs manifest predominantly in diffracted radiation and are bounded by the SPhP Reststrahlen bands. Infrared emissivity measurements using integrating-sphere FTIR experiments provide direct experimental evidence of these modes, with emissivity enhancements up to 200% near polaritonic resonances in SiO₂-coated cavities.

Beyond the cavity itself, we show that these effects naturally extend into the Fresnel zone, where thermal emission is governed by diffraction and interference rather than by Planckian far-field assumptions. Our results establish TEGMs as a robust physical mechanism bridging near-field polaritonics and far-field radiation, opening new perspectives for mesoscale thermal management, directional emitters, and radiative thermal devices.

Manipulation of phonon heat flow by nanostructuring of semiconductors: from room temperature to very low temperatures

Thursday, 23rd April - 14:00: Invited - Invited talk

Dr. Olivier Bourgeois¹

1. Institut Néel, CNRS, 25 avenue des Martyrs, 38000 Grenoble, France

The precise control of phonon fluxes—essential for heat management—plays a critical role in various domains such as energy harvesting, heat dissipation, and thermal regulation in quantum technologies. At the nanoscale, manipulating phonon transport becomes then particularly important. This presentation will highlight experimental approaches to measuring phonon transport in nanostructures, including nanowires, nanomembranes, 2D materials, and thermal metamaterials. These studies address key challenges in nanoscale energy management across a wide temperature range, from room temperature down to 50 mK.

Our research group has focused on nanostructuring semiconducting materials to modulate thermal conductivity. For example, in germanium matrices containing GeMn nano-inclusions, we observed a significant reduction in thermal conductivity. Similarly, silicon, germanium, and silicon-germanium nanowires exhibited a tenfold decrease in thermal conductivity, offering promising potential for nanothermoelectric modules.

To measure thermal conductivity at these microscales, we developed innovative 3-omega methods. For even finer resolution, we introduced a technique combining atomic force microscopy (AFM) and niobium nitride thermometry, known as Scanning Thermal Microscopy. This method enables thermal property measurements at the nanoscale, and we will present examples of its application on various materials.

Finally, at very low temperatures, where phonon mean free paths and wavelengths exceed 100 nanometers, new opportunities arise, such as accessing the ballistic, non-Fourier regime—including the Landauer regime. Using a suspended double-membrane sensor, we investigated phonon thermal transport in nanostructured SiN membranes. With state-of-the-art niobium nitride thermometry achieving attowatt sensitivity, we demonstrated ballistic phonon transport over micrometer-scale distances and observed non-trivial heat rectification in asymmetric samples. These findings open pathways for designing novel thermal phonon metamaterials that can be useful for heat management in Qbit technologies.

[1] J. Paterson, S. Mitra, Y.Q. Liu, M. Boukhari, D. Singhal, D. Lacroix, E. Hadji, A. Barski, D. Tainoff, and O. Bourgeois, *Appl. Phys. Lett.* **124**, 181902 (2024)

[2] F. Mazzelli, J. Paterson, F. Leroy, and O. Bourgeois, *J. Appl. Phys.* **137**, 015106 (2025).

[3] R. Swami, G. Julié, S. Le-Denmat, D. Singhal, J. Paterson, J. Maire, J.F. Motte, G. Pernot, H. Guillou, S. Gomès, and O. Bourgeois, *Rev. Sci. Instrum.* **95**, 054904 (2024).

[4] C.A. Polanco, A. van Roekeghem, B. Brisuda, L. Saminadayar, O. Bourgeois, and N. Mingo, *Sci. Adv.* **9**, eadi7439 (2023).

[5] A. Tavakoli, K. Lulla, T. Crozes, E. Collin, and O. Bourgeois, *Nature Commun.* **9**, 4287 (2018).

[6] B. Brisuda, J. Canosa Diaz, C. Polanco, V. Doebele, T. Crozes, J.-F. Robillard, N. Mingo, L. Saminadayar, O. Bourgeois, article in preparation.

Layer- and Field-Dependent Magnetic Order in 2D CrSBr Revealed by Pulsed Nanocalorimetry

Thursday, 23rd April - 14:50: 1D and 2D Heat conduction - Oral

Dr. Aitor Lopeandia¹, **Mr. Hugo Gómez Torres**¹, **Dr. Roop K. Mech**², **Dr. Alessandra Canetta**², **Dr. Llibertad Abad**³, **Dr. Pascal Gehring**², **Prof. Javier Rodriguez-Viejo**⁴

1. Catalan Institute of Nanoscience and Nanotechnology, 2. Institute of Condensed Matter and Nanosciences, Université Catholique de Louvain, 3. Institut de Microelectrònica de Barcelona, Centre Nacional de Microelectrònica, CSIC, 4. Universitat Autònoma de Barcelona, Campus UAB, ES-08193 Bellaterra, Spain

We report the first direct determination of the heat capacity (Cp) of few-layer CrSBr, a layered van der Waals antiferromagnet, using a microsecond-pulsed nanocalorimetry technique with sub-picojoule sensitivity. The onset of magnetic order in CrSBr is reflected in Cp(T) through a distinct anomaly associated with the magnetic entropy change at the Néel transition. This approach enables quantitative calorimetric measurements on encapsulated flakes down to a few atomic layers, providing direct thermodynamic access to the antiferromagnetic transition in the 2D limit.

The Cp(T) curves shown in the figure exhibit a pronounced antiferromagnetic anomaly whose amplitude, sharpness, and transition temperature systematically evolve with the number of CrSBr layers, highlighting how magnetic order develops with dimensionality. This method also enables in-situ calorimetry under applied in-plane magnetic fields, revealing that the antiferromagnetic transition is reversibly suppressed above a critical field that strongly depends on layer number, increasing progressively from few-layer to bulk-like samples.

These results establish microsecond-pulsed nanocalorimetry as a powerful platform to probe emergent magnetism and spin–lattice coupling in 2D materials, providing unprecedented thermodynamic insight into the dimensional evolution of magnetic order in Van der Waals systems.

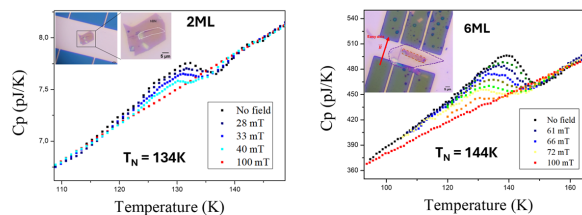


Figure: Heat capacity (Cp) as a function of temperature for two CrSBr samples with different thicknesses: **(left)** 2 monolayers (2ML) and **(right)** 6 monolayers (6ML). Measurements were performed under various magnetic fields applied along the easy axis of magnetization. The antiferromagnetic transition is observed at $T_N=134$ K for the 2ML sample and $T_N=144$ K for the 6ML sample. Increasing the magnetic field progressively suppresses the anomaly associated with the transition, highlighting the influence of the field on the magnetic order. Insets show the flake onto the nanocalorimeters membrane used and the orientation of the applied field.

Figura mnht 2026.png

High electrical conductivity in PdCoO₂ epitaxial films: A pathway to next generation interconnects beyond copper

Thursday, 23rd April - 15:10: 1D and 2D Heat conduction - Oral

***Ms. Shivashree Shivamade Gowda*¹, *Mr. Bilal Azhar*², *Ms. Ramya Mohan*¹, *Dr. Saman Zare*¹, *Mr. Nazmun Sadat*¹, *Mr. Chung Ma*¹, *Prof. Ethan Scott*¹, *Prof. Ashutosh Giri*³, *Prof. Joseph Poon*¹, *Prof. Hari Nair*², *Prof. Patrick Hopkins*¹**

1. University of Virginia, 2. Cornell University, 3. University of Maryland

Metallic delafossites are a class of quasi-two-dimensional materials with high in-plane electrical conductivity, and are less sensitive to size effects than conventional metals when confined to nanoscale dimensions, which makes them appealing for next-generation interconnects in CMOS devices. Among them, the metallic delafossite PdCoO₂ is of particular interest due to its unique crystal structure, which comprises alternating layers of highly conductive Pd and Mott-insulating CoO₂. Here, we report on the exceptionally high in-plane thermal conductivity of a series of PdCoO₂ epitaxial films on sapphire substrates measured using beam-offset time-domain thermoreflectance (BO-TDTR) and time-resolved magneto-optic Kerr effect (TR-MOKE) techniques. Our measurements yield in-plane thermal conductivities of approximately 150 and 270 W·m⁻¹·K⁻¹ for the 20 nm and 60 nm films, respectively, which rival that of copper films of equivalent thicknesses. We further demonstrate the electrical characteristics of PdCoO₂ thin films using ultrafast pump-probe microscopy and spectroscopic ellipsometry to determine electron mean free path (MFP) and carrier scattering dynamics, respectively. These factors – MFP, electron scattering, and the in-plane thermal conductivity – collectively depict the electron-driven heat transport mechanism in the PdCoO₂ film.

Resolved thermal contact resistances in 1D and 2D nanomaterials using the 3-probe method

Thursday, 23rd April - 15:30: 1D and 2D Heat conduction - Oral

*Dr. Jose Manuel Sojo Gordillo*¹, *Mr. Alex Rodriguez-Iglesias*², *Mr. Dominik M. Koch*¹, *Dr. Marta Fernandez-Regulez*², *Dr. Marc Salleras*², *Prof. Ilaria Zardo*¹

1. University of Basel, 2. Institute of Microelectronics of Barcelona

Thermal conductivity measurements of one-dimensional (1D) and structures, such as nanowires, as well as in-plane measurements of 2D materials are typically conducted using thermal bridging techniques.[1] However, these methods often fall short in accurately assessing the impact of contact resistance on the overall sample conductance. In numerous instances within the literature, this crucial contact contribution tends to be overlooked, despite its substantial influence on the determination of thermal properties. To address this limitation, some attempts using micro-Raman thermography have been conducted. This technique enables mapping of the thermal profile in nanostructures.[2] However, this is often a time-consuming approach with limited sensitivity, thus requiring relatively large temperature differences—typically above 50K—to achieve sufficient signal, which drives the system out of the linear regime.[3] Alternatively, the 3-probe method, in which a focused heating beam (electrons in the original implementation) is used to establish a heat balance, allows to spatially resolve the thermal resistance of the sample.[4,5] This approach, relying solely on electrical measurements, is significantly faster and offers high accuracy—within the 300mK range. Consequently, it enables a more precise estimation of the material's thermal conductivity while minimizing artifacts arising from thermal contact resistance. However, the required setup—a scanning electron microscope equipped with electrical feedthroughs—is not widely available and generally restricts the application of this technique to room temperature.

In this work, we show numerically—with Finite Element Analysis (FEA)—and experimentally, how the 3-probe technique can be implemented using a focused laser into a cryostat and how it can be used to resolve thermal conductivities without thermal contact resistance artifacts. Firstly, we illustrate the concept of this technique (Figure 1). Subsequently, we numerically demonstrate how, despite the increased beam size of the laser (1 μ m range) as compared with the electron beam, the same spatial resolution can be achieved provided that sample size allows (Figure 2). We also study the error of the technique in 2D samples as compared with the ideal case of a linear heating source. Secondly, we showcase several examples of thin films that have been measured using this technique (Figure 3), and are experimentally compared with the results from the bridge method alone (Figure 4). The discrepancies found underscore the significance of accounting for thermal contact resistance in accurately characterizing the thermal properties of 2D systems.

References:

- [1] L. Shi, *Journal of Heat Transfer*, 125(2003)881.
- [2] J.M. Sojo-Gordillo, *Nanoscale Horiz.* (2024)10.1039.D4NH00114A.
- [3] Y. Kaur, *ACS Appl. Mater. Interfaces*, 17(2025)1883–1891.
- [4] D. Liu, *Nano Lett.*, 14(2014)806–812.
- [5] P.-Y. Huang, *Applied Physics Letters*, 124(2024)182201.

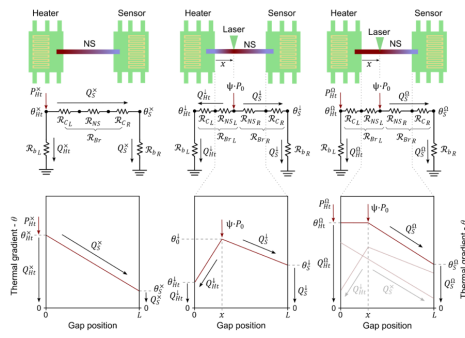


Figure 1. Sketches of the different steps of the method. a) Standard bridge method measurement that determines the heating of the sensor side through the sample $\partial\theta_s/\partial P_{in}$. b) Heating with laser step for determining the rise in temperature and heat flow in the sensor side θ_s^L , Q_S^L , and the absorption ψ . c) Balancing step achieved by inserting a balance power at the heater side P_B^L . The shaded lines illustrate how the temperature in the heater section is balanced by the superposition of the two heat sources. In these conditions the heater and sensor temperatures θ_H^L and θ_H^R are measured to determine what was the temperature at the laser position in the previous step θ_s^L .

Figure1.png

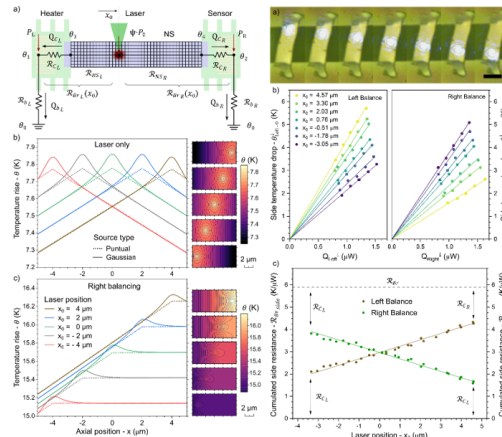


Figure 2. a) Sketch of the FEA 2D model, with a discretized 2D sample and a lumped resistive model for the contact resistance and the platform beams. b) Temperature rise produced by a laser gaussian source at different x_L . c) Temperature rise profile cuts at $y = 0$ when a balance with the right-side platform is established. In the last two plots, the left chart shows the temperature profile cuts (solid) at $y = 0$ extracted from the temperature maps illustrated at the right side, while the dashed lines represent the ideal profile arising from a linear source (0D approximation with the thermal resistance circuit model).

Figure2 3.png

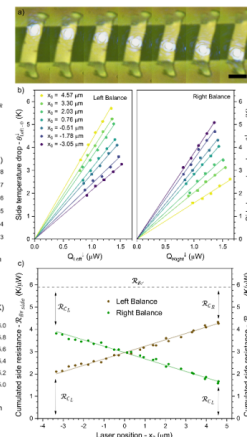


Figure 3. a) Optical images of the Laser beam focused along the longitudinal axis of the measured sample (a membrane in this case). b) Example curves illustrating the fitting of the temperature difference between beam spot and platforms as a function of the heat flux $(\theta_s^L - \theta_{side}^L)/Q_{side}^L(x)$ at each laser position. c) Example of the resulting cumulated thermal resistance curves $R_{T,side}(x)$. The top line shows the calculated total resistance from the bridge method R_B for comparison. Fitting these curves yields the thermal conductivity of the sample and the contact resistances at each side.

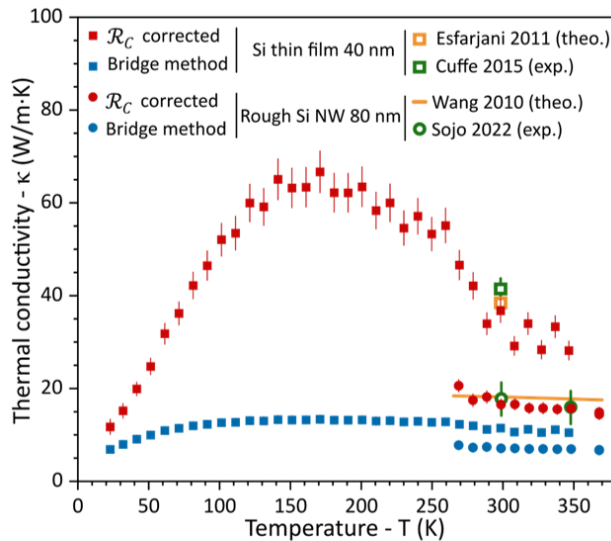


Figure 4. Temperature dependent thermal conductivity study of ~ 40 nm thick Si thin films (squares) and rough silicon nanowires with ~ 80 nm diameter (circles) comparing the obtained values as measured using the bridge method alone (red) with the corrected values using the 3-probe method (blue). A reasonable agreement is found for both samples with experimental and theoretical values of literature.

Figure4.png

Optical characterization of anisotropic thermal conductivity in sub 50 nm thin single-wall carbon nanotube films

Thursday, 23rd April - 15:50: 1D and 2D Heat conduction - Oral

Dr. Timm Swoboda¹, **Dr. Martin Magg**², **Mr. Cristian Borja Peña**³, **Mr. JiaQi Yang**¹, **Mr. Daniel Capolat Palomar**¹, **Mr. Pu Tan**¹, **Prof. Wim Wenseleers**⁴, **Prof. Sofie Cambré**⁵, **Dr. Benjamin Flavel**², **Prof. Javier Rodríguez Viejo**⁶, **Dr. Marianna Sledzinska**¹

1. Catalan Institute of Nanoscience and Nanotechnology, 2. Institute of Nanotechnology, Karlsruhe Institute of Technology, 3. Theory and Spectroscopy of Molecules and Materials, Department of Physics, University of Antwerp & Nanostructured and Organic Optical and Electronic Materials, Department of Physics, University of Antwerp, 4. Nanostructured and Organic Optical and Electronic Materials, Department of Physics, University of Antwerp, 5. Theory and Spectroscopy of Molecules and Materials, Department of Physics, University of Antwerp, 6. Universitat Autònoma de Barcelona, Campus UAB, ES-08193 Bellaterra, Spain

Thermal management remains a major challenge for the reliability and performance of modern small-scale electronic devices.[1] As a result, studies on materials with strong heat-spreading characteristics remain crucial. Nanoscale materials with a high thermal anisotropy ($k_{\text{in-plane}}/k_{\text{out-of-plane}}$) are especially attractive, as they can efficiently spread heat along the device while limiting heat flow towards heat sensitive components.[2] Single-wall carbon nanotube (SWCNT) films are particularly promising due to their exceptionally high in-plane thermal conductivity, while CNT assemblies can exhibit reduced thermal conductivity in the out-of-plane direction.[2] To evaluate the thermal conductivity of such anisotropic materials, typically optical techniques such as frequency-domain thermoreflectance (FDTR) and Raman thermometry are employed. In FDTR, a frequency modulated pump laser periodically heats the sample, while a reflected probe laser measures the resulting temperature dependent reflectance.[3] Such measurements typically require the deposition of a metallic transducer to achieve sufficiently high thermoreflectance. The thermal penetration depth of the heat inversely correlates with the pump-laser frequency, enabling the extraction of information from different depths within the sample. The phase lag between probe and pump signals as a function of the modulation frequency thus effectively provides direct depth-dependent insights into the dominant out-of-plane heat conduction of the samples. In this work, we used an FDTR setup to measure the out-of-plane thermal resistance of highly continuous, randomly oriented SWCNT films transferred onto sapphire substrates. SWCNT films with thicknesses between 15 nm and 45 nm were studied. The inner channels of the nanotubes were filled with different molecules to achieve p- or n-type doping. Gold transducers with a thickness of 100 nm were evaporated onto the films. By comparing the results across the films of different thicknesses, we fitted the effective interfacial resistances between the films and the substrates to calculate the intrinsic out-of-plane thermal conductivity of the films. We observed an ultralow out-of-plane thermal conductivity averaging around 0.09 ± 0.004 W/(m·K) with a low variation depending on the filling and the thickness of the films. Combined with previously obtained in-plane thermal conductivity values, these findings confirm the strong thermal anisotropy potential of such CNT films exceeding thermal anisotropy ratios of approximately 400, being among the highest values reported so far.

References

- [1] Shi, L. et al. Taylor & Francis, 19, 127-165, 2015.
- [2] Yamaguchi, S. et al. Applied Physics Letters, 115, 223104, 2019.
- [3] Kirsch, D. et al. Review of Scientific Instruments, 95, 103006, 2024.

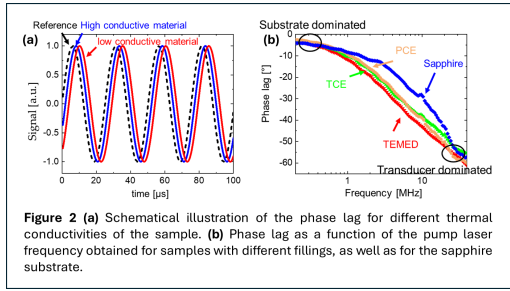


Figure 2.png

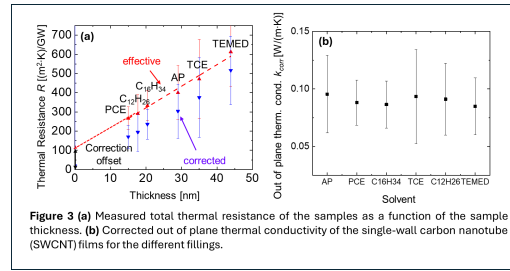


Figure 3.png

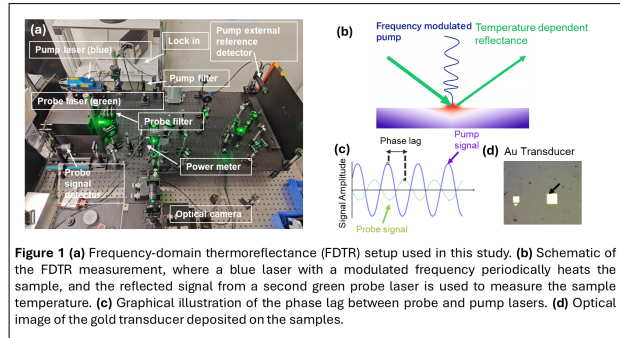


Figure 1.png

Microfabricated Si-based planar μ TEG platform for the integration and evaluation of novel thin-film thermoelectric materials

Thursday, 23rd April - 16:50: Poster II - Poster

Mr. Marc Aceituno Pimentel¹, Mr. Alex Rodriguez-Iglesias¹, Dr. Joaquin Santander¹, Mr. Shahadev Rodriguez-Miguel¹, Dr. Iñigo Martín-Fernández¹, Dr. Luis Fonseca¹, Dr. Llibertat Abad¹, Dr. Marc Salleras¹

1. Institute of Microelectronics of Barcelona

Thermoelectric materials (TE) enable direct heat-to-electricity conversion, offering compact and solid-state power solutions for autonomous IoT nodes, especially in harsh environments where batteries are impractical or unreliable. While most efforts focus on improving material zT , device architecture and thermal management are equally critical to maximizing performance [1].

Our group has previously developed silicon-based micro-thermoelectric generator (μ TEG) platforms integrating nanostructured materials in the form of thin films [2], nanowires [3], and microbeams [4]. Here, we present a microfabricated silicon-based planar μ TEGs platform designed for the integration of novel thermoelectric materials in thin-film form. This approach leverages CMOS-compatible microfabrication and miniaturization while enabling the use of a wide range of thermoelectric materials based on abundant, low-toxicity and fabrication-flow-compatible materials, such as silicides, together with their specific growth or deposition techniques.

As a proof of concept, 50 nm thick CrSi_2 films are integrated into the planar Si-based μ TEG structure [5]. The films are grown by solid-state reaction at 550°C from Poly-Si and Cr initial layers. The platform also allows the extraction of the material's Seebeck coefficient and electrical conductivity, yielding values of approximately 35 $\mu\text{V K}^{-1}$ and $1.52 \cdot 10^3 \text{ S cm}^{-1}$, respectively, resulting in a power factor ($\text{PF}=\sigma S^2$) of $\approx 0.2 \text{ mW m}^{-1} \text{ K}^{-2}$.

The results demonstrate the adaptability of the fabricated μ TEG platform as a reliable tool for the evaluation of novel thin-film thermoelectric materials integrated into a fully operating device and under realistic operating conditions.

[1] Ferrando-Villalba et al., *Nanomaterials*, 9, 653 (2019).

[2] A.P. Perez-Marín et al. *nanoEnergy*, 4, 73-80 (2014)

[3] D. Dávila et al., *Nano Energy*, 1(6), 812 (2012).

[4] A. Stranz et al. *Nanomaterials*, 12 (8) 1326 (2022)

[5] In preparation.

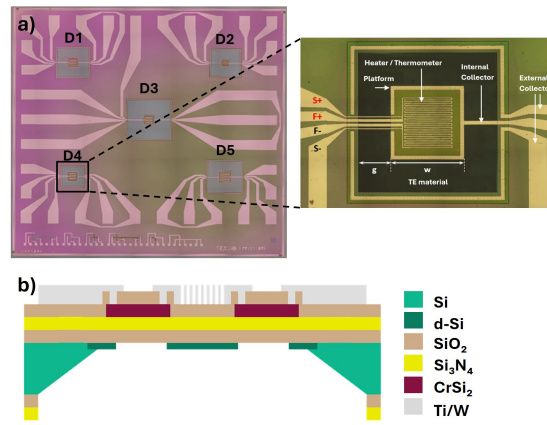


Fig 1. a) Top view of the chip showing the five suspended μ TEG platforms, with a detailed view of a single platform and its components. b) Schematic cross-section showing the different layers of the μ TEG platform.

Figure1-uteg platform.jpg

Ultrafast phonon dynamics in free-standing and substrate-supported nanocrystalline silicon

Thursday, 23rd April - 16:50: Poster II - Poster

Dr. Tiago Magalhães¹, **Dr. Housseem Rezgui**¹, **Dr. Gloria Conte**¹, **Dr. Tânia Ribeiro**¹, **Dr. Oili Ylivaara**², **Prof. Jouni Ahopelto**², **Prof. Clivia Sotomayor-Torres**¹

1. International Iberian Nanotechnology Laboratory (INL), Braga 4715-330, Portugal, 2. VTT, Espoo, Finland

Nanocrystalline silicon (ncSi) has emerged as a potential material for integrated nanoelectro-opto-mechanical platforms and optomechanical systems due to its CMOS technology compatibility and tunable optical, mechanical, and thermal properties. In particular, the annealing process in ncSi fabrication determines different structural properties such as grain size distribution and stress [1]. Recent studies have demonstrated that ncSi enables strong photon-phonon interactions, GHz-frequency mechanical modes, and nonlinear phenomena such as self-pulsing and phonon lasing in optomechanical cavities [2]. These features, combined with the ability to tailor grain size, stress, and layer thickness, make ncSi an attractive alternative to crystalline silicon for scalable photonic and phononic devices. Despite these advances, the microscopic mechanisms underlying ultrafast energy relaxation remain insufficiently understood, making it difficult to define clear strategies to reduce noise dissipation in ncSi-based devices.

In this work, we investigate the ultrafast phonon dynamics of ncSi using pump-probe spectroscopy, in particular, the asynchronous optical sampling (ASOPS) technique. The latter is used to measure carrier and phonon lifetimes, as well as characteristic frequencies, which are important parameters that govern energy dissipation, mechanical damping, and thermal transport [3]. Measurements were performed on both free-standing membranes and substrate-supported ncSi. In the free-standing membranes, the first generated coherent acoustic mode exhibits lifetimes extending into the nanosecond regime.

[1] Navarro-Urrios, D., et al. “Room-Temperature Silicon Platform for GHz-Frequency Nanoelectro-Opto-Mechanical Systems.” *ACS Photonics* 9, 413–419 (2022).

[2] Navarro-Urrios, D., et al. “Nanocrystalline silicon optomechanical cavities.” *Optics Express* 26, 9829–9839 (2018).

[3] J. Cuffe et al., “Lifetimes of Confined Acoustic Phonons in Ultrathin Silicon Membranes,” *Phys. Rev. Lett.* 110, 095503 (2013).

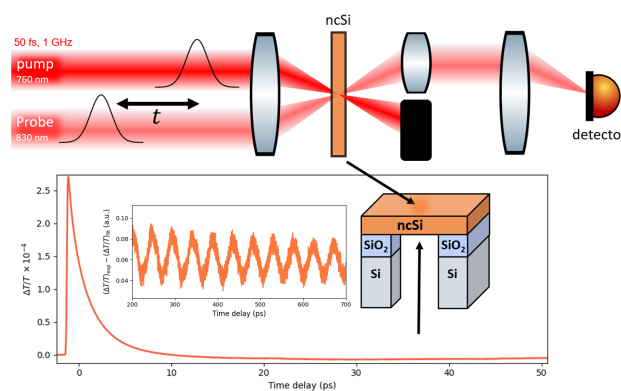


Fig1 corr2.png

Micro-Thermometry via Plasmon-Enhanced Metal Luminescence

Thursday, 23rd April - 16:50: Poster II - Poster

Ms. Athena Majlesi¹, Mr. Jan Kutschera¹, Dr. Marc Herzog¹, Prof. Matias Bargheer¹, Dr. Wouter Koopman¹

1. University of Potsdam, Institute of Physics and Astronomy

Surface-Enhanced Raman Scattering (SERS) is a popular method for studying reactions at the nanoscale [1]. However, these reactions are strongly influenced by local temperature of plasmonic substrate, which can significantly differ from the temperature of the environment due to optical heating. Therefore, an accurate determination of the temperature is crucial. Contactless optical methods are advantageous as they avoid perturbing the measurement by the probe. However, the plasmon resonance modifies key optical properties of the SERS substrate.

Here, we present a contactless optical method to determine the temperature of nanostructured plasmonic SERS substrates using the metal's intrinsic emission. Metal luminescence, while extremely weak in bulk metal, is often observed from structured plasmonic SERS substrates, since the emission probability is significantly enhanced by the plasmon resonance [2]. Crucially, luminescence emitted at energies above the excitation wavelength (i.e. in the anti-Stokes region), carries the signature of the thermal energy distribution of charges at finite temperatures (Figure 1).

To accurately extract the temperature, we utilize an iterative calibration procedure [3] that eliminates both the influence of plasmon resonance and laser heating effects by comparing spectra at varying excitation intensities and extrapolating to zero power (Figure 2). Our method extends the previous procedure by Cahill et al. such that temperatures can be compared across different positions with different local plasmon enhancement spectra. We achieve a millikelvin-level precision in determining the absolute nanoparticle temperature.

This technique offers a new powerful tool for contactless, micro-thermometry, essential for understanding and controlling photothermal effects in plasmonic catalysis, photovoltaics and real-time chemical reactions monitoring by SERS.

References

- [1] Koopman et al., *Adv. Mater. Interf.* **2021**, 8 (22), 2101344, doi: 10.1002/admi.202101344.
- [2] Koopman, *ACS Nano* **2025**, 19 (39), 34517, doi: 10.1021/acsnano.4c10812.
- [3] Xie & Cahill, *Appl. Phys. Lett.* **2016**, 109, 183104

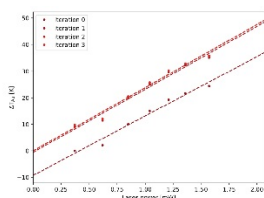


Figure 2: Iterative temperature calibration extending Xie and Cahill [3]. Temperature deviation ΔT from the known environment temperature is plotted against laser power for successive iterations. In iteration 0, the reference temperature is assumed equal to the environment. Linear extrapolation to zero power reveals the offset due to this assumption. The reference is then corrected and the process repeated until the extrapolated temperature converges to the environment value within ± 10 mK (iteration 3).

2.jpg

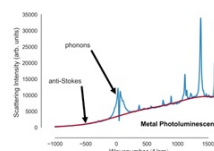


Figure 1: SERS spectrum of gold nanostructures showing molecular Raman peaks in the Stokes region and the continuous anti-Stokes luminescence background. The slope of the anti-Stokes emission directly encodes the nanoparticle temperature

1.jpg

Inverted temperature gradients in Au-Pd and Au-Rh core-satellite systems

Thursday, 23rd April - 16:50: Poster II - Poster

***Ms. Lisa Mehner*¹, *Ms. Maja Ruprecht*¹, *Mr. Ankit Dhankhar*², *Prof. Pramod Pillai*², *Ms. Shivani Kesarwani*¹, *Dr. Florian Schulz*³, *Dr. Felix Stete*¹, *Prof. Matias Bargheer*¹**

1. University of Potsdam, Institute of Physics and Astronomy, 2. Indian Institute of Science Education and Research (IISER), Department of Chemistry, 3. University of Hamburg, Institute for Nano Structure- and Solid State Physics

Nanoscale heat transport plays a central role in plasmon-driven catalysis, where localized temperature gradients and hot-carrier dynamics can be exploited to drive or support chemical reactions. Recent transient absorption studies on hybrid Au–Pd nanoparticle systems have demonstrated that, following optical excitation, energy can transiently localize in Pd satellites due to their faster electron–phonon coupling and larger electronic heat capacity. The temperature increase in Pd can be up to 200 K higher than in the light absorbing Au core (see Fig. 1 for schematic illustration) [1].

In the present work, we extend transient absorption measurements on Au–Pd hybrid systems to samples based on Au nanorod cores, complementing the previous studies that focused on spherical nanoparticles.

Building on these findings, we investigate nanoscale energy flow in hybrid structures consisting of Au nanorods decorated with Rh spikes [2]. Three distinct spatial distributions of Rh spikes around the Au nanorods are examined to elucidate the role of geometry on ultrafast energy redistribution. Using optical transient absorption spectroscopy, we probe the energy distribution in Au nanorods following femtosecond optical excitation. Our measurements reveal an accelerated decay of the transient Au response in hybrid Au–Rh nanostructures compared to bare Au nanorods, consistent with behavior previously observed in Au–Pd systems. Ongoing analysis of recent data will assess whether variations in the spatial distribution of the Rh spikes lead to measurable differences in the ultrafast dynamics.

Fig. 1 (from ref. [1]): Schematic illustration of the ultrafast energy flow in an Au-Pd hybrid system where Pd particles are in metallic contact to the Au core as satellites. The Au core is optically excited, generating hot electrons that ballistically or diffusively enter the Pd. The electrons in Pd quickly couple to the phononic system and transfer their energy. Since the electron phonon coupling in Au is slower, a strong temperature gradient between Pd and the Au core is created. After a few picoseconds, heat conduction equilibrates the temperatures over the system.

[1] Nat. Commun. 16, 8168 (2025), <https://doi.org/10.1038/s41467-025-63327-z>

[2] Chem. Mater. 2024, 36, 20, 10227–10237, <https://doi.org/10.1021/acs.chemmater.4c01966>

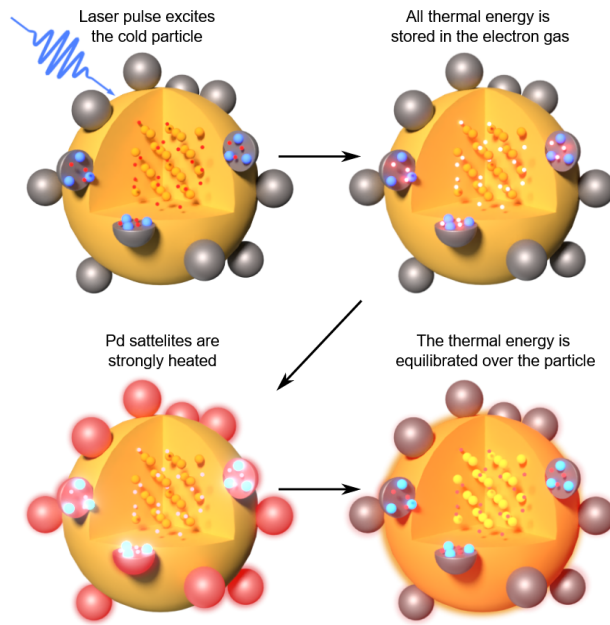


Fig1 au-pd.png

Thickness- and temperature-dependent thermal conductivity of ScN using Time-Domain Thermoreflectance

Thursday, 23rd April - 16:50: Poster II - Poster

Mr. Moritz Metschl¹, **Mr. Pouria Emtenani**², **Mr. Jamal Abou Haibeh**³, **Dr. Felix Nippert**¹, **Dr. Duc Vinh Dinh**⁴, **Mr. Abhilash Sanjay Ulhe**⁵, **Prof. Gregor Koblmüller**⁶, **Prof. Samuel Huberman**³, **Prof. Christian Thomsen**¹, **Prof. Markus Raphael Wagner**⁷

1. Technische Universität Berlin, Institute of Physics and Astronomy, Hardenbergstr. 36, 10623 Berlin, Germany, **2.** Institute of Physics and Astronomy, Technische Universität Berlin, 10623 Berlin, Germany, **3.** Department of Chemical Engineering, McGill University, Montréal, QC H3A 0C5, Canada, **4.** Paul-Drude-Institut für Festkörperelektronik (PDI), 10117 Berlin, Germany, **5.** Walter Schottky Institut and Physics Department, Technical University of Munich (TUM), 85748 Garching, Germany, **6.** Technische Universität Berlin, Institute of Physics and Astronomy, Hardenbergstr. 36, 10623 Berlin, Germany and Walter Schottky Institut and Physics Department, Technical University of Munich (TUM), 85748 Garching, Germany, **7.** Technische Universität Berlin, Institute of Physics and Astronomy, Hardenbergstr. 36, 10623 Berlin, Germany and Paul-Drude-Institut für Festkörperelektronik (PDI), 10117 Berlin, Germany

Rock-salt ScN and its ternary alloys are being investigated for their thermoelectric properties and piezoelectric properties and are also studied in the context of ultra-wideband communication. Over the past decade, varying results for the thermal conductivity (TC) of ScN have been published, ranging between 11 W/mK [1] for a 130 nm thin sample and (54 ± 3) W/mK [2] for a 2 mm quasi-bulk sample at room temperature. The aim of this work is to identify the mechanisms responsible for the differing results.

The TC of three ScN samples grown by molecular beam epitaxy on sapphire substrate [3] with thicknesses of 85 nm, 200 nm, and 500 nm was investigated as a function of temperature using Time-Domain Thermoreflectance (TDTR). At room temperature the TC of the ScN samples was determined to be (10.9 ± 0.8) W/mK, (13.4 ± 0.7) W/mK, and (23.5 ± 1.6) W/mK, respectively. The increasing TC can be attributed to the increasing layer thickness. The TDTR measurements were performed in a temperature range from 60 K to 400 K (see Figure 1(a)). To verify the results, the TC of ScN was calculated using the Boltzmann Transport Equation (BTE). The BTE results can be used to demonstrate the plausibility of the TDTR results (see Figure 1(b)) and to break down the influence of boundary and Umklapp scattering. Boundary scattering dominates at low temperatures but diminishes at higher temperatures, so that Umklapp scattering significantly determines TC above room temperature.

In addition, six ScN samples grown between 200°C and 1000°C were examined using TDTR. Figure 2 shows that the TC of the six ScN samples increases with rising growth temperature. The results range from 1 W/mK to 10 W/mK. Based on X-ray diffraction measurements, this can be attributed to an increase in crystal quality with rising growth temperature.

Since the electronic TC of ScN can be significant, it was considered using Hall measurements and the Wiedemann-Franz law [2].

The investigations conducted on layer thickness, growth temperature, and electronic TC have identified them as important factors influencing the TC of ScN, the interplay of which reconciles a large proportion of the published results on the TC of ScN.

References

- [1] Tureson, N. et al. J. Appl. Phys. 122, 025116 (2017).
- [2] Al-Atabi, H. et al. Appl. Phys. Lett. 116, 132103 (2020).
- [3] Dinh, D. V. et al. Appl. Phys. Lett. 123, 112102 (2023).

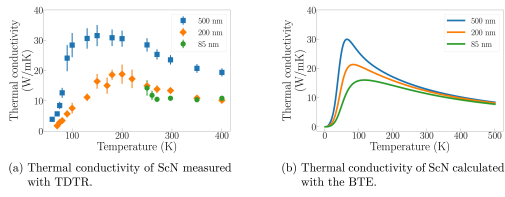


Figure 1: Thickness and temperature-dependent thermal conductivity of ScN measured and calculated.

Scn tc thickness and temperature dependent.jpg

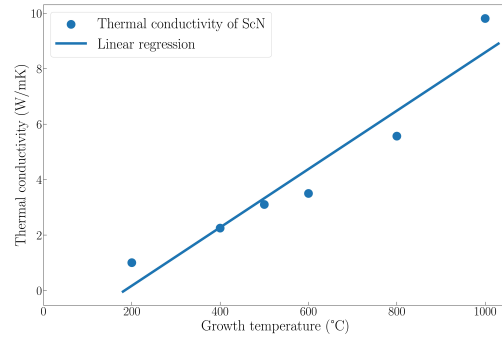


Figure 2: The thermal conductivity of six ScN samples with varying growth temperatures and a layer thickness of 100 nm is shown.

Scn tc growth temperature dependent.jpg

Effect of Π -conjugation in nanoscale heat transport

Thursday, 23rd April - 16:50: Poster II - Poster

Mr. Nelson Elías Rivas Chacón¹, **Mr. Pablo Martínez**¹, **Prof. Juan Carlos Cuevas**², **Dr. Guilherme Vilhena**³

1. Instituto de Ciencia de Materiales de Madrid, 2. Departamento de Física Teórica de la Materia Condensada, Universidad Autónoma de Madrid, 3. Instituto de Ciencia de Materiales de Madrid, Madrid, Spain

Understanding and controlling heat transport at the nanoscale is arguably one of the largest pending challenges of Nanoscience. The field has witnessed a renewed interest with recent spectacular experiments including measuring heat transport through single-atom contacts [1], then through single molecule junctions [2] and later the realization of the first molecular-sized nano-refrigerator. However, a fundamental understanding of the novel and exotic heat transport phenomena at these scales remains elusive, ultimately hindering a de-novo design of novel nano-materials with tailored heat transport properties. In this work, we employ advanced all-atom non-equilibrium molecular dynamics simulations to obtain an atomistic view of heat transport in model π -conjugated systems with tunable structural features such as optically-activated molecular switches and length-variable hydrocarbon chains. Our simulations, quantitatively reproduce experimental data [2], but most importantly they provide an atomically detailed understanding on the breakdown of Fourier's classical law for heat transport as new a form of coherent heat transport (ballistic) emerges. We employ the JOYCE 3.0 framework to construct quantum-mechanically derived intramolecular-specific force fields, yielding a more accurate transport description compared to that predicted using other general-purpose parametrization schemes. We further examine how chemical or mechanical modifications of these systems can modulate transport regimes and the overall thermal conductance, providing general design principles for nanoscale thermal devices and revealing fundamental factors governing nanoscale heat transport.

References

- [1] L. Cui *et al*, *Science* **355**, 1192-1195 (2017)
- [2] S.C. Yelishala *et al*, *Nat. Mater.* **24**, 1258-1264 (2025)
- [3] S. Giannini *et al*. *Journal of Chemical Theory and Computation* **21 (6)**, 3156-3175 (2025)

Ultrafast heat transport in metallic heterostructures tracked via strain responses measured by femtosecond X-ray diffraction

Thursday, 23rd April - 16:50: Poster II - Poster

*Dr. Jan-Etienne Pudell*¹, *Dr. Maximilian Mattern*², *Dr. Marc Herzog*³, *Dr. Alexander von Reppert*³, *Dr. Jasmin Jarecki*², *Dr. Jörg Hallmann*¹, *Prof. Matias Bargheer*³, *Prof. Anders Madsen*¹

1. European X-ray Free-Electron Laser, 2. Max-Born-Institut, 3. Uni Potsdam

Understanding how thermal energy is deposited, redistributed, and transformed in metallic heterostructures is essential for describing their functional behavior on ultrafast timescales. Femtosecond X-ray diffraction provides a powerful, material-resolved probe by measuring lattice strain as a direct indicator of the energy stored in each constituent subsystem. The lattice strain acts as an ultrafast thermometer, capable of resolving temperature dynamics far below the optical penetration depth. This enables tracking of heat flow across nanoscale interfaces, even when optical methods fail to discriminate between adjacent layers.

We investigate a broad range of samples, including ultrathin films, multilayers, and metal-metal superlattices. In particular, by comparing Bragg peak intensity and strain as indicators of layer temperature, we confirm that in-plane expansion is suppressed on picosecond timescales in continuous thin films. This suppression fundamentally alters the effective thermal expansion coefficients relevant for ultrafast experiments.

Such ultrafast, layer-specific thermometry is especially powerful in metallic heterostructures, where electron and lattice temperatures can evolve at vastly different rates, and where heat transport may range from diffusive to ballistic depending on the energy carriers and structural dimensions. On this poster, we present examples of heat transport in ultrathin metallic bilayers, energy transport through 100 nm of Cu without significant lattice heating, and lattice expansion in metal superlattices driven by electron pressure.

Why hybrid perovskites possess an ultralow thermal conductivity?

Thursday, 23rd April - 16:50: Poster II - Poster

Ms. Qinqin He¹, Prof. Yanguang Zhou¹

1. Hong Kong University of Science and Technology (HKUST)

Hybrid perovskites are constructed from an octahedral lattice framework with organic molecules confined within these octahedral cages, which therefore makes their thermal transport behave different from that in conventional crystals. It has been widely accepted that the thermal conductivity of hybrid perovskites is significantly low and possesses a weak temperature dependence. However, the origin for this is in debate and much less well documented. In this paper, we demonstrate that the origin of the ultralow thermal conductivity of hybrid perovskites is the static disorder introduced by organic molecules. This disorder, caused by organic molecules, strongly scatters the lattice vibrations and hinders the thermal transport in hybrid perovskites. Consequently, the temperature dependence of the corresponding thermal conductivity transits from $\sim T^0$ to $\sim T^{-1}$, and the thermal conductivity doubles at room temperature and increases fourfold at 150 K when the static disorder introduced by organic molecules is excluded. Meanwhile, the thermal energy in hybrid perovskites is found to be transferred by both the vibrations of the lattice framework ($\sim 48\%$ to $\sim 65\%$) and the interaction among organic molecules ($\sim 35\%$ to $\sim 52\%$). Our results map heat transport through the inorganic octahedral cage and the organic cations, clarify the mechanisms of their mutual coupling and interference, and provide guidance for thermal management in perovskites.

Optimizing Energy Conversion in Feedback-Controlled Nano Processes: Harnessing Time-Dependent Information

Thursday, 23rd April - 16:50: Poster II - Poster

Mr. Rasmus Hagman¹, **Dr. Jonas Berx**², **Prof. Janine Splettstoesser**¹, **Dr. Henning Kirchberg**¹

1. Chalmers University of Technology, 2. University of Copenhagen

Nanoscale devices that convert energy into useful work are becoming increasingly prevalent. A critical challenge in this area is managing energy transduction at the nanoscale. Quantum measurement and the associated acquisition of information can be harnessed to guide and enhance work output through feedback control. In this context, we explore a quantum information engine (QIE) as a prototype energy-transducing nanodevice controlled by measurement [1]. This engine leverages the information exchange between a working medium, represented by a two-level system, and a meter, modeled as a quantum harmonic oscillator. However, this information transfer is not instantaneous; it relies on the measurement time, which is the duration needed to establish a correlation between the quantum system and the meter. This measurement time sets a lower limit on the cycle time of the QIE, making time-dependent information acquisition a crucial resource for the process. We examine the relationship between the energetic cost of quantum measurement, the associated acquisition of information, and the potential extractable work during finite-time operations. To achieve this, we investigate performance quantifiers, including the conversion of information to extractable work, the efficiency of converting input energy to net extracted work, and power, defined as the rate of net work extraction during the cycle operation. Our findings indicate that all these factors are influenced by measurement time in various ways. For example, achieving high efficiency necessitates a long measurement time, but this, in turn, reduces power. To identify an optimal balance among these performance indicators, we employ Pareto optimization, a multi-objective optimization method, to determine ideal measurement times. We also discuss ways to extend our considerations using these concepts, such as in measurement-enhanced photochemical reactions [2].

[1] R. Hagman, J. Berx, J. Splettstoesser and H. Kirchberg: Optimising finite-time quantum information engines using Pareto bound, accepted in *New J. Phys.* **27**, 114507 (2025)

[2] H. Kirchberg and A. Nitzan: Quantum information engines: Bounds on performance metrics by measurement time, *Phys. Rev. A* **112**, 032201 (2025)

Phonon-mediated heat conduction in GaN/AlN superlattices grown on silicon

Thursday, 23rd April - 16:50: Poster II - Poster

Mr. Guillaume Würsch¹, Mr. Pouria Emtenani², Dr. Sebastian Tamariz³, Dr. Tim Grieb¹, Mr. Mahmoud Elhajhasan¹, Ms. Katharina Dudde¹, Ms. Jana Lierath¹, Prof. Nicolas Grandjean³, Prof. Markus R. Wagner⁴, Prof. Gordon Callsen¹

1. Universität Bremen, 2. Technische Universität Berlin, 3. Ecole polytechnique fédérale de Lausanne (EPFL), 4. Paul-Drude-Institut für Festkörperelektronik

Over the preceding decade, coherent heat conduction by phonons has been revealed in superlattices (SLs) [1]. Most related measurements relied on time-domain thermoreflectance (TDTR), a well-established technique that is often used, e.g., for the precise determination of the thermal conductivity κ . First, with increasing interface density (d) of the SL, one observes a decrease of κ due to phonon interface scattering. However, as a certain value of d , one observes a turn-on towards inquiring κ values, which is frequently interpreted in terms of coherent phonons heat conduction [1].

In this work, we analysed wurtzite GaN/AlN SLs, which are known for their high crystalline and interface quality, aiming to explore coherent heat conduction [2]. Our samples were grown by ammonia molecular beam epitaxy (MBE) on (111)-silicon wafers, which were first covered by a 20-nm-thick layer of AlN to enhance the quality of the following SL stack [3]. Subsequently, six different GaN/AlN SLs were grown, featuring identical layer thickness scaling from 1 monolayer (ML) up to 32 ML, while the entire thickness of all SL samples was kept constant at $t \approx 200$ nm. As a result, d for the GaN/AlN interface varies from 0.12 nm^{-1} to 3.8 nm^{-1} in our samples. We performed reflectometry, spectroscopic ellipsometry, and low-temperature photoluminescence measurements to carefully pre-characterize our SL samples. In addition, we undertook scanning transmission electron microscopy to check the structural quality of our layers with focus on their composition and interface quality. An example of such imaging is given for our 4 ML sample in Fig. 1. Furthermore, a random alloy $\text{Al}_{0.5}\text{Ga}_{0.5}\text{N}$ sample ($t \approx 200$ nm) was grown and compared to, e.g., the digital alloy represented by our 1 ML SL sample. Based on this approach, we aim to ensure that the interpretation of our measured $\kappa(d)$ trends can be linked to coherent heat conduction and not to other effects related to the sample quality. The frequency-domain thermoreflectance (FDTR) technique is selected for measuring κ . Furthermore, we validate FDTR analysis by comparing our results to TDTR measurements.

[1] J. Ravichandran *et al.*, *Nature Material* **13**, 168-172 (2014).

[2] Y. K. Koh *et al.*, *Advanced Functional Materials* **19**, 610-615 (2009).

[3] S. Tamariz *et al.*, *Journal Crystal Growth* **476**, 58-63 (2017).

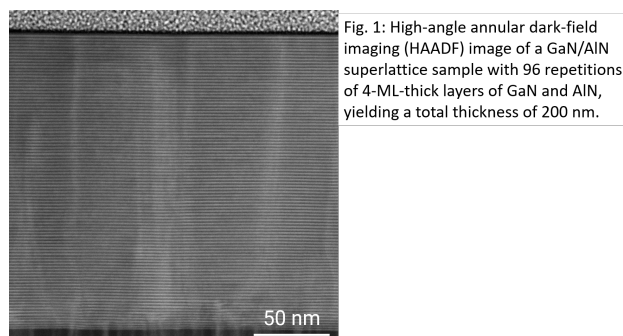


Fig. 1: High-angle annular dark-field imaging (HAADF) image of a GaN/AlN superlattice sample with 96 repetitions of 4-ML-thick layers of GaN and AlN, yielding a total thickness of 200 nm.

Fig1 nmht26 wuersch.png

Accurate Thermal Conductivity Measurement for Nano/Microscale Thermal Management: Advanced Models and Regression Methods for the Transient Plane Source Technique

Thursday, 23rd April - 16:50: Poster II - Poster

Mr. Jiaqi GU¹, Prof. Qiye Zheng¹

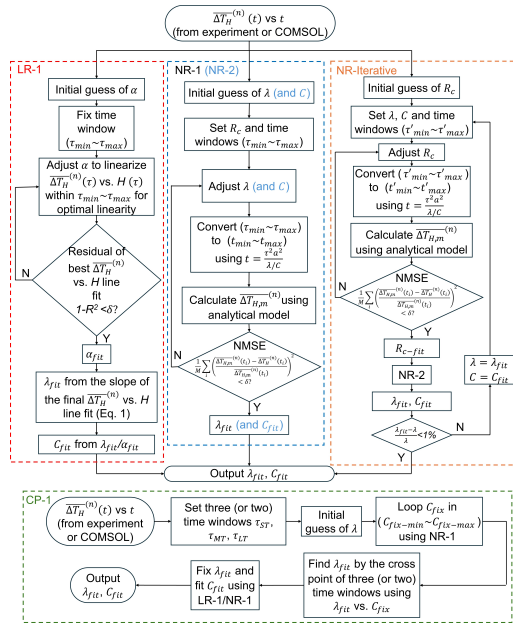
1. The Hong Kong University of Science and Technology

Accurate thermal conductivity (λ) measurement is critical for thermal management in advanced nano/microscale systems, including electronics cooling, aerospace components, and energy devices. Among contact methods, the transient plane source (TPS) method (ISO 22007-2:2022) is widely used for its efficiency in characterizing bulk solid samples. However, for high- λ materials ($\lambda > 30$ W/(m·K))—common in thermal management applications such as heat spreaders, heat sinks, and thermoelectric devices—TPS measurements suffer from significant systematic errors up to 97% due to limitations of traditional analytical models in addressing sensor/sample interface thermal resistance (R_c) and heat conduction within the sensor itself.

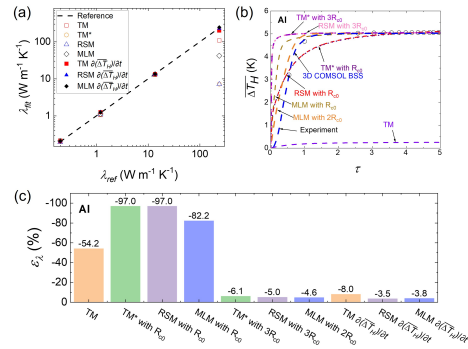
This study develops advanced analytical and regression frameworks to enable accurate thermal characterization of materials used in nano/microscale thermal management devices. We present: (1) two novel analytical models—realistic sensor model (RSM) and multilayer model (MLM)—that account for heat transfer within the sensor and R_c effects, both critical for high- λ materials used in thermal devices; (2) an innovative temperature derivative-based analysis approach using nonlinear regression (NR) that effectively suppresses R_c and sensor geometry influences, outperforming conventional iterative linear regression; and (3) systematic sensitivity analysis of key parameters via singular value decomposition (SVD), providing insights into optimal fitting procedures for thermal property determination.

We validate our approach using 3D finite element models (FEM) replicating the bifilar spiral structure of real TPS sensors, alongside experiments on four representative materials (PMMA, borosilicate glass, 304 stainless steel, and aluminum) and simulations spanning $\lambda = 0.1$ –400 W/(m·K). The derivative-based approach combined with two-parameter NR (NR-2) reduces errors from 50–97% to <10% for high- λ materials, remaining robust against R_c variations of one to two orders of magnitude. For materials with known heat capacity, one-parameter NR improves computational efficiency by 30–80% while maintaining <5% error. A derivative ratio model analysis further relaxes sample size requirements.

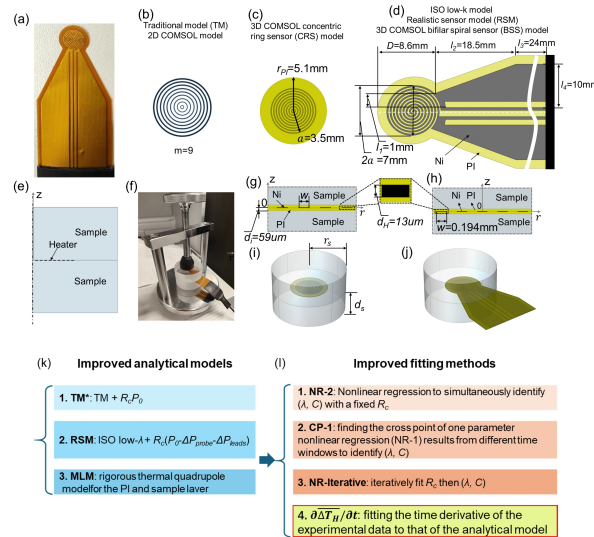
This comprehensive framework advances thermal characterization capabilities essential for designing and optimizing thermal management systems in nano/microscale devices, enabling more accurate material selection and performance prediction in energy components, heat spreaders, and thermal interface materials.



Flow chart of fitting approaches.jpg



The challenge in accurately analyzing high thermal conductivity materials.jpg



Schematic of the experimental setup and numerical modeling for the tps method.jpg

Thermophotonic coupling as a function of distance between the LED and the photovoltaic cell

Thursday, 23rd April - 16:50: Poster II - Poster

*Ms. Wissal Sghaier*¹, *Mr. Luc M. van der Krabben*², *Dr. Natasha Gruginskie*², *Dr. John J. Schermer*²,
*Dr. Somendu Maurya*³, *Dr. Jonna Tiira*³, *Dr. Tuomas Vaimala*³, *Dr. Kirsi Tappura*³, *Prof. Mika Prunnila*³,
*Dr. Benoit Behaghel*⁴, *Dr. Ivan Radevici*⁴, *Dr. Ahmad Shahahmahdi*⁴, *Dr. Jani Oksanen*⁴,
*Dr. P-Olivier Chapuis*¹

1. CETHIL, CNRS-INSA Lyon, France, 2. Radboud University, Nijmegen, The Netherlands, 3. VTT, Espoo, Finland, 4. Aalto University, Finland

Thermal radiation exchange between two surfaces at different temperatures is bounded by Planck's blackbody flux. As a result, the flux harvested by a photovoltaic (PV) cell facing a hot emitter has an upper bound. In order to convert more radiation into electricity than what is allowed by this bound, one has to emit more than thermal radiation. This is possible by replacing the passive hot emitter by a light-emitting device (LED), which however requires to be supplied with some electrical power to be active. Such a device coupling an LED to a PV cell is termed a thermophotonic device [1]. If the bandgaps of the two devices are matched, i.e. that the flux emitted by the LED and reaching the PV cell is narrow-band just above the bandgap energy, conversion efficiency could be very large. This requires quantum efficiency of both LED and PV cell being close to optimum: the power fed to the LED can then be harvested back in the PV cell. The output power comes then from the temperature difference between LED and PV cell, as the overall device can be understood as a heat engine. Interestingly, a refrigerating device can also be obtained if the temperature of the LED is initially lower than ambient [2]. We have implemented an experiment in order to analyze the pros and cons of thermophotonic coupling with devices based on GaAs ($E_g=1.42$ eV at room temperature). The experiment allows positioning one millimetric device with respect to the second one with nanometric accuracy down to a micrometric distance, i.e. with view factor close to unity. We report on the values of the Coupling Quantum Efficiency (CQE), defined as the ratio of output PV current to input LED one, as a function of the distance between the LED and PV cell. We demonstrate that CQE can be used for improving the positioning process. We also vary the temperature of the LED up to 120°C and observe a thermoradiative behaviour [3].

Fig. 1. Schematic of experiment in the thermal-energy harvesting mode.

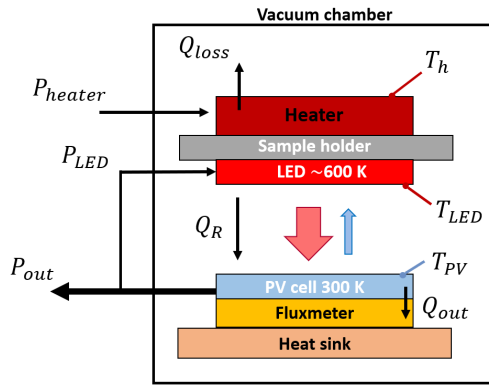
Fig. 2. Current harvested in the photovoltaic cell for a fixed LED current (0.38 mA, top) and CQE as a function of distance between the surfaces.

[1] N.P. Harder and M.A. Green, SST 18, S270 (2003)

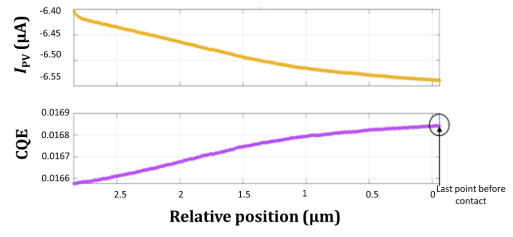
[2] T. Sadi et al., Nature Photonics 14, 205 (2020)

[3] M.P. Nielsen et al., Nature Photonics 18, 1137 (2024)

We acknowledge funding from EU projects TPX-Power&OPTAGON.



Wissalsghaier-fig1.png



Wissalsghaier-fig2.png

Direct Measurement of the Heat Capacity of Monolayer MoSe₂ by Ultrafast Nanocalorimetry

Thursday, 23rd April - 16:50: Poster II - Poster

***Mr. Hugo Gómez Torres*¹, *Dr. Sebin Varghese*², *Prof. Klaas-Jan Tielrooij*², *Dr. Aitor Lopeandia*³, *Prof. Javier Rodríguez-Viejo*³**

1. Catalan Institute of Nanoscience and Nanotechnology, 2. Eindhoven University of Technology, 3. Universitat Autònoma de Barcelona, Campus UAB, ES-08193 Bellaterra, Spain

The thermodynamic properties of two-dimensional (2D) materials remain largely unexplored due to the experimental difficulty of accessing their intrinsic heat capacity, which is typically masked by dominant substrate contributions. Here, we report the first direct measurement of the heat capacity (C_p) of few-layer down to monolayer MoSe₂, a 2D semiconductor, using a microsecond pulse-heating nanocalorimetry technique.

This approach relies on ultrafast, localized Joule heating of a suspended Pt/SiN nanocalorimetric platform, enabling the direct extraction of C_p from the temperature response with sub-picojoule sensitivity. The technique combines micro-scale energy sensitivity with sub-nanometer resolution in thickness, allowing heat capacity to be resolved at the level of individual atomic layers, as required for two-dimensional materials. In contrast to relaxation-based or optomechanical approaches that infer C_p indirectly from secondary parameters, this method provides direct access to the intrinsic heat capacity of atomically thin layers, establishing a new experimental route for quantitative thermodynamic measurements in the 2D limit.

The measured $C_p(T)$ exhibits clear deviations from bulk MoSe₂ behavior, highlighting the impact of reduced dimensionality and phonon confinement on lattice dynamics. Particular care is taken to quantify and subtract residual contributions from surface transfer contaminants, such as PDMS, ensuring isolation of the intrinsic MoSe₂ signal. These results provide a benchmark for the heat capacity of 2D semiconductors and demonstrate the capability of ultrafast nanocalorimetry to probe fundamental thermal properties of low-dimensional materials.

Controlling phonon transport in low-dimensional structures using phonon tunneling

Thursday, 23rd April - 16:50: Poster II - Poster

Prof. Ilari Maasilta¹, Dr. Zhuoran Geng¹

1. Nanoscience Center, Department of Physics, University of Jyväskylä

Acoustic phonons dominate heat transport in insulating solids at cryogenic temperatures, where micron-scale thermal wavelengths enable phononic engineering to tailor dispersion and thermal conduction. Because phonons are collective lattice excitations, they are generally confined to solids and cannot cross vacuum gaps. Although theory predicts phonon tunneling mediated by van der Waals or electrostatic interactions, such coupling is typically restricted to sub-nanometer separations under practical conditions [1,2].

Here we investigate piezoelectricity as a longer-range mechanism for acoustic phonon tunneling through vacuum [3,4]. Thermally excited acoustic phonons incident on a free surface of a piezoelectric solid generate evanescent electric fields that penetrate the vacuum and decay exponentially. When a second piezoelectric body lies within the interaction range set by the field decay length and the phonon wavelength, these fields couple coherently to its lattice vibrations, enabling contactless phonon-mediated energy transfer. We identify resonant tunneling conditions under which selected phonon modes achieve unity transmission [5]. Experiments using two independently suspended piezoelectric beams separated by a vacuum gap at cryogenic temperatures show energy transfer well above classical Planck radiation and substantially larger than in non-piezoelectric reference devices.

We further extend numerical studies to lower-dimensional piezoelectric structures, including two-dimensional plates and one-dimensional beams. Overlapping evanescent fields produce symmetric and antisymmetric coupled states, yielding hybridized phonon modes and splitting of phonon branches. This coherent modification of dispersion impacts ballistic heat transport and offers a gap- and geometry-tunable route to control thermal conductance. Selective excitation of one structure can also drive phonon “shuttling,” observed as periodic oscillations of energy exchange between the two bodies.

References

- [1] J. B. Pendry, K. Sasihithlu, and R. V. Craster, *Phys. Rev. B* **94**, 075414 (2016).
- [2] A. I. Volokitin, *J. Phys. Condens. Matter* **32**, 215001 (2020).
- [3] M. Prunnila and J. Meltaus, *Phys. Rev. Lett.* **105**, 125501 (2010).
- [4] Z. Geng and I. J. Maasilta, *Phys. Rev. Research* **4**, 033073 (2022).
- [5] Z. Geng and I. J. Maasilta, *Commun. Phys.* **6**, 178 (2023).

Thermal Transport Evolution in WS₂ Polymorphs: From 2H to the Low-Symmetry 2M Phase

Thursday, 23rd April - 16:50: Poster II - Poster

***Dr. Qi Ren*¹, *Ms. Marta Loletti*¹, *Dr. Riccardo Rurali*¹**

1. Institut de Ciència de Materials de Barcelona, ICMAB-CSIC, ES-08193 Bellaterra, Spain

Designing materials with tailor made thermal properties is an important challenge in current condensed matter and nanoscience, particularly for the implications on efficient thermal management in electronics and for applications related to energy harvesting, such as thermoelectricity. Polymorphism in layered transition metal dichalcogenides (TMDs) allows for significant changes in the structure and properties, and can sometimes be triggered with various external stimuli, such as charge transfer, temperature, electrostatic gating or strain. This makes TMD an ideal platform for exploring the structure-property relationship and phase transition control engineering of low-dimensional materials.

As a prototypical TMDs, the 2H phase of WS₂ has been extensively studied and applied; however, it is only very recently that the elusive 2M phase has been successfully synthesized. The rare 2M phase of WS₂ exhibits superconductivity [1] and, due to its low-symmetry layered structure, holds potential for non-trivial topological states, making it an ideal platform for exploring phase-transition-driven superconducting and topological phenomena [2]. While the electronic properties of 2M WS₂ have been extensively explored, their thermal transport characteristics remain virtually unknown. Moreover, the newly reported room-temperature Na-intercalation synthesis route [3] enables a controlled 2H → 2M phase transition, creating intermediate metastable structures whose heat-transport behavior has never been investigated. This provides a timely opportunity to understand how structural symmetry breaking, intercalation chemistry and polymorphism collectively affect phonon transport.

In this work, we present a comprehensive thermal transport investigation of pristine 2M WS₂ and of the intermediate Na-intercalated configurations along the 2H → 2M transition pathway. Using density functional theory (DFT) combined with phonon Boltzmann transport calculations beyond the relaxation-time approximation, we compute second- to fourth-order interatomic force constants (IFCs) for WS₂ polymorphs and quantify their full phonon-phonon scattering phase space. To address the large supercells required for the intercalated phases, we integrate machine-learning interatomic potentials (MACE) to generate harmonic and anharmonic IFCs with substantially reduced computational cost, validating their accuracy against benchmark DFT phonon dispersions. Our results reveal significant variations in lattice thermal conductivity across the different polymorphs and intercalated structures, exploring polymorph-driven thermal switching as a method for actively controlling heat flux in van der Waals materials.

Reference

- [1] Nature Physics 19, 106 (2023)
- [2] Nature Communications 15, 1263 (2024)
- [3] Chemistry of Materials, 37, 129 (2025)

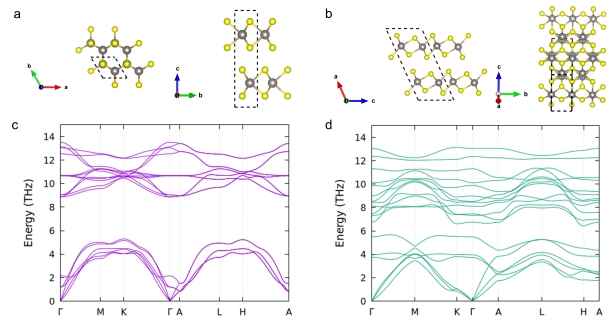


Figure 1. Top and side view of crystal structure of (a) 2H and (b) 2M phase WS₂. Phonon dispersion of (c) 2H and (d) 2M phase WS₂.

Abstract figure.png

Studying Phonon vs. Electron Contributions to Heat Transport of Single-Flake Metallic Ti₃C₂T_x MXene using Spatiotemporal Microscopy

Thursday, 23rd April - 16:50: Poster II - Poster

Mr. Max van Hemert¹, **Dr. Hugh Ramsden**¹, **Dr. Sebin Varghese**¹, **Dr. Bohai Lui**¹, **Ms. Elvira Tornero**²,
Dr. Stefano Ippolito³, **Dr. Miguel Muñoz**², **Prof. Yury Gogotsi**³, **Dr. Hai Wang**⁴, **Prof. Klaas-Jan Tielrooij**¹

1. Eindhoven University of Technology, 2. Instituto de Ciencia de Materiales de Madrid, Madrid, Spain, 3. Drexel University, 4. Utrecht University

MXenes are an up-and-coming class of two-dimensional materials, which are relatively easily produced at large scale using wet-chemical etching from the MAX phase [1]. This makes these materials attractive for application in, for example, electromagnetic interference shielding, thermal management, sensing and energy storage. Because of its importance for applications, it is important to understand their thermal properties. Although Ti₃C₂T_x is the most well-studied MXene, reported values for the in-plane thermal conductivity vary substantially between different sources. Furthermore, despite the metallic nature of Ti₃C₂T_x MXene [2], it is still unknown whether electrons or phonons mainly contribute to its plane heat conduction.

We address these issues by studying in-plane heat transport in single-flake Ti₃C₂T_x MXene, eliminating effects caused by the interaction of multiple flakes in films. Using spatiotemporal microscopy [3,4], we directly visualise the heat transport in space and time. From these measurements, we find a thermal diffusivity of 0.05 cm²s⁻¹, which corresponds to an in-plane thermal conductivity of 13.5 Wm⁻¹K⁻¹.

To investigate the role of electrons in the thermal transport, we assess their contribution using the Wiedemann-Franz law. From the upper limit of electrical conductivity of 10⁶ Sm⁻¹, we find that the electrons contribute less than 50% to the thermal conductivity in Ti₃C₂T_x MXene. This contrasts with the usual domination of electrons to the thermal conductivity of metals. This could open new ways to control the thermal transport of MXenes.

[1] Naguib, M. *et al.* 25th Anniversary Article: MXenes: A New Family of Two-Dimensional Materials. *Advanced Materials* **26**, 992–1005 (2014).

[2] Lipatov, A., Bagheri, S. & Sinitskii, A. Metallic Conductivity of Ti₃C₂T_x MXene Confirmed by Temperature-Dependent Electrical Measurements. *ACS Materials Lett.* **6**, 298–307 (2024).

[3] Varghese, S. *et al.* A pre-time-zero spatiotemporal microscopy technique for the ultrasensitive determination of the thermal diffusivity of thin films. *Review of Scientific Instruments* **94**, 034903 (2023).

[4] Vazquez, G. D. B. *et al.* Spatiotemporal Microscopy: Shining Light on Transport Phenomena. *Adv Elect Materials* **2300584** (2023).

Investigating the effect of temperature and relative humidity on thermal transport in Covalent organic frameworks (COFs)

Thursday, 23rd April - 16:50: Poster II - Poster

Ms. Sudeshna Sahoo¹, Mr. Yannick Eich¹, Prof. Seema Agarwal¹, Prof. Juergen Senker¹, Prof. Markus Retsch¹

1. University of Bayreuth

Covalent organic frameworks (COFs) are a class of highly ordered crystalline porous materials synthesized by linking organic building blocks via covalent bonds that lead to a well-defined porosity. Different pore sizes and linker groups have been shown to influence heat transport in the COF materials.¹ As the pore size of the COFs increases, the overall thermal conductivity decreases because solid heat-conduction pathways are diminished due to lower material density, and phonon scattering at the pore surfaces is enhanced.² Temperature also plays a key role in modulating the thermal conductivity of COFs by affecting heat transport through the covalent backbone.³ Owing to the large surface area and open porous nature of COFs, a substantial degree of water adsorption can occur depending on the relative humidity.

In this contribution, we systematically elucidate how temperature and humidity can influence the thermal conductivity of COFs with various pore sizes and functional groups. In particular, hydrophilic linker groups such as -SO₃H, which act as chemical anchors for water molecule adsorption, are of interest as this increases the effective heat conduction pathways. Consequently, the combined effect of temperature and relative humidity can enhance heat transport within these COFs, a phenomenon validated through thermal conductivity measurements of COF powders using the Modified Transient Plane Source (MTPS) technique. We elucidate the reversibility of the temperature- and humidity-dependent thermal conductivity to provide a fundamental understanding of the interplay between the COF structure, its chemical functionalization, and water adsorption.

(1) Freitas, S. K. S.; Borges, R. S.; Merlini, C.; Barra, G. M. O.; Esteves, P. M. Thermal Conductivity of Covalent Organic Frameworks as a Function of Their Pore Size. *Journal of Physical Chemistry C* **2017**, *121* (48), 27247-27252. DOI: 10.1021/acs.jpcc.7b10487.

(2) Thakur, S.; Giri, A. Supramolecular reinforcement drastically enhances thermal conductivity of interpenetrated covalent organic frameworks. *Journal of Materials Chemistry A* **2023**, *11* (35), 18660-18667. DOI: 10.1039/d3ta04161a.

(3) Kwon, J.; Ma, H.; Giri, A.; Hopkins, P. E.; Shustova, N. B.; Tian, Z. T. Thermal Conductivity of Covalent-Organic Frameworks. *Acs Nano* **2023**, *17* (16), 15222-15230. DOI: 10.1021/acsnano.3c03518.

Thermal anisotropy in layered oxide Bragg stacks

Thursday, 23rd April - 16:50: Poster II - Poster

***Mr. Simon Freund*¹, *Mr. Ingmar Pietsch*¹, *Prof. Josef Breu*¹, *Prof. Markus Retsch*¹**

1. University of Bayreuth

Several layered oxide materials can be gently delaminated in water via osmotic forces to form large single-layer nanosheets in a liquid crystalline dispersion. Spray-coating such dispersions yields films of nanosheet stacks with high regularity along the stacking direction (Bragg stacks). In the case of Sodium-Fluorohectorite, such Bragg stack films exhibit much faster thermal transport along the films as compared to through the stacks ($\kappa_{\parallel} / \kappa_{\perp} > 25$). [1,2]

However, we observed that depending on the specific Bragg stack material, the thermal anisotropy can also be as low as $\kappa_{\parallel} / \kappa_{\perp} = 3$, even though the structural properties of the films are comparable.

This contribution discusses why the thermal anisotropy can vary so much depending on the specific Bragg stack material. We present thermal transport measurements of various layered oxide Bragg stack films fabricated via spray-coating, ranging from different silicates to titanate and niobate films. To study the directional thermal properties of the films, we employ different frequency-domain laser heating techniques that probe the temperature evolution via infrared emission (Lock-In Thermography), the photoacoustic effect (Photoacoustic Method), or the thermorefectance effect (Frequency-Domain Thermorefectance).

References:

- [1] Z. Wang, K. Rolle, T. Schilling, P. Hummel, A. Philipp, B. Kopera, A. Lechner, M. Retsch, J. Breu, and G. Fytas, *Angew. Chem. Int. Ed.* **59**, 1286–1294 (2020).
- [2] A. Philipp, P. Hummel, T. Schilling, P. Feicht, S. Rosenfeldt, M. Ertl, M. Schöttle, A. M. Lechner, Z. Xu, C. Gao, J. Breu, and M. Retsch, *ACS Appl. Mater. Interfaces* **12**, 18785–18791 (2020).

Localizing heat at the nanoscale via dissipation – Testing 3-temperature models by ultrafast x-ray diffraction and transient absorption

Friday, 24th April - 09:00: Invited - Invited talk

Prof. Matias Bargheer¹

1. University of Potsdam, Institute of Physics and Astronomy / HZB Helmholtz-Zentrum Berlin

Ultrafast optical excitation initiates energy transfer processes at the nanoscale with extraordinary and surprising phenomena, due to non-equilibrium conditions between electrons and phonons. Focusing on well-defined model systems composed of nanolayered metal heterostructures we provide experimental crosschecks of two- or three-temperature models via ultrafast x-ray thermometry for the following phenomena: After a nearly homogenous optical pulse, the energy deposited in the electron system spontaneously localizes in thin layers significantly below the skin depth (Fig. 1). While the electrons are significantly hotter than the phonons, electronic pressure acts on metal-metal interfaces, although the latter are transparent to electronic energy transport. Once electron-phonon coupling sets in, very large temperature gradients can persist across the metallic interface for several tens of picoseconds.

The main ingredient in these observations is that metals with d-orbitals at the Fermi level (Pt, Pd, Ni, Fe, Co...) have a significantly larger thermally accessible electronic density of states, which increases the electronic heat capacity and the electron-phonon coupling. Combining such materials with more noble metals like Au and Cu leads to counterintuitive phenomena, which can be unraveled by ultrafast X-ray diffraction, a unique material-specific and time-resolved thermometer.

The described phenomena have applications in thermal transport, engineering light-driven chemistry and THz manipulation of functional materials.

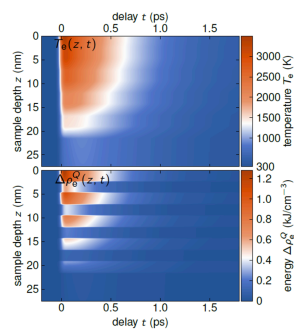


Fig. 1: Spatiotemporal temperature and electronic energy density in a Pt/Cu superlattice with about 5nm period. The electrons rapidly thermalize which leads to a sharply localized energy density due to the material differences in specific heat.

Bargheer nmht fig1.png

Couplings between heat carriers (electrons, phonons and magnons) in complex systems

Friday, 24th April - 10:00: Complex, Multi-Agent Transport - Oral

Prof. Yanguang Zhou¹

1. Hong Kong University of Science and Technology (HKUST)

The interaction among electrons, phonons, and magnons is a key focus in solid-state physics. While experiments can measure the overall strength of coupling between them, it is challenging for experimentalists to obtain the detailed dynamics of the couplings between these heat carriers.

Atomistic simulations, on the other hand, can provide detailed dynamic information and mechanisms of the couplings between these heat carriers. For example, the electron-phonon coupling (EPC) in simple crystals can be determined by the electron-phonon scattering matrix and Eliashberg spectral function, which can be calculated from density functional theory (DFT) simulations. Meanwhile, numerical studies usually focus on simple systems, e.g., bulk crystals and nanocrystals, with tens of atoms due to computational limitations.

In real situations, however, many materials exist in the form of polycrystals which include many planar defects, i.e., grain boundaries. These planar defects may largely affect the EPC, and then the related electrical and thermal properties. For instance, Yazdani *et al.* found that the planar defect, i.e., free surfaces, can largely increase the strength of the EPC in nanocrystals using *ab initio* molecular dynamics (AIMD) simulations. It is therefore necessary to systematically investigate the couplings among various heat carriers in complicated systems, and the underlying mechanism behind the relation between the couplings among various heat carriers and planar defects, which remains largely unexplored.

In this talk, we will introduce the Langevin dynamics simulations with spatial correlations, which can systematically study the EPC in polycrystals, and a new computational tool to capture the dynamics of phonon-magnon couplings (PMC) in magnetic systems. We find that the EPC constant of polycrystalline silicon is larger than that of single-crystalline silicon and increases with the decrease of grain size. Our results also reveal that high-frequency phonon-magnon scattering rates are one order of magnitude larger than those at low frequencies due to energy scattering conservation rules and high densities of states.

References:

- 1, Wenxiang Liu, Xing Xiang and Yanguang Zhou*, Electron-phonon Coupling in Polycrystalline Silicon. *Phys. Rev. B* **112**, 155301 (2025).
- 2, Yanguang Zhou, Julien Tranchida*, Yijun Ge, Jayathi Y. Murthy* and Timothy S. Fisher*, Atomistic Simulations of Phonon and Magnon Thermal Transport in Magnetic Materials. *Phys. Rev. B* **101**, 224303 (2020).
- 3, Yanguang Zhou, and Ming Hu*, Full Quantification of Three-phonon Scattering Process at Interface from Non-Equilibrium Molecular Dynamics Simulation. *Phys. Rev. B* **95**, 115313 (2017).

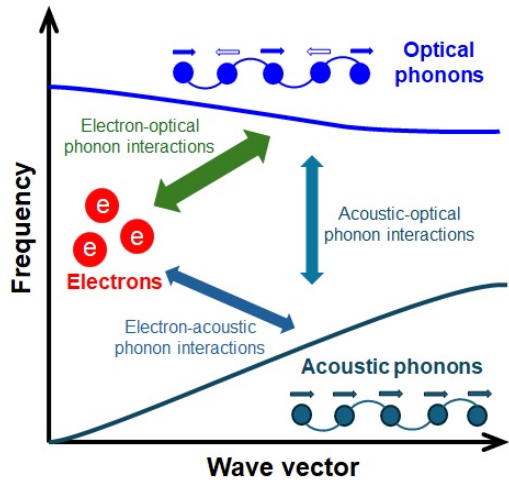


Fig3-1.jpg

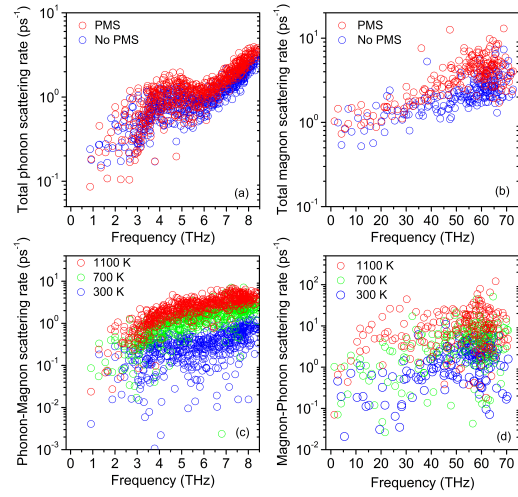


Fig 3.jpg

Engineering Transport and Thermoelectric Properties of Cs₂NaYbCl₆ Perovskite via Doping and Nanoengineering

Friday, 24th April - 10:20: Complex, Multi-Agent Transport - Oral

***Dr. Antonio Cappai*¹, *Prof. Claudio Melis*¹, *Prof. Luciano Colombo*¹**

1. University of Cagliari

We present a first-principles investigation of the combined effects of chemical doping and nanostructuring on thermoelectric performance of the double halide perovskite Cs₂NaYbCl₆. Using Density Functional Theory and Boltzmann transport calculations, we explicitly include all relevant scattering mechanisms (namely, electron–phonon, phonon–phonon, Coulomb impurity, phonon–impurity, and grain boundary scattering) to evaluate electrical and thermal transport coefficients. Our results show that Coulomb scattering from dopants is strongly screened and negligible compared to dominant electron–phonon interactions. Thus, both n- and p-type doping enhance electrical conductivity while only moderately reducing the Seebeck coefficient, leading to a significant increase in power factor. Phonon–impurity scattering is found to be minimal, while grain boundary scattering effectively reduces lattice thermal conductivity without strongly affecting carrier mobility. Combining optimal n-type doping (10^{19} cm⁻³) with nanoscale grains (10 nm), the figure of merit ZT increases from $\sim 10^{-8}$ in the pristine crystal to ~ 0.12 . These findings demonstrate a viable pathway for improving thermoelectric efficiency in wide-bandgap, lead-free perovskites through controlled extrinsic modifications.

Fast Ionic Transport Governed by Collective Vibrational Dynamics

Friday, 24th April - 10:40: Complex, Multi-Agent Transport - Oral

*Dr. Yixin Xu*¹, *Prof. Yanguang Zhou*¹

1. Hong Kong University of Science and Technology (HKUST)

We elucidate the role of collective vibrational dynamics in governing the ionic transport in solids. It is demonstrated that the ionic transport is mediated through a synergistic interplay between unstable and stable vibrational modes. Unstable vibrational modes directly initiate the hopping of ions by displacing ions from their equilibrium sites. Stable vibrational modes, in parallel, facilitate the ion diffusion indirectly by amplifying the separation of local ionic pairs through coordinated collective rearrangements. The interaction between unstable and stable vibrational modes collectively results in the high ionic diffusivity in solids. The “vibration-ion” interaction is further designed via defect engineering. Our results show that the population of unstable vibrational modes is increased by tailoring the vibrational spectrum using intrinsic ionic vacancies. This concurrently strengthens the direct ionic translation and the coupling between unstable and stable vibrational modes. As a result, the ionic diffusivity of the example system Ag_2Te increases from $0.84 \times 10^{-5} \text{ cm}^2/\text{s}$ to $1.54 \times 10^{-5} \text{ cm}^2/\text{s}$ at 500 K when 10% Te^{2-} vacancies are introduced. Our work here establishes a physical picture to bridge the microscopic vibrational dynamics to macroscopic diffusion properties.

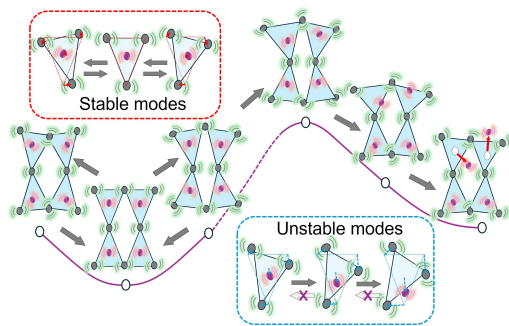


Figure vibration ion schematic.jpg

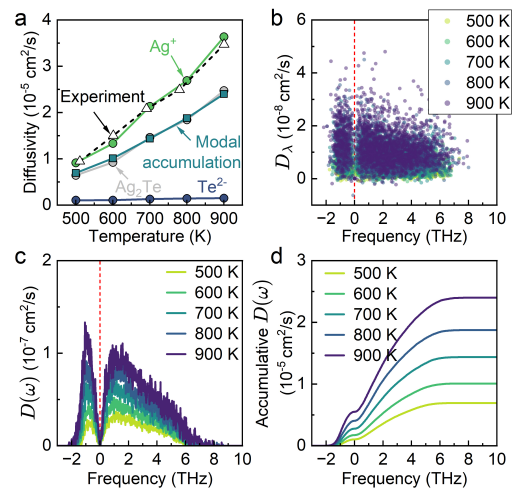


Figure modal diffusion.jpg

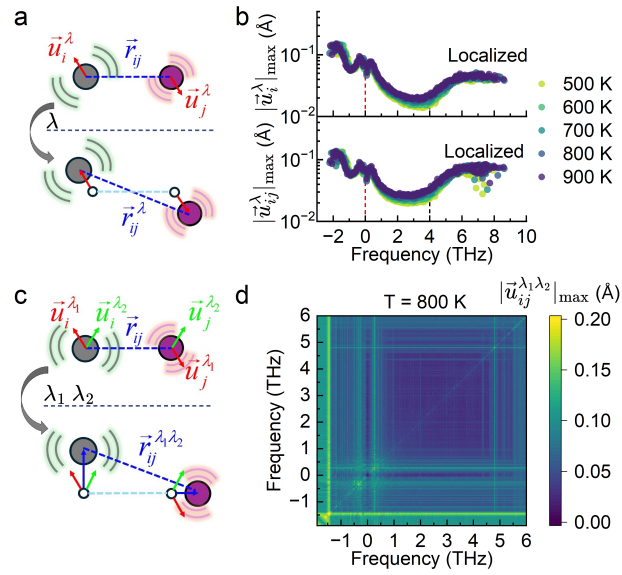


Figure modal separation.jpg

Anomalous thermal transport in 2D layered metal organic frameworks

Friday, 24th April - 11:00: Complex, Multi-Agent Transport - Oral

***Dr. Riccardo Dettori*¹, *Prof. David Beljonne*², *Prof. Luciano Colombo*¹, *Prof. Claudio Melis*¹**

1. University of Cagliari, 2. University of Mons

Two-dimensional metal–organic frameworks (2D MOFs) combine soft lattices and tunable interlayer coupling, making them an appealing platform to engineer directional heat transport. In this work, we investigate lattice dynamics and thermal conduction in layered copper benzenehexathiolate (Cu₃BHT) as a function of stacking pattern (AA, AB, and C) using a fully first-principles workflow. Density-functional-theory simulations coupled with lattice dynamics calculations reveal that AB stacking is dynamically unstable, while the C phase is the thermodynamic ground state and features covalent Cu–S interlayer bridges that stiffen shear/breathing modes and strongly enhance through-plane transport. In evaluating thermal conductivity, we find that heat conduction is dominated by low-frequency interlayer modes, resulting in ultralow thermal conductivity and pronounced anisotropy. Moreover, coherent (Wigner) contributions substantially increase κ and weaken the classical T^{-1} trend to $\kappa \propto T^{-\alpha}$ with $\alpha < 1$, indicating a mixed particle-/wave-like transport regime in these soft, near-degenerate phonon manifolds. [1]

Building on this ab initio benchmark, we outline the generation of a machine-learned interatomic potential for Cu₃BHT using the linearly parametrized ChIMES framework trained on DFT energies/forces/stress tensor across representative stacking registries, low-frequency distortions, and thermally sampled configurations. This potential will enable large-scale equilibrium and non-equilibrium molecular dynamics to quantify the impact of microstructure, stacking disorder, and defects on nanoscale heat transport while preserving fidelity to the first-principles phonon physics highlighted here. [2,3]

[1] Dettori, R. *et al.* Scientific Reports, 2025, 15(1), 41337

[2] Dettori, R. *et al.* Nano Express, 2025, 6(4), 045004

[3] Dettori, R. *et al.* Nanotechnology, 2025, 36(15), 155703

Using heterodyned, deep-ultraviolet transient gratings to measure non-diffusive heat transport in crystalline silicon membranes

Friday, 24th April - 11:50: Semiconductors and Thermoelectricity - Featured talk

***Ms. Emma Nelson*¹, *Mr. Yunhao Li*¹, *Mr. Theodore Culman*¹, *Ms. Jiayi Liu*¹, *Dr. Albert Beardo*², *Dr. Brendan McBennett*³, *Prof. Joshua Knobloch*⁴, *Prof. Henry Kapteyn*¹, *Prof. Margaret Murnane*¹**

1. University of Colorado, Boulder, 2. Universitat Autònoma de Barcelona, Campus UAB, ES-08193 Bellaterra, Spain, 3. National Institute of Standards and Technology, 4. Utah State University

To push the limits of computing power and speed, next-generation devices will utilize novel materials, small features, and complex geometries. To meet these demands, characterization techniques that can capture the nanoscale properties of semiconductors in transient situations that mimic their use in real devices are crucial. Transient grating (TG) experiments, where two laser beams are crossed on a sample to create a nanoscale excitation, are one method traditionally used to measure nanoscale transport in semiconductors. Most tabletop transient gratings are limited to excitation periods >500 nm by the use of visible lasers, so to reach smaller length scales, ultraviolet light is needed [1]. Extreme ultraviolet light has been used for TG at facility-scale sources, but these setups are not as accessible [2].

Here, we present a novel, all-reflective, heterodyned TG experiment using deep-ultraviolet (DUV, ~ 200 nm) light to directly excite ultrawide-bandgap semiconductor materials. We generate DUV light using nonlinear optical crystals to upconvert to the fourth harmonic of the fundamental Ti:sapphire pulse. This short wavelength is necessary to reach nanoscale transient grating periods, as TG period scales with pump laser wavelength, and to directly excite ultrawide-bandgap materials that are transparent to visible light.

The first iteration of the experiment used lenses to create the transient grating, generating TG patterns down to 287nm. We first validated the DUV TG setup by measuring the acoustic wave velocity in a gold thin film, and then we characterized carrier diffusion in diamond, an ultrawide bandgap material [3]. However, the lens geometry does not allow for heterodyne detection, in which the diffracted probe beam interferes with a static reference beam on the detector to increase the signal-to-noise ratio [1].

To increase the experimental sensitivity using heterodyne detection, we implement an all-reflective geometry using off-axis parabolic mirrors to cross the DUV beams on the sample. This detection scheme also allows us to optimize the thermal response relative to the electronic contribution to the signal. With this novel heterodyned geometry, we characterize non-diffusive thermal transport in <50 nm thick silicon membranes and compare our measurements of their thermal conductivity to values calculated using approximate solutions to the Boltzmann Transport equation, including both hydrodynamic and ballistic models. We observe an unexpected interplay between cross-plane and in-plane effects in the membrane thermal conductivities.

[1] Johnson et al., *PRL* **10**, 025901 (2013)

[2] Bencivenga et al., *Sci. Adv.* **5**, eaaw5805 (2019)

[3] Nelson et al., *Phys. Rev. Applied* **22**, 054007 (2025)

Thermoelectric characterization of 2D materials on a micro-chip platform

Friday, 24th April - 12:20: Semiconductors and Thermoelectricity - Oral

Dr. Nathan Aubergier¹, **Dr. Peng Xiao**², **Dr. Eva Desgue**³, **Dr. Pierre Legagneux**³, **Mr. Nicolas Claus**¹,
Dr. Daniel Bourgault¹, **Dr. Paolo Bondavalli**³, **Dr. Aymen Mahjoub**³, **Dr. Olivier Bourgeois**¹

1. Institut Néel, CNRS, 25 avenue des Martyrs, F-38000 Grenoble, France, 2. Univ. Bordeaux, CNRS, LOMA UMR 5798, Talence, France, 3. Thales Research & Technology, 1 avenue Augustin Fresnel, 91767 Palaiseau, France

Fabrication progress of new material compatible with clean-room procedures leads a promising way to thermoelectric generators (TEGs). Indeed, while energy harvesting can arise from the MW to the μW , an effort is made to develop scalable nanometer sized TEG (nanoTEG) for large-market applications at the μW scale (e.g. internet of things, IoT)¹. For that usage, TE conversion efficiency of such materials needs to be characterized, mainly the Seebeck coefficient S and the electrical conductivity σ which are both included in the figure of merit ZT . ZT is equal to $S^2\sigma T/\kappa$ and dictates the overall TEG performance, where κ is the thermal conductivity and T the absolute temperature. For IoT applications, materials with important power factor ($P_F = S^2\sigma$) need to be found. Promising candidates are various, from thinned-down well-established bulk materials like Bi_2Te_3 to more exotic 2D based materials with particular band structure like topological insulators made by layered or epitaxial transition-metal dichalcogenide (TMDC). Characterisation of 2D TE materials can then be challenging considering that the temperature gradient across the material of interest must be precisely controlled and measured. For that purpose, we developed a lab-on-chip platform to probe locally and in a well-controlled environment the Seebeck coefficient as well as the electrical conductivity in a wide temperature range². In this work, we report the characterization (DC and AC modes) to probe the thermoelectric properties of materials with different thicknesses, from thin FeVAl film (100nm), Bi_2Te_3 (300nm) to layered materials like SnSe_2 (10nm) and epitaxied PtSe_2 (15nm) (Fig. 1). A fine temperature control is shown and small temperature gradients along the sample which are as low as 5mK at room temperature can be used. In such a small gradient, parasitic Seebeck contribution can arise from other temperature gradients in the measurement line, this is why we developed an AC mode in order to couple the localised temperature gradient with an identified voltage contribution. Fig. 2 shows different Seebeck characterisations for thin film FeVAl (A-B) and SnSe_2 flakes as well as Bi_2Te_3 -based thin film. With the ability to characterize the Seebeck coefficient precisely at low temperature, such micro-chip platforms can be used to characterize promising low-temperature thermoelectric phenomena like the phonon-drag effect in heterostructures.

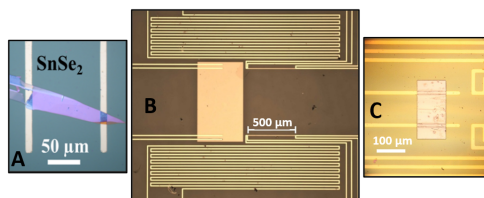


Fig 1. Optical image of the measurement chip featuring a dry-transferred SnSe_2 flake (A), a MBE grown PtSe_2 (B) and a sputtered n-type Bi_2Te_3 film (C). The panel B show a zoom-out view of the lab-on-chip devices. Top and bottom mazes are symmetrical heater to reverse the temperature gradient. Voltage probes are strategically aligned parallel to the Seebeck electrodes to ensure that both voltage and thermal gradients were measured along the same axis.

Aubergier nmht fig1.png

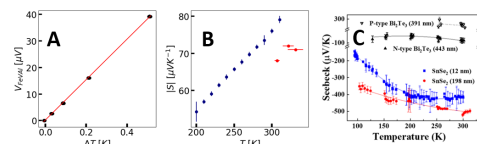


Fig 2. A. FeVAl Seebeck coefficient measurement in AC mode at $T_{\text{bath}} = 300\text{K}$ were power dissipated in the chip that create the in plane temperature gradient range from 0mW at $\Delta T = 0\text{K}$ to 400mW at $\Delta T = 500\text{mK}$. We observe a important temperature control even at room temperature, the minimum temperature gradient measured is $\Delta T = 10\text{mK}$. B. Temperature-dependent Seebeck coefficients for FeVAl thin film in blue. Red dots are macroscopic measurements using a temperature gradient which is about 20K. C. Temperature-dependent Seebeck coefficients for crystalline SnSe_2 flakes (198 nm and 12 nm) and both n- and p-type Bi_2Te_3 -based thin films [2].

Aubergier nmht fig2.png

Non-local heating in semiconductor membranes

Friday, 24th April - 12:40: Semiconductors and Thermoelectricity - Oral

**Mr. Mahmoud Elhajhasan¹, Ms. Katharina Dudde¹, Ms. Elena Trukhan², Mr. Guillaume Würsch¹,
Mr. Julian Themann¹, Ms. Jana Lierath¹, Dr. Nakib Protik², Dr. Giuseppe Romano³,
Prof. Gordon Callsen¹**

1. Universität Bremen, 2. Humboldt-Universität zu Berlin, 3. MIT-IBM Watson AI Lab

Heating of photonic and electronic semiconductor devices limits their performance and lifetime, which must be encountered by thermal management starting at the heat source. It is a common assumption that the heat source and the resulting heat spot locally coincide for length scales exceeding the mean free paths of the main heat carriers in a semiconductor, the phonons. We show that this paradigm of heat locality already breaks down on a few micrometer length scale, and non-local heating can appear.

We developed a thermal imaging system based on two-laser Raman thermometry (2LRT) relying on $4f$ -imaging, to directly illustrate phonon-induced local and non-local heating phenomena in semiconductor membranes. First, we tested our experimental setup by analyzing extended membranes made of Si [1] and mainly GaN [2]. For our most recent generation of samples we added lateral boundaries (counted by n) to our GaN membranes (≈ 250 -nm-thick), allowing us to form edges ($n = 1$), corners ($n = 2$), and hexagons ($n = 6$). In addition to the common laser-induced heat spot (see Fig. 1 A, $n = 2$), we observe a heating of boundaries (semiconductor/vacuum interfaces) in these samples at a distance of a few micrometers to the heat spot (see Fig. 1 B), if the laser power suffices. We find that this non-local heating phenomenon persists well above room temperature and intensifies with increasing n .

We interpret our experimental finding in terms of phonons propagating with a long mean free path that are generated in the laser-induced heat spot, but do not predominantly contribute to a temperature rise in this location, as they travel to the edges of the membrane. Here, these phonons scatter and deposit their thermal energy, leading to non-local, so-called, “edge heating“. Interestingly, our observation is not limited to cryogenic temperatures, because it occurs even well above room temperature with maximal lattice temperatures reaching up to 970 K ($n = 6$). We link this observation to the importance of 4-phonon scattering at such temperatures, enabling the generation of low-energy phonons with long mean free paths in GaN. Our observation highlights the importance of heat generation via light absorption for modeling thermal transport. Overall, boundaries similar to the edges that heat in these structures appear in any real-world device and must be considered for thermal management.

[1] K. Dudde *et al.*, *Material Today Physics* **57**, 101784 (2025).

[2] M. Elhajhasan *et al.*, *Phys. Rev. B* **108**, 235313 (2023).

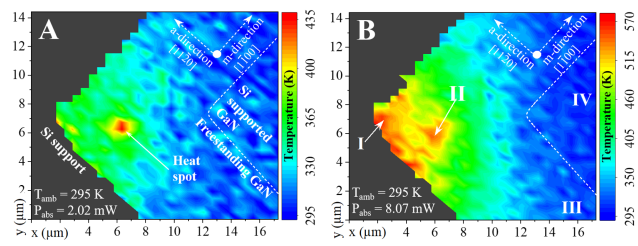


Fig. 1. Thermal imaging of a GaN membrane corner ($n = 2$) by 2LRT. (A) Temperature mapscan at a corner ($n = 2$) with the heat laser (absorbed laser power of $P_{abs} = 2.02$ mW) placed at a distance of $d = 3.5 \pm 0.3$ μm away from the lateral membrane boundaries. The laser-induced, local heat spot is clearly visible. **(B)** Increasing P_{abs} to 8.07 mW yields a temperature mapscan that shows heating at the position of the heat laser (II) and at the edge of the membrane (I) in the corner region. Here, III marks the free-standing GaN membrane and IV the GaN film that is still supported by the Si substrate.

Figure 1.png

Out-of-plane thermal conductivity of $\text{Ti}_3\text{C}_2\text{T}_x$ MXene flakes depending on temperature and thickness

Friday, 24th April - 13:00: Semiconductors and Thermoelectricity - Oral

*Ms. Elvira Tornero*¹, *Dr. Bohai Lui*², *Dr. Stefano Ippolito*³, *Mr. Max van Hemert*², *Dr. Hugh Ramsden*², *Dr. David Saleta*⁴, *Dr. Aaron Schmidt*⁵, *Dr. Katja Klinar*⁶, *Prof. Yury Gogotsi*³, *Prof. Klaas-Jan Tielrooij*², *Dr. Miguel Muñoz*¹

1. Instituto de Ciencia de Materiales de Madrid, Madrid, Spain, 2. Eindhoven University of Technology, 3. Drexel University, 4. Catalan Institute of Nanoscience and Nanotechnology, 5. Fourier Scientific, 6. University of Ljubljana

Transition metal carbides or nitrides, referred to as MXenes, is a family of two-dimensional materials with intriguing properties for electronic, insulating, and thermoelectric applications. Within these applications, understanding the heat transport across MXenes is essential for reliable device operation. However, the mechanisms governing heat conduction in these materials, particularly along the out-of-plane direction, are not yet fully understood. In this study, we examine the out-of-plane thermal conductivity dependence on both thickness and temperature in $\text{Ti}_3\text{C}_2\text{T}_x$, i.e. one of the most extensively investigated MXenes. Frequency-domain thermoreflectance (FDTR) measurements are performed on individual multilayer flakes with thicknesses ranging between 15 and 76 nm. At ambient conditions, the measured out-of-plane thermal conductivity remains constant across this thickness range, yielding an impressive low value of $0.18 \pm 0.02 \text{ W m}^{-1} \text{ K}^{-1}$. When varying temperature from 150 K to 450 K, the thermal conductivity displays a non-monotonic trend, increasing up to 375 K before decreasing at higher temperatures with an approximate T^{-1} dependence. A maximum value of $0.21 \text{ W m}^{-1} \text{ K}^{-1}$ is observed at 375 K. These findings support a phonon-mediated diffusive transport regime in the out-of-plane direction. This work sheds light to the mechanisms that govern heat transport in $\text{Ti}_3\text{C}_2\text{T}_x$ and show the potential of MXenes for thermal management applications.

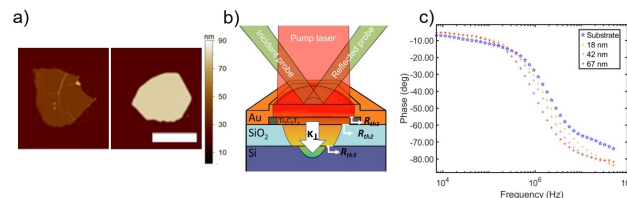


Figure 1. a) Topography maps of two $\text{Ti}_3\text{C}_2\text{T}_x$ with different thicknesses (scale bar is 10 μm). b) Schematic drawing of FDTR measurements on $\text{Ti}_3\text{C}_2\text{T}_x$ flakes supported on SiO_2/Si substrates. c) FDTR phase vs frequency measurements for both the substrate and $\text{Ti}_3\text{C}_2\text{T}_x$ flakes with different thicknesses. The signal difference between samples allow us to distinguish between different flake's thermal resistance.

Fig 1. out-of-plane thermal conductivity mxene flakes depending on temperature and thickness.jpg

Experimental Study of Atomic and Single-Molecule Scale Heat Transport: From molecular phononics to near-field hot-carrier thermal radiation

Friday, 24th April - 14:30: Molecular and Atomic Contacts - Featured talk

Dr. Longji Cui¹

1. University of Colorado Boulder

Understanding thermal transport at extreme length scales down to single atoms and molecules is both fundamentally important and technologically transformative, yet progress remains constrained by the resolution limits of current probes. While atoms and molecules serve as the smallest functional building blocks in modern devices and have enabled breakthroughs from atomic clocks to single-atom catalysis, thermal phenomena at these scales remain largely unexplored, despite heat accounting for ~90% of global energy use and ~60% of energy waste. This gap stems from the formidable challenges of stabilizing systems at such small scales and detecting heat currents at the picowatt or even sub-picowatt level, especially under conditions where coherence and nonequilibrium dynamics emerge.

This talk explores two frontiers of nanoscale heat transport: molecular phononics and hot-carrier-induced near-field thermal radiation. First, we report the room-temperature observation of destructive phonon interference in single-molecule junctions, enabled by a custom-built, ultrastable twin-tip scanning thermal microscopy (SThM) platform capable of simultaneous electrical and thermal measurements. In para- and meta-connected oligophenylene-ethynylene (OPE3) trimers, we observe a pronounced suppression of thermal conductance in the meta isomer. Quantum-accurate molecular dynamics simulations reproduce both the magnitude and the interference-induced suppression, attributing it to cancellation among vibrational pathways along the kinked aromatic backbone. These findings confirm that coherent phonon transport can persist even at ambient conditions, when confined to molecular dimensions.

To advance beyond these measurements, we present a theoretical framework for near-field hot-carrier nanoscopy, where a scanning nanotip placed nanometers from a photoexcited material detects ultrafast thermal emission through absorption and scattering of extreme-near-field radiation. This model bridges multi-temperature nonequilibrium transport theory with fluctuational electrodynamics, and resolves how hot electrons and individual phonon branches contribute to the spatiotemporal evolution of local thermal signals. Using monolayer graphene as a model system, we identify signatures of supercollision cooling, second sound, and nonlocal phonon transport that are currently inaccessible to far-field or electrical probes.

Overall these studies establish new experimental and theoretical routes for probing and controlling heat flow, from the single-molecule limit to ultrafast hot-carrier dynamics, opening pathways toward coherent molecular-scale thermal devices and time-resolved near-field thermal imaging in quantum materials.

References:

1. Phonon interference in single-molecule junctions, *Nature Materials*, 24, 258–1264 (2025).
2. Near-field thermal radiation as a probe of nanoscale hot electron and phonon transport. *ACS Nano* 2025 19 (6), 6033-6043.
3. Thermal conductance of single-molecule junction, *Nature* 572, 628-633 (2019).

Room-temperature phonon interference in single-molecule junctions

Friday, 24th April - 15:00: Molecular and Atomic Contacts - Oral

Mr. Sai C. Yelishala¹, **Dr. Yunxuan Zhu**¹, **Mr. Pablo Martinez**², **Dr. Hongxuan Chen**¹, **Mr. Mohammad Habibi**¹, **Dr. Giacomo Prampolini**³, **Prof. Juan Carlos Cuevas**⁴, **Prof. Wei Zhang**¹, **Dr. Guilherme Vilhena**², **Dr. Longji Cui**¹

1. University of Colorado Boulder, 2. Instituto de Ciencia de Materiales de Madrid, 3. Istituto di Chimica dei Composti Organometallici, 4. Departamento de Física Teórica de la Materia Condensada, Universidad Autónoma de Madrid

Wave interference allows unprecedented coherent control of various physical properties and has been widely studied in electronic and photonic materials. However, the interference of phonons, or thermal vibrations, central to understanding coherent thermal transport in all electrically insulating materials, has been poorly characterized due to experimental challenges. In this work [1], we report the first direct observation of vibrational interference at room temperature, which was measured in two molecular-scale junctions. This is enabled by custom-developed scanning thermal probes with combined high stability and sensitivity, allowing quantification of heat flow through molecular junctions one molecule at a time. Using isomers of oligo(phenylene ethynylene)₃ with either *para*- or *meta*-connected central rings, our experiments revealed a remarkable reduction in thermal conductance in *meta*-conformations. We make use of quantum-mechanically derived force fields [2] to accurately model the vibrational properties of the molecular compounds within classical non-equilibrium molecular dynamics (NEMD). Our simulations confirm the experimental observations regardless of the specific lead geometry under consideration. Further analysis through Green's function methods supports the presence of vibrational interference in both species. Fine sampling of the conformations spanned through the dynamics reveal that thermal fluctuations hinder interferences in *para*-OPE3, thus explaining the difference with respect to *meta*-OPE3. This work opens opportunities for studying numerous wave-driven material properties of phonons down to the single-molecule level that have remained experimentally inaccessible.

References:

- [1] Yelishala, S.C., Zhu, Y., Martinez, P.M. et al. *Nat. Mater.* **24** 1258 (2025)
[2] S. Giannini et al. *J. Chem. Theory Comput.* **21** 3156 (2025)

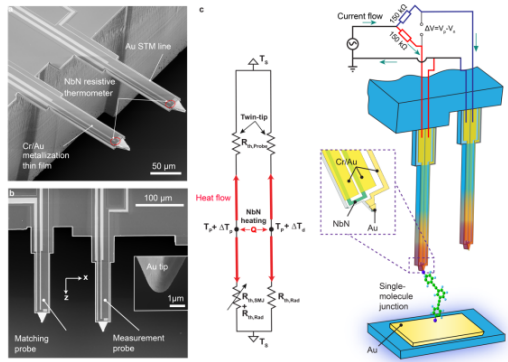


Fig 1: **a**, SEM image of a twin-tip STM probe featuring NbN thermometers with Cr/Au metallization on two geometrically identical beams, and gold electrode lines for current measurement. **b**, SEM image of a probe showing the proximity of the twin tip. Inset: end of a gold-coated tip. **c**, Measurement scheme for quantifying the thermal conductance of a single-molecule junction, which is trapped between the gold sample and the longer tip of the twin-tip probe.

Experimental setup.png

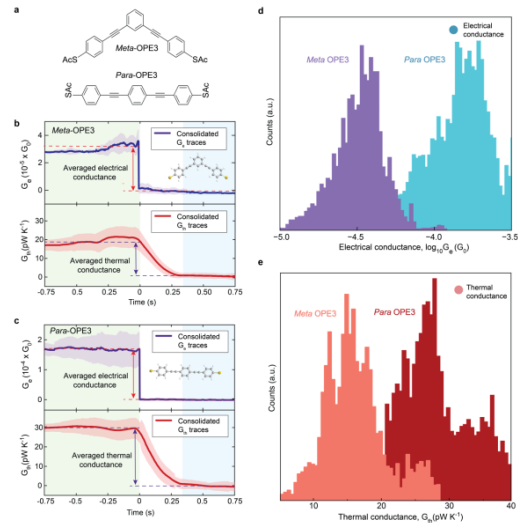


Fig 2: **a**, Chemical structure of meta- and para-OPE3 molecules. **b, c**, Consolidated electrical and thermal conductance traces for meta-OPE3 (**b**) and para-OPE3 (**c**) from approximately 50 measurements, where the shaded regions represent 1 s.d. **d**, Electrical histograms of OPE3 molecules constructed from the data traces in **b**, showing nearly an order of magnitude difference in electrical conductance due to destructive electrical quantum interference. **e**, The corresponding thermal histograms of two OPE3 molecules show a difference of 50% due to destructive phonon interference.

Measurements.png

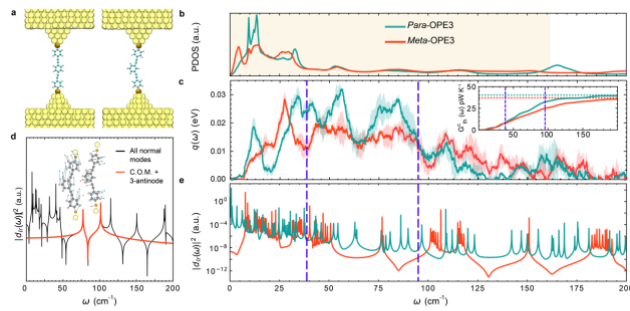


Fig 3: **a**, Schematics of the contact geometries of para- and meta-OPE3 molecules bonded to gold electrodes. **b**, Phonon DOS computed from the MD trajectories for the junctions shown in **a**. The yellow shaded region represents the allowed frequencies inside the contacts, that is, the Debye frequency of gold ($\sim 161 \text{ cm}^{-1}$). **c**, The corresponding averaged spectral heat current computed over three independent simulations as a function of frequency and the associated s.d. (represented as the shaded area). Inset: cumulative thermal conductance obtained by integrating the spectral conductance. **d**, Kernel of the transmission function ($|d_n(\omega)|^2$) as a function of frequency for the meta-OPE3 coupled to single gold atoms. The black line includes all vibration modes; the red line corresponds to the contribution of the two modes represented as insets. **e**, Averaged transmission function kernels computed for several geometries sampled within a cMD trajectory.

Simulations.png

Cryogenic STM Break Junction Measurements of Heat Transport in Atomic Contacts

Friday, 24th April - 15:20: Molecular and Atomic Contacts - Oral

Ms. Valentina Grieci¹, Dr. Bernd Gotsmann¹

1. IBM Research Zurich

Heat dissipation is one of the key limitations in the miniaturization of high-performance electronic devices. Unlike electrical transport, thermal transport mechanisms at the extreme nanoscale remain poorly understood. This work aims to deepen our understanding of heat flow through atomic junctions, where transport channels are quantized and quantum effects dominate.

Atomic junctions are formed using the Scanning Tunneling Microscope Break Junction (STM-BJ) technique (Fig. 1). By integrating the STM-BJ with a suspended MEMS device acting as an ultrasensitive thermal sensor, we perform simultaneous measurements of electrical and thermal conductance with pW/K sensitivity, enabling direct correlation between charge and heat transport through individual quantum channels.

At room temperature, thermal conductance quantization has been observed in metallic atomic contacts, confirming the Wiedemann–Franz law in the quantum regime [1]. Here, we extend these measurements to the cryogenic regime, where deviations from the Wiedemann–Franz law are expected due to phononic contributions to heat transport [2]. Measurements are performed down to 15 K, well below the Debye temperature of the metal forming the contact (Au), accessing regimes where ballistic phonon transport and discrete vibrational modes are expected to become relevant.

Achieving stable atomic contacts at low temperatures represents a major experimental challenge due to vibrations induced by the cooling cycle. As described in [3], this is addressed by integrating a pulse-tube cryocooler mechanically decoupled from the STM through a passive damping architecture (Fig. 2), reducing cold-head vibrations from micrometers to picometers at the tip–sample junction. Low-temperature operation also requires enhanced thermal sensitivity, since the quantum of thermal conductance scales linearly with temperature. The MEMS sensors were therefore redesigned to increase thermal isolation while preserving mechanical stiffness, yielding a substantial improvement in sensitivity (Fig. 3). Finally, surface cleanliness of the MEMS device is crucial: due to the lack of in-situ cleaning in the setup, a dedicated preparation and handling protocol was developed to ensure MEMS surface cleanliness.

This work establishes a robust platform for probing the crossover between electronic and phononic heat transport at the atomic scale, offering new insights into quantum heat conduction.

[1] *Nature Nanotechnology* 12, 430–433 (2017).

[2] *Nano Lett.* 2018, 18, 7358–7361.

[3] *Rev. Sci. Instrum.* 92, 123704 (2021).

Fig. 1: Schematic of the STM-BJ experiment. The gold electrode temperature (T_H) is monitored by measuring the four-probe voltage (V_{4P}) and heater current (I_H). The tunneling current (I_{STM}) is used to extract the junction's electrical resistance, with an external resistor (R_{EXT}) limiting the current.

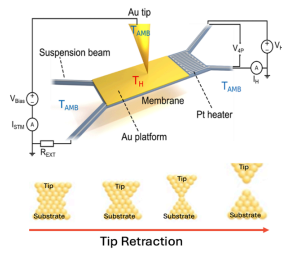


Fig.1-stmbjexperiment.png

Fig. 2: Cryogenic STM break junction setup. (Left) External view showing the mechanically decoupled pulse-tube cryocooler and main vacuum chamber. (Right) Scanning stage inside the thermal radiation shield, suspended by Be-Cu springs for vibration isolation.

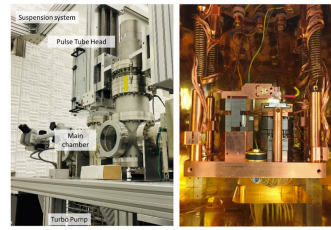


Fig.2-cryogenicstm.png

Fig. 3: Power vs. temperature rise measurements used to extract the thermal conductance G_{th} of MEMS sensors, which directly determines their sensitivity. The blue curve corresponds to previous designs, while the yellow curve shows the improved performance of a new geometry engineered to enhance thermal isolation, as confirmed by the reduced thermal conductance slope.

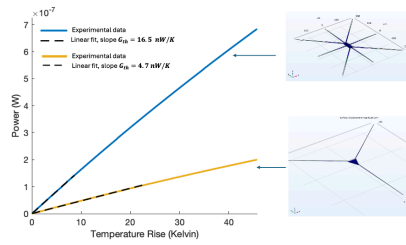


Fig.3-memsdesignsensitivity.png

Reverse design of $\text{Sm}_x\text{Nd}_{1-x}\text{NiO}_3$ thin films for radiative transfer applications

Friday, 24th April - 15:40: Conduction and Radiation - Oral

*Mr. Pierre-Antoine Tostivint*¹, *Dr. Jérémie Drévilion*², *Dr. Simon Hurand*², *Dr. Arthur Tausch*², *Dr. Fabien Capon*¹

1. IJL, Université de Lorraine, 2. Institut Pprime

Thermochromism, the faculty of a material to change his radiative properties with temperature, can be an alternative to various problematics such as radiative cooling or infrared stealth. Belonging to these thermochromics materials are rare-earth nickelates which present a metal-insulator transition with temperature. By adjusting the size of the rare earth in insertion in the unit cell, it is possible to adapt the insulator to metal transition in the temperature range that we want.

This study presents how it is possible to couple a physical model describing the dielectric function of $\text{Sm}_x\text{Nd}_{1-x}\text{NiO}_3$ depending on the energy, the temperature and the Sm/Nd ratio, with an S-matrix/metaheuristics algorithm enabling the determination of multilayer thicknesses and the ideal chemical composition of nickelates to address a given problem such as infrared stealth.

The empirical dielectric function model was realized using temperature dependent infrared spectroscopic ellipsometry data obtained on SmNiO_3 , NdNiO_3 and $\text{Sm}_{0.65}\text{Nd}_{0.35}\text{NiO}_3$ sputtered thin films. Fig. 1. presents the evolution of the extinction coefficient k at $10\ \mu\text{m}$ of $\text{Sm}_x\text{Nd}_{1-x}\text{NiO}_3$, depending on the temperature and the rare-earth composition. This figure allows us to see the dependence of the metal insulator transition temperature on the rare-earth content.

By coupling this model with an S-matrix/metaheuristics algorithm, it is possible to determine the optimum thicknesses and composition of a multi-layer stack (Fig. 2(a)), minimizing for example the difference between the exitance of the environment at room temperature and the contribution emitted and reflected by our material. Fig. 2(b) represents the spectral exitance from -50 to 150°C with a linear step of 50 values of an optimized multilayer and compared with exitance of the atmosphere considered as a black body at 25°C . We can then obtain, from the spectral exitance data, the evolution of the temperature observed by infrared camera. This can be seen in Fig 2(c) representing the infrared temperature corresponding to two spectral ranges where the atmosphere is transparent, allowing the camera operation. If we consider a delta of 5°C around room temperature and the range $8\text{-}12\ \mu\text{m}$, we can obtain a furtive material between 0 and 70°C .

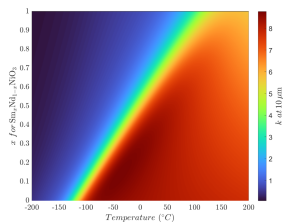


Fig. 1. Map of the extinction coefficient centered at $10\ \mu\text{m}$ versus the chemical composition and the temperature.

Extinction coefficient map.png

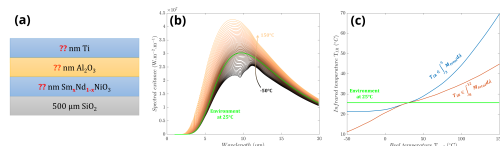


Fig. 2. (a) Example of multilayer stack optimized by the S-matrix/Metaheuristics algorithm, (b) Spectral exitance of the multilayer $30\ \text{nm Ti} / 225\ \text{nm Al}_2\text{O}_3 / 125\ \text{nm Sm}_x\text{Nd}_y\text{NiO}_3$ from -50 to 150°C

Exitance irtemperature figure.png

Ballistic phonon dissipation in 2D, thermal conductivity suppression function and the ‘collective diffusion’ regime

Friday, 24th April - 16:00: Conduction and Radiation - Poster

*Dr. Juan Carlos ACOSTA ABANTO*¹, *Dr. Raja Sen*², *Dr. Jelena Sjakste*², *Dr. Nathalie Vast*², *Dr. Ali Alkurdi*¹, *Dr. Carolina Abs Da Cruz*¹, *Dr. Elyes Nefzaoui*³, *Dr. Severine Gomes*¹, *Dr. P-Olivier Chapuis*¹

1

1. CETHIL, CNRS-INSA Lyon, France, 2. LSI, CNRS, Ecole Polytechnique, Palaiseau, France, 3. ESYCOM, Univ. Gustave-Eiffel, France

Heat dissipation by phonons from nanoscale sources is constrained by a maximal flux associated with ballistic transport and thermal boundary resistances. In one-dimensional configuration, it is well understood that reducing the thickness of a thin film leads to a decrease in apparent thermal conductivity. The effect can be seen by introducing an average mean free path Λ of the order of 200 nm in silicon. If one includes the complete phonon mean-free path distribution function, the shape of thermal conductivity as a function of thickness changes slightly, but the overall behaviour stays the same.

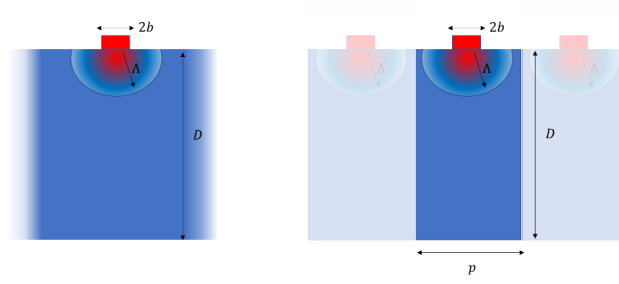
For finite sources, the situation is different and a thermal conductivity ‘suppression function’ was introduced in [1] in order to quantify the flux deviation to the prediction with the diffusive heat equation. The authors derived a suppression function that depends only on the mean free path distribution and on the heat source characteristic size. The same was postulated in [2]. However, the ‘suppression function’ can be understood in steady state as the ratio between the correct thermal conductance to the prediction with heat diffusion. This dependency highlights the necessity for a more-complex expression than that postulated in [2], and various geometrical parameters such as medium size (i.e. distance to heat bath), pitch in the case of periodic configuration and Λ enter into play. As a result, the suppression function is not a universal function of the heat source size. For instance, it depends on the frequency of excitation of the thermal wave ω in the electrothermal 3ω method. In [3], the function was taken from numerical computation but the diffusive part was not fully accounted for. Here, we compare simple analytical approximations to solutions of the Boltzmann transport equation for phonons (EPRT approximation) in order to provide guidelines in various two-dimensional cases. One result is that the ‘collective-diffusion’ regime highlighted in [2] and termed ‘disparate’ in [3] can simply be seen as a consequence of the interplay between four sizes, i.e. Λ , the heat source size, the pitch and the distance to the heat bath, which can be treated with the Matthiessen rule and series resistances within a reasonable error budget.

[1] A. Maznev et al., PRB 84, 195206 (2011)

[2] K. Hoogeboom-Pot et al., PNAS 112, 4846 (2015)

[3] L. Zeng et al., Sci. Rep. 5, 17131 (2015); A 116, 064307 (2014)

We acknowledge funding from projects EFICACE/NanoHeat (ANR), QuantiHeat/EFINED (EU), and thank D. Lemonier.



Carlosacosta-fig.png

A Novel High-Throughput Approach to Studying the Quasi-Ballistic Thermal Transport Regime

Friday, 24th April - 16:20: Conduction and Radiation - Oral

Dr. Sebastian Reparaz¹, **Dr. Kai Xu**², **Dr. Clemens Petersen**³, **Dr. Filippo Bencivenga**⁴, **Dr. Laura Foglia**⁴, **Dr. Riccardo Mincigrucci**⁴, **Prof. Markus R. Wagner**⁵, **Dr. Holger von Wenckstern**³, **Dr. Riccardo Rurali**²

1. Universitat Autònoma de Barcelona, Campus UAB, ES-08193 Bellaterra, Spain, 2. Institut de Ciència de Materials de Barcelona, ICMAB-CSIC, ES-08193 Bellaterra, Spain, 3. University of Leipzig, 4. Elettra Synchrotron Trieste, 5. Technische Universität Berlin, Institut für Festkörperphysik

Despite substantial theoretical and computational progress in elucidating spectral phonon MFP distributions and their influence on thermal transport, few experimental techniques reliably deliver precise and self-consistent data. The thermal transient method (TTG), correlating phonon mean free path (MFP) reduction directly with induced grating spatial wavelengths, has emerged as particularly effective but inherently suffers from a fundamental optical diffraction limit. Specifically, the minimum achievable grating spatial scale is constrained by the laser wavelength, impeding access to phonon transport phenomena occurring at sub-optical scales. Consequently, overcoming these spatial resolution limitations has become a significant challenge, motivating research into advanced optical and alternative experimental methods.

In this talk, we introduce a novel experimental approach designed to systematically investigate phonon contributions with varying MFPs to thermal conductivity in thin films. Our method specifically targets the quasi-ballistic regime, characterized by phonon MFPs exceeding the film thickness. To achieve this, we fabricated gradient samples featuring continuously decreasing thicknesses reaching sub-10 nm scales, enabling unprecedented spatial resolution and direct access to quasi-ballistic transport phenomena.

Counterintuitively, our findings reveal that phonon suppression with reduced thickness is not uniform but significantly influenced by thermal boundary conductance at the film-substrate interface. Particularly, minimal interface conductance markedly reduces the suppression of phonons with longer MFPs, underscoring the crucial role of interfaces in governing quasi-ballistic thermal transport. Complementary in-plane TTG experiments performed at the FERMI synchrotron facility confirm our observations, indicating consistency with established harmonic suppression functions typical of TTG experiments. Conversely, frequency-domain thermorefectance measurements demonstrate that suppression functions significantly deviate from steady-state assumptions and closely align with forms observed in TTG studies. We discuss the choice of a specific suppression function tailored to our experimental geometry and boundary conditions, highlighting its complexity and sensitivity to experimental parameters. This comprehensive analysis clarifies the interplay among phonon mean free paths, interface thermal conductance, and various transport regimes, offering valuable insights critical for nanoscale thermal management strategies.

We further demonstrate the versatility and robustness of our methodology by applying it to various technologically important oxide materials and polymer gradient films. In each case, we directly obtain the phonon accumulation function as a function of maximum phonon MFPs, delivering an intrinsic material property independent of specific excitation conditions and boundary constraints. Our approach thus provides a simple yet powerful technique for detailed studies of phonon MFP spectra at length scales below 10 nm, significantly advancing our understanding of nanoscale heat transport mechanisms.

Authors Index

| | | | |
|-----------------------|--------------------|----------------------|-----------------------------|
| Abad Mayor, B. | 13 | Biermann, K. | 100 |
| Abad, L. | 42, 108, 114 | Blandre, E. | 63 |
| Abdul Rasheed, R. | 47 | Boland, J. | 48 |
| Abou-Hamdan, L. | 85 | Bondavalli, P. | 146 |
| Abs Da Cruz, C. | 156 | Borja Peña, C. | 112 |
| Aceituno Pimentel, M. | 42, 114 | Bouchon, P. | 85 |
| ACOSTA ABANTO, J. | 31, 156 | Bourgault, D. | 146 |
| Acosta Abanto, J. | 5 | Bourgeois, O. | 24, 107, 146 |
| Adessi, C. | 26, 31 | Bourouina, T. | 47 |
| Agarwal, S. | 136 | Breu, J. | 137 |
| Agrait, N. | 105 | Brisuda, B. | 24 |
| Ahmadi, B. | 99 | Brouillard, M. | 5, 31 |
| Ahopelto, J. | 116 | Buhmann, S. | 15 |
| Aldave, D. | 19, 55 | C. Yelishala, S. | 151 |
| Alfaro Mozaz, F. | 14 | Caballero Calero, O. | 76 |
| Alkurdi, A. | 156 | Callsen, G. | 27, 126, 147 |
| Alvarez, F. | 4, 7, 9, 28 | Camacho, J. | 4, 28 |
| Amrit, J. | 59 | Cambré, S. | 112 |
| Antony, A. | 47 | Canetta, A. | 108 |
| Ares, P. | 19, 55 | Canosa Diaz, J. | 24 |
| Armstrong, I. | 56 | Capolat Palomar, D. | 57, 79, 112 |
| Aubergier, N. | 146 | Capon, F. | 155 |
| AUFFEVES, A. | 96 | Cappai, A. | 141 |
| Azhar, B. | 109 | Cartoixa, X. | 88 |
| Baba, T. | 38 | Caviglia, A. | 65 |
| Bafaluy, J. | 4 | Chakrabarty, T. | 63 |
| Barabashko, M. | 23 | Chang, K. | 89 |
| Bargheer, M. | 117, 118, 123, 138 | Chang, Z. | 21 |
| Barros, E. | 66 | Chapuis, P. | 5, 31, 51, 52, 83, 129, 156 |
| Baudin, E. | 85 | Chavez, E. | 69 |
| Beardo, A. | 4, 7, 9, 28, 145 | Chen, H. | 151 |
| Behaghel, B. | 129 | Chen, Z. | 46 |
| Beljonne, D. | 144 | Chevalier, S. | 74 |
| Ben Abdallah, P. | 1 | Chirtoc, M. | 31 |
| Bencivenga, F. | 158 | Ciavatta, A. | 62 |
| Benyattou, T. | 83 | Claus, N. | 146 |
| BERCU, N. | 5, 31 | Cobian, M. | 26, 103 |
| Berx, J. | 125 | Colombo, L. | 141, 144 |
| Bescond, M. | 29 | Conte, G. | 116 |
| Bhat, S. | 100 | Cresson, P. | 63 |
| Biehs, S. | 16, 60, 102 | Cueff, S. | 20 |

| | | | |
|--------------------------------|-------------------|----------------------|---------------|
| Cuevas, J. | 56, 105, 122, 151 | Galland, C. | 95 |
| Cui, L. | 150, 151 | Garcia Fernandez, J. | 29 |
| Culman, T. | 145 | Garcia Loureiro, A. | 29 |
| Cummings, A. | 79 | Geesmann, F. | 102 |
| Danielsson, E. | 10 | Gehring, P. | 108 |
| de Pablo, P. | 19 | Geng, Z. | 132 |
| De SanFeliciano, M. | 26 | Ghanem, M. | 11 |
| Denis, S. | 40 | Giordano, V. | 22 |
| Desgue, E. | 146 | Giraudet, L. | 5, 31 |
| Detcheverry, F. | 26 | Giri, A. | 109 |
| Dettori, R. | 144 | Goblot, V. | 95 |
| Dhankhar, A. | 118 | Gogotsi, Y. | 135, 149 |
| Di Lucente, E. | 95 | Gomes, S. | 5, 31, 156 |
| Diaz Serrano, A. | 4, 9 | Gordievskaya, Y. | 41 |
| Dimoulas, A. | 77 | Gotsmann, B. | 153 |
| Dinh, D. | 120 | Graczykowski, B. | 37, 88 |
| Dollfus, P. | 11 | Grandjean, N. | 126 |
| Douri, S. | 92 | Greffet, J. | 85 |
| Dovbeshko, G. | 23 | Grieb, T. | 126 |
| Drévilion, J. | 155 | Grieci, V. | 153 |
| Dubois, E. | 63 | Gruginskie, N. | 129 |
| Dudde, K. | 27, 126, 147 | GU, J. | 127 |
| Délvallée, A. | 92 | Guillemot, V. | 17 |
| Díez-Martínez, A. | 19 | Gómez Torres, H. | 108, 131 |
| Eich, Y. | 136 | Gómez-Herrero, J. | 19, 55 |
| El Hajj, J. | 26 | Habibi, M. | 151 |
| Elhajhasan, M. | 27, 126, 147 | Hagman, R. | 125 |
| Elsachat, A. | 48, 77 | Haibeh, J. | 120 |
| Emtenani, P. | 66, 100, 120, 126 | Hallmann, J. | 123 |
| Eserin, S. | 48 | Hamaoui, G. | 20 |
| Esplandiu, M. | 57, 79 | Hameury, J. | 92 |
| Feltin, N. | 92 | Han, Z. | 7 |
| Fernandez-Regulez, M. | 42, 110 | Harford, J. | 4 |
| Fernández-Tresguerres Mata, A. | 17 | Hay, B. | 92 |
| Feulner, S. | 88 | He, Q. | 124 |
| Finch, S. | 77 | Heinz, H. | 56 |
| Fischer, S. | 82 | Henkel, C. | 44, 45 |
| Flavel, B. | 112 | HERVE, A. | 47 |
| Fleurence, N. | 92 | Herz, F. | 60 |
| Foglia, L. | 158 | Herzog, M. | 117, 123 |
| Fonseca, L. | 42, 114 | Hopkins, P. | 109 |
| Franca Santiago, O. | 15 | Horny, N. | 5, 20, 26, 31 |
| Freund, S. | 137 | Hortvík, V. | 94 |
| Förbom, C. | 36 | Huberman, S. | 91, 101, 120 |
| Galazka, Z. | 66 | Hurand, S. | 155 |
| | | Hätinen, J. | 36 |

| | | | |
|----------------------|--------------|----------------------|------------------|
| Ippolito, S. | 135, 149 | Liu, X. | 48 |
| Ishikawa, K. | 38 | Liu, Z. | 21 |
| Jacob, D. | 47 | Loletti, M. | 54, 66, 100, 133 |
| Jaramillo Concha, C. | 95 | Lomadze, N. | 41 |
| Jarecki, J. | 123 | Lopeandia, A. | 79, 108, 131 |
| Jeannot, S. | 63 | Lopez-Nebreda, R. | 105 |
| Jeong, C. | 89 | Loreto, R. | 36 |
| Jeong, J. | 19, 55 | Lui, B. | 135, 149 |
| Jeong, M. | 89 | Luomahaara, J. | 36 |
| Jezowski, A. | 23 | Luzik, V. | 59 |
| Joulain, K. | 50 | Ma, C. | 109 |
| Journet-Gautier, C. | 69 | Maasilta, I. | 37, 132 |
| Kapteyn, H. | 145 | Madsen, A. | 123 |
| Kas, J. | 2 | Magalhães, T. | 116 |
| Kaya, O. | 69, 79 | Magg, M. | 112 |
| Kemppinen, A. | 36 | Mahjoub, A. | 146 |
| Kesarwani, S. | 41, 118 | Maire, J. | 74 |
| Kim, D. | 89 | Majlesi, A. | 45, 117 |
| Kirchberg, H. | 10, 125 | Marichy, C. | 69 |
| Kiselev, M. | 97 | Martin, E. | 20 |
| Kittel, A. | 102 | Martin, T. | 97 |
| Klapetek, P. | 94 | Martin-Gonzalez, M. | 76 |
| Klinar, K. | 149 | Martinek, J. | 94 |
| Knobloch, J. | 4, 145 | Martinez, P. | 105, 122, 151 |
| Koblmüller, G. | 120 | Martín-Fernández, I. | 42, 114 |
| Koch, D. | 65, 110 | Marzari, N. | 95 |
| Kolosov, O. | 48, 77 | Massengale, J. | 52 |
| Kontou, K. | 83 | Mateos-Lopez, O. | 56, 105 |
| Koopman, W. | 45, 117 | Mattern, M. | 123 |
| Korkiamäki, T. | 37 | Maurya, S. | 129 |
| Kretinin, A. | 77 | McBennett, B. | 145 |
| Krivchikov, A. | 23 | McIntosh, N. | 21 |
| Kumar, A. | 36 | Mech, R. | 108 |
| Kutschera, J. | 117 | Medapalli, R. | 48 |
| Lange, H. | 41 | Mehner, L. | 118 |
| Lazar, M. | 20 | Meißner, M. | 2 |
| Le-Friec, Y. | 63 | Melis, C. | 141, 144 |
| Leclercq, J. | 83 | Merabia, S. | 26, 31, 103 |
| Legagneux, P. | 146 | Merchiers, O. | 51, 83 |
| Letessier, J. | 74 | Metschl, M. | 120 |
| Li, L. | 52 | Mincigrucci, R. | 158 |
| Li, Y. | 145 | Mohan, R. | 109 |
| Liberal, I. | 14 | Mori, T. | 38 |
| Lierath, J. | 27, 126, 147 | Morán-Meza, J. | 92 |
| Linseis, V. | 88 | Murdin, B. | 48 |
| Liu, J. | 145 | Murnane, M. | 145 |
| | | Muñoz, M. | 56, 135, 149 |

| | | | |
|-----------------------------|------------------|------------------------|-----------------------------------|
| Mykkänen, E. | 36 | Ribeiro, T. | 116 |
| Müller-Plathe, F. | 68 | Rivas Chacón, N. | 122 |
| Müller-Werkmeister, R. | 45 | Robillard, J. | 5, 24, 31, 63 |
| | | Roche, S. | 69, 79 |
| Naeimi, A. | 16, 60 | Rodehuts Kors, S. | 102 |
| Nair, H. | 109 | Rodríguez-Iglesias, A. | 42, 110, 114 |
| Nefzaoui, E. | 47, 156 | Rodríguez-Miguel, S. | 114 |
| Nelson, E. | 145 | Rodríguez-Viejo, J. | 57, 79, 108, 131 |
| Nguyen, T. | 97 | Rodríguez Viejo, J. | 112 |
| Niehaus, T. | 103 | Romano, G. | 27, 147 |
| Niemchenko, K. | 59 | Ronzani, A. | 36 |
| Niemchenko, Y. | 59 | Roschier, L. | 35 |
| Nigro, A. | 42 | Rossi, T. | 2 |
| Nippert, F. | 66, 100, 120 | Rousseau, L. | 20 |
| Noell, M. | 44, 45 | Roux, B. | 52 |
| | | Ruan, X. | 7 |
| O'Shaughnessy-Gutierrez, M. | 48 | Rubeck, S. | 63 |
| Oksanen, J. | 129 | Ruprecht, M. | 118 |
| OLLAIC, G. | 20 | Rurali, R. | 21, 54, 65, 66, 88, 100, 133, 158 |
| | | Rössle, M. | 2 |
| Patil, A. | 63 | | |
| Paulatto, L. | 62 | Sadat, N. | 109 |
| Perez-Murano, F. | 42 | Sahoo, S. | 136 |
| Petersen, C. | 158 | Saint Martin, J. | 11 |
| Pich, A. | 41 | Salami, N. | 103 |
| Pietsch, I. | 137 | Saleta, D. | 149 |
| Pillai, P. | 118 | Salleras, M. | 42, 110, 114 |
| Pompidou, Q. | 31 | Santander, J. | 114 |
| Poon, J. | 109 | Santer, S. | 41 |
| Poulos, M. | 71 | Santos, M. | 52 |
| Poulose, H. | 45 | Sarkar, J. | 100 |
| Prampolini, G. | 151 | Sarkar, S. | 51 |
| Protik, N. | 27, 147 | Sarr, J. | 51 |
| Prunnila, M. | 36, 129 | Schermer, J. | 129 |
| Pudell, J. | 123 | Schmidt, A. | 149 |
| Puurtinen, T. | 37 | Schmitt, A. | 85 |
| Pérez Picazo, E. | 76 | Schneider, E. | 48 |
| | | Schulz, F. | 118 |
| Raciti, G. | 13 | Scott, E. | 109 |
| Radevici, I. | 129 | Segantini, G. | 65 |
| Rajabpour, A. | 103 | Sen, R. | 11, 156 |
| Ramsden, H. | 135, 149 | Senker, J. | 136 |
| Rantanen, T. | 36 | Seoane, N. | 29 |
| Rech, J. | 97 | Sergeev, D. | 38 |
| Rehr, J. | 2 | Sghaier, W. | 129 |
| Ren, Q. | 54, 133 | Shahahmahdi, A. | 129 |
| Reparaz, S. | 66, 88, 100, 158 | Sharma, D. | 13 |
| Retsch, M. | 72, 136, 137 | Sheikh, R. | 31 |
| Rezgui, H. | 33, 116 | | |

| | | | |
|----------------------|-----------------------|---------------------|----------------------------|
| Shinoda, Y. | 38 | Ulhe, A. | 120 |
| Shivamade Gowda, S. | 109 | Vaillon, R. | 52 |
| Simoncelli, M. | 95, 101 | Vaimala, T. | 129 |
| Sivan, A. | 13, 65 | Valtr, M. | 94 |
| Sjakste, J. | 11, 156 | van der Krabben, L. | 129 |
| Skorda, S. | 77 | van der Veen, R. | 2 |
| Sledzinska, M. | 57, 69, 79, 112 | van Dijck, B. | 91 |
| Sojo Gordillo, J. | 13, 42, 65, 110 | van Hemert, M. | 91, 135, 149 |
| Sokolov, A. | 101 | Varghese, S. | 28, 91, 131, 135 |
| Sotomayor-Torres, C. | 33, 69, 116 | Vast, N. | 156 |
| Souvignet, T. | 69 | Vertiz, A. | 14 |
| Splettstoesser, J. | 10, 125 | Vicente Manzano, C. | 76 |
| Stete, F. | 118 | Viisanen, K. | 36 |
| Strauß, N. | 15 | Vikhtynska, T. | 59 |
| Sun, Y. | 87 | Vilhena, G. | 56, 105, 122, 151 |
| Surblys, D. | 71 | VOLZ, S. | 106 |
| Swoboda, T. | 57, 79, 112 | von Reppert, A. | 123 |
| Szewczyk, D. | 23 | von Wenckstern, H. | 158 |
| Tabatabaei, F. | 103 | Wagner, M. | 66, 88, 100, 120, 126, 158 |
| Tamariz, S. | 126 | Wang, H. | 135 |
| Tan, P. | 57, 79, 112 | Wenseleers, W. | 112 |
| Tappura, K. | 129 | Wilde, Y. | 17, 85 |
| Taskinen, J. | 36 | Worbes, L. | 102 |
| Tausch, A. | 155 | Wu, K. | 95 |
| Tellal, A. | 83 | Würsch, G. | 27, 126, 147 |
| Tenaguillo, M. | 76 | Xiao, P. | 69, 146 |
| Termentzidis, K. | 71 | Xu, K. | 88, 100, 158 |
| Themann, J. | 27, 147 | Xu, Y. | 142 |
| Thomas, M. | 52 | Yan, Y. | 47 |
| Thomsen, C. | 66, 120 | Yang, J. | 57, 69, 79, 112 |
| Thurau, P. | 102 | Yang, R. | 52 |
| Tielrooij, K. | 28, 91, 131, 135, 149 | Ylivaara, O. | 116 |
| Tiira, J. | 129 | Zardo, I. | 13, 42, 65, 110 |
| Tonkonozhenko, A. | 59 | Zare, S. | 109 |
| Tornero, E. | 56, 135, 149 | Zenji, A. | 13 |
| Tostivint, P. | 155 | Zhang, W. | 151 |
| Trautvetter, J. | 65 | Zheng, Q. | 46, 73, 127 |
| Trukhan, E. | 27, 147 | Zhou, Y. | 124, 139, 142 |
| Tsipas, P. | 77 | Zhu, Y. | 95, 151 |
| Tsukamoto, O. | 38 | Ziehm, T. | 102 |
| Tubal, M. | 36 | | |
| Tur Prats, J. | 4, 7, 9, 28 | | |
| Tyagi, S. | 29 | | |

